UNIVERSITÀ DELLA CALABRIA

UNIVERSITÀ DELLA CALABRIA

Dipartimento di Ingegneria Civile

Dottorato di Ricerca in

Ingegneria Civile e Industriale

CICLO

XXXII

A COMPREHENSIVE ANALYSIS OF HYDROLOGICAL BENEFITS OF LOW IMPACT DEVELOPMENT TECHNIQUES: EXPERIMENTAL INVESTIGATION AND NUMERICAL MODELING

Settore Scientifico Disciplinare ICAR/02

Coordinatore: Ch.mo Prof. Franco Furgiuele

Firma _____

Supervisore/Tutor: Ch.ma Prof.ssa Patrizia Piro

Firma _____

Dottorando: Dott.ssa Stefania Anna Palermo

Firma _____

I would like to dedicate this thesis to my birth family
and to Vito, my future husband.

Declaration

I hereby declare that except where specific reference is made to the work of others, the contents of this dissertation are original and have not been submitted in whole or in part for consideration for any other degree or qualification in this, or any other University. This dissertation is the result of my own work and includes nothing which is the outcome of work done in collaboration, except where specifically indicated in the text.

Dott.ssa Stefania Anna Palermo

2019

Acknowledgements

I would like to thank all the people that supported me during this path.

First, my birth family (mum, dad and Rocco), Vito, my future husband, and his birth family. All of them have encouraged and backed me from the beginning. Thank to make me happy during my daily life.

A special thanks to my scientific supervisor, Prof. Patrizia Piro, who have supported my project, contributed to improve my knowledge and given me the opportunity to increase my cultural and human luggage, by working together on innovative aspects of urban drainage, allowing me to spend a period in an abroad university for my academic growth, granting me to participate to many conference all over the world. I would like to thank her for giving me this great opportunity, for her constant encouragement, and, above all, for the strength she gave me during these years.

I would also to thank Prof. Wolfgang Rauch and Prof. Robert Sintzfrei for their hospitality, availability and scientific support and supervision, during my research period at University of Innsbruck, as well as I would to thank all the other professors and my "Austrian" colleagues and friends who maked me feel at home despite the distance.

And thanks to all my Italian friends and to the LIU (Urban Hydraulic and Hydrology Laboratory) colleagues to have been a part of this travel.

Abstract

Urban floods, recently increasing due to the combine effect of climate change and urbanization, represent a potential risk to human life, economic assets and environment. In this context, the traditional urban drainage techniques seem to be inadequate for the purpose, therefore a transition towards an innovative sustainable and resilient urban stormwater management is a valid solution. One promising strategy is the implementation of decentralized stormwater controls, also known as Low Impact Development (LID) systems that provide several benefits at multiple scales. Despite several studies demonstrated the LIDs' capability in terms of surface runoff reduction, the transition towards a sustainable urban drainage system, which includes these techniques, seems to be very slow. One of the key scientific limiting factors can be found in the lack of comprehensive analyses able to highlight the hydrological performance and the physical processes involved in LID systems at multiple spatial scale and by considering long-term experimental data. The complexity of the physical processes, involved in each specific LIDs stratigraphy, requires modeling tools able to accurately interpret their hydraulic behaviour, as well as to correlate their hydrologic efficiency with the management of stormwater in the surrounding urban area. For these reasons, so far different empirical, conceptual and mechanistic models have been proposed, however in many of these studies, the hydrological parameters, as well as the physical ones were not properly investigated, limiting the analysis only to specific factors, or by considering literature values for the numerical modeling. Thus, principal aim of this thesis is to present a comprehensive analysis of the hydrological benefits of LID techniques by experimental investigation and numerical modeling. To achieve this goal, several analyses were carried out by considering different: LID systems, spatial scales, weather conditions, modeling investigation, as well as mathematical optimization approaches. Monitored data at the full scale implementation and laboratory measurements were used to support the numerical modeling. More in detail, first a global sensitivity analysis (GSA), based on the Elementary Effect Test (EET) was applied to a PCSWMM hydrodynamic model of the University Campus Innsbruck, which combines traditional drainage infrastructures and low impact development techniques, as Rain Gardens. In this regard, main findings have showed that soil hydraulic parameters considered in the model, (i.e., principally Soil Hydraulic Conductivity and Seepage Rate) were the most sensitive parameters. Therefore, the identification of these properties for LID

systems is crucial in order to correctly evaluate their hydraulic performance. Starting from this finding the analysis of the hydrological efficiency of a full-scale extensive green roof, located at University of Calabria in Mediterranean Climate was assessed, by considering field monitored hydrological data, as well as soil hydraulic properties evaluated in lab, and a modeling analysis. Thus, first a field monitoring campaign for one year was carried out, and then hydrological performance indices on an event scale were evaluated. The findings have revealed the optimal behaviour of the specific green roof in Mediterranean climate, which presents an average value of Subsurface Runoff Coefficient of 50.4% for the rainfall events with a precipitation depth more than 8 mm. Later, to evaluate the influence of increasing values of substrate depths (6 cm, 9 cm, 12 cm, 15 cm) on green roof retention capacity, the hydraulic properties of the soil materials were first investigated in Laboratory, by the simplified evaporation method, and then considered for the implementation of the mechanistic model HYDRUS 1D. The results obtained in this phase have showed how the considered substrate depths were able to achieve a runoff volume reduction of 22% to 24%. Thus, as the outflow volume reduction achieved by increasing the soil depth was not significant, the ideal depth for specific soil substrate would be 6 centimetres. Following this study, and based on the findings obtained at building scale, next phase was focused on the analysis of hydrological effectiveness of Low Impact development solutions at large-urban scale in a south Italian case study. This investigation was carried out by considering different LID conversion scenarios by a predictive conceptual model (PCSWMM). In this regards, a specific permeable pavement and green roof, developed and installed at University of Calabria, were considered for the model implementation. Globally, modeling results have confirmed the suitability of these LID solutions to reduce surface runoff even if just a small percentage (30%) of the impervious surfaces is converted. By considering all of the findings, previous achieved by experimental and modelig investigation, it emerged that many aspects related to LIDs design and operation, as well as the choice of the facility and its location can affect the results in terms of hydraulic efficiency. In this regard, a mathematical optimization approach to consider several aspects together could be a suitable tool for designers of LID systems and experts in the field. Therefore, in the last part of the work, new Mathematical Optimization Approaches for LID techniques were evaluated. More in detail, the optimization of rainwater harvesting systems, by using TOPSIS (Technique for Order Preference by Similarity to Ideal Solution) and Rough Set method as Multi-Objective Optimization approaches, was carried out. The results have demonstrated

that these approaches could provide an additional tool to identify the ideal system. In conclusion, main findings of this thesis confirm the suitability of LID systems for urban stormwater management providing useful suggestions for their design and tools for assessing their hydrological effectiveness, analysing physical and hydrological parameters that affect their operation, introducing advanced concepts for the optimization of LID systems, therefore providing a significant and innovative contribution for the improvement of scientific research in the field and the spread of these sustainable techniques.

Sommario

Gli allagamenti delle aree urbane, recentemente aumentati a causa dell'effetto combinato dei cambiamenti climatici e dell'urbanizzazione, rappresentano un potenziale rischio per la vita umana, i beni economici e l'ambiente. Questo fenomeno evidenzia l'inadeguatezza dei sistemi di drenaggio urbano tradizionali, e, per tale ragione, una transizione verso una gestione innovativa, sostenibile e resiliente delle acque piovane è una valida soluzione. In questo contesto, una strategia promettente è l'implementazione di sistemi in grado di effettuare controlli decentralizzati delle acque piovane, noti anche come sistemi LID (Low Impact Development) che offrono numerosi vantaggi su più scale. Tuttavia, nonostante diversi studi abbiano dimostrato la capacità dei sistemi LID nel ridurre il deflusso superficiale, la transizione verso un sistema di drenaggio urbano sostenibile, che include queste tecniche, sembra essere ancora molto lenta. Uno dei principali fattori limitanti si riscontra nella mancanza di studi completi in grado di evidenziare le prestazioni idrologiche e i processi fisici coinvolti nei sistemi LID considerando differenti scale spaziali e dati sperimentali a lungo termine. La complessità dei processi fisici, coinvolti in ogni specifica stratigrafia dei sistemi LID, richiede strumenti di modellazione in grado di interpretarne accuratamente il comportamento idraulico, nonché di correlare l'efficacia idrologica di tali sistemi con la gestione delle acque piovane nell'area urbana circostante. Finora sono stati proposti diversi modelli empirici, concettuali e meccanicistici, tuttavia, in molti di questi studi, i parametri idrologici, oltre che quelli fisici, non sono stati adeguatamente analizzati, limitandone lo studio solo a parametri specifici o considerando valori di letteratura per l'implementazione modellistica. Pertanto, scopo principale del presente lavoro di tesi è presentare un'analisi completa dei benefici idrologici delle tecniche LID mediante indagini sperimentali e modellazione numerica. Per raggiungere tale obiettivo, sono state condotte diverse analisi considerando differenti: sistemi LID, scale spaziali, condizioni climatiche, modelli numerici, nonché approcci di ottimizzazione matematica. Per supportare l'analisi numerica e quella modellistica, nel presente lavoro sono state considerate misurazioni su larga scala e di laboratorio. Nello specifico, nella prima fase, è stata inizialmente applicata un'analisi di sensibilità globale (Elementary Effect Test) a un modello idrodinamico, sviluppato in ambiente PCSWMM, che simula la risposta idrologica del nuovo sistema di drenaggio del Campus universitario di Innsbruck, che combina infrastrutture di drenaggio tradizionali e sistemi LID, quali i giardini di pioggia. I principali risultati hanno mostrato

che i parametri idraulici del suolo, considerati nel modello (principalmente la conduttività idraulica del suolo e anche velocità di infiltrazione), erano i parametri più sensibili. Pertanto, l'identificazione di tali proprietà dei sistemi LID è fondamentale per valutare correttamente le loro prestazioni idrauliche. A partire da questo risultato è stata effettuata l'analisi dell'efficienza idrologica di un tetto verde estensivo installato presso l'Università della Calabria, in clima Mediterraneo, considerando: i dati idrologici monitorati sul sito sperimentale, le proprietà idrauliche del suolo valutate in laboratorio e un'analisi modellistica. È stata, dunque, inizialmente condotta una campagna di monitoraggio di un anno e, successivamente, sono stati valutati gli indici di prestazione idrologica a scala di evento. Dall'analisi dei risultati è emerso che il tetto verde specifico presenta un valore medio del coefficiente di deflusso del 50.4% per eventi con altezza di pioggia superiore a 8 mm. Successivamente, per valutare l'influenza di valori crescenti di profondità del substrato (6 cm, 9 cm, 12 cm, 15 cm) sulla capacità di ritenzione del tetto verde, le proprietà idrauliche del substrato di suolo sono state valutate in laboratorio con il metodo evaporimetro, e, in seguito, considerate per l'implementazione del modello meccanicistico HYDRUS 1D. I risultati ottenuti in questa fase hanno mostrano una variazione del deflusso dal 22% al 24% in funzione delle profondità di substrato. Non avendo ottenuto una significativa riduzione del volume di deflusso all'aumentare della profondità del substrato, si può considerare quale la profondità ideale in clima Mediterraneo quella di 6 centimetri. A seguito di questa analisi, condotta su un singolo tetto verde installato su un edificio reale, la fase successiva si è concentrata sull'efficacia idrologica delle soluzioni LID su scala urbana considerando un caso studio localizzato nel sud Italia. Nello specifico, l'analisi è stata condotta considerando diversi scenari di conversione LID, mediante modellazione concettuale (PCSWMM) predittiva. Per l'implementazione modellistica sono state considerate la pavimentazione permeabile e il tetto verde sperimentale, sviluppati e installati presso l'Università della Calabria. A livello globale, i risultati della modellazione hanno confermato l'idoneità delle tecniche LID nella riduzione del deflusso superficiale anche se a essere convertita è solo una piccola percentuale (30%) delle superfici impermeabili. Considerando tutti i risultati ottenuti in precedenza da analisi sperimentali e modellistiche, è emerso che molti aspetti relativi alla progettazione e al funzionamento dei sistemi LID, nonché la scelta della tecnica specifica e la sua localizzazion possono influenzare i risultati in termini di efficacia idraulica. In tale contesto, un approccio di ottimizzazione matematica che consideri insieme diversi aspetti potrebbe, dunque, essere

uno strumento adatto per i progettisti di sistemi LID e per gli esperti del settore. Nell'ultima parte del lavoro, sono stati, pertanto, valutati nuovi approcci di ottimizzazione matematica per le tecniche LID. Più nel dettaglio, si è focalizzata l'attenzione sull'ottimizzazione di un sistema di raccolta e riuso dell'acqua meteorica utilizzando il metodo TOPSIS (Technique for Order Preference by Similarity to Ideal Solution) e il metodo Rough Set come approcci di ottimizzazione multi-obiettivo. I risultati hanno dimostrato che questi approcci potrebbero essere uno strumento aggiuntivo per identificare il sistema ottimale. In conclusione, i principali risultati di questa tesi confermano l'idoneità dei sistemi LID per la gestione delle acque piovane urbane, fornendo utili suggerimenti per la loro progettazione e strumenti per valutare la loro efficacia idrologica, analizzando i parametri fisici e idrologici che influenzano il loro funzionamento, introducendo concetti avanzati per l'ottimizzazione dei sistemi stessi, fornendo, quindi, un contributo significativo e innovativo per il miglioramento della ricerca scientifica nel settore e la diffusione di queste tecniche sostenibili.

Contents

LIST OF ABBREVIATIONS

ADWP	Antecedent Dry Weather Period
BMPs	Best Management Practices
CSOs	Combined Sewer Overflows
CSSs	Combined Sewer Systems
D	Rainfall Duration
DMs	Decision Makers
EET	Elementary Effect Test
EPA	Environmental Protection Agency
GF	Green Facades
GI	Green Infrastructure
GR	Green Roof
GSA	Global Sensitivity Analysis
GW	Green Wall
i	Rainfall intensity
IR	Impervious Roof
IDF	Intensity–Duration–Frequency
IoT	Internet of Things
LID	Low Impact Development
LW	Living Wall
OC	Open Channel
PA	Porous Asphalt
PC	Pervious Concrete
PD	Precipitation Depth
PFL	Peak Flow Lag-time
PFR	Peak Flow Reduction
PICPs	Permeable Interlocking Concrete Pavers
PP	Permeable Pavement
RC	Runoff Coefficient
RD	Runoff Depth
RG	Rain Garden
RP	Return Period
RR	Runoff Reduction
RMSE	Root Mean Square Error
RWH	Rainwater Harvesting
SA	Sensitivity Analysis
SRBs	Smart Rain Barrels
SRC	Subsurface Runoff Coefficient

SUDS	Sustainable Urban Drainage Systems
SWMM	Storm Water Management Model
SWRC	Soil Water Retention Curve
TOPSIS	Technique for Order Preference by Similarity to Ideal Solution
TSR	Time to Start of Runoff
UDS	Urban Drainage System
VGM	Van Genuchten Mualem
WSUD	Water Sensitive Urban Design

LIST OF FIGURES

LIST OF TABLES

LIST OF PAPERS

The following papers are an integral part of this thesis. They are annexed to this thesis in the printed version, by permission of the journal publishers or conference organisers. Copies of the papers may be obtained from journal publishers or conference organisers.

Paper I - **Palermo S.A.**, Zischg J., Sitzenfrei R., Rauch W., Piro P. (2019a) Parameter Sensitivity of a Microscale Hydrodynamic Model. In: Mannina G. (eds) New Trends in Urban Drainage Modelling. UDM 2018. Green Energy and Technology. Springer, Cham. https://doi.org/10.1007/978-3-319-99867-1_169

Paper II - **Palermo, S. A.**, Turco, M., Principato, F., & Piro, P. (2019b). Hydrological Effectiveness of an Extensive Green Roof in Mediterranean Climate. Water, 11(7), 1378. https://doi.org/10.3390/w11071378

Paper III - Piro, P., Carbone, M., Morimanno, F., & **Palermo, S. A.** (2019a). Simple flowmeter device for LID systems: From laboratory procedure to full-scale implementation. Flow Measurement and Instrumentation, 65, 240-249. https://doi.org/10.1016/j.flowmeasinst.2019.01.008

Paper IV - Oberascher M., Zischg J., **Palermo S.*A.***, Kinzel C., Rauch W., Sitzenfrei R. (2019). Smart Rain Barrels: Advanced LID Management Through Measurement and Control. In: Mannina G. (eds) New Trends in Urban Drainage Modelling. UDM 2018. Green Energy and Technology. Springer, Cham. https://doi.org/10.1007/978-3-319-99867-1_134

Paper V - Piro P., Turco M., **Palermo S.A.**, Principato F., Brunetti G. (2019b). A Comprehensive Approach to Stormwater Management Problems in the Next Generation Drainage Networks. In: Cicirelli F., Guerrieri A., Mastroianni C., Spezzano G., Vinci A. (eds) The Internet of Things for Smart Urban Ecosystems. Internet of Things (Technology, Communications and Computing). Springer, Cham. https://doi.org/10.1007/978-3-319-96550-5_12

Paper VI - **Palermo, S. A.**, Talarico, V. C., & Turco, M. (2020a). On the LID systems effectiveness for urban stormwater management: case study in Southern Italy. In IOP Conference Series: Earth and Environmental Science (Vol. 410, No. 1, p. 012012). IOP Publishing. https://doi.org/10.1088/1755-1315/410/1/012012

Paper VII - **Palermo, S. A.**, & Turco, M. (2020). Green Wall systems: where do we stand?. In IOP Conference Series: Earth and Environmental Science (Vol. 410, No. 1, p. 012013). IOP Publishing. https://doi.org/10.1088/1755-1315/410/1/012013

Paper VIII **- Palermo S.A.**, Talarico V.C., Pirouz B. (2020b) Optimizing Rainwater Harvesting Systems for Non-potable Water Uses and Surface Runoff Mitigation. In: Sergeyev Y., Kvasov D. (eds) Numerical Computations: Theory and Algorithms. NUMTA 2019. Lecture Notes in Computer Science, vol 11973. Springer, Cham. https://doi.org/10.1007/978-3-030-39081-5_49

Paper IX **-** Pirouz B., **Palermo S.A.**, Turco M., Piro P. (2020) New Mathematical Optimization Approaches for LID Systems. In: Sergeyev Y., Kvasov D. (eds) Numerical Computations: Theory and Algorithms. NUMTA 2019. Lecture Notes in Computer Science, vol 11973. Springer, Cham. https://doi.org/10.1007/978-3-030-39081-5_50

The following additional publications also resulted from the work during the PhD study. Although they are not part of this thesis, their contents are also related to the topics here discussed. Copies of the papers, already published, may be obtained from journal publishers or conference organizers.

Maiolo, M., Pirouz, B., Bruno, R., **Palermo, S. A.**, Arcuri, N., & Piro, P. (2020). The Role of the Extensive Green Roofs on Decreasing Building Energy Consumption in the Mediterranean Climate. Sustainability, 12(1), 359. https://doi.org/10.3390/su12010359

Pirouz, B., **Palermo, S.A.**, Arcuri, N., Piro, P. (2019). Decreasing Water Footprint of Electricity and Heat by Extensive Green Roofs in the Mediterranean climate. Under review in Journal of Environmental Management.

Piro, P., Ferrante, A.P., Frega, F., **Palermo, S.A.**, Principato, F. (2018). Mitigazione degli allagamenti urbani attraverso strategie di Controllo in Tempo Reale e sistemi LID. In Atti del XXXVI Convegno Nazionale di Idraulica e Costruzioni Idrauliche, IDRA 2018, Ancona, IT, 12- 14 September 2018, (pp. 184-17).

Palermo, S.A., Principato, F., Piro, P. (2017). Evaluation of hydrological performances of an extensive green roof at University of Calabria, Italy. In Proceedings of the IWA/IAHR 14th International Conference on Urban Drainage, ICUD2017, Prague, CZ, 10-15 September 2017, Oral Presentation, (pp. 835-838).

Principato, F., **Palermo, S.A.**, Nigro, G., Garofalo,G. (2017). Sustainable Strategies and RTC to mitigate CSO's impact: different scenarios in the highly urbanized catchment of Cosenza, Italy. In Proceedings of the 14th IWA/IAHR International

Conference on Urban Drainage, ICUD2017, Prague, CZ, 10-15 September 2017, Oral Presentation, (pp. 587-589).

Chapter 1 - Introduction

A Sustainable urban stormwater management is one of the main challenges towards which the scientific world is projected. In the last years, in fact, the coupled effect of urbanization and climate alteration led a drastic change on the natural hydrological cycle, making cities vulnerable to flooding risk. The growing frequency of urban flooding highlighted the inadequacy of traditional urban drainage systems, thus a transition towards sustainable, resilient and smart drainage systems is necessary.

In this context, the PhD project was focused on the Low Impact development (LID) techniques, which, due their capacity to reduce surface runoff and increase evapotranspiration and infiltration rates, represent valuable alternatives for stormwater management and natural hydrological cycle restoration in urban areas. In this regard, a comprehensive analysis of the hydrological benefits, by experimental investigations and numerical modeling, is here discussed.

This chapter first examines the issues that inspired the project, the new challenges and the promising solutions in the field of urban stormwater management. Then, the aims of the work will be specified and the structure of thesis as well as the annexed papers will be defined.

1.1 New challenges for the stormwater runoff management

The increase of impervious surfaces, due to urbanisation process, which represents one of the most significant trends of the 21st century, led several environmental and socio-economic impacts as: impoverishment of ecosystems, flooding risk, water quality deterioration, air pollution, urban heat island effect, and other socio-environmental problems (McDonald et al., 2014; Shuster et al., 2005; Gunn et al., 2012, Zhou et al. 2018). In this regard, more than twenty years ago, Arnold (1996) defined the impervious surfaces coverage as an environmental indicator. Based on the projection that world urban population will continuously increase, the urbanization will remain the biggest challenge for a sustainable urban design (Krebs et al., 2013).

From a hydraulic perspective, the exponentially development of built-up areas and motorways of the last decades have significant altered the natural hydrological cycle. In this regard, the constant loss of natural areas was reflected in the reduction of infiltration rate and groundwater recharge as well as in the decrease of interception and evapotranspiration processes, with an increase of surface runoff volumes. (Antrop, 2004; Shuster et al., 2005; Tang et al., 2005; Ahiablame et al., 2013).

Moreover, the growth of the frequency of extreme rainfall events, characterized by high intensity and short duration, due to the climate change (Kundzewicz et al. 2006), coupled with the effects of soil sealing, significantly affected urban water environment in terms of water management. More in detail, this negative combination, occurred during the post-urbanization, caused an alteration in the runoff hydrograph, which presents a much more runoff volume, a higher and more rapid peak flow than the situation of pre-development.

This amount of surface runoff is directly discharged in the existing drainage system, designed to collect and quickly transfer the runoff from urban areas, by sewer networks and water treatment facilities, to the receiving water bodies (Zhou, 2014). However, the existing drainage network, unable to manage this amount of runoff volume generated from extreme rainfall events, makes cities vulnerable to local flooding and combined sewer overflows (CSOs). The local urban flooding take place when during extreme rainfall events overload the urban drainage system (UDS), producing overflow from manholes onto surface streets. While the CSOs occurs when the wastewater treatment plant is unable to treat the wastewater delivered by the UDS, because the maximum treatment capacity is reached.

Therefore, the exceedances of sewage and wet weather flows are discharged directly into the receiving water bodies without receiving any treatment. For this reason, CSOs phenomena represents one of the major contributors to water pollution in rivers, lakes, etc. (Piro et al. 2019b).

In this context, it is detected the unsuitability of traditional UDS and starting from the assumption of Shishegar et al. (2018), whereby "stormwater management" refers to all the strategies for surface runoff control, water pollution mitigation, and ecosystem integrity restoration, an innovative and sustainable approach to manage the urban rainwater is necessary.

Thus, environmental sustainability has become a general goal of current urban water management (Marsalek et al. 2008) and there are several on-site management options that can be used in combination (Schreier et al., 2009).

1.2 Towards a Sustainable Urban Stormwater Management

To mitigate the environmental impact due to the combined effect of urbanization and climate change and overcome the unsuitability of the traditional drainage system, a transition towards an innovative, sustainable and resilient urban water management is required. In this regard, in the last years, nature-based approaches, that includes strategies for controlling stormwater by reusing unused public and residential areas, as rooftops, walls, car parks, and so on, have gained popularity.

These innovative sustainable urban stormwater management solutions include techniques known all over the world as: LID (Low Impact Development), BMPs (Best Management Practices), GI (Green Infrastructure), WSUD (Water Sensitive Urban Design), SUDS (Sustainable Urban Drainage Systems) and so on, all focused on the use of engineering or non-engineering practices, which share similar hydro-environmental processes to mitigate flooding risk, recharge groundwater, reduce air and water pollution, and other environmental issues (Fletcher et al., 2015, Mao et al., 2017; Zhang and Chui, 2018).

However, as stated in literature, BMPs mainly include engineering structural and non-structural practices, while LID and GI are more often related to urban macro-scale development systems, mainly implemented on site to control stormwater at source (Zhang and Chui, 2018).

In this dissertation, the term Low Impact Development "LID" will be used to consider a series of facilities whose aim is to replicate the site's pre-developed hydrological processes using system able to infiltrate, filter, store, evaporate, and detain runoff close to its source. Therefore, given their capability to mitigate urban surface runoff and their more environmentally characteristics, they can be easily integrated with the conventional drainage network or replaced to it in some situations.

However, although several studies demonstrated the LIDs' capability for surface runoff reduction (Gregoire and Clausen, 2011; Stovin et al., 2012; Garofalo et al., 2016; Bateni et al., 2019; Osheen, 2019), the transition towards sustainable urban stormwater management, that includes these techniques is very slow. One of the key scientific limiting factors can be found in the lack of comprehensive analysis able to highlight the hydrological performance and the physical processes involved in LID systems at multiple spatial scale and by considering long-term experimental data.

Moreover, the heterogeneity of the layers and materials that compose some LID systems - as green roof, green wall, rain gardens, permeable pavements, infiltration trenches - and consequently the complexity of the physical processes involved in each specific stratigraphy, require modeling tools able to accurately interpret their hydraulic behaviour, as well as to correlate their hydrologic efficiency with the management of stormwater in the surrounding urban area. In this regard, in literature several empirical, conceptual and mechanistic models have been proposed to simulate the hydraulic behaviour of some LID units, as well to evaluate the hydraulic effectiveness (Hilten et al., 2008; Kasmin et al., 2010; Stovin et al., 2012; Li et al., 2013; Garofalo et al., 2016; Brunetti et al., 2016; Peng and Stovin, 2017; Johannessen et al., 2019). Anyway, in some of these studies, the hydrological parameters (rainfall intensity, rainfall duration, antecedent dry weather period, runoff, etc.), as well as the physical ones (soil substrate hydraulic properties, soil depth, slope, etc.), which significantly affect the hydraulic efficiency of LID systems, are not evaluated in appropriate way. For instance, the hydraulic properties of the growing media, relevant element of some LID techniques (i.e green roof, green wall, rain garden and so on), are not generally investigate in a comprehensive way, limiting the analysis only to specific parameters, or by considering literature values for the numerical modeling. Furthermore, the availability of long-term hydrological (rainfall-runoff) monitored data recorded at a full-scale implementation represent another crucial factor that influence the analysis on the hydrological efficiency of these systems. Another key aspect

in the widespread of these solutions can be found in the lack of tools that evaluate the optimal integration of these systems with the conventional drainage network. Therefore, all these elements influence the analysis of the LID systems and contribute to limit their widespread at urban catchment scale.

1.3 Aims and structure of the Thesis

Based on the previous discussion, principal aim of this thesis is to present a comprehensive analysis of the hydrological efficiency of LID techniques by experimental investigation and numerical modeling. Therefore, this study tries to overcome the drawback factors previously identified as research gaps on the analysis of the hydraulic benefits of LID practices.

To achieve this main purpose several analyses were carried out by considering different: LID systems (rain garden, green roof, permeable pavement, rainwater harvesting system), spatial scales (full scale experimental site and urban/large scale), modeling tools (conceptual and mechanistic models), mathematical optimization approaches (Rough Set and Topsis method). Each case study, considered in this this thesis, allowed to investigate specific factors which affect the hydrologic/hydraulic behaviour of LID technique and to analyze the LID performances from the single scale units to large/urban scale implementation. Hydrological data monitored in full scale installation and laboratory measurements were used to support the numerical and modeling analysis. Some of these analyses have been already published in international peer-reviewed journals, books and indexed conference proceedings, annexed to this work.

In order to give an overview of this thesis and to show the relationship to the annexed papers, which are integral part of the work, the aim of each chapter is below specified. Anyway, this thesis presents not only the findings of the annexed papers, but also additional results, discussion and critical reflections and give a holistic overview of the entire context.

Following this chapter, *Chapter 2* is dedicated to an overview on the LID techniques, with specific reference to the practices considered in this dissertation. Therefore, all the papers annexed to this dissertation are linked with this chapter.

In *Chapter 3* are highlighted the most influential parameters in the development of a hydrodynamic model which combines a traditional drainage network and LID techniques, as rain gardens. To achieve this aim, a global sensitivity analysis (GSA), based on the Elementary Effect Test (EET), was applied to a PCSWMM hydrodynamic model of the University Campus Innsbruck. The findings in terms of the most influence parameters were considered as crucial factors in the investigation carried out in chapter 4, which is focused, as will be discussed then, on a full-scale LID implementation. Moreover, at the end of chapter 3 is also introduced a new concept of advanced LID Management Through a smart rain barrel, developed by considering microscale hydrodynamic of University Campus of Innsbruck. This chapter is connected to Paper I (Palermo et al., 2019a) and Paper IV (Oberascher et al., 2019).

If the previous chapter considers a real large scale case study in a Continental climate condition and it is finalised to obtain the most influential model parameters in a sustainable stormwater management system, *Chapter 4*, as briefly stated above, focuses on the analysis of the hydrological effectiveness of an experimental extensive green roof, located at University of Calabria (Italy) in Mediterranean climate region. More in detail, to investigate which parameter affects the hydrological response of the full-scale green roof, an in-depth empirical and modeling analysis is presented. Therefore, in this Chapter, which is linked to Paper II (Palermo et al., 2019b) and Paper III (Piro et al., 2019a), first an empirical analysis, based on one-year hydrological data collected on the experimental site was presented and then, a mechanistic model was used to evaluate the influence of the substrate depth on the hydrological efficiency of the specific LID practice. To achieve this last purpose and implement the model, based on findings obtained in the previous chapter, in terms of most influential LID model parameters that need to be evaluated in detail, the hydraulic properties of the soil substrate were measured in the Urban Hydraulic and Hydrology Laboratory (LIU) at University of Calabria (Italy) using a simplified evaporation method. Finally, a future research challenge in terms of smart optimization of the specific experimental site, connected to Paper V (Piro et al., 2019b) is here briefly presented.

Following this analysis, and based on the findings obtained at building scale, *Chapter 5* presents the analysis of hydrological effectiveness of LID systems at large-urban

scale, by modeling a highly urbanized area in south Italy under different LID conversion scenarios. In this regard, two LID systems, green roof and permeable pavement were considered for the numerical analysis carried out by the conceptual model PCSWMM. More in detail the model, here presented, can be considered as a predictive tool suitable to evaluate the effect of different LID conversion scenarios on the urban stormwater management. Given the unavailability of real flow data at the site specific, and to reduce the uncertainty, the model was developed by considering the data of drainage network, land use classification and land slope retrieved from design maps, while for the LID parameters, the green roof and permeable pavement, implemented at University of Calabria, whose soil hydraulic properties were previously evaluated in lab, were taken into account. The results of this chapter are linked to Paper VI (Palermo et al., 2020a).

By considering all of the findings, previous achieved by experimental and modelig investigation, it emerged that many aspects related to LIDs design and operation, as well as the choice of the facility and its location can affect the results in terms of hydraulic efficiency. In this regard, a mathematical optimization approach to consider several aspects together could be a suitable tool for designers of LID systems and experts in the field. Therefore, *Chapter 6* introduces the use of new Mathematical Optimization Approaches for LID techniques. To achieve this goal, TOPSIS (Technique for Order Preference by Similarity to Ideal Solution) and Rough Set method as Multi-Objective Optimization approaches by analyzing different case studies were considered. This methodology was applied to Rainwater harvesting system (RWH) whose results, reported in Paper VIII (Palermo et al., 2020b), are described in detail in this chapter. In addition, the same methodology was applied for LID practices selection, whose findings are reported in the annexed Paper IX (Pirouz et al., 2020).

Finally, *Chapter 7* states general conclusions, summarizes the novelty of this work and introduces recommendations for future studies.

1.4 References

Ahiablame, L. M., Engel, B. A., & Chaubey, I. (2013). Effectiveness of low impact development practices in two urbanized watersheds: Retrofitting with rain barrel/cistern and porous pavement. Journal of Environmental Management, 119, 151–161. https://doi.org/10.1016/j.jenvman.2013.01.019

Antrop, M. (2004). Landscape change and the urbanization process in Europe. Landscape and urban planning, 67(1-4), 9-26. https://doi.org/10.1016/S0169-2046(03)00026-4

Arnold Jr, C. L., & Gibbons, C. J. (1996). Impervious surface coverage: the emergence of a key environmental indicator. Journal of the American planning Association, 62(2), 243-258. http://dx.doi.org/10.1080/01944369608975688

Bateni, N., Lai, S. H., Putuhena, F. J., Mah, D. Y. S., Mannan, M. A., & Chin, R. J. (2019). Hydrological Performances on the Modified Permeable Pavement with Precast Hollow Cylinder Micro detention Pond Structure. KSCE Journal of Civil Engineering, 23(9), 3951-3960. https://doi.org/10.1007/s12205-019-2271-8

Brunetti, G., Simunek, J., Piro, P. (2016). A comprehensive numerical analysis of the hydraulic behavior of permeable pavement. J. Hydrol. 540, 1146–1161. https://doi.org/10.1016/j.jhydrol.2016.07.030

Fletcher, T. D., Shuster, W., Hunt, W. F., Ashley, R., Butler, D., Arthur, S., ... & Mikkelsen, P. S. (2015). SUDS, LID, BMPs, WSUD and more: The evolution and application of terminology surrounding urban drainage. Urban Water Journal, 12(7), 525–542. https://doi.org/10.1080/1573062X.2014.916314

Garofalo, G., Palermo, S., Principato, F., Theodosiou, T., & Piro, P. (2016). The influence of hydrologic parameters on the hydraulic efficiency of an extensive green roof in mediterranean area. Water, 8(2), 44. https://doi.org/10.3390/w8020044

Gregoire, B. G., & Clausen, J. C. (2011). Effect of a modular extensive green roof on stormwater runoff and water quality. Ecological Engineering, 37(6), 963-969. https://doi.org/10.1016/j.ecoleng.2011.02.004

Gunn, R., Martin, A., Engel, B., & Ahiablame, L. (2012). Development of two indices for determining hydrologic implications of land use changes in urban areas. Urban Water Journal, 9(4), 239–248. https://doi.org/10.1080/1573062X.2012.660957

Hilten, R. N., Lawrence, T. M., & Tollner, E. W. (2008). Modeling stormwater runoff from green roofs with HYDRUS-1D. Journal of hydrology, 358(3-4), 288-293. https://doi.org/10.1016/j.jhydrol.2008.06.010

Johannessen, B. G., Hamouz, V., Gragne, A. S., & Muthanna, T. M. (2019). The transferability of SWMM model parameters between green roofs with similar build-up. Journal of hydrology, 569, 816-828. https://doi.org/10.1016/j.jhydrol.2019.01.004

Kasmin, H., Stovin, V. R., & Hathway, E. A. (2010). Towards a generic rainfall-runoff model for green roofs. Water science and technology, 62(4), 898-905. https://doi.org/10.2166/wst.2010.352

Krebs, G., Rimpiläinen, U. M., & Salminen, O. (2013). How does imperviousness develop and affect runoff generation in an urbanizing watershed?. Fennia-International Journal of Geography, 191(2), 143-159. DOI: 10.11143/7794

Kundzewicz, Z. W., Radziejewski, M., & Pinskwar, I. (2006). Precipitation extremes in the changing climate of Europe. Climate Research, 31(1), 51-58. doi:10.3354/cr031051

Li, Y., & Babcock Jr, R. W. (2013). Green roof hydrologic performance and modeling: a review. Water Science and Technology, 69(4), 727-738. https://doi.org/10.1016/j.jhydrol.2008.06.010

Mao, X., Jia, H., & Shaw, L. Y. (2017). Assessing the ecological benefits of aggregate LID-BMPs through modelling. Ecological modelling, 353, 139-149. http://dx.doi.org/10.1016/j.ecolmodel.2016.10.018

Marsalek, J., Cisneros, B. J., Karamouz, M., Malmquist, P. A., Goldenfum, J. A., & Chocat, B. (2008). Urban Water Cycle Processes and Interactions: Urban Water Series-UNESCO-IHP (Vol. 2). CRC Press.

McDonald, R. I., Weber, K., Padowski, J., Flörke, M., Schneider, C., Green, P. A., ... & Boucher, T. (2014). Water on an urban planet: Urbanization and the reach of urban water infrastructure. Global Environmental Change, 27, 96-105. https://doi.org/10.1016/j.gloenvcha.2014.04.022

Osheen, Singh K.K.. (2019). Rain Garden—A Solution to Urban Flooding: A Review. In Sustainable Engineering (pp. 27-35). Springer, Singapore. https://doi.org/10.1007/978-981-13-6717-5_4

Peng, Z., & Stovin, V. (2017). Independent validation of the SWMM green roof module. Journal of Hydrologic Engineering, 22(9), 04017037. https://doi.org/10.1061/(ASCE)HE.1943-5584.0001558

Piro P., Turco M., Palermo S.A., Principato F., Brunetti G. (2019b) A Comprehensive Approach to Stormwater Management Problems in the Next Generation Drainage Networks. In: Cicirelli F., Guerrieri A., Mastroianni C., Spezzano G., Vinci A. (eds) The Internet of Things for Smart Urban Ecosystems. Internet of Things (Technology, Communications and Computing). Springer, Cham. https://doi.org/10.1007/978-3-319-96550-5_12

Schreier, H., & Marsalek, J. (2009). Innovative Stormwater Management in Canada. In Low Impact Development for Urban Ecosystem and Habitat Protection (pp. 1-10).

Shishegar, S., Duchesne, S., & Pelletier, G. (2018). Optimization methods applied to stormwater management problems: a review. Urban Water Journal, 15(3), 276–286. https://doi.org/10.1080/1573062X.2018.1439976

Shuster, W. D., Bonta, J., Thurston, H., Warnemuende, E., & Smith, D. R. (2005). Impacts of impervious surface on watershed hydrology: A review. Urban Water Journal, 2(4), 263-275. https://doi.org/10.1080/15730620500386529

Stovin, V., Vesuviano, G., & Kasmin, H. (2012). The hydrological performance of a green roof test bed under UK climatic conditions. Journal of hydrology, 414, 148-161. https://doi.org/10.1016/j.jhydrol.2011.10.022

Zhang, K., & Chui, T. F. M. (2018). A comprehensive review of spatial allocation of LID-BMP-GI practices: Strategies and optimization tools. Science of the total environment, 621, 915-929. https://doi.org/10.1016/j.scitotenv.2017.11.281

Tang, Z., Engel, B. A., Pijanowski, B. C., & Lim, K. J. (2005). Forecasting land use change and its environmental impact at a watershed scale. Journal of Environmental Management, 76(1), 35–45. https://doi.org/10.1016/j.jenvman.2005.01.006

Zhou, Q. (2014). A review of sustainable urban drainage systems considering the climate change and urbanization impacts. Water, 6(4), 976-992. https://doi.org/10.3390/w6040976

Zhou, L., Wu, Y., Woodfin, T., Zhu, R., & Chen, T. (2018). An Approach to Evaluate Comprehensive Plan and Identify Priority Lands for Future Land Use Development

to Conserve More Ecological Values. Sustainability, 10(1), 126. https://doi.org/10.3390/su10010126

Chapter 2 – Low Impact Development techniques: an overview

In this chapter an overview of Low Impact Development (LID) systems is presented. Starting from a general introduction on these techniques, an in-depth description of some practices, analyzed during the PhD project, is discussed. More in detail, this chapter is conceived and structured by considering principally the literature review carried out in all papers annexed to this dissertation and by adding other information and discussion. Therefore, first a general introduction on LID systems, linked to Paper IX (Pirouz et al., 2020), is presented; following this general section, sub-chapters on green roof, rain garden, green wall, permeable pavement and rainwater harvesting, partially related to Paper II (Palermo et al., 2019b); Paper VII (Palermo & Turco, 2020); Paper VIII (Palermo et al., 2020b) are exposed. Each practice is here first reviewed by analyzing the general design features and then the hydrological effectiveness is discussed by considering modeling and experimental results found in literature.

2.1 Low Impact Development (LID) techniques

Low Impact Development (LID) techniques are sustainable small-scale units, which providing several benefits at multiple scales (Zischg et al., 2018), are able to mitigate the environmental impacts caused by the combined effect of urbanization and climate change. In this regard, these systems are able to: improve biodiversity and wildlife community structures; reduce energy consumption, by increasing energy and cost savings for heating, cooling, and irrigation; mitigate urban heat island effects; restore water quality of the receiving water bodies; improve air quality, by enhancing carbon sequestration through preservation and planting of vegetation; reserve ecological and biological systems; enhance quality of life for inhabitants (Dietz, 2007; Ahiablame et al., 2012; Karteris et al., 2016).

Specifically, from a hydraulic point of view, LID techniques can be considered as an emerging stormwater management philosophy (Eckart et al., 2017) whose main purpose is to infiltrate, filter, store, evaporate, and detain runoff close to its source (Piro et al., 2019b). Therefore, their implementation in an urban area can create a complex system of temporal storage facilities for managing stormwater runoff (Palermo et al., 2019a), as well as favour consistent dry weather flow (baseflow) through groundwater recharge.

As reported in Ahiablame et al. (2012), these sustainable systems can provide several benefits correlated to hydraulic efficiency. They can: (i) integrate stormwater management approaches during the planning phase; (ii) manage the stormwater close to the source through small-scale units; (iii) encourage environmentally sensitive design; (iv) create a hydrologic multifunctional landscape; (v) prevent rather than mitigate and remediate; (vi) decrease construction and maintenance costs of drainage networks; (vii) promote public education and participation for environmental protection.

In recent years, the implementation of these sustainable solutions has attracted widespread interest from researchers, urban planners, and city managers (Jia et al., 2015) and several studies have been devoted to LID design, benefits, and simulation models to simulate their hydraulic efficiency in terms of urban flooding risk reduction (Elliot and Trowsdale, 2007; Jia et al, 2012; Zahmatkesh et al., 2014; Eckart et al., 2017; Mao et al., 2017; Zhang et al., 2018).

However, although their benefits at urban scale are largely recognised, as pointed out by Eckart et al. (2017), the main factors affecting LID performance can be summarized in the location dependencies of LID, rainfall and climate conditions. In agreement with the authors, in fact, the appropriate design of LID is affected by the site location in terms of

soil type/conditions, plants, rainfall regime, land use types and other meteorological and hydrological properties. In addition, the optimal selection and placement of LID is one of the most key components to consider for achieving the maximum efficiency at the minimum cost.

In this regard, in order to evaluate the hydraulic behaviour of some of these sustainable solutions, the analysis of the main design construction features is crucial, and, therefore, they will be discussed in the following sections.

2.2 LID types and design features

LID alternatives can be generally classified in two main categories (Fletcher et al., 2013; Eckart et al., 2017):

1. *Infiltration-based techniques,* whose main contribute is the restoration of base-flows through the subsurface flows and groundwater recharge.
2. *Retention-based techniques,* that can retain stormwater, by reducing runoff.

Based on this principal classification, swales, infiltration trenches, rain gardens, basins, sand filters, and permeable pavement belong to the first group. While ponds, wetlands, green roofs, green wall and rainwater harvesting are the most common retention-based techniques.

Starting on these main classification, the Ph.D project was focused on the analysis of some of these techniques, more specifically: green roof, green wall, rain garden, permeable pavement, rainwater harvesting systems. In this regard, more detail on the design features of each of these systems will be discussed in detail in the following sections. Green Roof, Green Wall and Rainwater Harvesting sections are linked to Paper II (Palermo et al., 2019b), Paper VII (Palermo & Turco, 2020), Paper VIII (Palermo et al., 2020b).

2.2.1 Green Roof

Green Roof (GR) by exploiting otherwise unused spaces, such as the roofs of the building, are particularly beneficial in densely built urban areas (Wang et al., 2017).

They represent a source of stormwater runoff mitigation by reducing the total runoff volume, peak flow rate, and delaying peak discharge time into the combined sewer systems (Voyde et al., 2010; Stovin et al., 2012; Garofalo et al., 2016).

GRs, which incorporate both the natural environment and engineered systems, offer a wide range of other benefits, including an enhancement of water quality, reduction in the building energy demand, attenuation of urban heat islands, decrease in air pollution and noise levels in urban spaces, increase in the building's aesthetic value, and wildlife and biodiversity growth (Vijayaraghavan, 2016; Pęczkowski et al., 2018; Bevilacqua et al., 2018; Santamouris, 2014; Rowe, 2011; Yang et al., 2012).

As an engineering system, green roof is composed of different components (Figure 2.1) including: growing substrate covered with vegetation, a filter layer, a drainage layer, a protection layer, a root barrier and a waterproofing membrane (Berndtsson, 2010; Vila et al., 2012; Vijayaraghavan and Raja, 2014; Hashemi et al., 2015).

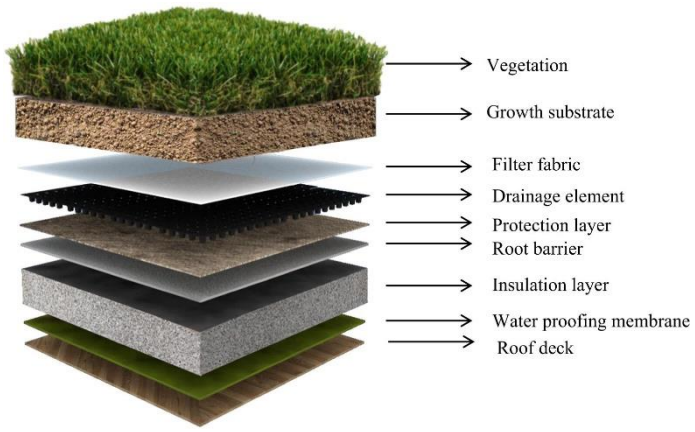

Figure 2.1: Green roof components (Vijayaraghavan, 2016).

Due to is for this specific configuration that green roofs technology can be considered as sustainable tool for stormwater runoff mitigation. The hydrological process operating within the green roof starts with the rainfall interception by the vegetation cover and proceeds with the infiltration of water in the soil substrate, where a part of the retained volume evaporates from the soil or is used by plants and a portion evapotranspires. The remaining portion passes through the filter layer and enters in the drainage elements, where water is detained. When the drainage space is completely utilized, the overflow drains out (Stovin et al. 2012, Vijayaraghavan, 2016).

Many studies agree on the classification of GRs into two main categories: extensive and intensive, which differ from each other regarding the depth of soil layer and vegetation.

Generally, extensive GRs have a thin soil layer of less than approximately 15 cm, whereas intensive soil layers exceed this value; shallow rooting and drought-resistant plants are used for the extensive GR, whereas deeper rooting plants are used for the intensive GRs. Therefore, due to its characteristics, the extensive GR is lighter, cheaper, and requires less maintenance than the intensive one. In addition, there is a semi-intensive green roof, that is a combination of the extensive and intensive types (Buccola et al., 2011; Krebs et al., 2016; Carson et al., 2013; Raji et al., 2015; Besir and Cuce, 2018). A schematic classification of green roofs according to type of usage, construction factors and maintenance requirements as reported in Raji et al. (2015) is shown in Figure 2.2.

Maintenance	Low	Periodically	High
Irrigation	No	Periodically	Regularly
Plant communities	Moss-Sedum-Herbs and Grasses	Grass-Herbs and Shrubs	Lawn or Perennials, Shrubs and Trees
System build-up height	60 - 200 mm	120 - 250 mm	150 - 400 mm on underground garages > 1000 mm
Weight	60 - 150 kg/m^2	120 - 200 kg/m^2	180 - 500 kg/m^2
Costs	Low	Middle	High
Use	Ecological protection layer	Designed Green Roof	Park like garden

Figure 2.2: Classification of green roofs according to type of usage, construction factors and maintenance requirements (Raji et al., 2015).

As reported in Garofalo et al. (2016), the hydraulic efficiency of the green roof in terms of water retention capacity is affected by:

- the *physical features of the green roof*, i.e. number of layers and materials, soil type and thickness, type of vegetation and percentage of roof covered, roof geometry;

- *the weather conditions,* i.e length of antecedent dry weather period, season/climate, characteristics of rain event like intensity and duration.

2.2.2 Green Wall

Green wall techniques, generally mentioned also as vertical greening/greenery systems, vertical garden, or bio-walls (Manso and Castro-Gomes 2015) represent one of the LID solutions able to increase the green spaces in urban area obtaining beneficial effects from the building to the urban scale. Specifically, at building scale, by optimizing the benefits of plants species, they can be considered passive design solutions which improve thermal comfort both in winter and summer, thereby reducing energy demand for heating and cooling (Wong et al., 2010; Perini et al., 2017). In addition, the implementation of a green wall increases the value of the real estate and allow sound insulation; while at urban scale, these systems can enhance air quality, urban biodiversity, mitigate urban heat island effect (Hadba et al., 2017; Francis and Lorimer, 2011). They represent also a control source of stormwater management at urban catchment scale (Lau and Mah, 2018). Moreover, from a social point of view, the implementation of vegetation on facades improve cities image and wellbeing, favouring the fruition of them (Sheweka and Magdy, 2011).

Although this system have gained popularity during the last years, their first applications can be found 2500 years ago in the hanging Gardens of Babylon; similar examples were also in the Roman Empire. Several applications occurred over the centuries, until the 19th century, when these techniques were used in several European and North America cities, as ornamental elements and for thermal purposes (Manso and Castro-Gomes, 2015; Dunnett and Kingsbury, 2008; Baran and Gültekin, 2018).

Nowadays, with “green wall” we refer to a vegetative system which is generally developed along the façade of a building consisting of different components, and it can be directly attached on the wall or supported by a structure (Manso and Castro-Gomes, 2015; Baran and Gültekin, 2018).

The general functional elements of green wall technique are: (i) supporting elements; (ii) growing media; (iii) vegetation; (iv) drainage; and (v) irrigation. As reported in Manso and Castro-Gomes (2015), based on the features of these elements and on the presence or absence of some of them, the green wall systems can be subdivided into two

macro-categories: Green Facades (hereafter named GFs) (Figure 2.3) and Living Walls (hereafter named LWs) (Figure 2.4).

The Green Facades (GFs) are characterized by a low systemic technology, few constituent elements, and a limited level of integration between plants and walls. They are light, easy to install and generally aimed at supporting the natural development of plants. The plants, mainly climbing, can have evergreen foliage or deciduous, and reach until 25 m of height, taking, however, some years for the full coverage of the wall (Manso and Castro-Gomes, 2015).

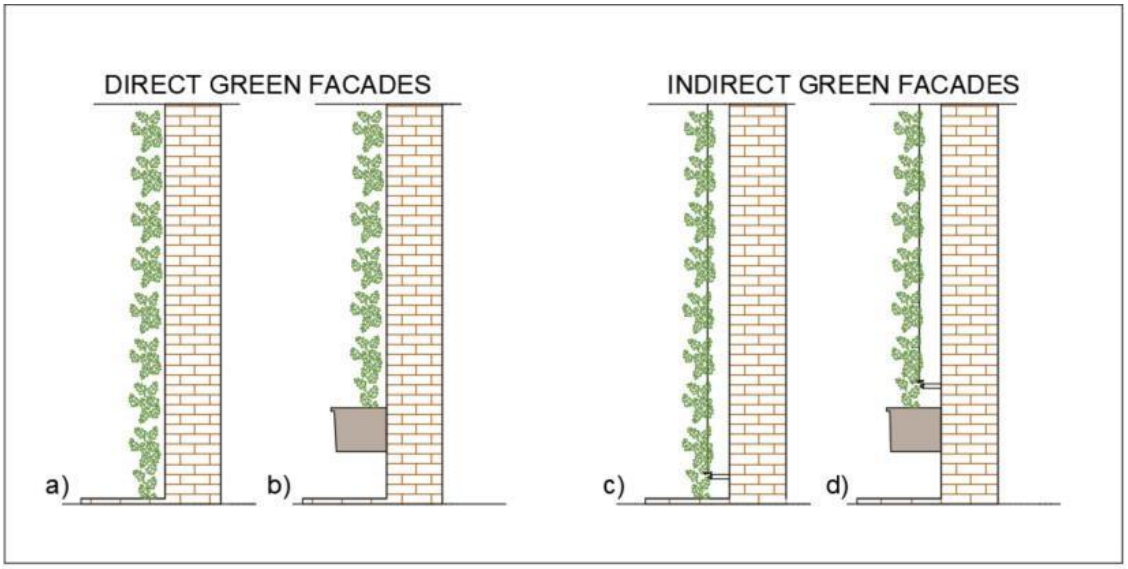

Figure 2.3: Different types of Green Facades: (a) Direct Green Facade with vegetation planted into the soil; (b) Direct Green Facade with plants rooted in the box; (c) Indirect Green Facade with vegetation planted into the soil; (d) Indirect Green Facades with plants rooted in the box. (Palermo & Turco, 2020).

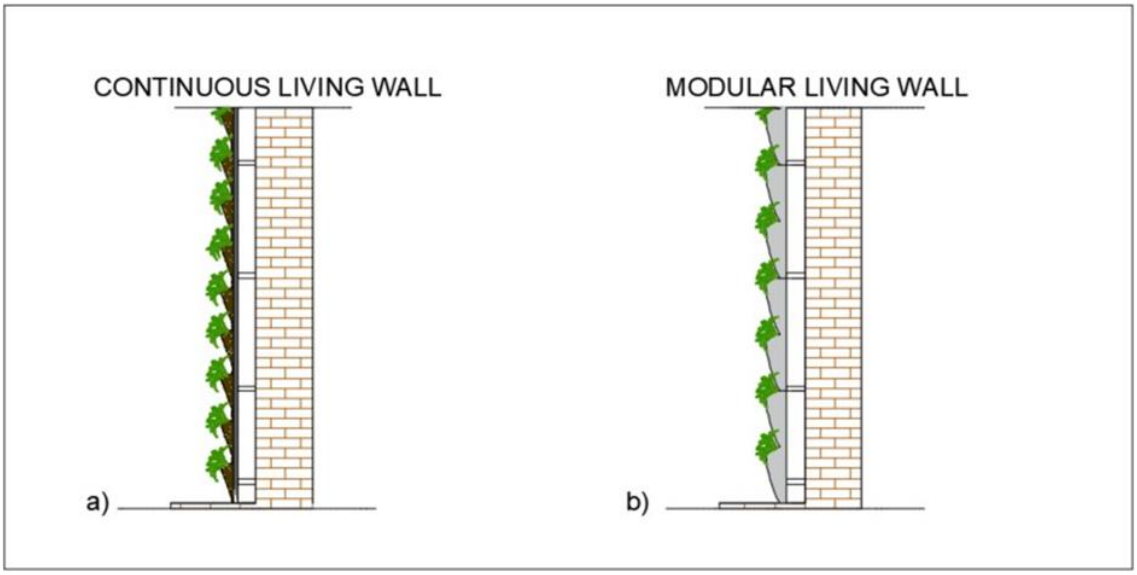

Figure 2.4: Different types of Living Walls: (a) Continuous Living Wall; (b) Modular Living Wall (Palermo & Turco, 2020).

The Living Walls (LWs), allowing the rapid coverage by vegetation of high building, represent a more recent innovation than the green facades. These types of green wall can use a wide variety of plants species (grasses, perennial plants, shrub, succulent, and so on), selected according to the climate condition, the drought tolerance, the root development, and specifically combined to achieve aesthetic effects Manso and Castro-Gomes, 2015).

More detail on the construction features of each types of green wall can be found in the annexed Paper VII (Palermo & Turco, 2020).

From the literature review, carried out in the annexed paper, it is emerged that, although these systems, like green roofs or rain gardens, can be valuable engineering solutions to reduce the stormwater discharged into the drainage systems, they were little investigated from this perspective. In this regard, only a study, carried out by Lau and Mah (2018), was found.

2.2.3 Rain Garden

Rain Gardens (RGs) or bioretention systems, were first coined for residential use by Dick Brinker in 1990 in Prince George's County, Maryland, as an alternative to the conventional ponds has acquired significant attention in the last decades (Malaviya et al., 2019; Osheen, 2019).

This LID technique is a vegetated depression that collects runoff discharged from the much-larger surrounding impervious areas (generally 1:10 – 1:20), as roof area or a car parks (Aravena & Dussaillant, 2009).

The conventional structural configuration of a RG generally consists of (i) *ponding area*, (ii) *inflow structure* and (iii) *outflow structure* (Katsifarakis, 2015; Basdeki et al., 2016; Malaviya et al., 2019).

The ponding area is a natural or artificial ground depression, with a porous soil medium layer, a surface mulch layer, and vegetation (Prince George's Country 2012) (Figure 2.5). More in detail, first the top of the ponding area is filled with mulch layer and then the top soil is added. In addition, when the RG is located in area with a soil of low permeability, thus the water infiltration rate in the underlying is not adequate, a gravel layer is put on bottom, or un under-drain pipe can also be used for the same purpose. The vegetation, that can consist of small plants, shrubs, trees, perennials, ferns, grasses and

groundcover species, preferably native plants, has a very crucial function to hold the soil, filter the pollutants and make the rain garden aesthetically pleasing. Therefore, the correct choice of vegetation influences the hydraulic efficiency of the system (Osheen, 2019; Malaviya et al., 2019.

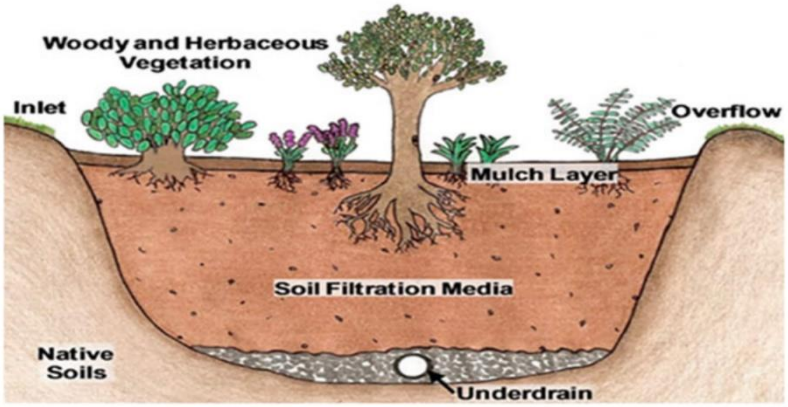

Figure 2.5: Schematic of a typical rain garden (Osheen, 2019).

The inflow or inlet structure provides to directly discharge of the runoff from the surrounding area (streets, sidewalks, etc.) into the ponding area. It can be a drain pipe, a hard surface or a grass strip. *While the overflow or outlet structure,* generally linked to the sewerage system, provides to discharge the water that exceed the ponding capacity of the rain garden (Katsifarakis, 2015; Malaviya et al., 2019; Osheen 2019; Robinson et al., 2019).

For highly engineered rain gardens, the excavated depression is covered by geotextile then protected by media that increase the roughness with depth (Ishimatsu, 2017).

Given this specifically structural configuration, RGs limit the discharge of water from impermeable surfaces to the drainage network, using the natural processes of storage, infiltration and evapotranspiration. These systems, favoring runoff infiltration and short-time storage, contribute to total runoff reduction as well as its peak (Katsifarakis et al. 2015; Siwiec et al., 2018).

The main hydrological processes occurring inside a RG during a storm event are: the retention of stormwater within the substrate's micropores until the field capacity is reached; the evapotranspiration of a portion of retained water; the increasing the soil moisture towards saturation once the media reached field capacity and any subsequent rainfall will fill the larger pores. Typically, RGs are designed to allow ponding to occur once the saturation reaches the surface. In addition, if the RG is unlined, the exceeding

moisture will be returned to the ground via infiltration, while if it is lined it is discharged into the linked sewer system. Therefore, as other LID infrastructures, like green roof, in a RG the stormwater control occurs by retention processes, i.e. the reduction of the runoff volume, that will be upper for a longer antecedent dry weather period (ADWP) and detention, i.e. delay and attenuation of the runoff hydrograph (Yuan et al., 2017).

Based on this hydrological processes, the capacity of a rain garden to infiltrate water is affected by the hydraulic properties of growing media (i.e. initial water content, capillary suction, saturated hydraulic conductivity, and pressure head from the ponded water), as well as the site-specific properties (catchment area and slope, surface types, and the time of concentration) (Siwiec et al., 2018).

As other LID techniques, RGs can provide several other benefits in addition to the stormwater quantity runoff control as: restore groundwater recharge; improve the water quality by filtering pollutants from stormwater runoff; increase air quality, by capture and storage CO2; reduce noise pollution; mitigate local climate; enhance biodiversity and visual amenity; favour pollination (Dietz & Clausen, 2005; Yang et al., 2009; Siwiec et al., 2018).

The widespread of this LID system is also justifying because RG are easy to install, inexpensive and require little maintenance after installation (Aravena & Dussaillant 2009).

2.2.4 Permeable Pavement

Permeable Pavement (PP), also called porous or pervious pavement is a paving structure which allows stormwater runoff to be infiltrated and conveyed through its material matrix (Drake et al., 2013).

It is one of the most widely used LID type as an alternative engineering infrastructure for pedestrian and/or vehicular traffic (pathways, driveways, parking lots and access roads). It is suitable for urban stormwater management and mitigate the problems caused by conventional road development (Scholz & Grabowiecki, 2007; Elizondo-Martínez et al., 2019; Turco et al., 2019).

PP system consist of a permeable paving surface as well as layers of coarse aggregate materials that function as reservoir, providing storage capacity during precipitation events (Drake et al., 2013). Generally, as reported in Figure 2.6, a typical PP consist of: a wear layer, a bedding layer, a base layer, a sub-base layer and un underdrain

(as required). Other components commonly used in the design of PP systems are geotextiles, and small aggregate filter or choker courses.

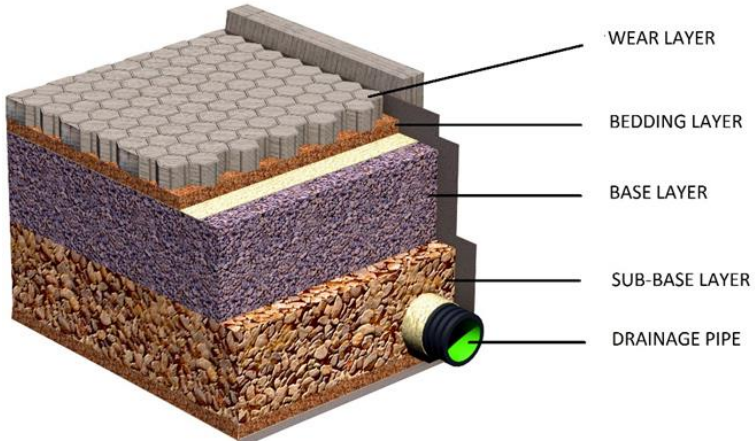

Figure 2.6: Cross section of a Permeable Pavement (Piro et al., 2019b).

The implementation of base layer and a sub-base layer, as the wear layer, is due to the structural integrity of the pavement system and it is strictly related to the traffic load. In this regard, one of the main principle construction design is that underlying layers distribute the concentrated loads from wheels below the road. Thus, traffic loads affect the choice of layers' thickness and the type of materials to be used (Knapton et al. 2012; Kellagher et al., 2015).

Different types of surface materials are commonly used for PP development, and based on the choice of the surface paving material, it is possible to classified different type of PPs. More in detail the top layer of the PPs can be monolithic (porous concrete/asphalt) or modular forms (interlocking porous concrete pavers and plastic grid) (Palla et al. 2015).

Based on the most commercially materials, PP can be classified in: Permeable Interlocking Concrete Pavers (PICPs), Pervious Concrete (PC), Porous asphalt (PA), Grass grid pavement.

- The *Permeable Interlocking Concrete Pavers (PICPs),* consisting of modular units separated by joint filled with open-graded aggregate, are generally used for pedestrian areas, pathways, car parks, private driveways.
- The *Pervious Concrete (PC),* generally used for car parks, and lightly trafficked roads, can be implemented as an independent surface or to improve structural stability at the base of PCIP in case if frequent traffic by heavy vehicles.

- The *Porous asphalt (PA)*, used for pedestrian areas, car parks, private driveways, and lightly trafficked roads, it is also able to reduce traffic noise and can be set as an independent surface or to provide a stronger base to PICP. For these two last types, the binding agent covers the aggregate particles without filling the voids between the particles.
- The *Grass grid pavement*, generally implemented for leisure facilities car parks, private driveways, and office car parks, it is an eco-friendly type of PP most suitable for lightly trafficked locations, where the grass usually is reinforced with plastic or concrete grids.

More details on this different types can be found in Drake et al., (2013) and Kuruppu et al., (2019).

As infiltration-based LID technique, the main operating principle in a PP is to collect, infiltrate, and eventually treat, the surface stormwater runoff. Moreover, if the infiltration into native soils is allowed, this system increase the groundwater recharge, otherwise the treated runoff is direct discharged into the receiving water bodies.

Given its hydrologic behaviour several studies have shown the efficiency of PPs in reducing surface runoff and peak flow, as well as delaying time to peak (Al-Rubaei et al., 2013; Lin et al., 2016; Kuruppu et al., 2019). This hydraulic efficiency, strongly correlated to the evaporation, drainage and retention process, is mainly influenced by the particle size distribution of the bedding material, and by the retention of water in the surface blocks (Marchioni & Becciu, 2015; Alsubih et al., 2017; Turco et al., 2017).

2.2.5 Rainwater Harvesting System

Rainwater Harvesting (RWH), considered an ancient practice used all over the world to meet the water demand, is now supported by many countries as a suitable solution to limit potable water demand, reduce frequency, peaks and volumes of stormwater runoff at the source, and contribute to the restoration of natural hydrological cycle (Petrucci et al., 2012; Amos et al., 2016; Campisano et al., 2017; Palla et al., 2017;).

The principal component of a conventional RWH system (Figure 2.7) is the rainwater tank which temporally stores the water from a capturing surface, normally the building roof or others impervious surfaces closely to the building. In a single-family

building, aboveground tank, named "rain barrels", are generally used for irrigation and runoff control, while, in the case of multi-story building, above or below-ground concrete cisterns are implemented. In addition, a system consisting of gutters and downspouts lead the runoff from the collecting surface to the tank, while a dedicated piping network is needed for rainwater reuse. One or more pumps can be used to guarantee the pressure head for different usages, while other devices as first flus diverters, debris screen, and filters are generally implemented for water quality control. These information and more specific detail regarding this technique can be found in several studies (Campisano et al., 2017; Herrmann & Schmida, 2000; GhaffarianHoseini et al., 2016).

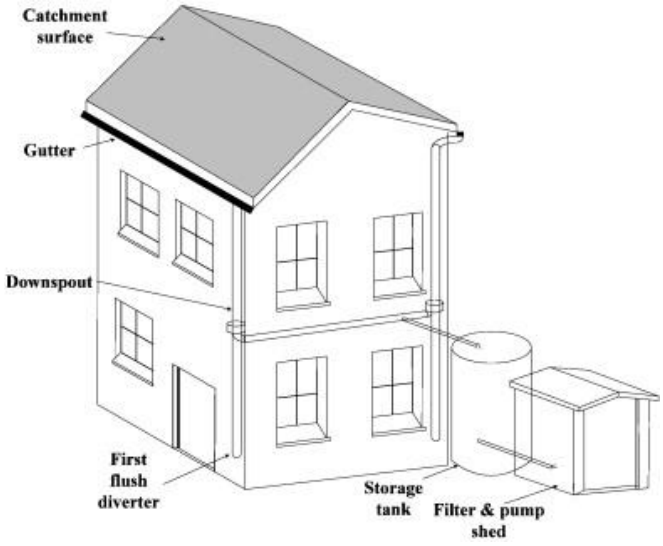

Figure 2.7: Principal components of a rainwater harvesting system (Li et al., 2010).

Recent advances have showed the possibility for real-time monitoring and control of these systems in order to increase their efficiency in terms of reduction of urban flooding or combined sewer overflows (Oberascher et al., 2019) and optimize the rainwater reuse.

Harvested rainwater can be considered a renewable water source that is perfect for different non-potable water uses, as toilet flushing, laundry, car washing, terrace cleaning, private garden irrigation and green roof irrigation (Herrmann & Schmida, 2000; Li et al., 2010; Campisano and Modica, 2015; Jones & Hunt, 2010; Domènech & Saurí, 2011; Cipolla et al., 2018; Piro et al., 2019)

In addition, as source control technology distributed at urban catchment scale, these systems are suitable to reduce stormwater runoff volume. In this regard, several studies have evaluated also the hydrological efficiency of RWH in terms of reduction of the runoff

volume and peak discharged to the sewer system (Palla et al., 2017; Herrmann and Schmida, 2000; Campisano & Modica 2015; Becciu et al., 2018).

Several studies have been carried out to analyze the RWH efficiency for water saving and runoff mitigation. In this regard, Campisano & Modica (2015) have showed that the RWH's performance depends of site-specific factors, such as roof type and surface, precipitation regime, demand usage, tank size, number of people in the household, etc.

2.3 Hydrological Effectiveness of LID systems

So far several studies have demonstrated the efficiency of LID techniques on urban stormwater runoff mitigation by experimental investigation and modeling analysis.
In this regard, a general overview on the studies which analyzed the hydrological effectiveness of the LID systems, whose design features were described in the previous section, is here presented by considering one LID techniques at time.

Therefore, in this overview the first LID technique that it will be considered is the green roof (GR) system. Many studies have shown the beneficial effects of GR in delaying the peak flow rate and reducing the runoff volume discharged into the combined sewer systems (CSSs) (Simmmons et al., 2008; Voyde et a., 2010; Stovin et al., 2012; Gromaire et al., 2013; Cipolla et al., 2016; Liu et al., 2019).

In this regard, Li & Babcock (2014) in their reviewer paper have showed that laboratory experiments and field measurements have demonstrated that green roofs are able to reduce stormwater runoff volume by 30% to 86%, reduce peak flow rate by 22% to 93% and delay the peak flow by 0 to 30 min.

Moreover, by the analysis of several studies carried out on the green roofs, it emerged, as reported in a previous study (Garofalo et al., 2016), that the hydraulic efficiency of a green roofs could be expressed by the runoff coefficient, evaluated as the ratio between the total runoff depth delivered from the green roof and the total rainfall depth. The analysis of this coefficient, strongly influenced by the storm events features, as well as by the geometrical characteristics of the green roof, is crucial for designing purposes and, therefore, it has to be properly defined. In this regard, in Garofalo et al., (2016) was carried out a summary of the subsurface runoff coefficient values found in literature (Table 2.1) by observing that it ranges between around 0.30 and 0.90.

Table 2.1: Subsurface runoff coefficient found in the literature studies for green roof (Garofalo et al., 2016).

References	*Climate Condition and Location*	*Subsurface runoff coefficient*
Carter and Rasmussen (2006)	*Humid sub-tropical – Athens (GE)*	0.38
Uhl and Schiedt (2008)	*Continental – Muenster (DE)*	0.32
Palla et al. (2010)	*Mediterranean – Genova (IT)*	0.48
Voyde et al. (2010)	*Sub-tropical – Auckland (NZ)*	0.34
Stovin et al. (2012)	*Temperate – Sheffield (UK)*	0.48
Gromaire et al. (2013)	*Temperate – Trappes (F)*	0.36 - 0.50
Locatelli et al. (2014)	*Ocean - Odense and Copenaghen (DK)*	0.43 - 0.68
Wong and Jim (2014)	*Humid sub-tropical – Hong Kong (CN)*	0.86 - 0.89

In addition to these studies others experimental works have been considered in this dissertation.

In 2008, in Muenster, DE, Uhl & Schiedt (2008) have presented the results of a monitoring campaign, carried out on 18 green roofs installed on a roof of 500 m^2, obtaining an average annual runoff coefficient of 32%.

In an another study, Lee et al., (2013), by considering extensive green-roof of 0.5 m (W) x 0.5 m (L) x 0.2 m (H), built in the laboratory for different rainfall events in Korea, have obtained a high water-retaining capacity response to rainfall of less than 20 mm/h.

While, in Australia, Razzaghmanesh & Beecham (2014) have evaluated the potential of green roofs as a source control device by considering 4 medium size green roof beds over a 2-year period. From the 226 rainfall events considered, representative of the Adelaide climate, they obtained an average retention coefficient of around 89% for intensive systems and of 74% for extensive ones.

Moreover, Stovin et al., (2015) have analyzed 4 years of rainfall and runoff data from a set of 9 parallel green roof test beds located in Sheffield, UK. They obtained a retention major than 80% for rainfall event less than 10 mm of precipitation depth, but considerably lower for rainfall depth greater. While, on average, for 65% of events with precipitation more than 5 mm the test beds retained the first 5 mm of rainfall.

While Nawaz et al. (2015) have analyzed the hydrologic performance of a full-scale extensive green roof in Leeds (UK) in temperate climate condition, considering 30 individual rainfall events individuated in a record dataset over a period of 3 years (2012–2014). The results showed that the green roof presented a mean retention value of 66%.

By the analysis of the state of art about the experimental results obtained on the green roof, it emerged that, while many studies have analyzed the hydrological

performance (runoff coefficient, runoff retention, peak flow reduction, peak flow lag-time) at seasonal and annual scales, only few have evaluated it at event-scale.

Moreover, despite the recognised hydrological benefits of green roof, literature studies that investigate their hydrological performance at full-scale implementation and for a long term monitoring period are less than those one carried out in lab or by test beds.

Finally, the complexity of the physical processes involved in green roof's stratigraphy, confirmed in all studies, require a properly investigation the soil hydraulic parameters that affect the hydraulic behaviour of such LID system.

Thus, this thesis, in the specific chapter related to the green roof case study, will overcome all of these issues by presenting a long-term analysis on the hydrological efficiency of a real full-scale experimental green roof, located at University of Calabria in Mediterranean Climate, carried out by considering field monitored hydrological data, as well as soil hydraulic properties evaluated in lab, and a modeling analysis.

While by the analysis of the state of art on the green wall systems, showed in Paper VII (Palermo & Turco, 2020), annexed to this dissertation, was found that in recent years numerous new applications have encouraged the growth of Green Wall techniques as an energy saving tool.

However, although these systems can also be considered valuable engineering solutions to reduce stormwater runoff discharged into drainage systems, it is emerged that green wall systems are little studied in this direction.

In this regard, only one study, conducted by Lau and Mah (2018), assessed the hydrological effectiveness of green walls, developing a USEPA SWEP model, which considers the green wall system as part of the urban drainage system. More in detail, the study is based on a modeling implementation of a modular system of green walls on the Central City commercial building, Kota Samarahan. The authors performed 4 simulation models, characterized by different conditions (soil texture classes: sand, clay sand, sandy clay and clay) and precipitation inputs. The results confirmed that green wall systems can be considered to reduce surface runoff.

Considering now the Rain Gardens (RGs) systems, from literature it is detected that even if they have been recognized as an effective LID technique for reducing stormwater runoff through the retention and infiltration processes, however so far their field

performance and regional effect have not been comprehensively investigated (Malaviya et al., 2019).

However, some studies have evaluated the rain gardens efficiency in terms of flow retention. In this regard, Hunt et al. (2008) have obtained that rain gardens can achieve about 46–100% flow reduction, depending by seasonal difference and stormwater characteristics.

In another study, Davis (2008) have found, by observing two bioretention cells for 49 runoff events in 2 years, mean peak reductions of 49% and 58% for the two cells, as well as significantly delayed of the flow peaks.

While Hatt et al. (2009), have observed different rain garden, obtaining peak flow reductions between 49% and 80%.

Recently, Li et al., (2018), by a modeling analysis at large scale, have obtained an overflow reduction rate between 6.74% to 65.23%.

Another study, conducted by Zhang et al. (2019) in Kyoto, Japan, has a shown a favourable storage/infiltration functions in two rain gardens, with a stormwater runoff control of more than 60%.

Permeable Pavement (PP) system, as green roof, is one of the most investigated LID techniques. In this regard, a large number of studies, conducted on its water quantity performance, have shown the capability of this technique for surface runoff reduction, peak flow attenuation and peak flow delay.

Collins et al., 2008, evaluating the performance of 4 types of PP and standard asphalt in eastern North Carolina, have obtained that for rainfall intensity of 25 mm/h, PP achieve 40–50% runoff volume reduction and about 90% of peak runoff attenuation.

Ball & Rnakin (2010), have found that the generation of surface runoff from the PP required a rainfall intensity exceeding 20 mm/h.

In another study, Alam et al. (2019) have examined the hydrologic performance of three different permeable pavement designs, observing a percentage of peak flow mitigation of 31–100%. Moreover, the Porous Concrete Pavement (PCP) was the most satisfactory in reducing surface runoff.

While, Vaillancourt et al. (2019) in their study obtained, in one of the 5 monitored sites, where rainfall and runoff were monitored for 12 months, peak flow delays ranging from 4 min to 4 h 42 min and runoff reductions ranging from 26% to 98%, depending on the rainfall event.

Finally, as last LID technique, considered in this overview, the Rainwater Harvesting (RWH) systems, as reported in Petrucci et al. (2012), have been evaluated from the researchers not only for their water saving aims, but also for their contribution to control stormwater runoff at the source by providing distributed retention storage at large scale.

In this regard, Campisano and Modica (2015) have evaluated the retention potential for roof runoff peak reduction of RWH system for single household. They observed that significant reduction of the peak depends on the tank size and on the water demand pattern. For a tank size (with a storage fraction s = 5), a peak reduction ranging between 30 – 68% for at least half of the considered events was obtained.

In another study Palla et al. (2016) have evaluated the hydraulic efficiency of domestic rainwater harvesting system at urban bock scale, achieving an average peak and volume reduction of 33% and 26% percent respectively by considering 2125 rainfall events.

A comprehensive review on this system was did by Campisano et al. (2017).

Through the literature review it emerged that several models on LID systems have been proposed, most of them focused on simulating the hydraulic/hydrologic behaviour of the single system other assessing the efficiency at urban-large scale (Hilten et al., 2008; Jia et al., 2012; Palla & Gnecco, 2015; Garofalo et al., 2016; Brunetti et al., 2016; Peng and Stovin, 2017; Li et al., 2019).

In this regard, as reported in Brunetti et al., (2017), three different categories of LID models can be classified: (1) *empirical model*, based on direct observation, measurement and extensive data records; (2) *conceptual model*, as SWMM, largely used in literature for the numerical analysis of LIDs, where the different components of the system are considered using conceptual entities (rain gauge, subcatchment, reservoir, LID control editor, and so on); (3) *mechanistic model*, as HYDRUS, where each component has a clear physical meaning, and each parameter can be measured independently.

2.4 Conclusions

In conclusion, although, as demonstrated in this chapter, several studies confirmed the LIDs' capability for surface runoff reduction, the large spread of these systems as urban stormwater management tools seem be very slow.

By considering this literature review, one of the key scientific limiting factors is the lack of comprehensive analysis finalized to evaluate the hydrological performance and the physical processes occurring in these systems, by considering both long-term experimental investigation and numerical modeling.

Another aspect to take into account is that all of LID systems are characterized by a heterogeneity stratigraphy, in terms of materials and components, and consequently the complexity of the physical processes, involved in these systems, require modeling tools able to accurately interpret their hydraulic behaviour and to correlate their hydrologic performance with the management of stormwater in the surrounding urban area.

However, in some of these studies, the physical parameters, specifically the soil hydraulic properties, which significantly affect the hydrological performance of LID systems, are not always investigated in a properly way. Sometimes the analysis is limited to specific parameters or literature values are considered to implement numerical modeling.

Similarly, the analysis of the most influential hydrological parameters is often quite limited for the missing of full-scale LID implementation, as well as for the unavailability of long-term hydrological monitored data.

Finally, another limiting aspect emerged from this literature review is the missing of tools able to evaluate the optimal solution in terms of LID system and site location by mathematical approaches.

In this context, this thesis aims to overcome the scientific gaps, highlighted in this section and in previous chapter, by carrying out a comprehensive analysis of different LID systems in order to investigate the hydrological benefits of these innovative and sustainable solutions at multiple spatial scales, considering experimental full-scale implementation and long-term monitored data as well as modeling large-scale implementation, lab experimental investigations, conceptual and mechanistic models, sensitivity analysis and mathematical optimization approaches.

2.5 References

Ahiablame, L. M., Engel, B. A., & Chaubey, I. (2012). Effectiveness of low impact development practices: literature review and suggestions for future research. Water, Air, & Soil Pollution, 223(7), 4253-4273. DOI 10.1007/s11270-012-1189-2

Alam, T., Mahmoud, A., Jones, K. D., Bezares-Cruz, J. C., & Guerrero, J. (2019). A Comparison of Three Types of Permeable Pavements for Urban Runoff Mitigation in the Semi-Arid South Texas, USA. Water, 11(10), 1992. https://doi.org/10.3390/w11101992

Al-Rubaei, A. M., Stenglein, A. L., Viklander, M., & Blecken, G. T. (2013). Long-term hydraulic performance of porous asphalt pavements in northern Sweden. Journal of Irrigation and Drainage Engineering, 139(6), 499-505. https://doi.org/10.1061/(ASCE)IR.1943-4774.0000569

Alsubih, M., Arthur, S., Wright, G., & Allen, D. (2017). Experimental study on the hydrological performance of a permeable pavement. Urban Water Journal, 14(4), 427-434. https://doi.org/10.1080/1573062X.2016.1176221

Amos, C., Rahman, A., & Mwangi Gathenya, J. (2016). Economic analysis and feasibility of rainwater harvesting systems in urban and peri-urban environments: A review of the global situation with a special focus on Australia and Kenya. Water, 8(4), 149. https://doi.org/10.3390/w8040149

Aravena, J. E., & Dussaillant, A. (2009). Storm-water infiltration and focused recharge modeling with finite-volume two-dimensional Richards equation: Application to an experimental rain garden. Journal of Hydraulic Engineering, 135(12), 1073-1080. https://doi.org/10.1061/(ASCE)HY.1943-7900.0000111

Ball, J. E., & Rankin, K. (2010). The hydrological performance of a permeable pavement. Urban Water Journal, 7(2), 79-90. https://doi.org/10.1080/15730620902969773

Baran Y., Gültekin A.B. (2018) Green Wall Systems: A Literature Review. In: Fırat S., Kinuthia J., Abu-Tair A. (eds) Proceedings of 3rd International Sustainable Buildings Symposium (ISBS 2017). ISBS 2017. Lecture Notes in Civil Engineering, vol 7. Springer, Cham. https://doi.org/10.1007/978-3-319-64349-6_8

Basdeki, A., Katsifarakis, L., & Katsifarakis, K. L. (2016). Rain Gardens as integral parts of urban sewage systems-a case study in Thessaloniki, Greece. Procedia engineering, 162, 426-432. https://doi.org/10.1016/j.proeng.2016.11.084

Becciu, G., Raimondi, A., & Dresti, C. (2018). Semi-probabilistic design of rainwater tanks: a case study in Northern Italy. Urban Water Journal, 15(3), 192-199. https://doi.org/10.1080/1573062X.2016.1148177

Berndtsson, J. C., 2010. Green roof performance towards management of runoff water quantity and quality: a review. Ecological Engineering, 36(4), 351-360. https://doi.org/10.1016/j.ecoleng.2009.12.014

Besir, A. B., & Cuce, E. (2018). Green roofs and facades: A comprehensive review. Renewable and Sustainable Energy Reviews, 82, 915-939. https://doi.org/10.1016/j.rser.2017.09.106

Bevilacqua, P., Mazzeo, D., & Arcuri, N. (2018). Thermal inertia assessment of an experimental extensive green roof in summer conditions. Building and Environment, 131, 264-276. https://doi.org/10.1016/j.buildenv.2017.11.033

Buccola, Norman, and Graig Spolek. (2011). A pilot-scale evaluation of greenroof runoff retention, detention, and quality. Water, Air, & Soil Pollution 216.1-4: 83-92. https://doi.org/10.1007/s11270-010-0516-8

Brunetti, G., Simunek, J., Piro, P. (2016). A comprehensive numerical analysis of the hydraulic behavior of permeable pavement. J. Hydrol. 540, 1146–1161. https://doi.org/10.1016/j.jhydrol.2016.07.030

Brunetti, G. (2017). On the use of mechanistic modeling for the numerical analysis of Low Impact Development techniques. PhD Thesis. Department of Civile Engineering. University of Calabria.

Drake, J. A., Bradford, A., & Marsalek, J. (2013). Review of environmental performance of permeable pavement systems: state of the knowledge. Water Quality Research Journal, 48(3), 203-222. https://doi.org/10.2166/wqrjc.2013.055

Campisano, A., & Modica, C. (2015). Rainwater harvesting as source control option to reduce roof runoff peaks to downstream drainage systems. Journal of Hydroinformatics, 18(1), 23-32. https://doi.org/10.2166/hydro.2015.133

Campisano, A., Butler, D., Ward, S., Burns, M. J., Friedler, E., DeBusk, K., ... & Han, M. (2017). Urban rainwater harvesting systems: Research, implementation and future perspectives. Water research, 115, 195-209. https://doi.org/10.1016/j.watres.2017.02.056

Carson, T. B., Marasco, D. E., Culligan, P. J., & McGillis, W. R. (2013). Hydrological performance of extensive green roofs in New York City: observations and multi-

year modeling of three full-scale systems. Environmental Research Letters, 8(2), 024036. http://dx.doi.org/10.1088/1748-9326/8/2/024036

Carter, T., & Rasmussen, T. (2006). Evaluation of the hydrologic behavior of green roofs. Journal of the American Water Resources Association, 42, 1261-1294.

Cipolla, S. S., Maglionico, M., & Stojkov, I. (2016). A long-term hydrological modelling of an extensive green roof by means of SWMM. Ecological Engineering, 95, 876-887. https://doi.org/10.1016/j.ecoleng.2016.07.009

Cipolla, S. S., Altobelli, M., & Maglionico, M. (2018). Decentralized water management: Rainwa-ter harvesting, greywater reuse and green roofs within the GST4Water project. In Multidis-ciplinary Digital Publishing Institute Proceedings, 2(11), p. 673.

Collins, K. A., Hunt, W. F., & Hathaway, J. M. (2008). Hydrologic comparison of four types of permeable pavement and standard asphalt in eastern North Carolina. Journal of Hydrologic Engineering, 13(12), 1146-1157. https://doi.org/10.1061/(ASCE)1084-0699(2008)13:12(1146)

Davis, A. P. (2008). Field performance of bioretention: Hydrology impacts. Journal of Hydrologic Engineering, 13(2), 90-95. https://doi.org/10.1061/(ASCE)1084-0699(2008)13:2(90)

Dietz, M. E., & Clausen, J. C. (2005). A field evaluation of rain garden flow and pollutant treatment. Water, Air, and Soil Pollution, 167(1-4), 123-138. https://doi.org/10.1007/s11270-005-8266-8

Dietz, M. E. (2007). Low impact development practices: A review of current research and recommendations for future directions. Water, air, and soil pollution, 186(1-4), 351-363. https://doi.org/10.1007/s11270-007-9484-z

Domènech, L., & Saurí, D. (2011). A comparative appraisal of the use of rainwater harvesting in single and multi-family buildings of the Metropolitan Area of Barcelona (Spain): social experience, drinking water savings and economic costs. Journal of Cleaner production, 19(6-7), 598-608. https://doi.org/10.1016/j.jclepro.2010.11.010

Dunnett, N., & Kingsbury, N. (2008). Planting green roofs and living walls. Portland, OR: Timber press.

Eckart, K., McPhee, Z., & Bolisetti, T. (2017). Performance and implementation of low impact development–A review. Science of the Total Environment, 607, 413-432. https://doi.org/10.1016/j.scitotenv.2017.06.254

Elizondo-Martínez, E. J., Andrés-Valeri, V. C., Jato-Espino, D., & Rodriguez-Hernandez, J. (2019). Review of porous concrete as multifunctional and sustainable pavement. Journal of Building Engineering, 100967. https://doi.org/10.1016/j.jobe.2019.100967

Elliott, A. H., & Trowsdale, S. A. (2007). A review of models for low impact urban stormwater drainage. Environmental modelling & software, 22(3), 394-405. https://doi.org/10.1016/j.envsoft.2005.12.005ù

Fletcher, T. D., Andrieu, H., & Hamel, P. (2013). Understanding, management and modelling of urban hydrology and its consequences for receiving waters: A state of the art. Advances in water resources, 51, 261-279. http://dx.doi.org/10.1016/j.advwatres.2012.09.001

Francis, R. A., & Lorimer, J. (2011). Urban reconciliation ecology: the potential of living roofs and walls. Journal of environmental management, 92(6), 1429-1437. https://doi.org/10.1016/j.jenvman.2011.01.012

Garofalo, G., Palermo, S., Principato, F., Theodosiou, T., & Piro, P. (2016). The influence of hydrologic parameters on the hydraulic efficiency of an extensive green roof in mediterranean area. Water, 8(2), 44. https://doi.org/10.3390/w8020044

GhaffarianHoseini, A., Tookey, J., GhaffarianHoseini, A., Yusoff, S. M., & Hassan, N. B. (2016). State of the art of rainwater harvesting systems towards promoting green built environments: a review. Desalination and Water Treatment, 57(1), 95-104. https://doi.org/10.1080/19443994.2015.1021097

Gromaire, M. C., Ramier, D., Seidl, M., Berthier, E., Saad, M., & De Gouvello, B. (2013). Impact of extensive green roofs on the quantity and the quality of runoff–first results of a test bench in the Paris region. NOVATECH 2013.

Hadba, L., Mendonça, P., & Silva, L. T. (2017). Green walls: an efficient solution for hygrothermal, noise and air pollution control in the buildings. In Living and Sustainability: An Environmental Critique of Design and Building Practices, Locally and Globally. AMPS, Architecture_MPS. London South Bank University.

Hashemi, S. S. G., Mahmud, H. B., & Ashraf, M. A., 2015. Performance of green roofs with respect to water quality and reduction of energy consumption in tropics: a review. Renewable and Sustainable Energy Reviews, 52, 669-679. https://doi.org/10.1016/j.rser.2015.07.163

Hatt, B. E., Fletcher, T. D., & Deletic, A. (2009). Hydrologic and pollutant removal performance of stormwater biofiltration systems at the field scale. Journal of Hydrology, 365(3-4), 310-321. https://doi.org/10.1016/j.jhydrol.2008.12.001

Herrmann, T., & Schmida, U. (2000). Rainwater utilisation in Germany: efficiency, dimensioning, hydraulic and environmental aspects. Urban water, 1(4), 307-316. https://doi.org/10.1016/S1462-0758(00)00024-8

Hilten, R. N., Lawrence, T. M., & Tollner, E. W. (2008). Modeling stormwater runoff from green roofs with HYDRUS-1D. Journal of hydrology, 358(3-4), 288-293. https://doi.org/10.1016/j.jhydrol.2008.06.010

Hunt, W. F., Smith, J. T., Jadlocki, S. J., Hathaway, J. M., & Eubanks, P. R. (2008). Pollutant removal and peak flow mitigation by a bioretention cell in urban Charlotte, NC. Journal of Environmental Engineering, 134(5), 403-408. https://doi.org/10.1061/(ASCE)0733-9372(2008)134:5(403)

Ishimatsu, K., Ito, K., Mitani, Y., Tanaka, Y., Sugahara, T., & Naka, Y. (2017). Use of rain gardens for stormwater management in urban design and planning. Landscape and Ecological Engineering, 13(1), 205-212. https://doi.org/10.1007/s11355-016-0309-3

Jia, H., Lu, Y., Shaw, L. Y., & Chen, Y. (2012). Planning of LID–BMPs for urban runoff control: The case of Beijing Olympic Village. Separation and Purification Technology, 84, 112-119. https://doi.org/10.1016/j.seppur.2011.04.026

Jia, H., Wang, X., Ti, C., Zhai, Y., Field, R., Tafuri, A. N., ... & Shaw, L. Y. (2015). Field monitoring of a LID-BMP treatment train system in China. Environmental monitoring and assessment, 187(6), 373. https://doi.org/10.1007/s10661-015-4595-2

Jones, M. P., & Hunt, W. F. (2010). Performance of rainwater harvesting systems in the southeastern United States. Resources, Conservation and Recycling, 54(10), 623-629. https://doi.org/10.1016/j.resconrec.2009.11.002

Karteris, M., Theodoridou, I., Mallinis, G., Tsiros, E., Karteris, A., 2016. Towards a green sustainable strategy for Mediterranean cities: Assessing the benefits of large-scale green roofs implementation in Thessaloniki, Northern Greece, using environmental modelling, GIS and very high spatial resolution remote sensing data. Renew. Sustain. Energy Rev. 58, 510–525. doi:10.1016/j.rser.2015.11.098

Katsifarakis, K. L., Vafeiadis, M., & Theodossiou, N. (2015). Sustainable drainage and urban landscape upgrading using rain gardens. Site selection in Thessaloniki,

Greece. Agriculture and agricultural science procedia, 4, 338-347. https://doi.org/10.1016/j.aaspro.2015.03.038

Kellagher, R., Martin, P., Jefferies, C., Bray, R., Shaffer, P., Wallingford, H. R., ... & Woods Ballard, B. (2015). Construction Industry Research and Information Association, Great Britain, Department of Trade and Industry, Environment Agency. The SUDS manual, Ciria, London C, 697.

Knapton, J., Morrell, D., & Simeunovich, M. (2012). Structural Design Solutions for Permeable Pavements. Landscape, 44(1422), 312000.

Krebs, G., Kuoppamäki, K., Kokkonen, T., & Koivusalo, H. (2016). Simulation of green roof test bed runoff. Hydrological processes, 30(2), 250-262. https://doi.org/10.1002/hyp.10605

Kuruppu, Upeka, Ataur Rahman, and M. Azizur Rahman. "Permeable pavement as a stormwater best management practice: a review and discussion." Environmental Earth Sciences 78.10 (2019): 327. https://doi.org/10.1007/s12665-019-8312-2

Lau, J. T., & Mah, D. Y. S. (2018). Green Wall for Retention of Stormwater. Pertanika Journal of Science and Technology, 1, 283.

Lee, J. Y., Moon, H. J., Kim, T. I., Kim, H. W., & Han, M. Y. (2013). Quantitative analysis on the urban flood mitigation effect by the extensive green roof system. Environmental Pollution, 181, 257-261. https://doi.org/10.1016/j.envpol.2013.06.039

Li, Y., & Babcock Jr, R. W. (2014). Green roof hydrologic performance and modeling: a review. Water science and technology, 69(4), 727-738. https://doi.org/10.2166/wst.2013.770

Li, Z., Boyle, F., & Reynolds, A. (2010). Rainwater harvesting and greywater treatment systems for domestic application in Ireland. Desalination, 260(1-3), 1-8. https://doi.org/10.1016/j.desal.2010.05.035

Li, J., Zhang, B., Li, Y., & Li, H. (2018). Simulation of Rain Garden Effects in Urbanized Area Based on Mike Flood. Water, 10(7), 860. https://doi.org/10.3390/w10070860

Li, Q., Wang, F., Yu, Y., Huang, Z., Li, M., & Guan, Y. (2019). Comprehensive performance evaluation of LID practices for the sponge city construction: a case study in Guangxi, China. Journal of environmental management, 231, 10-20. https://doi.org/10.1016/j.jenvman.2018.10.024

Lin, W., Park, D. G., Ryu, S. W., Lee, B. T., & Cho, Y. H. (2016). Development of permeability test method for porous concrete block pavement materials considering

clogging. Construction and Building Materials, 118, 20-26. https://doi.org/10.1016/j.conbuildmat.2016.03.107

Liu, W., Feng, Q., Chen, W., Wei, W., & Deo, R. C. (2019). The influence of structural factors on stormwater runoff retention of extensive green roofs: new evidence from scale-based models and real experiments. Journal of hydrology, 569, 230-238. https://doi.org/10.1016/B978-0-12-812843-5.00020-4

Locatelli, L., Mark, O., Mikkelsen, P. S., Arnbjerg-Nielsen, K., Jensen, M. B., & Binning, P. J. (2014). Modelling of green roof hydrological performance for urban drainage applications. Journal of hydrology, 519, 3237-3248. https://doi.org/10.1016/j.jhydrol.2014.10.030

Malaviya, P., Sharma, R., & Sharma, P. K. (2019). Rain Gardens as Stormwater Management Tool. In Sustainable Green Technologies for Environmental Management (pp. 141-166). Springer, Singapore. https://doi.org/10.1007/978-981-13-2772-8_7

Manso, M., & Castro-Gomes, J. (2015). Green wall systems: a review of their characteristics. Renewable and Sustainable Energy Reviews, 41, 863-871. https://doi.org/10.1016/j.rser.2014.07.203

Mao, X., Jia, H., & Shaw, L. Y. (2017). Assessing the ecological benefits of aggregate LID-BMPs through modelling. Ecological modelling, 353, 139-149. http://dx.doi.org/10.1016/j.ecolmodel.2016.10.018

Marchioni, M., & Becciu, G. (2015). Experimental results on permeable pavements in urban areas: a synthetic review. International Journal of Sustainable Development and Planning, 10(6), 806-817. DOI: 10.2495/SDP-V10-N6-806-817

Nawaz, R., McDonald, A., & Postoyko, S. (2015). Hydrological performance of a full-scale extensive green roof located in a temperate climate. Ecological Engineering, 82, 66-80. https://doi.org/10.1016/j.ecoleng.2014.11.061

Oberascher M., Zischg J., Palermo S.A., Kinzel C., Rauch W., Sitzenfrei R. (2019) Smart Rain Barrels: Advanced LID Management Through Measurement and Control. In: Mannina G. (eds) New Trends in Urban Drainage Modelling. UDM 2018. Green Energy and Technology. Springer, Cham. https://doi.org/10.1007/978-3-319-99867-1_134

Osheen, Singh K.K. (2019) Rain Garden—A Solution to Urban Flooding: A Review. In: Agnihotri A., Reddy K., Bansal A. (eds) Sustainable Engineering. Lecture Notes in

Civil Engineering, vol 30. Springer, Singapore. https://doi.org/10.1007/978-981-13-6717-5_4

Palermo S.A., Zischg J., Sitzenfrei R., Rauch W., Piro P. (2019a) Parameter Sensitivity of a Microscale Hydrodynamic Model. In: Mannina G. (eds) New Trends in Urban Drainage Modelling. UDM 2018. Green Energy and Technology. Springer, Cham. https://doi.org/10.1007/978-3-319-99867-1_169

Palermo, S. A., & Turco, M. (2020). Green Wall systems: where do we stand?. In IOP Conference Series: Earth and Environmental Science (Vol. 410, No. 1, p. 012013). IOP Publishing. https://doi.org/10.1088/1755-1315/410/1/012013

Palla, A., Gnecco, I., & Lanza, L. G. (2010). Hydrologic restoration in the urban environment using green roofs. Water, 2(2), 140-154. https://doi.org/10.3390/w2020140

Palla, A., Gnecco, I., Carbone, M., Garofalo, G., Lanza, L. G., & Piro, P. (2015). Influence of stratigraphy and slope on the drainage capacity of permeable pavements: laboratory results. Urban Water Journal, 12(5), 394-403. https://doi.org/10.1080/1573062X.2014.900091

Palla, A., & Gnecco, I. (2015). Hydrologic modeling of Low Impact Development systems at the urban catchment scale. Journal of hydrology, 528, 361-368. https://doi.org/10.1016/j.jhydrol.2015.06.050

Palla, A., Gnecco, I., & La Barbera, P. (2017). The impact of domestic rainwater harvesting systems in storm water runoff mitigation at the urban block scale. Journal of environmental management, 191, 297-305. https://doi.org/10.1016/j.jenvman.2017.01.025

Pęczkowski, G., Kowalczyk, T., Szawernoga, K., Orzepowski, W., Żmuda, R., & Pokładek, R. (2018). Hydrological performance and runoff water quality of experimental green roofs. Water, 10(9), 1185. https://doi.org/10.3390/w10091185

Peng, Z., & Stovin, V. (2017). Independent validation of the SWMM green roof module. Journal of Hydrologic Engineering, 22(9), 04017037. https://doi.org/10.1061/(ASCE)HE.1943-5584.0001558

Perini, K., Bazzocchi, F., Croci, L., Magliocco, A., & Cattaneo, E. (2017). The use of vertical greening systems to reduce the energy demand for air conditioning. Field monitoring in Mediterranean climate. Energyand Buildings, 143, 35-42. https://doi.org/10.1016/j.enbuild.2017.03.036

Petrucci, G., Deroubaix, J. F., De Gouvello, B., Deutsch, J. C., Bompard, P., & Tassin, B. (2012). Rainwater harvesting to control stormwater runoff in suburban areas. An experimental case-study. Urban Water Journal, 9(1), 45-55. https://doi.org/10.1080/1573062X.2011.633610

Piro P., Turco M., Palermo S.A., Principato F., Brunetti G. (2019b) A Comprehensive Approach to Stormwater Management Problems in the Next Generation Drainage Networks. In: Cicirelli F., Guerrieri A., Mastroianni C., Spezzano G., Vinci A. (eds) The Internet of Things for Smart Urban Ecosystems. Internet of Things (Technology, Communications and Computing). Springer, Cham. https://doi.org/10.1007/978-3-319-96550-5_12

PRINCE GEORGE'S, C. O. U. N. T. Y. (2002). Bioretention manual, Prince George's County Government, Department of Environmental Protection, Landover, MD, USA.

Raji, B., Tenpierik, M. J., & van den Dobbelsteen, A. (2015). The impact of greening systems on building energy performance: A literature review. Renewable and Sustainable Energy Reviews, 45, 610-623. https://doi.org/10.1016/j.rser.2015.02.011

Razzaghmanesh, M., & Beecham, S. (2014). The hydrological behaviour of extensive and intensive green roofs in a dry climate. Science of the total environment, 499, 284-296. http://dx.doi.org/10.1016/j.scitotenv.2014.08.046

Robinson, T., Schulte-Herbrüggen, H., Mácsik, J., & Andersson, J. (2019). Raingardens for stormwater management: Potential of raingardens in a Nordic climate.

Rowe, D. B. (2011). Green roofs as a means of pollution abatement. Environmental pollution, 159(8-9), 2100-2110. https://doi.org/10.1016/j.envpol.2010.10.029

Santamouris, M. (2014). Cooling the cities–a review of reflective and green roof mitigation technologies to fight heat island and improve comfort in urban environments. Solar energy, 103, 682-703. https://doi.org/10.1016/j.solener.2012.07.003

Sheweka, S., & Magdy, A. N. (2011). The living walls as an approach for a healthy urban environment. Energy Procedia, 6, 592-599. https://doi.org/10.1016/j.egypro.2011.05.068

Simmons, M. T., Gardiner, B., Windhager, S., & Tinsley, J. (2008). Green roofs are not created equal: the hydrologic and thermal performance of six different extensive green roofs and reflective and non-reflective roofs in a sub-tropical climate. Urban Ecosystems, 11(4), 339-348. https://doi.org/10.1007/s11252-008-0069-4

Scholz, M., & Grabowiecki, P. (2007). Review of permeable pavement systems. Building and environment, 42(11), 3830-3836. https://doi.org/10.1016/j.buildenv.2006.11.016

Siwiec, E., Erlandsen, A. M., & Vennemo, H. (2018). City greening by rain gardens-costs and benefits. Ochrona Srodowiska i Zasobów Naturalnych, 29(1), 1-5. DOI 10.2478/oszn-2018-0001

Stovin, V., Vesuviano, G., & Kasmin, H. (2012). The hydrological performance of a green roof test bed under UK climatic conditions. Journal of hydrology, 414, 148-161. http://dx.doi.org/10.1016/j.jhydrol.2011.10.022

Stovin, V., Poë, S., De-Ville, S., & Berretta, C. (2015). The influence of substrate and vegetation configuration on green roof hydrological performance. Ecological Engineering, 85, 159-172. https://doi.org/10.1016/j.ecoleng.2015.09.076

Turco, M., Kodešová, R., Brunetti, G., Nikodem, A., Fér, M., & Piro, P. (2017). Unsaturated hydraulic behaviour of a permeable pavement: Laboratory investigation and numerical analysis by using the HYDRUS-2D model. Journal of hydrology, 554, 780-791. https://doi.org/10.1016/j.jhydrol.2017.10.005

Turco M., Brunetti G., Porti M., Grossi G., Maiolo M., Piro P. (2019) Metals Potential Removal Efficiency of Permeable Pavement. In: Mannina G. (eds) New Trends in Urban Drainage Modelling. UDM 2018. Green Energy and Technology. Springer, Cham. https://doi.org/10.1007/978-3-319-99867-1_29

Uhl, M., & Schiedt, L. (2008, August). Green roof storm water retention–monitoring results. In 11th International Conference on Urban Drainage, Edinburgh, UK (Vol. 31).

Vaillancourt, C., Duchesne, S., & Pelletier, G. (2019). Hydrologic Performance of Permeable Pavement as an Adaptive Measure in Urban Areas: Case Studies near Montreal, Canada. Journal of Hydrologic Engineering, 24(8), 05019020. https://doi.org/10.1061/(ASCE)HE.1943-5584.0001812

Vijayaraghavan, K., & Raja, F. D., (2014). Design and development of green roof substrate to improve runoff water quality: Plant growth experiments and adsorption. Water research, 63, 94-101. https://doi.org/10.1016/j.watres.2014.06.012

Vijayaraghavan, K. (2016). Green roofs: A critical review on the role of components, benefits, limitations and trends. Renewable and sustainable energy reviews, 57, 740-752. https://doi.org/10.1016/j.rser.2015.12.119

Vila, A., Pérez, G., Solé, C., Fernández, A. I., & Cabeza, L. F., 2012. Use of rubber crumbs as drainage layer in experimental green roofs. Building and Environment, 48, 101-106. https://doi.org/10.1016/j.buildenv.2011.08.010

Voyde, E., Fassman, E., & Simcock, R. (2010). Hydrology of an extensive living roof under sub-tropical climate conditions in Auckland, New Zealand. Journal of hydrology, 394(3-4), 384-395. https://doi.org/10.1016/j.jhydrol.2010.09.013

Wang, X., Tian, Y., & Zhao, X. (2017). The influence of dual-substrate-layer extensive green roofs on rainwater runoff quantity and quality. Science of the Total Environment, 592, 465-476. https://doi.org/10.1016/j.scitotenv.2017.03.124

Wong, N. H., Tan, A. Y. K., Chen, Y., Sekar, K., Tan, P. Y., Chan, D., & Wong, N. C. (2010). Thermal evaluation of vertical greenery systems for building walls. Building and environment, 45(3), 663-672. https://doi.org/10.1016/j.buildenv.2009.08.005

Wong, G. K., & Jim, C. Y. (2014). Quantitative hydrologic performance of extensive green roof under humid-tropical rainfall regime. Ecological Engineering, 70, 366-378. https://doi.org/10.1016/j.ecoleng.2014.06.025

Yang, H., Florence, D. C., McCoy, E. L., Dick, W. A., & Grewal, P. S. (2009). Design and hydraulic characteristics of a field-scale bi-phasic bioretention rain garden system for storm water management. Water Science and Technology, 59(9), 1863-1872. https://doi.org/10.2166/wst.2009.186

Yang, H. S., Kang, J., & Choi, M. S. (2012). Acoustic effects of green roof systems on a low-profiled structure at street level. Building and Environment, 50, 44-55. https://doi.org/10.1016/j.buildenv.2011.10.004

Yuan, J., Dunnett, N., & Stovin, V. (2017). The influence of vegetation on rain garden hydrological performance. Urban Water Journal, 14(10), 1083-1089. https://doi.org/10.1080/1573062X.2017.1363251

Zahmatkesh, Z., Burian, S. J., Karamouz, M., Tavakol-Davani, H., & Goharian, E. (2014). Low-impact development practices to mitigate climate change effects on urban stormwater runoff: Case study of New York City. Journal of Irrigation and Drainage Engineering, 141(1), 04014043. DOI: 10.1061/(ASCE)IR.1943-4774.0000770

Zhang, K., & Chui, T. F. M. (2018). A comprehensive review of spatial allocation of LID-BMP-GI practices: Strategies and optimization tools. Science of the total environment, 621, 915-929. https://doi.org/10.1016/j.scitotenv.2017.11.281

Zhang, L., Oyake, Y., Morimoto, Y., Niwa, H., & Shibata, S. (2019). Rainwater storage/infiltration function of rain gardens for management of urban storm runoff in Japan. Landscape and Ecological Engineering, 15(4), 421-435. https://doi.org/10.1007/s11355-019-00391-w

Zischg, J., Zeisl, P., Winkler, D., Rauch, W., & Sitzenfrei, R. (2018). On the sensitivity of geospatial low impact development locations to the centralized sewer network. Water science and technology, 77(7), 1851-1860. https://doi.org/10.2166/wst.2018.060

Chapter 3 – Parameter sensitivity analysis of a microscale hydrodynamic model of University Campus Innsbruck

This chapter presents the results of a global sensitivity analysis (GSA) applied to a microscale hydrodynamic model, developed based on the new configuration of the drainage network of University Campus Innsbruck, which combines pipe infrastructure and small-scale source treatments in terms of Rain Gardens (RGs). The aim is to identify the most influential model parameters. For the model creation and simulation, the Storm Water Management Model (SWMM) is used. For the GSA method the Elementary Effect Test (EET) is applied, where uncertainties to 18 model input parameters, comprising 10 subcatchment and 8 Low Impact Development (LID) parameters, are assigned and analyzed by 1,900 simulations. The model's responses are evaluated at four main RGs and four model outputs: *(1) total inflow, (2) surface level, (3) storage level,* and *(4) surface runoff* at the RGs. Finally, based on this model configuration, the idea on the development of an advanced LID management (as smart rain barrels) through measurement and control is briefly presented. These findings are already published and are linked to Paper I (Palermo et al., 2019a) and Paper IV (Oberascher et al., 2019).

3.1 Introduction

The design of conventional sewer systems, based on historical observations of precipitation and land use, require significant investments to meet challenges imposed by rapid urbanization, evolving regulations and an uncertain climate (Kerkez et al., 2016).

Therefore, in this context a transition from traditional drainage infrastructure towards a sustainable, smart and resilient urban water management is required.

To apply this innovative concept of manage the urban stormwater, one promising strategy is the implementation of decentralized stormwater controls, also known as e.g. Green Infrastructure (GI) or Low Impact Development (LID), which provide several benefits at multiple scales (Zischg et al. 2018, Maiolo et al. 2017). Another additional solution, that can be integrated with the previous one, is to improve urban water flow and quality by equipping the drainage systems with low-cost sensors and controllers, in order to achieve a new generation of intelligent green and gray stormwater networks, highly adaptive in function of the external environmental (Kerkez et al., 2016). In this regard, recent advances in the field of Internet of Things (IoT) have opened up new possibilities for real-time monitoring and control of such structures, that enable the reduction of urban flooding or combined sewer overflows.

So far, many literature studies have investigated the hydraulic efficiency of LID systems, showing their strong variability according to several factors, including the characteristics of storm events, as well as many numerical and physical models were developed to prove their feasibility and performance (Garofalo et al. 2016). By implementing multiple small-scale units in urban areas, a complex system of temporal storage facilities for managing stormwater runoff can be created.

The implementation of LID techniques strongly affects the hydraulic performance of the drainage system. Therefore, the identification of most influential parameters in a system which combines sustainable systems and conventional pipe infrastructures for urban stormwater management become a key factor to investigate.

In this regard, this work provides a first step towards the sustainable operation of the newly set up “Smart Campus” at the University of Innsbruck, where recently LID systems have been implemented. The first objective of this study is to present the development of a detailed micro-scale hydrodynamic model by using the PCSWMM software, based on the data retrieved on the site specific. Secondly, the most influencing model parameters are identified through a sensitivity analysis, including the uncertainties

of subcatchment and LID parameters. Finally, starting from the microscale model configuration, the idea on advanced LID (smart rain barrels) management through measurement and control is briefly presented.

3.2 Materials and Methods

3.2.1 Case Study Description

The case study area is the University Campus Innsbruck, in Tyrol, Austria (47° 15'50.87" N 11°20'40.17" E), where 12 Rain Gardens (RGs), 1 Green Roof (GR) and 3 Gravel Roofs were implemented to enable a more sustainable water management strategy and to make the Campus more attractive and resilient to flooding risk.

To connect impervious surface areas (e.g. pavements, streets) to those LIDs a new drainage system, consisting of a network of open channels (OCs) with a parabolic cross-section and PVC conduits (DN200) was built. This system supports the existing underground drainage network, composed of around 420 m of conduits (DN200÷DN600), which collect the rainwater only from the roofs.

Thus, the total drainage system can be divided into two independent systems: one related to the RGs; and the second one concerning the old drainage network.

Four RGs with an area of 65 m^2 each are located at the centre of the main square and receive the rainwater collected only by the OCs system (Figure 3.1, top). The others RGs (Figure 3.1, below), ranging from 16 m^2 to 43 m^2, intercept the stormwater runoff from different areas.

Even if the RGs differ from each other regarding the area and the storage depth, they have identical stratigraphy (Fig. 3.2), and consist of the following horizontal layers (from top to bottom):

1. a *surface vegetated layer* vegetated with a berm height of 26 cm;
2. a *soil layer* with a thickness of 30 cm;
3. a *storage layer* with varying depths;
4. an *underdrain pipe*.

Figure 3.1: Pictures of the two different types of RGs at University Campus Innsbruck, the circular ones on the top, where is possible to observe the open channel too, and the semi-rectangular one, below.

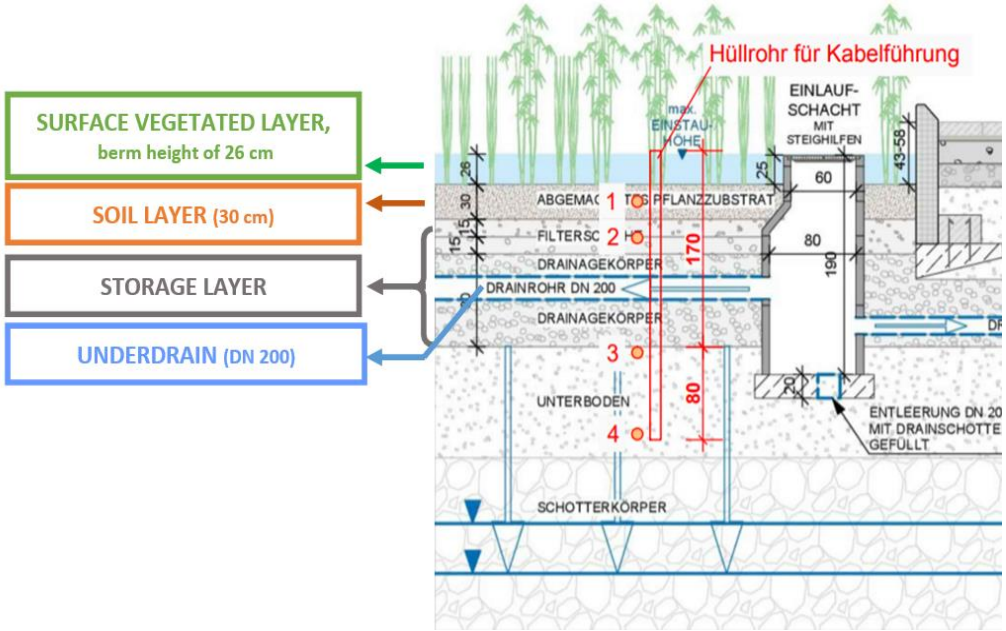

Figure 3.2: Cross section of the Circular RG located at the University Campus Innsbruck (adapted picture from the design map by Karl Grimm – Landschaftsarchitekten - Grimm, 2016).

3.2.2 Model Development

A detailed hydrodynamic model was developed considering the entire Campus drainage system previous described. To achieve this aim, the dynamic rainfall-runoff simulation model PCSWMM (CHI PCSWMM), based on the EPA-SWMM version 5.1.012 (Rossman 2015), was used.

SWMM, is widely known model generally used for hydrodynamic approaches, but it allows also to implement different versions LID control units, represented by a combination of vertical layers with properties defined on a per-unit-area basis (Goncalves et al., 2018). Therefore, it is a suitable model for the main purpose of this study.

The model was built considering topographical data, land use classification, new and existing stormwater system, RG details, taken from construction plans and site measurements.

To obtain a detailed microscale model, the study area of 3.02 ha was divided into several subcatchments, which were precisely defined depending on changes of the surface slope and the land use.

The subcatchment width, that describes the overland flow characteristic, is generally an important and sensitive model parameter, especially for large subcatchments. For this microscale model, knowing all geometrical features of the system, it was calculated as the fraction between the subcatchment area and the flow length.

To simulate the LID solutions, the model was integrated with the use of the LID Control Editor, an additional SWMM module developed to simulate the hydrological behaviour of source control solutions (Rossman, 2010). Recently studies confirm the suitability of SWMM to assess the LID performances and to support their implementation at catchment scale (Palla & Gnecco, 2015; Ahiablame & Shakya, 2016). For the specific case study, the bio-retention cell SWMM module was selected for the model implementation of the RG. To assign the properties for each layer, required by the LID Control section, the stratigraphy features and the physical parameters were considered based on the design features, retrieved in the maps and reports by the designer and developers. Finally, since the RGs differ from each other for the thickness of the storage layer, 12 “bioretention cells” LID control were implemented.

The Soil Conservation Service (SCS) Curve Number (CN) method was considered for the infiltration method and the flow routing computations were based on the Dynamic Wave Equations.

3.2.3 Sensitivity Analysis

Taking into account that the implementation of the LID structures strongly influences the hydraulic performance of the drainage system and that most model input parameters are uncertain, a Global Sensitivity Analysis (GSA) was carried out.

Sensitivity Analysis allows to investigate how the variation in the model output (y) can be attributed to variations of its input factors (x_1, x_2, …, x_m).

In this case, due the number of considered parameters and the features of the decentralized LID system, the Morris screening method (Morris 1991), also known as *Elementary Effect Test* (EET), was used (Saltelli et al. 2008).

As reported in Pianosi et al., (2016), the mean of r finite differences ("*Elementary Effects*" or "EEs") is considered as a measure of global sensitivity, i.e.:

$$S_i = \frac{1}{r}\sum_{j=1}^{r} EE^j = \frac{1}{r}\sum_{j=1}^{r} \frac{g\left(\bar{x}_1^j,\dots,\bar{x}_i^j+\Delta_i^j,\dots,\bar{x}_M^j\right)-g\left(\bar{x}_1^j,\dots,\bar{x}_i^j,\dots,\bar{x}_M^j\right)}{\Delta_i^j} c_i \qquad [3.1]$$

Two sensitivity measures, the *standard deviation* of the EET (σ) and the *mean* of EET (μ) are calculated. The standard deviation of the EEs provides information on the degree of interaction of their input factor with the others, thus a high standard deviation indicates that a factor is interacting with others because its sensitivity changes across the variability space (Pianosi et al. 2016).

For the sampling strategy to select the points $x^j(j = 1, \dots, r)$ and the input variations Δ_i, the sampling strategy proposed by Morris (1991) was chosen.

This strategy defines r trajectories in the input space, each composed of M+1 points, where M is the number of input factors subject to SA, (here assumed equal to 100). This strategy selects the starting point randomly over a uniform grid of the parameter space and the subsequent points by moving one factor at a time by a fixed amount Δ, so that each trajectory allows for evaluating one Elementary Effect (EE) per factor. The grid size is determined through the "number of levels" L (chosen by the user), as $1/(L-1)$ of the

range of variability of input factor; while the size of variation Δ is evaluated as $L/[2 \cdot (L-1)]$ (Pianosi et al., 2016)

To consider the spatial variability of the model results *("prediction function")*, the outcome of the four main circular RGs was evaluated at different horizontal layers for the presented case study (see Sect. 3.2.1).

Starting from the assumption that the site-specific subcatchment parameters, *slope*, *width* and *area* are measured physical features; the following 18 input parameters (10 related to the subcatchments and 8 to the RGs) were selected for the GSA (Table 3.1). For each parameter, the range of variability was chosen based on of their physical attributes and by considering reported values in the SWMM Manual (Rossman 2015).

The interval size to define the grid over the input parameter space was set to 10.

Table 3.1: Input parameters for GSA, meaning and corresponding range of variability taken from User SWMM Manual (Rossman,2015) (Palermo et al., 2019a)

	N	Name of parameter	Meaning	Value range
Subcatchemnet Parametrs	1	Imperv (%)	*Percent of impervious area*	90 - 100
	2	Perv (%)	*Percent of pervious area*	0 -10
	3	Destore-Imperv (mm)	*Depth of depression storage on impervious area*	1.27 - 2.54
	4	Destore-Perv (mm)	*Depth of depression storage on pervious area*	2.54 - 5.08
	5	N-Imperv	*Manning's roughness coefficient for impervious area*	0.012 - 0.014
	6	N-Perv	*Manning's roughness coefficient for pervious area*	0.13 - 0.24
	7	CN-Imperv	*SCS runoff curve number for impervious area*	90 - 98
	8	CN-Perv	*SCS runoff curve number for pervious area*	30 - 61
	9	Drying Time (days)	*Time for a fully saturated soil to be completely dry*	2 - 14
	10	OpenChannel Roughness	*Manning's roughness coefficient for Open Channel*	0.022 - 0.026
RG parameters	11	Vegetative Volume (fraction)	*Fraction of volume within the surface storage depth filled with vegetation*	0.1 - 0.2
	12	Porosity (volume fraction)	*The volume of pore space relative to total volume of soil*	0.42 - 0.437
	13	Field Capacity (FC) (volume fraction)	*Volume of pore water relative to total volume after the soil has been allowed to drain fully*	0.062 - 0.105
	14	Wilting Point (WP) (volume fraction)	*Volume of pore water relative to total volume for a well dried soil where only bound water remain*	0.024 - 0.047
	15	Conductivity (Kf) (mm/hr)	*Hydraulic conductivity for the fully saturated soil*	30 - 180
	16	Conductiity Slope (Kslope)	*Slope of the curve of log(conductivity) versus soil moisture content (dimensionless)*	30 - 60
	17	Seepage rate (mm/hr)	*The rate at which water seeps into the native soil below the layer*	30 - 180
	18	Drain coefficient (mm/hr)	*The drain coefficient C which determines the rate of flow through a drain*	3 - 6

As previously mentioned, the four main circular RGs were considered for the sensitivity analysis of this study.

The effect of the variability of each parameter was analyzed by considering four different model outputs for the four RGs: *(1) LID Total Inflow, (2) LID Surface Level, (3) LID Storage Level* and *(4) LID Surface Runoff*. The first one, the *LID Total Inflow* considers the total runoff intercepted in each RG and takes into account the influence of the subcatchment parameters, while the other three model outputs evaluate the hydrological performance of the RGs. To summarize the four main RGs with similar physical characteristics, but different intercepted surfaces, the mean values of these outputs are built.

For the hydrodynamic simulation, design storm event with a return period of one year (1.13 mm/min) was used.

For carrying out the GSA 1,900 model runs are performed through a Matlab Script which uses SWMM and integrates the SAFE-toolbox (Pianosi et al. 2015).

3.3 Results and Discussion

3.3.1 Numerical Model

Based on the information described in section 3.2.1, the final model configuration, obtained by using the software PCSWMM is shown in Figure 3.3, where is it possible to observe the land use in terms of impervious percentage.

To obtain a detailed microscale model, the study area of 3.02 ha was divided into 252 subcatchments, defined depending on changes of the surface slope and the land use.

In this regard, each LID unit occupies the entire pervious subcatchment, and receive the surface runoff from the surrounding impervious area through the open channel or a specific system of slope.

The main conventional drainage system collet the rainwater from the roof surfaces to rapid move it in the final outfall located at the top of the figure, that is connected with the urban sewer system.

Globally the whole modeling drainage system, consisting of the two independent system (decentralized LIDs and central stormwater system) consists of: 139 Junctions, 139 Conduits and 13 LID Controls (12 RG and 1 GR).

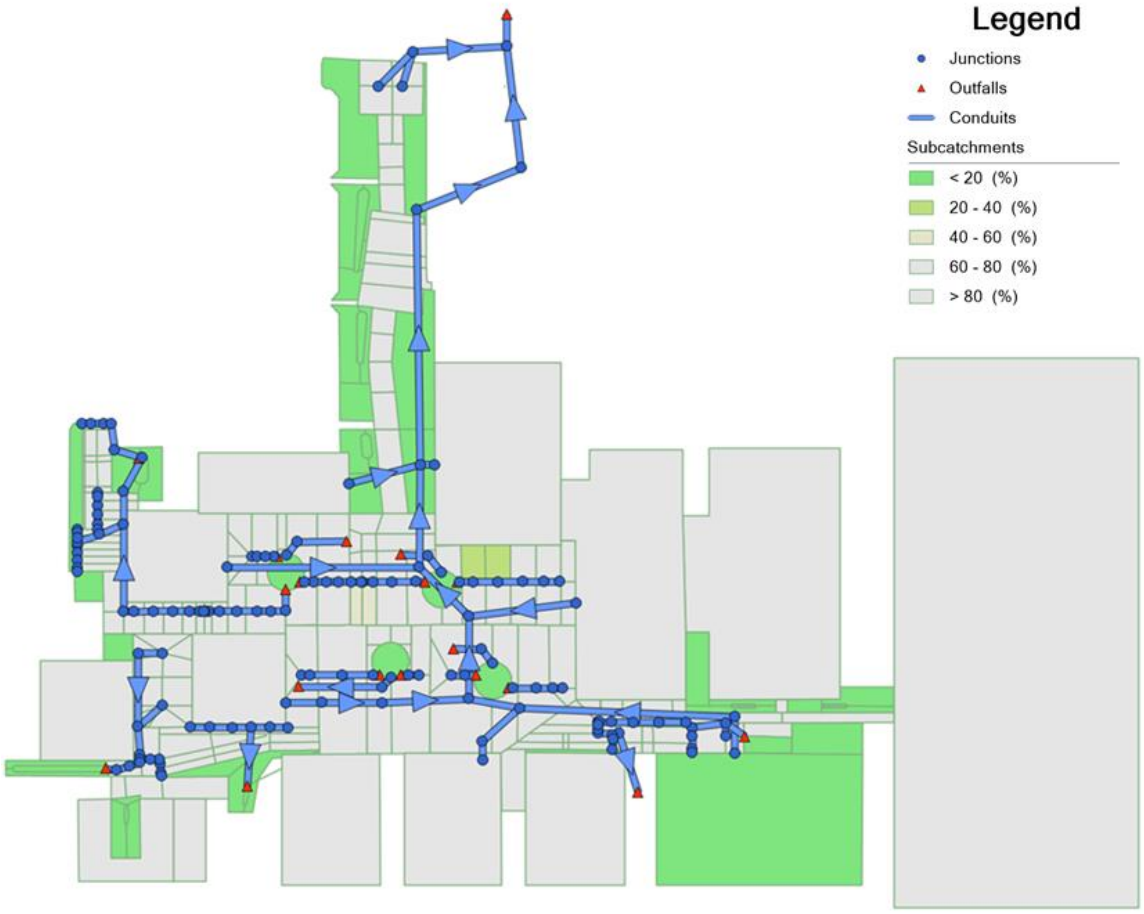

Figure 3.3: Final model configuration of the University Campus Innsbruck implemented by PCSWMM

3.3.2 Analysis of the most influential model parameters

Results of the EET Sensitivity Analysis are reported in Fig. 3.4, where the Mean of EEs (μ) versus their standard deviation (σ) (left side) and the Convergence plots (right side) are shown. In the graphs on the left side - where each input factor corresponds with one point - the point located at the righter side along the horizontal axis (μ) is the more influential one, while the higher up referring to the vertical axis (σ) is that one presents the larger degree of interactions with other factors (Pianosi et al. 2016).

Being the μ of EEs a measure on the global sensitivity, the findings show that the most influential factor for the *LID Total Inflow* output is the *Depression Storage Impervious* (3), the second one is the *Percent of Impervious Area* (1). Even if, the higher σ is reached

by the *CN-Impervious* (7), the factor (1) presents also a high σ, and this means that these two factors (7 and 1) have a huge degree of interaction with the other factors.

While the most influential factor for the LID Surface Level is the *Soil Hydraulic Conductivity* (15), which presents also the higher degree of interaction with the other parameters. In agreement with this last result it is also the finding obtained for the *LID Surface Runoff outcome*, where the *Soil Hydraulic Conductivity* (15) is the most sensitive parameter and it presents also the greatest degree of interaction with the other factors. In addition, in this case, *Percent of Impervious Area* (1), *Vegetative Volume* (11), and the *Depression Storage Impervious* (3) follow this result.

Finally, when the *LID Storage Level* output is considered, the factor located at the righter side along the horizontal axis, i.e. the more influential one, is the *Seepage Rate* (17), which present also the higher degree of interaction with the other parameters. Following this value, *Soil Hydraulic Conductivity* (15).

In the graphs on the right side (Fig. 3.4), the sensitivity indexes are estimated using an increasing sample size by considering one line per factor, while the dashed lines represent confidence bounds (Pianosi et al., 2016). In this regard, the results found confirm previous findings in terms of most influential factors, also providing other details about the number of model evaluations needed to reach the convergence.

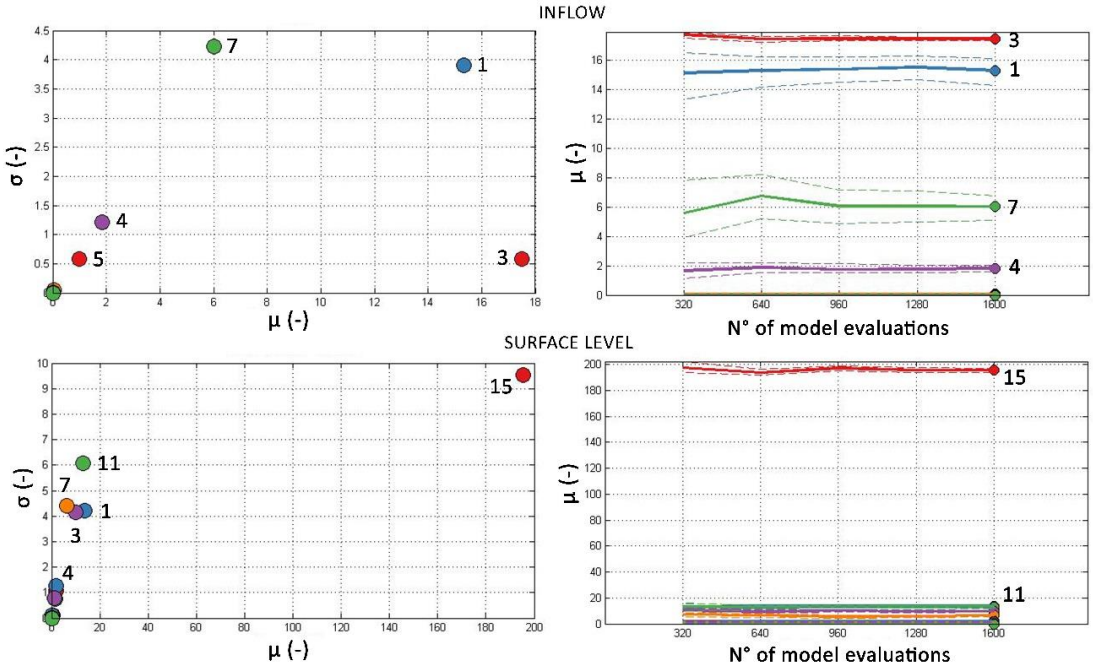

Figure 3.4: Results of GSA for the 4 model outputs in terms of: mean of EEs vs their standard deviation (left side) and the Convergence plots (right side). The number of each parameter are the same reported in Table 3.1. (Figure adapted and integrated from Palermo et al., 2019a).

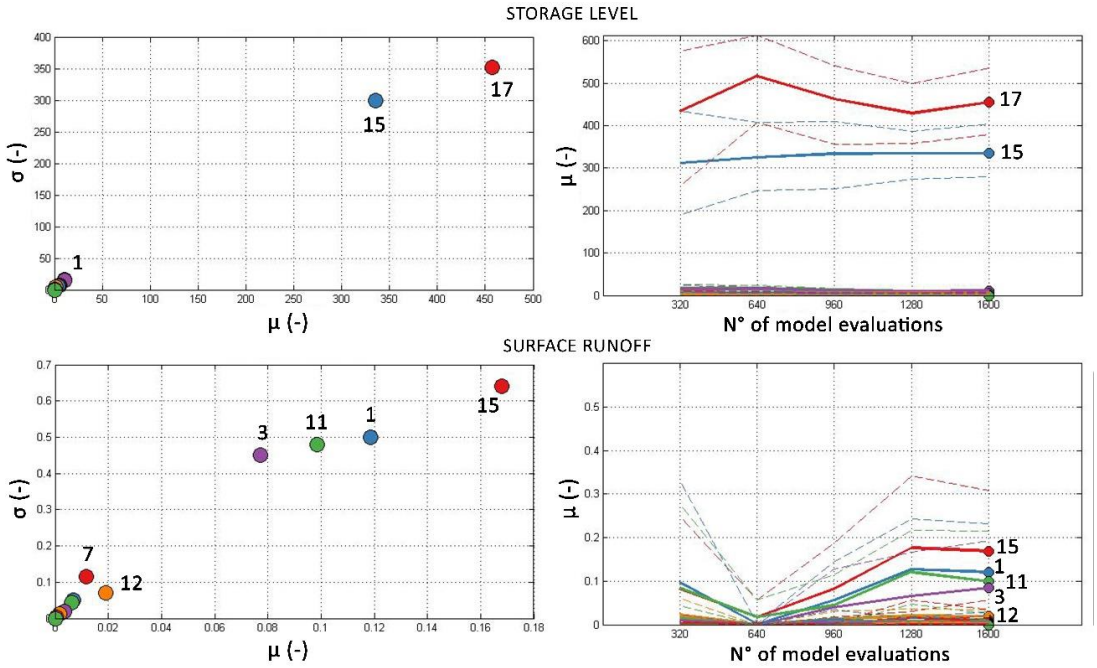

Figure 3.4. *Cont.*

3.4 New trends: advanced LID management through measurement and control

Based on the final configuration of the hydrodynamic micro-scale model, previous discussed, a study already published by Oberascher et al. (2019), corresponding to Paper IV annexed to this thesis, was carried out in order to present a concept for using real-time controlled smart rain barrels integrated into a smart city pilot project. More in detail, this study aims to support the development of a prototypes of Smart Rain barrels (SRBs) (e.g. choice of sizes and locations) for the real implementation.

The study was born from the consideration on recent advances in the field of Internet of Things (IoT), that have opened up new opportunities for real-time monitoring and control of drainage network, allowing urban flooding or combined sewer overflows (CSOs) the reduction. In paper IV, IoT and rain barrels are linked together, resulting in a smart rain barrel.

However, despite the idea of a smart rain barrel is nothing totally new, as the large number of some publicly available products shows (RainGrid n.d., Sieker n.d.), SRBs, here presented, are integrated into a pilot project for smart cities, where LIDs will interact among each other and be connected with the RTC system. Within the Smart Water Control project,

every water inflow and outflow from the University Campus in Innsbruck (Austria) will be measured in real-time. In combination with weather forecasts, these data will be used for RTC of the smart rain barrels to optimize the efficiency of the LID purposes.

In this context, this paper considers the conceptual implementation of Smart Rain Barrels (SRBs) into the existing stormwater system at the university campus in Innsbruck (Austria). As discussed in section 3.2.1, the campus area is currently divided into two independent drainage systems: RGs which receive from the surface areas (pavements, streets, green spaces) runoff and central stormwater system where roof areas runoff are directly discharged. This latter system is used for the implementation of the SRBs, but the SRBs can also be used to connect the central and decentral systems, by discharging into the LIDs and fully utilizing their capacities, or by directly discharging to the central system.

The model, developed by EPA Storm Water Management Model SWMM (see section 3.2.2), was considered as starting point for the purpose. Then to show the advantages of the SRBs under design conditions, the diameters were artificially reduced to 200 mm and 300 mm to observe flooding when applying the design rain events.

As first step, a simplified model for the SRBs was created, by considering the filling level in the sewer system for RTC. Since the main objective was to reduce the peak runoff rate in the conventional drainage network, the SRBs were implemented as additional storage volume and placed between the roof subcatchments and the inlet of the sewer system. The SRBs were controlled by rules consisting of a conditional clause (e.g. filling level of the sewer systems) and an action clause (e.g. different outflows from the rain barrel). more in detail, the outlet from the SRBs was closed when the filling level at the closest manhole was higher than a predefined height. As an initial assumption, a filling level of 60% at the manhole was used for peak runoff reduction in the sewer system. When the storage volume of the SRB was full, the overflow was routed into the drainage system.

First results showed that accumulated flood volume reductions of 18 – 40% can be achieved and that the location of the smart rain barrel and the storage size are important factors to reduce flooding. By this result emerged the capability on the rain barrels as urban stormwater management tool and not only as optimal device for water saving, even if this is the main purpose for which it is generally used.

Finally, the smart rain barrels could also be used to connect the central and decentral drainage systems, by discharging outflow into the LID systems or by directly draining the runoff into the central system.

3.5 Conclusions

In this chapter, the development of a microscale hydrodinamic model which combines traditional drainage infrastructures and LID system for enhancing the implementation of tools, devices and methods related to the smart campus project, i.e. smart water management case study at the University Innsbruck was presented.

Moreover, a global sensitivity analysis (GSA) of the model was carried out in order to identify the most influential parameters. The model's performances were analyzed at four rain gardens and for four model outputs: *Total Inflow, Surface Level, Storage Level* and *Surface Runoff* at the rain gardens. Results showed that, in terms of global sensitivity, an important role is taken by the *Depression Storage Impervious*, parameter related to the Inflow outcome, followed by the *Percentage of Impervious Area*. While, the findings obtained for the other three model outputs related to the rain gardens, emerged that the *Soil Hydraulic Conductivity* is one of the most sensitive parameters and it presents also the greater degree of interaction with the other factors. Only when the *Storage Level* output is considered, the *Seepage Rate parameter* precedes the soil hydraulic conductivity as most influential factors.

Therefore, in agreement with the studies, discussed in chapter 2, the soil hydraulic properties of infiltration/retention-based LID techniques, as rain garden, green roof or permeable pavement, take an important role for the hydraulic efficiency of the systems in terms of retention and detention of stormwater runoff. Thus, the identification of the soil hydraulic properties for LID system is crucial in order to correctly evaluate the hydraulic performance of such techniques. This main conclusion can be considered as useful suggestion for designers and experts in the field which have the aims to install and/or investigate LID full-scale implementation system. In this regard, this main conclusion was considered during the investigation on the extensive green roof located at University of Calabria, that will be presented in next chapter. Based on this results, in fact, the soil hydraulic properties of the extensive green roof were evaluated in laboratory using a simplified evaporation method.

Finally, the development of this model allowed also to elaborate the concept of an advanced LID systems, by the modeling implementation of a smart rain barrels, which represents a future research direction.

3.6 References

Ahiablame, L., & Shakya, R. (2016). Modeling flood reduction effects of low impact development at a watershed scale. Journal of environmental management, 171, 81-91. https://doi.org/10.1016/j.jenvman.2016.01.036

CHI PCSWMM. https://www.pcswmm.com/. Accessed 20 Mar 2018

Garofalo, G., Palermo, S., Principato, F., Theodosiou, T., & Piro, P. (2016). The influence of hydrologic parameters on the hydraulic efficiency of an extensive green roof in mediterranean area. Water, 8(2), 44. https://doi.org/10.3390/w8020044

Goncalves, M., Zischg, J., Rau, S., Sitzmann, M., Rauch, W., & Kleidorfer, M. (2018). Modeling the effects of introducing low impact development in a tropical city: A case study from Joinville, Brazil. Sustainability, 10(3), 728. https://doi.org/10.3390/su10030728.

Grimm K. (2016). Planinhalt: D – Raingarden und Baumgrube. Projekt/Objekt: Sanierung Campus Technikerstrasse – Aussenanlagen. Planverfasser: Karl Grimm – Landschaftsarchitekten.

Kerkez, B., Gruden, C., Lewis, M., Montestruque, L., Quigley, M., Wong, B., ... & Poresky, A. (2016). Smarter stormwater systems. DOI: 10.1021/acs.est.5b05870.

Maiolo, M., Carini, M., Capano, G., & Piro, P. (2017). Synthetic sustainability index (SSI) based on life cycle assessment approach of low impact development in the Mediterranean area. Cogent Engineering, 4(1), 1410272. https://doi.org/10.1080/23311916.2017.1410272

Morris, M. D. (1991). Factorial sampling plans for preliminary computational experiments. Technometrics, 33(2), 161-174.

Palla, A., & Gnecco, I. (2015). Hydrologic modeling of Low Impact Development systems at the urban catchment scale. Journal of hydrology, 528, 361-368. https://doi.org/10.1016/j.jhydrol.2015.06.050

Pianosi, F., Sarrazin, F., & Wagener, T. (2015). A Matlab toolbox for global sensitivity analysis. Environmental Modelling & Software, 70, 80-85. https://doi.org/10.1016/j.envsoft.2015.04.009

Pianosi, F., Beven, K., Freer, J., Hall, J. W., Rougier, J., Stephenson, D. B., & Wagener, T. (2016). Sensitivity analysis of environmental models: A systematic review with practical workflow. Environmental Modelling & Software, 79, 214-232. https://doi.org/10.1016/j.envsoft.2016.02.008

RainGrid. (n.d.). Stormwater Smartgrids. https://www.raingrid.com/stormwater-smartgrids/Accessed 26 Mar 2018

Rossman, L. A. (2010). Modeling low impact development alternatives with SWMM. Journal of Water Management Modeling.

Rossman, L. A. (2015). Storm Water Management Model User's Manual Version 5.1. Office of Research and Development. Water Supply and Water Resources Division. US Environmental Protection Agency.

Saltelli, A., Ratto, M., Andres, T., Campolongo, F., Cariboni, J., Gatelli, D., Saisana, M., Tarantola, S. (2008). Global Sensitivity Analysis. The Primer. Wiley, Hoboken

Sieker. (n.d.). Smart Cistern - Efficient rainwater usage based on precipitation forecast. http://www.sieker.de/en/products-and-services/product/smart-cistern-40.html. Accessed 26 Mar 2018

Zischg, J., Zeisl, P., Winkler, D., Rauch, W., & Sitzenfrei, R. (2018). On the sensitivity of geospatial low impact development locations to the centralized sewer network. Water science and technology, 77(7), 1851-1860. https://doi.org/10.2166/wst.2018.060

Chapter 4 - Hydrological Effectiveness of an Extensive Green Roof in Mediterranean Climate

In urban water management, green roofs provide a sustainable solution for flood risk mitigation. Numerous studies have investigated green roof hydrologic effectiveness and the parameters that influence their operation; many have been conducted on the pilot scale, whereas only some of these have been executed on full-scale rooftop installations. Several models have been developed, but only a few have investigated the influence of green roof physical parameters on performance. From this broader context, this chapter presents the results of a monitoring analysis of an extensive green roof located at the University of Calabria, Italy, in the Mediterranean climate region. Moreover, a modeling approach was used to evaluate the influence of the substrate depth on green roof retention. To achieve this last purpose and implement the model, based on findings obtained in the chapter 3, the soil hydraulic properties were measured in Laboratory. The findings of this chapter are already published in Palermo et al., 2019b (Paper II), but it is also linked with Paper III (Piro et al., 2019a). Finally, a future research direction in terms of smart optimization of the specific experimental site, linked to Paper V (Piro et al., 2019b) is here briefly presented.

4.1 Introduction

As discussed in section 2.2.1, green roof represent a source of storm water runoff mitigation by reducing the total runoff volume, peak flow rate, and delaying peak discharge time into the combined sewer systems.

So far several studies have analyzed green roofs (GRs) retention performance worldwide; many of these have been conducted on a pilot scale, generally consisting of different test beds or similar modules (Stovin et al., 2012; Buccola et al., 2011; Krebs et al., 2016); others have been conducted on a full-scale rooftop (Voyde et al., 2010; Carson et al., 2013; Fassman-Beck et al., 2013). However, not all of these have analyzed the GR behavior for a continuous monitoring period, evaluating each parameter on an event scale.

The hydraulic behavior of GRs has also been analyzed from a modeling point of view. Numerical models have been developed using software such as the Environmental Protection Agency (EPA)'s Storm Water Management Model (SWMM) (Krebs et al., 2016; Peng & Stovin, 2017; Cipolla et al., 2016; Principato et al., 2019), Soil, Water, Atmosphere, and Plant (SWAP) model (Metselaar, 2012), and HYDRUS model (Hilten et al., 2008; Palla et al., 2012; Li & Babcock, 2015; Brunetti et al., 2016;)

From the analysis of these studies, some indicators (runoff volume reduction, peak flow reduction, peak flow lag-time, etc.) have been used to estimate GR hydraulic effectiveness. As discussed in chapter 2, another useful lumped parameter, crucial for designing purposes is the subsurface runoff coefficient (SRC). In this regard, from a literature review completed by Garofalo et al. (2016), the SRC presented a large variability in mean value, ranging from 0.30 to 0.90. This wide range can be explained by analyzing, for each study, the climate conditions of the GR site, the GR's size (full-scale or pilot system), period of data analysis, the time step resolution, and the hydraulic and physical features.

Factors that typically influence GR water retention capacity can be grouped in two main categories: weather conditions (length of the antecedent dry weather period, season/climate, characteristics of rainfall event) and the GR's physical features (number of layers and materials, substrate depth, its hydraulic characteristics, type of vegetation, percentage of roof covered, roof geometry, and green roof age). Being unable to intervene in the weather conditions of the site where the installation is located, the choice of the physical characteristics of the substrate is crucial. In this regard, many studies have

observed that the hydraulic behavior of a GR is influenced by the substrate depth and type (Liu & Fassman-Beck, 2017; Feitosa & Wilkinson, 2016; Soulis et al., 2017). Some of these studies were conducted in the laboratory by considering constant rainfall data and not real data recorded by a rain gauge, whereas others considered the results of modeling simulations based on literature hydraulic soil properties and not real substrate hydraulic properties.

From this broader context, the first objective of this study was to present the field hydrological monitoring results of a specific extensive GR that has been installed at the University of Calabria, Italy, in a Mediterranean climate. To complete this analysis, first, one year of rainfall data (October 2015 to September 2016) recorded by a rain gauge located on the experimental site was selected. Secondly, the corresponding runoff from the GR was evaluated and compared with the runoff from an impervious roof, which was located at the same site. Thirdly, to analyze the green roof's hydraulic efficiency, the response in terms of the SRC, peak flow reduction (PFR), peak flow lag-time (PFL), and time to start of runoff (TSR) were determined on an event scale. The second objective of the study was to evaluate the influence of the soil depth on the retention capacity of a substrate soil for an extensive green roof in Mediterranean climate by considering the measured soil hydraulic properties and varying the thickness (from 9 to 15 cm) by means of the HYDRUS-1D model.

4.2 Materials and Methods

4.2.1 Experimental Site

The experimental green roof (Figure 4.1) was built in 2012 on the terrace of the Department of Mechanical, Energy and Management Engineering (DIMEG), at the University of Calabria, Italy, located 221 m above sea level in the Vermicelli Catchment. The University is in the south of Italy in the vicinity of Cosenza (39°18′ N 16°15′ E), under a Mediterranean climate condition, which is characterized by an average annual precipitation of 881.2 mm/year and a mean annual temperature of 15.5 °C (Brunetti et al., 2016).

Figure 4.1: The experimental green roof (GR) located at the University of Calabria, Italy. A map of Italy, with the location of the green roof (left), the GR experimental site (middle), and an axonometric detail stratigraphy (right). All the figures were captured or created by the Urban Hydraulic and Hydrology Laboratory, University of Calabria, Italy (Palermo et al., 2019b).

The green roof (GR) was built according to Italian regulation UNI 11235, and from top to bottom consisted of:

(1) a surface layer, vegetated with three native Mediterranean species;
(2) a commercial soil substrate, called "Terra Mediterranea" (Harpo spa, Trieste, Italy), with a maximum depth of 8 cm composed of a mineral terrain;
(3) a permeable geotextile with a weight of 105 g/m^2 to prevent fine soil particles from moving into the underlying layers;
(4) a drainage layer in polystyrene foam with a water storage capacity of 11 L/m^2 and a drainage capacity of 0.46 L·s^{-1}m^{-2};
(5) an anti-root layer consisting of a waterproof bituminous membrane with an anti-root additive, specific for green roof installation;
(6) an additional recovery waterproof membrane in elastobituminous membrane.

In detail, as discussed in depth by Brunetti et al. (2016), the soil substrate consists of a mineral soil with 74% gravel, 22% sand, and 4% silt and clay; it presents a measured bulk density of 0.86 g·cm^{-3} and 8% organic matter, which was determined in the laboratory using the Walkley–Black method. Among the three native Mediterranean species, two are herbaceous plants that are suited for well-drained soils (*Dianthus gratianopolitanus and Cerastium tomentosum*), and one is a succulent plant (*Carpobrotus edulis*), which is characterized by a high drought tolerance. More detail on the specific soil substrate hydraulic properties are reported in the results section, where the measurements recorded in the laboratory are provided.

To evaluate the hydraulic efficiency of this specific stratigraphy, the outflow collected from the GR, which is characterized by an area of 50 m^2 and a slope of 1%, was compared with that discharged by an impervious roof (IR) located on the same site, which presented an area of 40 m^2. The different areas of the GR and IR were considered during the outflow comparison analysis.

The GR water supply is guaranteed only by reusing the green roof's outflow, which was collected in a specific storage tank and distributed through a drip irrigation system. This irrigation system is activated during drought periods, generally occurring in summer when the precipitation volume for the specific climate condition is low and very high temperatures are recorded in accordance with low values of soil moisture measured in the soil substrate. By analyzing the whole dataset, the irrigation, actioned only during the driest days, did not affect the runoff results.

Rainfall depth was measured every minute using a tipping bucket rain gauge with a resolution of 0.254 mm, which was located on the roof.

The outflow rates were collected by a flow meter device, previously developed in Lab and installed at the base of the building, which consists of a vertically developed system, formed by a polyvinyl chloride (PVC) pipe with a sharp-crested weir. More detail on the design phase, experimental analysis and obtained calibrated equations can be found in Paper III (Piro et al., 2019a) and briefly described in section 4.2.1.1. The water level in the device was measured by a pressure transducer (Ge Druck PTX1830, GE Measurement & Control Solutions, Groby Leicester, UK), with a measurement range of 75 cm and an accuracy of 0.1% of the full scale, previously calibrated in the laboratory by using a water column to identify the relationship between the output signal in mA, obtained through a digital bench multimeter, and the water tension h, measured by a graduated rod. The water levels thus measured were continuously recorded in a SQLITE database system with a resolution of 1 min.

4.2.1.1 Green roof's flow measurement

In order to estimate the hydraulic benefits of LID solutions, an appropriate evaluation of the outflow rate is important. Therefore, the selection of a specific flowmeter device for LID system, which can also estimate the minimum flow rates released following small rain events, is necessary.

In this regard, as it is described in detail in Paper III (Piro et al., 2019a) to measure the outflow rates from several full-scale LID systems, including the extensive green roof located in the Urban Hydraulic Park at the University of Calabria, an innovative and simple flowmeter device was previously created in the laboratory.

As shown in Figure 4.2, the "measuring pipe", first developed in Lab and then installed at the experimental green roof site, consists of a vertical PVC pipe DN200 with a rectangular weir with a width (*b*) 12 mm. While, a system consisting of a concentric DN100 pipe, approximately 50 cm long, with openings at the bottom, was placed within the DN200 pipe to inject and dissipate the water energy mass. Moreover, to collect the water from the surface and infiltration systems with ease, the dissipation system was connected to the top by means of a special piece (diameter reducer DN200-DN100), thereby obtaining a total device length of 58 cm.

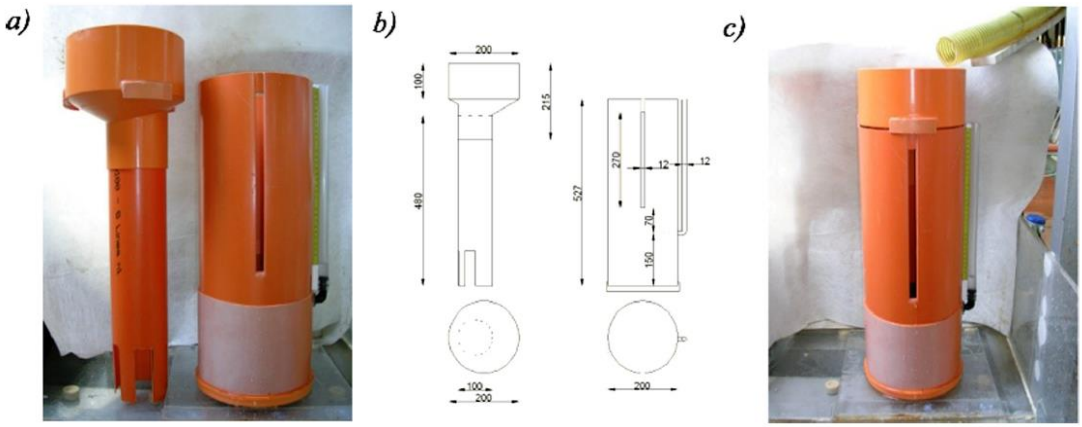

Figure 4.2: a) Energy sink and measuring tube not yet assembled; b) final dimensions of two elements; c) device prototype in vertical position, ready for laboratory tests (Piro et al., 2019a).

Final result of the study (Piro et al., 2019a) was the definition of the final discharge coefficient equation [4.1] expressed as function of *h/b* parameter and, therefore, of the theoretical flow rate expressed through the *discharge law* [4.2].

$$C_d = 0.77988 - 0.017232\left(\frac{h}{b}\right)^{0.5} \quad [4.1]$$

$$Q_{theoretical} = \frac{2}{3}\left[0.77988 - 0.017232\left(\frac{h}{b}\right)^{0.5}\right]\sqrt{2g}bh^{1.5} \quad [4.2]$$

where *h* is the upstream head over weir (mm), *b* is the weir width (mm), and *Q* is flow rate discharge by weir (l/s).

A high correlation with R^2 = 99.97% was achieved when comparing the flow (Q) obtained using equation [4.2] and that measured during the laboratory tests.

4.2.2 Data Analysis

For this study, rainfall and runoff data with one-minute time resolution that were recorded at the experimental site between October 2015 and September 2016 were considered.

In the first phase, from all the data collected, only the events with a precipitation depth greater than 2 mm were selected. This assumption was supported by an analysis of the recorded rainfall events. It was found that the 51 events (total volume around 28 mm) with rainfall depths less than 2 mm are unlikely to produce runoff volume for the specific site, confirming the assumption of Voyde et al. (2010). Individual events were also defined as being separated by continuous dry periods of at least six hours (Getter et al., 2007; Voyde et al. 2010; Stovin et al., 2012).

To consider the hydrological features of each storm event, the precipitation depth (PD), rainfall duration (D), rainfall intensity (i), antecedent dry weather period (ADWP, defined as the dry weather period between two independent rainfall events), and event return period (RP, defined as the average recurrence interval between events equaling or exceeding a specific magnitude (Shiau, 2003)), were evaluated at the event scale. To use a more rigorously probabilistic method, the characteristics of the selected storm events were evaluated by considering the local precipitation pattern. For the evaluation of the return period (RP) event, the experimental rainfall events were compared with the historical records obtained from the Regional Agency Prevention Environment in Calabria Region, Italy (ARPACAL) (Arpacal, 2019). To consider all the rainfall events here with a duration of more than one day, the intensity–duration–frequency (IDF) relationships were computed by analyzing the historical records of the annual maximum series for rainfall durations of 1, 3, 6, 12, and 24 hours (1923–2012) and for rainfall durations of 1, 2, 3, 4, and 5 days (1935–1999) according to data from the rain gauge station in Cosenza.

In the second phase, for each selected rainfall event and by using the data collected from the flux meter devices, the corresponding total outflow rate in terms of runoff depth (RD) from the GR and IR were evaluated. To obtain two comparable values, despite the

two different areas of the GR and IR, it was chosen to show the results in terms of runoff depth (mm) and not in terms of runoff flow (L/s or m^3/s)

Finally, in order to determine the green roof (GR) hydraulic effectiveness, precipitation hyetographs and corresponding hydrographs of GR and IR on event scale were elaborated and the hydrological indicators, reported below, were estimated.

- Subsurface Runoff Coefficient (SRC), expressed as percentage ratio between the total Runoff Depth from GR (RD_{GR}) and the total Precipitation Depth (PD):

$$SRC[\%] = \frac{RD_{GR}}{PD} \cdot 100 \quad [4.3]$$

- Peak Flow Reduction (PFR), calculated as the percentage difference between the hydrographs peak of IR (PF_{IR}) and GR (PF_{GR}):

$$\mathrm{PFR}[\%] = \frac{\mathrm{PF_{IR}} - \mathrm{PF_{GR}}}{\mathrm{PF_{IR}}} \cdot 100 \quad [4.4]$$

- Peak Flow Lag-time (PFL), determined as the time difference between the peak of precipitation hyetograph (t_P) and the peak of GR hydrograph ($t_{P_{GR}}$):

$$PFL[min] = t_{P_{GR}} - t_P \quad [4.5]$$

- Time to Start of Runoff (TSR), evaluated, according to Stovin et al. (2012), as the time difference between the start of rainfall (t_0) and the time at which the total runoff exceeded 0.01 mm ($t_{RD>0.01\mathrm{mm}}$):

$$TSR[min] = t_{RD>0.01mm} - t_0 \quad [4.6]$$

4.2.3 Soil hydraulic Properties

To evaluate the influence of the substrate depth on green roof retention capacity, a six-month dataset (January 2016 to June 2016) was selected from a weather station that measured the precipitation, velocity and direction of wind, air humidity, air temperature,

atmospheric pressure, and global solar radiation. The weather station is located at the University of Calabria, next to the experimental site (the Green Roof) cited in this chapter. Data from the station were collected online and were processed and stored in an SQL database. Reference evapotranspiration was calculated using the Penman–Monteith equation (Allen et al., 1998). An average value of albedo of 0.23 was assumed considering that the albedo for vegetated areas was 0.23 in a similar study conducted on a green roof (Lazzarin et al., 2005).

In order to assess the hydrological response of the green roof by variating the soil substrate depth using the HYDRUS model, the hydraulic properties of the soil materials were investigated.

There are many methods to assess the hydraulic properties of soils in different conditions (Arya, 2002; Dane & Hopmans, 2002). Among these, the simplified evaporation method (Schindler, 1980) is one of the most popular. This method is based on measuring both soil moisture and pressure head during a soil drying cycle under the effect of evaporation. The method was developed by Wind (1969), who introduced an iterative graphical procedure to estimate, first, the water retention curve from the average soil moisture and pressure head readings, and to define hydraulic conductivities from measured pressure head profile and variations in the water content distribution. Afterwards, several authors proposed simplifications to this method (Peters & Durner, 2008; Schindler et al., 2010a; Schindler et al., 2010b).

In this work, the hydraulic properties of the soil substrate were measured in the Urban Hydraulic and Hydrology Laboratory, University of Calabria, Italy using a simplified evaporation method proposed by Schindler et al. (2010a, 2010b) using the HYPROP® device (METER Group AG, Munich, Germany) (UMS GmbH, 2015). With this method, two tensiometers are placed at two depths of a soil sample sitting in a sample ring. The plane in the middle between the two tensiometers is identical to the horizontal symmetry plane of the column. The sample is saturated with water, basally closed, and set on a balance. The soil surface is open to the ambient atmosphere so that the soil water can evaporate. HYPROP® (METER Group AG, Munich, Germany) measures the water tension in two horizons of the soil sample over the evaporation process by means of two vertical tension shafts. The changing mass of the sample over time is assessed by weighing. The medial water content is calculated based on the mass change. This results in one measuring value per point in time for the retention curve.

The soil substrate of the green roof for the laboratory analysis was packed using a stainless-steel sampling ring with a volume of 250 mL. Then, the soil sample was saturated from the bottom before starting the evaporation test. The measurement unit and the tensiometers were degassed using a vacuum pump to reduce the potential nucleation sites in the demineralized water. At the end of the experiment, the sample was placed in an oven at 105 °C for 24 h; then, the dry weight was measured. For a complete description of the system, please refer to the UMS (UMS GmbH, 2015).

The numerical optimization procedure, HYPROP-FIT (Pertassek, et al.,2015), was used to simultaneously fit the retention and hydraulic conductivity functions to the experimental data obtained using the evaporation method. Fitting was accomplished using a non-linear optimization algorithm that minimizes the sum of the weighted squared residuals between model predictions and measurements.

The unimodal van Genuchten–Mualem model (Van Genuchten,1980) was evaluated for the description of soil hydraulic properties:

$$\Theta = \begin{cases} \frac{1}{(1+(\alpha|h|)^n)^m} & \text{if } h \leq 0 \\ 1 & \text{if } h > 0 \end{cases} \quad [4.7]$$

$$\Theta = \frac{\theta - \theta_r}{\theta_s - \theta_r} \quad [4.8]$$

$$K = \begin{cases} K_s \Theta^L \left[\left(1 - \left(1 - \Theta^{\frac{1}{m}} \right) \right)^m \right]^2 & \text{if } h < 0 \\ K_s & \text{if } h > 0 \end{cases} \quad [4.9]$$

$$m = 1 - \frac{1}{n} \quad [4.10]$$

where Θ is the effective saturation; α is a parameter related to the inverse of the air-entry pressure head (L^{-1}); θ_s and θ_r are the saturated and residual water contents,

respectively (–); n and m are pore-size distribution indices; K_s is the saturated hydraulic conductivity ($L \cdot T^{-1}$); and L is the tortuosity and pore-connectivity parameter.

4.2.4 Simulation Procedure

Based on the hydraulic properties measured by the simplified evaporation method proposed by Schindler et al. (2010a; 2010b) using the HYPROP® device (METER Group AG, Munich, Germany) UMS (2015), the runoff volume from a specific substrate for an extensive green roof by considering increasing values of soil depth using the HYDRUS-1D model was analyzed. In detail, the cumulative runoff volume from the green roof, in response to a continuous period of six months of rainfall events, was evaluated by varying the depth of the soil from time to time, not exceeding the maximum soil thickness of 15 cm generally attributed to an extensive green roof (6 cm, 9 cm, 12 cm, and 15 cm).

To run a simulation by varying the soil substrate, the HYDRUS-1D model (Šimůnek, et al., 2016) was used. HYDRUS-1D is a one-dimensional finite element model that is used for simulating the movement of water, heat, and multiple solutes in variably saturated porous media. HYDRUS-1D implements multiple uniform (single-porosity) and nonequilibrium (dual-porosity and dual-permeability) water flow models (Šimůnek et al., 2016).

The studied green roof was interpreted as a one-dimensional, single-porosity, porous medium system, which could be described by the Richards equation in the following form:

$$\frac{\partial \theta}{\partial z} = \frac{\partial}{\partial z}\left[K(h)\frac{\partial h}{\partial z} + 1\right] - S \qquad [4.11]$$

where θ is the volumetric water content, h is the soil water pressure head (L), $K(h)$ is the unsaturated hydraulic conductivity (LT^{-1}), z is the soil depth (L), and S is a sink term ($L^3L^{-3}T^{-1}$), which is defined as a volume of water removed from a unit volume of soil per unit of time due to plant water uptake. Feddes et al. (1978) defined S as:

$$S(h) = a(h) \cdot S_p \quad [4.12]$$

where *a(h)* is a dimensionless water stress response function that depends on the soil pressure head *h* and has a range of values between 0 ÷ 1, and S_p is the potential root water uptake rate.

Feddes et al. (1978) proposed a water stress response function, in which water uptake is assumed to be zero close to soil saturation and for pressure heads higher than the wilting point. Water uptake is assumed to be optimal between two specific pressure heads, which depend on a particular plant. Feddes parameters were assumed according to the HYDRUS database considering the vegetation as grass.

4.2.5 Numerical Domain and Boundary Conditions

The numerical domain representing the stratigraphy of the green roof consisted of one layer. An atmospheric boundary condition was applied at the soil surface using the precipitation and meteorological conditions measured. A seepage face boundary condition was specified at the bottom of the layer. A seepage face boundary acts as a zero-pressure head boundary when the bottom boundary node is saturated, and as a no-flux boundary when it is unsaturated. The initial pressure head was assumed to be constant in the entire domain and was set to −100 cm.

4.3 Results and Discussion

4.3.1 Rainfall Events

The whole studied period was characterized by 62 rainy events and one snowy event (19 January 2016), which was not considered in this study (Table 4.1), for a total precipitation depth (PD) of 1256.3 mm ranging from 2.0 mm to 120.1 mm with a mean value of 20.3 mm. For the whole dataset and the specific climate conditions, more than half (51.6%) of the rainfall events had a precipitation depth less than 10 mm, while 24.2% had a precipitation depth between 10–30 mm, 16.1% had a precipitation depth between 30–50 mm, 3.2% had a precipitation depth between 50–70 mm, 1.6% (one event) had a

precipitation depth between 70–90 mm, one event had a precipitation depth between 90–110 mm, and one had a precipitation depth greater than 110 mm. This analysis is representative of the specific precipitation pattern where the experimental site is located, and therefore is affected by the Mediterranean climate condition characterized by hot and dry summers and cool and wet winters (Garofalo et al., 2016).

Table 4.1: Hydrological characteristics of each rainfall event collected from October 2015 to September 2016 on the experimental site. *PD*: precipitation depth, *D*: rainfall duration, Mean *i*: mean rainfall intensity, *Max i*: maximum rainfall intensity, *ADWP*: antecedent dry weather period, and *RP*: return period (Palermo et al., 2019b).

No.	Date	PD	D	Mean i	Max i	ADWP	RP
	(dd/mm/yyyy; hh:mm)	(mm)	(hh:mm)	(mm/h)	(mm/h)	(hh:mm:ss)	(years)
1	07/10/2015; 07:47	42.2	15:05	2.8	121.9	-	<1
2	09/10/2015; 19:21	24.1	16:32	1.5	167.6	43:40	<1
3	10/10/2015; 23:25	48.3	17:11	2.8	106.7	11:33	<1
4	15/10/2015; 08:01	6.4	04:24	1.4	15.2	90:45	<1
5	21/10/2015; 14:51	120.1	42:55	2.8	45.7	146:25	<20
6	29/10/2015; 13:10	63.3	35:32	1.8	61.0	147:25	<2
7	21/11/2015; 23:26	37.1	10:37	3.5	30.5	526:45	<1
8	23/11/2015; 16:30	13.0	04:19	3.0	15.2	30:28	<1
9	24/11/2015; 17:24	97.3	61:31	1.6	76.2	20:34	<3
10	28/11/2015; 08:49	2.8	01:53	1.5	15.2	25:54	<1
11	10/12/2015; 13:05	8.4	02:48	3.0	15.2	290:22	<1
12	03/01/2016; 06:04	66.3	36:28	1.8	76.2	566:10	<2
13	05/01/2016; 02:51	3.3	08:15	0.4	30.5	08:19	<1
14	06/01/2016; 05:45	24.6	24:08	1.0	30.5	18:37	<1
15	07/01/2016; 19:36	9.9	08:58	1.1	15.2	13:43	<1
16	12/01/2016; 19:02	6.1	08:43	0.7	30.5	110:28	<1
17	15/01/2016; 21:39	24.9	25:51	1.0	15.2	58:22	<1
18	11/02/2016; 08:01	23.4	04:54	4.8	30.5	519:58	<1
19	12/02/2016; 06:25	18.8	07:07	2.6	45.7	17:30	<1
20	12/02/2016; 23:22	74.9	35:24	2.1	76.2	09:49	<3
21	18/02/2016; 05:26	45.2	18:25	2.5	45.7	90:40	<1
22	20/02/2016; 12:15	4.6	00:48	5.7	30.5	36:24	<1
23	23/02/2016; 22:11	3.1	02:55	1.0	15.2	81:07	<1
24	26/02/2016; 03:52	10.9	19:30	0.6	30.5	50:46	<1
25	01/03/2016; 00:00	4.1	01:21	3.0	15.2	72:37	<1
26	01/03/2016; 07:19	31.0	15:33	2.0	45.7	05:58	<1
27	03/03/2016; 06:13	40.9	18:14	2.2	61.0	31:21	<1
28	07/03/2016; 06:13	7.4	14:36	0.5	15.2	77:46	<1
29	09/03/2016; 14:42	4.8	06:51	0.7	15.2	41:52	<1
30	12/03/2016; 06:27	6.1	08:03	0.8	15.2	56:54	<1
31	15/03/2016; 08:06	9.1	01:49	5.0	30.5	65:36	<1
32	16/03/2016; 14:38	27.9	20:10	1.4	30.5	29:33	<1
33	23/03/2016; 07:43	34.3	22:30	1.5	91.4	140:55	<1
34	24/03/2016; 23:08	2.8	01:15	2.2	15.2	16:55	<1
35	08/04/2016; 08:33	5.3	00:54	5.9	30.5	344:10	<1
36	08/04/2016; 21:12	2.3	02:12	1.0	15.2	11:46	<1
37	09/04/2016; 20:39	15.7	08:36	1.8	30.5	21:13	<1
38	23/04/2016; 18:12	8.1	00:36	13.5	61.0	325:01	<1
39	24/04/2016; 04:00	11.2	11:12	1.0	106.7	09:13	<1
40	25/04/2016; 04:38	2.5	02:00	1.3	15.2	13:27	<1

Table 4.1 *Cont.*

No.	Date	PD	D	Mean i	Max i	ADWP	RP
	(dd/mm/yyyy; hh:mm)	(mm)	(hh:mm)	(mm/h)	(mm/h)	(hh:mm:ss)	(years)
41	25/04/2016; 12:45	8.1	05:36	1.5	76.2	06:07	<1
42	28/04/2016; 21:44	14.7	08:36	1.7	15.2	75:25	<1
43	01/05/2016; 11:00	3.3	07:50	0.4	15.2	52:40	<1
44	02/05/2016; 06:28	23.9	24:54	1.0	15.2	11:40	<1
45	04/05/2016; 03:49	5.3	04:00	1.3	15.2	20:25	<1
46	12/05/2016; 03:47	3.6	09:36	0.4	30.5	188:01	<1
47	14/05/2016; 19:09	35.6	21:42	1.6	61.0	53:48	<1
48	20/05/2016; 09:15	2.5	02:48	0.9	15.2	112:27	<1
49	13/06/2016; 01:01	2.8	03:30	0.8	15.2	564:57	<1
50	19/06/2016; 11:34	2.5	06:00	0.4	15.2	151:06	<1
51	24/06/2016; 03:34	7.9	01:42	4.6	15.2	106:03	<1
52	26/07/2016; 14:43	2.0	00:12	10.2	45.7	777:28	<1
53	07/08/2016; 13:28	8.4	10:24	0.8	15.2	286:34	<1
54	11/08/2016; 22:29	2.3	00:12	11.5	30.5	391:36	<1
55	23/08/2016; 14:51	22.4	22:06	1.0	76.2	280:10	<1
56	31/08/2016; 23:31	6.9	06:54	1.0	30.5	178:37	<1
57	06/09/2016; 03:44	36.3	07:12	5.0	76.2	117:21	<1
58	08/09/2016; 03:50	13.7	07:18	1.9	15.2	40:52:48	<1
59	13/09/2016; 15:29	12.5	02:42	4.6	91.4	124:24	<1
60	17/09/2016; 04:22	7.9	05:48	1.4	45.7	82:10	<1
61	18/09/2016; 23:19	38.9	20:48	1.9	61.0	37:10	<1
62	22/09/2016; 05:49	2.3	00:42	3.3	15.2	57:40	<1
	Mean	20.3	11:47	2.5	40.8	129:27	
	Minimum	2.0	00:12	0.4	15.2	05:58	
	Maximum	120.1	61:31	13.5	167.6	777:28	
	Sum	1256.3					

October 2015, with 340.4 mm of precipitation depth (24.2% of the total considered period), was the wettest month, whereas July 2016, with only 2.0 mm, was the driest month in this experimental period.

By comparing all the 62 monitored storms events in terms of total rainfall depth and duration with the relevant intensity–duration–frequency (IDF) curves, which considered the event return periods found using the historical data collected from the rain gauge station in Cosenza, it emerges that most of the rainfall events fall below the one-year return period threshold. This finding is important for the analysis of the precipitation events, and for the subsequent evaluations of the hydraulic efficiency of the green roof.

4.3.2 Green Roof Hydrologic Effectiveness

To evaluate the hydrological performance of the experimental green roof, the runoff volume - which was generated in response to the 62 rainfall events recorded at the experimental site - and the hydrological indicators, were both analyzed.

Table 4.2 reports the results obtained in terms of total runoff depth (RD) and subsurface runoff coefficient (SRC) for each event. For peak flow reduction (PFR), peak flow lag-time (PFL), and time to start runoff (TSR), only the results for rainfall events with a precipitation depth (PD) greater than 8 mm are shown. In detail, the choice to evaluate the PFR, PFL, and TSR indexes for only for some events was based on the evaluations conducted on rainfall events with precipitation depths less than 8 mm, which were almost completely preserved by the green roof. In this regard, having found a minimal runoff for these events, it was difficult to identify a demarcated hydrograph peak as well as the start of the hydrograph, which was considerably delayed. The same situation was found for event 53, which, despite having a rainfall depth of 8.4 mm, had a minimal runoff volume that was probably affected by the long event duration and the high temperature of the period (August), and therefore was not suitable for the analysis. Table 4.2 also reports the mean, minimum, and maximum values for each hydrological indicator.

Table 4.2: Hydrological performance indicators for GR at event scale. *PD*—precipitation depth, *RD*—runoff depth, *SRC*—subsurface runoff coefficient, *PFR*—peak flow reduction, *PFL*—peak flow lag-time, *TSR*—time to start runoff (Palermo et al., 2019b).

No.	Date	PD	RD	SRC	PFR	PFL	TSR
	(dd/mm/yyyy; hh:mm)	(mm)	(mm)	(%)	(%)	(min)	(min)
1	07/10/2015; 07:47	42.2	20.0	47.4	65.4	6.0	17.0
2	09/10/2015; 19:21	24.1	10.8	44.8	17.9	5.0	23.0
3	10/10/2015; 23:25	48.3	31.0	64.2	13.3	2.0	10.0
4	15/10/2015; 08:01	6.4	0.4	6.3	-	-	-
5	21/10/2015; 14:51	120.1	100.0	83.3	28.3	9.0	30.0
6	29/10/2015; 13:10	63.3	46.4	73.3	52.6	531.0	51.0
7	21/11/2015; 23:26	37.1	13.0	35.0	83.0	468.0	200.0
8	23/11/2015; 16:30	13.0	4.2	32.3	82.0	197.0	60.0
9	24/11/2015; 17:24	97.3	79.5	81.7	44.3	207.0	10.0
10	28/11/2015; 08:49	2.8	0.4	14.3	-	-	-
11	10/12/2015; 13:05	8.4	1.6	19.0	95.2	168.0	15.0
12	03/01/2016; 06:04	66.3	32.7	49.3	75.5	1647.0	54.0
13	05/01/2016; 02:51	3.3	0.3	9.1	-	-	-
14	06/01/2016; 05:45	24.6	12.9	52.4	51.3	57.0	5.0
15	07/01/2016; 19:36	9.9	6.4	64.6	36.6	369.0	3.0
16	12/01/2016; 19:02	6.1	1.1	18.0	-	-	-
17	15/01/2016; 21:39	24.9	13.2	53.0	29.6	1447.0	24.0
18	11/02/2016; 08:01	23.4	4.1	17.5	79.7	18.0	42.0
19	12/02/2016; 06:25	18.8	11.1	59.0	27.6	58.0	102.0
20	12/02/2016; 23:22	74.9	56.0	74.8	22.5	8.0	5.0
21	18/02/2016; 05:26	45.2	30.4	67.3	33.6	55.0	39.0
22	20/02/2016; 12:15	4.6	0.9	19.6	-	-	-
23	23/02/2016; 22:11	3.1	0.1	3.2	-	-	-
24	26/02/2016; 03:52	10.9	4.6	42.2	73.6	13.0	42.0
25	01/03/2016; 00:00	4.1	0.7	17.1	-	-	-
26	01/03/2016; 07:19	31.0	19.9	64.2	32.1	49.0	73.0
27	03/03/2016; 06:13	40.9	29.4	71.9	41.3	1280.0	154.0
28	07/03/2016; 06:13	7.4	2.1	28.4	-	-	-
29	09/03/2016; 14:42	4.8	0.9	18.8	-	-	-
30	12/03/2016; 06:27	6.1	1.6	26.2	-	-	-

Table 4.2 *Cont.*

No.	Date	PD	RD	SRC	PFR	PFL	TSR
	(dd/mm/yyyy; hh:mm)	(mm)	(mm)	(%)	(%)	(min)	(min)
31	15/03/2016; 08:06	9.1	3.8	41.8	44.9	124.0	3.0
32	16/03/2016; 14:38	27.9	19.4	69.5	41.6	897.0	73.0
33	23/03/2016; 07:43	34.3	16.1	46.9	74.5	9.0	26.0
34	24/03/2016; 23:08	2.8	0.1	3.6	-	-	-
35	08/04/2016; 08:33	5.3	0.3	5.7	-	-	-
36	08/04/2016; 21:12	2.3	0.0	0.0	-	-	-
37	09/04/2016; 20:39	15.7	5.8	36.9	86.5	8.0	11.0
38	23/04/2016; 18:12	8.1	1.8	22.2	92.9	11.0	15.0
39	24/04/2016; 04:00	11.2	2.9	25.9	62.1	4.0	10.0
40	25/04/2016; 04:38	2.5	0.2	8.0	-	-	-
41	25/04/2016; 12:45	8.1	4.2	51.9	73.3	1.0	4.0
42	28/04/2016; 21:44	14.7	5.8	39.5	*	521.0	108.0
43	01/05/2016; 11:00	3.3	0.3	9.1	-	-	-
44	02/05/2016; 06:28	23.9	16.9	70.7	72.8	1253.0	399.0
45	04/05/2016; 03:49	5.3	1.3	24.5	-	-	-
46	12/05/2016; 03:47	3.6	0.0	0.0	-	-	-
47	14/05/2016; 19:09	35.6	23.3	65.4	38.3	512.0	132.0
48	20/05/2016; 09:15	2.5	0.0	0.0	-	-	-
49	13/06/2016; 01:01	2.8	0.0	0.0	-	-	-
50	19/06/2016; 11:34	2.5	0.0	0.0	-	-	-
51	24/06/2016; 03:34	7.9	0.2	2.5	-	-	-
52	26/07/2016; 14:43	2.0	0.0	0.0	-	-	-
53	07/08/2016; 13:28	8.4	0.2	2.4	-	-	-
54	11/08/2016; 22:29	2.3	0.0	0.0	-	-	-
55	23/08/2016; 14:51	22.4	7.2	32.1	93.0	5.0	1.0
56	31/08/2016; 23:31	6.9	0.0	0.0	-	-	-
57	06/09/2016; 03:44	36.3	13.4	36.9	*	34.0	28.0
58	08/09/2016; 03:50	13.7	5.1	37.2	74.2	324.0	5.0
59	13/09/2016; 15:29	12.5	4.4	35.2	89.5	8.0	3.0
60	17/09/2016; 04:22	7.9	0.4	5.1	-	-	-
61	18/09/2016; 23:19	38.9	20.9	53.7	19.0	16.0	45.0
62	22/09/2016; 05:49	2.3	0.0	0.0	-	-	-
	Mean (**)	20.3	11.1	32.0			
	Minimum (**)	2.0	0.0	0.0			
	Maximum (**)	120.1	100.00	83.3			
	Sum (**)	1256.3	689.7				
	Mean (***)	32.5	19.4	50.4	56.0	294.9	52.1
	Minimum (***)	8.1	1.6	17.5	13.3	1	1
	Maximum (***)	120.1	100	83.3	95.2	1647	399
	Sum (***)	1137.0	678.2				

* Due to an interruption of the sensor signal, it was not possible to evaluate the runoff from the conventional roof (IR); thus, the result in terms of PFR was not evaluated; ** Values evaluated considering the whole dataset (62 rainfall events); *** Values estimated by excluding the storm events with rainfall depth less than 8 mm and the rainfall event 53.

By analyzing the results in Table 4.2, it was found that the SRC exhibits a high variability, ranging from 0% to 83.3% with a mean value of 32.0% when the whole dataset (62 storms event) was considered; meanwhile, it ranges from 17.5% to 83.3% with a mean value of 50.4% for storm events with rainfall depths more than 8 mm (26 events) and excluding event 53, too. In this regard, this increase of the mean value of SRC is due to the

exclusion by the average evaluation of 27 storm events, which were almost totally retained by the green roof, and are the same events that are not considered also for the other indexes (PFR, PFL and TSR). This first result, in accordance with a previous study carried out for an extensive green roof in Mediterranean climate (Cipolla et al.2016) and fully falling within the range of the variation mentioned in Section 4.1 (30–90%), confirms the good response of the specific GR, but simultaneously highlights how the SRC index is strongly influenced by weather conditions. For example, by comparing two events with different rainfall depths, such as Event 9 (PD = 97.3 mm) and Event 18 (PD = 23.4 mm), the SRC values were 81.7% and 17.5%, respectively. Two events with similar rainfall depths, such as Event 7 (PD = 37.1 mm) and Event 27 (PD = 40.9 mm), produced SRC values of 35.0% and 71.9%, respectively. These differences in SRC given similar precipitation can be understood by observing the antecedent dry weather period (ADWP) of the two events, which affects the initial soil moisture condition and therefore the soil retention capacity. Event 7, with a retention of 65.0% (SRC = 35.0%), occurred after more than 20 continuous dry days, whereas when Event 27 happened, at the beginning of the event, the soil substrate had a reduced retention capacity due to the short ADWP (just over one day); therefore, this results in a higher SRC than Event 7.

A similar conclusion can be reached by observing the other three indices (PFR, PFL, and TSR) in Table 4.2. It was found that PFR, PFL, and TSR - with mean values of 56.0%, 294.9 min, and 52.1 min, respectively - were highly variable, and principally associated with the climate condition before the beginning of the storm events, and therefore, with the initial humidity of the soil.

By considering the results in Figure 4.3, which show the regression plots (significance level equal of 0.5) estimated for selected hydrological parameters, it is noted a linear strong relationship ($R^2 = 0.95$) between RD and PD (Figure 4.3a) and a logarithmic relationship ($R^2 = 0.77$) between SRC and PD (Figure 4.3b). By analyzing the Figure 4.3a, it was found that RD tended to be 0 to 10 mm for PD values lower than 20 mm, whereas Figure 4.3b shows SRC values ranging between 75–85% for PD greater than 70 mm, and a significant variation in the SRC value for PD less than 10 mm, principally depending on the ADWP.

All these findings confirm the findings reported in the literature (Stovin et al., 2012; Garofalo et al., 2016), which identified ADWP as a significant determinant of hydrological performance. This specific hydrological parameter, which ranged from around 6 hours to more than 777 hours in this study (Table 4.1), significantly affects the substrate moisture conditions and thus the green roof hydrological response in terms of SRC, PFR, PFL, and TSR indexes.

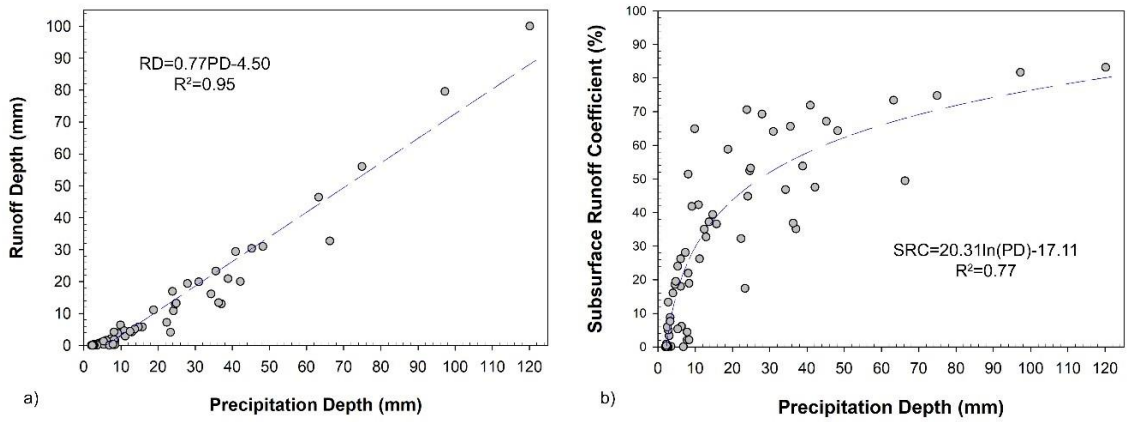

Figure 4.3: Regression plots (significance level = 0.05) for selected key parameters, by using all the rainfall events: (a) runoff depth (RD) as a function of precipitation depth (PD) and (b) subsurface runoff coefficient (SRC) as a function of precipitation depth (PD) (Palermo et al., 2019b).

All the results that were analytically evaluated in terms of runoff volume, rainfall intensity, and hydrological indexes, provided excellent feedback, as shown in Figure 4.4, where hyetographs and corresponding hydrographs of the GR (black line) and the IR (grey color) are shown for eight selected rainfall events. These storms events were selected to cover a wide range of precipitation depths, durations, and antecedent dry weather conditions.

The events shown in Figure 4.4 confirm the hydrological efficiency of the experimental green roof in terms of runoff volume reduction and peak hydrograph mitigation compared to the conventional roof, and the delay in peak flow compared with the hyetograph.

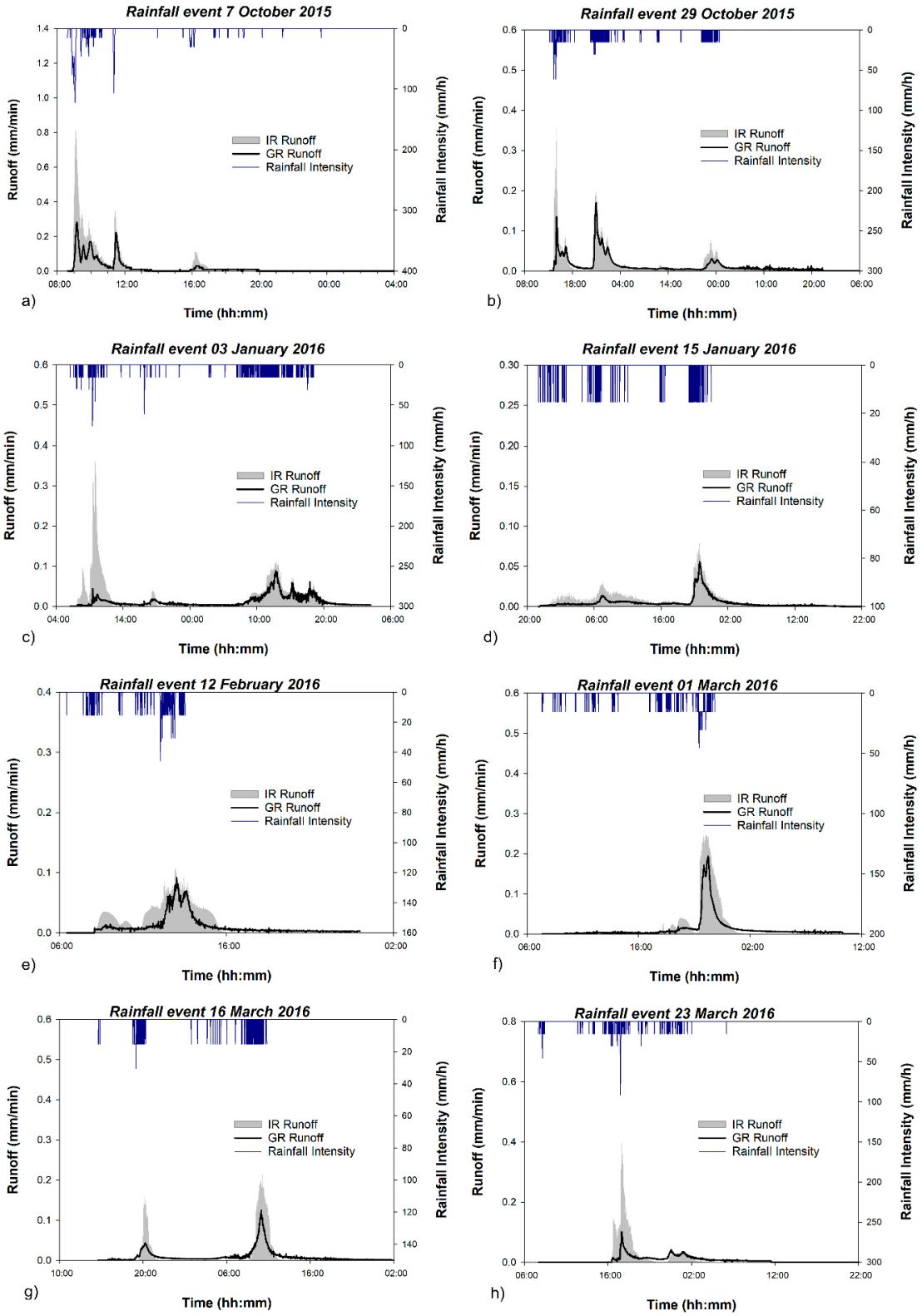

Figure 4.4: Hyetographs and corresponding green roof (GR) and impervious roof (IR) runoff hydrographs for eight selected rainfall events: (a) 7 October 2015 (total precipitation depth (PD) = 42.2 mm and total green roof runoff depth (GR-RD) = 20.0 mm); (b) 29 October 2015 (PD = 63.3 mm and GR-RD = 46.4 mm); (c) 03 January 2016 (PD = 66.3 mm and GR-RD = 32.7 mm); (d) 15 January 2016 (PD = 24.9 mm and GR-RD = 13.2 mm); (e) 12 February 2016 (PD = 18.8 mm and GR-RD = 11.1 mm); (f) 01 March 2016 (PD = 31.0 mm and GR-RD = 19.9 mm); (g) 16 March 2016 (PD = 27.9 mm and GR-RD = 19.4 mm); (h) 23 March 2016 (PD = 34.3 mm and GR-RD = 16.1 mm) (Palermo et al., 2019b).

4.3.3 Soil Hydraulic Properties

The soil hydraulic properties of the soil substrate measured with the evaporation method are shown in Figure 4.5. The measured soil water retention curve (SWRC) is well described across the entire water content range (blue points in Figure 4.5a), whereas the measured points of the hydraulic conductivity function (blue points in Figures 4.5b and 4.5c) are concentrated in the dry range between 10–30% of the volumetric water content. The measured data were imported into HYPROP-FIT (METER Group AG, Munich, Germany) software to fit the analytical hydraulic property functions.

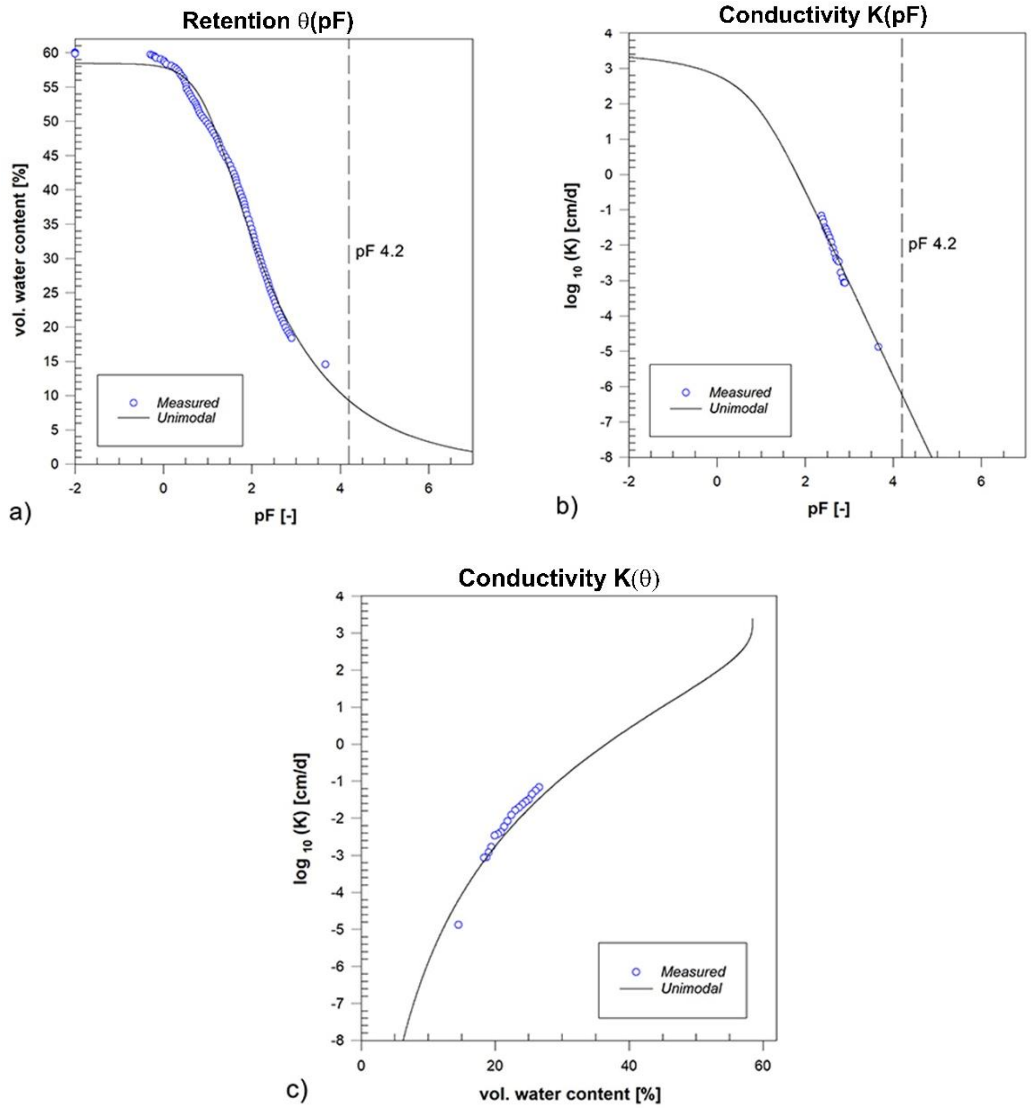

Figure 4.5: (a) The soil water retention curve showing the volumetric water content (θ) versus *pF* (decimal log of tension, expressed as pressure head in the unit of cm); (b) the conductivity curves showing the log of the hydraulic conductivity (*K*) versus *pF*, and (c) the log of hydraulic conductivity versus volumetric water content (θ) (Palermo et al., 2019b).

The unimodal van Genuchten Mualem model (VGM) (Van Genuchten,1980) was fitted (Figure 4.5, black line). The root mean square error (RMSE) values for retention and conductivity functions were 0.01 cm^3cm^{-3} and 0.16 log K, cm/day, respectively.

The hydraulic properties obtained by fitting the van Genuchten Mualem model and their limit of confidence are described in Table 4.3, where α is a parameter related to the inverse of the air-entry pressure head (L^{-1}); θ_s and θ_r are the saturated and residual water contents, respectively; n is a pore-size distribution index; K_s is the saturated hydraulic conductivity (LT^{-1}); and l is the tortuosity and pore-connectivity parameter.

Table 4.3: Estimated soil hydraulic parameters. θr, residual water content; θs, saturated water content; α, inverse of the air-entry pressure head; n, pore-size distribution index; and l, tortuosity (Palermo et al., 2019b).

Parameter	Value	Lower Limit	Upper Limit	Unit of Measure
θr	0.00	0	0.07	cm^3cm^{-3}
θs	0.58	0.57	0.59	cm^3cm^{-3}
α	0.09	0.07	0.11	cm^{-1}
n	1.25	1.20	1.32	-
Ks	3000	0.00	4000	cm day^{-1}
l	0.5	-	-	-

The model used indicates a soil characterized by a very high permeability, which corresponds well with the textural composition of the GR substrate. This characteristic is well suited for green roof substrates, which must guarantee fast drainage and avoid water ponding on the surface, even during intense precipitation. Narrow confidence intervals for parameters indicate high confidence in their estimation, whereas a huge range in the estimation of K_s indicates that the evaporation method is not accurate for the determination of the hydraulic conductivity near saturation, and this is reflected in the estimation of K_s. To improve the accuracy in the estimation of the hydraulic conductivity near saturation, other methods and devices should be used such as Ksat (UMS GmbH, 2012) based on the Darcy experiment.

4.3.4 Green Roof Hydraulic Behavior for Different Soil Depths

As stated above, the hydraulic parameters of the soil substrate were used in HYDRUS-1D to describe the hydrological behavior of the green roof with different soil depths.

Cumulative inflow and outflow fluxes of the green roof are reported in Figure 4.6. By increasing the soil substrate depth, the green roof was able to reduce the total runoff

volume from 22% to 24% in response to the same total precipitation during the considered period.

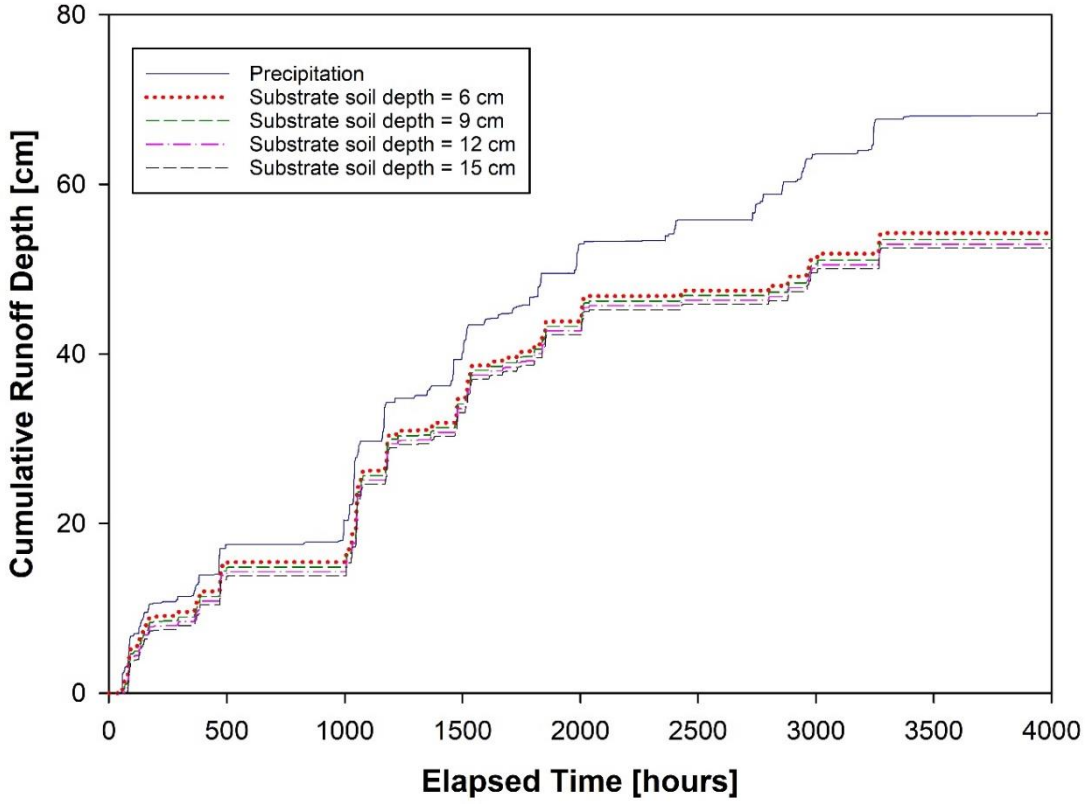

Figure 4.6: Cumulative rainfall and cumulative modeled runoff for different values of soil depth (*H*) by considering a six-month dataset (*January–June 2016*) (Palermo et al., 2019b).

The steep gradients in the cumulative outflow indicate that the green roof responded quickly to precipitation. This aspect is directly related to the limited thickness of the substrate, which reduces the possible delay.

During simulations, mass balance errors were always below 1%, which is generally considered acceptable at these low levels.

As shown in Figure 4.6, the outflow volume reduction achieved by doubling the soil substrate depth under the same climate conditions was not significant. This result, which confirms the findings of Feitosa and Wilkinson (2016), can be justified by observing that the six-month dataset used for these simulations was obtained in winter and spring, where evapotranspiration is not predominant. Based on these findings, since the adoption of a deeper soil depth does not contribute to a significant increase in the retention capacity, it would only represent a structural overloading, while a substrate depth of six centimeters would be an ideal soil depth for extensive green roofs.

4.4 Future Perspective: GR and RHW from a Smart and Innovative Point of View

Evaluated the hydrological effectiveness of the extensive green roof located at University of Calabria, by considering experimental analysis and modeling investigation, in this section a future research challenge is discussed. The idea, here presented, is already presented in the Paper V (Piro et al., 2019b) published and annexed to this thesis.

The integration of Green Roof (GR) and RainWater Harvesting (RWH) system, like in the case of the experimental site of University of Calabria, allows considerable benefits in terms of rational management of water resource. Furthermore, different studies have considered the RWH systems as a good strategy to limit environmental impacts that the on-going urbanization produce on the drainage network and receiving water bodies, but only few have analyzed these ones as smart objects for an integrated management of the water resource.

Therefore, an innovation in the field of Urban drainage is look at the single techniques GR and RWH as smart objects, optimizing them with ICT technologies, based on the IoT (Internet of Things) paradigm.

A new aspect, in fact, could lie in the integration of GRs and RWH techniques through a complex network equipped with: *sensors*, which allow rapid quantitative assessments from a hydraulic, energy and environmental point of view; *regulators* or *actuators*, able to modify the processes in progress; *transducers* that allow the conversion of the data detected in command; *control units* that report the variables to the pre-established threshold values.

According on what was previously discussed about Green Roof experimental site of University of Calabria, the rainwater collected in the storage tank is re-introduced through the irrigation system at fixed time and in quantity set by the operator of the experimental site. The optimization of this system could be achieved by considering the smart automation through the estimation of water content and the evaluation on the wheatear situation. More in detail, when the water content, monitored by specific sensors dislocated within the layers of the green roof, falls below a threshold value that causes the plant water stress, the smart system sends a command to activate the irrigation withdrawing the water from the storage tank in the needed rates to re-reach the appropriate water content. The Weather Station located at the experimental site offers also the opportunity to make

preventive estimates, based on the rainfall regime and solar radiation recorded on the site, so as to better calibrate the operation of the irrigation system.

Through these innovative strategies, in fact, not only a hydraulic benefit would be obtained, optimizing the reuse of the rainwater and reducing the flow to the drainage system, but also a thermo-energetic one. The activation of the irrigation system could also be carried out following the temperature measurements in the rooms below in order to improve the summer thermal comfort of the building.

4.5 Conclusions

Green roofs may be a solution for minimizing the impact of urbanization on the hydrologic cycle. Given the important role they play in the mitigation of urban flooding several studies have focused on the analysis of their hydraulic behavior.

In this study, a field monitoring campaign for one year on a full-scale extensive green roof was conducted. Hydrological indices (*subsurface runoff coefficient, peak flow reduction, peak flow lag-time*, and *time to start runoff*) were estimated on an event scale, and possible correlations between these indicators and hydrological features of storm events were evaluated. The findings showed that the subsurface runoff coefficient (SRC) ranges from 17.5% to 83.3% with an average value of 50.4% for the rainfall events with a precipitation depth more than 8 mm (35 rainfall events) and by excluding Event 53, which presents an average value of 32.0% for the whole dataset (62 rainfall events). This result, which is evaluated by considering an event scale analysis, falls in the range (around 30–90%) evaluated in literature (Garofalo et al., 2016) under different climate conditions and temporally scales. In addition, as the subsurface runoff coefficient is an extremely useful index to quantify the hydraulic efficiency of a green roof, this finding confirms the optimal retention capacity of the experimental green roof in the Mediterranean climate. Therefore, the average value of the subsurface runoff that was obtained in this study for the specific green roof can be taken into account during preliminary design choices for the construction of green roofs in Mediterranean climate conditions.

Finally, to evaluate the influence of soil thickness on the hydraulic behavior of a green roof, the HYDRUS 1D model was used to consider green roofs with soil depths of 6 cm, 9 cm, 12 cm, and 15 cm. The results obtained in this phase show how the considered substrate depths for green roofs were able to achieve a runoff volume reduction of 22% to

24% during the selected period for the Mediterranean climate conditions without observing flow over the top surface of the soil. These findings are in accordance with the literature (Feitosa and Wilkinson, 2016), which may be explained by the dataset used in these simulations being obtained during winter and spring where evapotranspiration, one of the key factors reducing storm water in the hydrological cycle, was not predominant. Thus, in the field of extensive green roofs, as the outflow volume reduction achieved by increasing the soil depth was not significant, the ideal depth for soil substrate would be six centimeters. Finally, since the outflow volume reduction achieved by doubling the soil substrate depth under the same climate conditions is not significant, the maximum depth of 15 cm is not recommended for adoption considering the structural overloading.

Future research challenge is look at the single techniques green roof and rainwater harvesting, located at University of Calabria, as smart objects, optimizing their benefits by ICT technologies, based on the IoT (Internet of Things) paradigm.

Following this study and based on the findings obtained at building scale, next chapter was focused on the analysis of hydrological effectiveness of Low Impact development solutions at large-urban scale in a south Italian case study.

4.6 References

Allen, R.G.; Pereira, L.S.; Raes, D.; Smith, M. (1998). FAO Irrigation and Drainage Paper No. 56: Crop Evapotranspiration; FAO: Rome, Italy.

Arya, L.M. (2002). Wind and hot-air methods. In Methods of Soil Analysis; Part 4. Physical Methods; Dane, J.H., Topp, G.C., Eds.; SSSA: Madison, WI, USA; 916–926. https://doi.org/10.1016/j.enbuild.2005.02.001

Arpacal, 2019. Available online: http://www.cfd.calabria.it/index.php/dati-stazioni/dati-storici (accessed on 24 January 2019).

Buccola, N., & Spolek, G. (2011). A pilot-scale evaluation of greenroof runoff retention, detention, and quality. Water, Air, & Soil Pollution, 216(1-4), 83-92. https://doi.org/10.1007/s11270-010-0516-8

Brunetti, G., Šimůnek, J., & Piro, P. (2016). A comprehensive analysis of the variably saturated hydraulic behavior of a green roof in a mediterranean climate. Vadose Zone Journal, 15(9). doi:10.2136/vzj2016.04.0032

Carson, T. B., Marasco, D. E., Culligan, P. J., & McGillis, W. R. (2013). Hydrological performance of extensive green roofs in New York City: observations and multi-year modeling of three full-scale systems. Environmental Research Letters, 8(2), 024036. http://dx.doi.org/10.1088/1748-9326/8/2/024036

Cipolla, S. S., Maglionico, M., & Stojkov, I. (2016). A long-term hydrological modelling of an extensive green roof by means of SWMM. Ecological Engineering, 95, 876-887. https://doi.org/10.1016/j.ecoleng.2016.07.009

Dane, J.H.; Hopmans, J.W. (2002). Pressure plate extractor. In *Methods of Soil Analysis*; Part 4. Physical Methods; Dane, J.H., Topp, G.C., Eds.; SSSA: Madison, WI, USA, 688–690.

Feddes, R.A.; Kowalik, P.J.; Zaradny, H. (1978). Simulation of Field Water Use and Crop Yield; PUDOC: Wageningen, The Netherlands.

Fassman-Beck, E., Voyde, E., Simcock, R., & Hong, Y. S. (2013). 4 Living roofs in 3 locations: Does configuration affect runoff mitigation?. Journal of Hydrology, 490, 11-20. https://doi.org/10.1016/j.jhydrol.2013.03.004

Feitosa, R. C., & Wilkinson, S. (2016). Modelling green roof stormwater response for different soil depths. Landscape and Urban Planning, 153, 170-179. https://doi.org/10.1016/j.landurbplan.2016.05.007

Garofalo, G., Palermo, S., Principato, F., Theodosiou, T., & Piro, P. (2016). The influence of hydrologic parameters on the hydraulic efficiency of an extensive green roof in mediterranean area. Water, 8(2), 44. https://doi.org/10.3390/w8020044

Getter, K. L., Rowe, D. B., & Andresen, J. A. (2007). Quantifying the effect of slope on extensive green roof stormwater retention. Ecological engineering, 31(4), 225-231. https://doi.org/10.1016/j.ecoleng.2007.06.004

Krebs, G., Kuoppamäki, K., Kokkonen, T., & Koivusalo, H. (2016). Simulation of green roof test bed runoff. Hydrological processes, 30(2), 250-262. https://doi.org/10.1002/hyp.10605

Hilten, R. N., Lawrence, T. M., & Tollner, E. W. (2008). Modeling stormwater runoff from green roofs with HYDRUS-1D. Journal of hydrology, 358(3-4), 288-293. https://doi.org/10.1016/j.jhydrol.2008.06.010

Lazzarin, R. M., Castellotti, F., & Busato, F. (2005). Experimental measurements and numerical modelling of a green roof. Energy and Buildings, 37(12), 1260-1267. https://doi.org/10.1016/j.enbuild.2005.02.001

Li, Y., & Babcock Jr, R. W. (2015). Modeling hydrologic performance of a green roof system with HYDRUS-2D. Journal of Environmental Engineering, 141(11), 04015036. https://doi.org/10.1061/(ASCE)EE.1943-7870.0000976

Liu, R., & Fassman-Beck, E. (2017). Hydrologic response of engineered media in living roofs and bioretention to large rainfalls: experiments and modeling. Hydrological processes, 31(3), 556-572. https://doi.org/10.1002/hyp.11044

Metselaar, K. (2012). Water retention and evapotranspiration of green roofs and possible natural vegetation types. Resources, conservation and recycling, 64, 49-55. https://doi.org/10.1016/j.resconrec.2011.12.009

Palermo, S. A., Turco, M., Principato, F., & Piro, P. (2019b). Hydrological Effectiveness of an Extensive Green Roof in Mediterranean Climate. Water, 11(7), 1378. https://doi.org/10.3390/w11071378

Palla, A., Gnecco, I., & Lanza, L. G. (2012). Compared performance of a conceptual and a mechanistic hydrologic models of a green roof. Hydrological Processes, 26(1), 73-84. https://doi.org/10.1002/hyp.8112

Peng, Z., & Stovin, V. (2017). Independent validation of the SWMM green roof module. Journal of Hydrologic Engineering, 22(9), 04017037. https://doi.org/10.1061/(ASCE)HE.1943-5584.0001558

Peters, A., & Durner, W. (2008). Simplified evaporation method for determining soil

hydraulic properties. Journal of Hydrology, 356(1-2), 147-162. https://doi.org/10.1016/j.jhydrol.2008.04.016

Pertassek, T.; Peters, A.; Durner, W. (2015). HYPROP-FIT Software User's Manual, V.3.0; UMS GmbH: München, Germany.

Piro, P., Carbone, M., Morimanno, F., & Palermo, S. A. (2019a). Simple flowmeter device for LID systems: From laboratory procedure to full-scale implementation. Flow Measurement and Instrumentation, 65, 240-249. https://doi.org/10.1016/j.flowmeasinst.2019.01.008

Piro P., Turco M., Palermo S.A., Principato F., Brunetti G. (2019b) A Comprehensive Approach to Stormwater Management Problems in the Next Generation Drainage Networks. In: Cicirelli F., Guerrieri A., Mastroianni C., Spezzano G., Vinci A. (eds) The Internet of Things for Smart Urban Ecosystems. Internet of Things (Technology, Communications and Computing). Springer, Cham. https://doi.org/10.1007/978-3-319-96550-5_12

Principato F., Ferrante A.P., Frega F., Bartolo M., Piro P. (2019) Mitigation of Urban Surface Runoff Through LID Solutions: Case Study in Mediterranean Area. In: Mannina G. (eds) New Trends in Urban Drainage Modelling. UDM 2018. Green Energy and Technology. Springer, Cham. https://doi.org/10.1007/978-3-319-99867-1_115

Shiau, J. T. (2003). Return period of bivariate distributed extreme hydrological events. Stochastic environmental research and risk assessment, 17(1-2), 42-57. https://doi.org/10.1007/s00477-003-0125-9

Schindler, U. (1980). Ein Schnellverfahren zur Messung der Wasserleitfähigkeit im teilgesättigten Boden an Stechzylinderproben. Arch. Für Acker-Und Pflanzenbau Und Bodenkd. 24, 1–7.

Schindler, U., Durner, W., Von Unold, G., Mueller, L., & Wieland, R. (2010a). The evaporation method: Extending the measurement range of soil hydraulic properties using the air-entry pressure of the ceramic cup. Journal of plant nutrition and soil science, 173(4), 563-572. https://doi.org/10.1002/jpln.200900201

Schindler, U., Durner, W., von Unold, G., & Müller, L. (2010b). Evaporation method for measuring unsaturated hydraulic properties of soils: Extending the measurement range. Soil science society of America journal, 74(4), 1071-1083. doi:10.2136/sssaj2008.0358

Šimůnek, J., Van Genuchten, M. T., & Šejna, M. (2016). Recent developments and

applications of the HYDRUS computer software packages. Vadose Zone Journal, 15(7). doi:10.2136/vzj2016.04.0033

Soulis, K. X., Ntoulas, N., Nektarios, P. A., & Kargas, G. (2017). Runoff reduction from extensive green roofs having different substrate depth and plant cover. Ecological engineering, 102, 80-89. https://doi.org/10.1016/j.ecoleng.2017.01.031

Stovin, V., Vesuviano, G., & Kasmin, H. (2012). The hydrological performance of a green roof test bed under UK climatic conditions. Journal of hydrology, 414, 148-161. https://doi.org/10.1016/j.jhydrol.2011.10.022

UMS GmbH. (2012). KSAT: Operation Manual; Umwelt Monitoring System; GmbH: Munich, Germany.

UMS GmbH. (2015). UMS: Manual HYPROP, Version 2015-01; UMS GmbH: München, Germany, 8137; Volume 37.

Van Genuchten, M. T. (1980). A closed-form equation for predicting the hydraulic conductivity of unsaturated soils 1. Soil science society of America journal, 44(5), 892-898. doi:10.2136/sssaj1980.03615995004400050002x

Voyde, E., Fassman, E., & Simcock, R. (2010). Hydrology of an extensive living roof under sub-tropical climate conditions in Auckland, New Zealand. Journal of hydrology, 394(3-4), 384-395. https://doi.org/10.1016/j.jhydrol.2010.09.013

Wind, G.P. (1969) Capillary conductivity data estimated by a simple method. Available online: https://library.wur.nl/WebQuery/wurpubs/fulltext/350954 (accessed on 3 July 2019).

Chapter 5 - On the LID systems effectiveness for urban stormwater management at large scale: case study in Southern Italy

Starting from the analysis on the hydrological behaviour of a single LID unit, discussed in the previous chapter, in this section the hydrological effectiveness of Low Impact development (LID) solutions at large scale, by modeling a highly urbanised area located in South Italy, is presented. For the model creation and simulation, PCSWMM was used. The analysis was carried out by considering different land use conversion scenarios including the implementation of LID practices. The model has the aim to be a predictive tool to understand the effect of the implementation of different percentage of LID systems on urban stormwater management, by evaluated three hydrological performance indexes (Runoff Coefficient, Runoff Reduction and Peak Flow Reduction). Given the unavailability of real runoff data at the site specific, and to reduce the uncertainty, the model was developed by considering topographical data, land use classification and data on the existing stormwater system, already investigated in a previous study, as well as for the LID parameters, the specific green roof and permeable pavement implemented at University of Calabria were taken into account. This chapter is linked to Paper VI (Palermo et al., 2020a) annexed to this dissertation.

5.1 Introduction

To enhance the environmental quality and restore the exosystemic balance affected by urbanization and climate change, sustainable solutions and assessment methodologies at different spatial scale (urban, peri-urban, watershed, and so on) are become a priority, and in this direction several studies have been carried out (Razdar et al., 2010; Javadinejad et al., 2014; Talarico et al., 2018).

Focusing on urban environment, the highly imperviousness led a drastic change in the natural hydrological cycle components with consequences in terms of reduction of infiltration and evapotranspiration as well as increase of runoff volumes. Therefore, during extreme stormwater events such volumes can overload the sewer systems causing local floods (Piro et al., 2019a).

In this scenario, as stated above, is relevant to find solutions to reduce the impacts (Razdar et al., 2010) and the implementation of decentralized stormwater controls, also known as LIDs (Low Impact Development), whose investigation on hydrological benefits is the main objective of this dissertation, can provide a promising answer to the current environmental challenges.

Specifically, green roofs and permeable pavements, largely investigated, have been considered among the most efficient strategies in terms of urban flooding risk mitigation, water quality enhancement, and urban heat islands reduction (Fassman & Blackbourn, 2010; Berndtsson, 2010; Li et al., 2014; Vijayaraghavan, 2016; Maiolo et al., 2017; Turco et al., 2018; Kuruppu et al., 2019).

Therefore, based on this framework, and after the analysis conducted in the previous chapter on the hydrological behaviour of a single LID unit, the main objective of this section is to analyze how the implementation of Low Impact Development systems (LIDs) can contribute to mitigate the effect of climate change and urbanization in terms of surface runoff reduction and, consequently, urban flooding risk mitigation at large urban scale.

To achieve this main objective, the hydrological response of a small selected urban area of Municipality of Paola in Calabria Region - located in Southern Italy – under Mediterranean climate condition, was investigated by considering different LIDs conversion scenarios. In this regard, a modeling implementation of the Green Roofs and Permeable Pavements, installed at University of Calabria, was carried out by using the PCSWMM software (CHI PCSWMM).

5.2 Materials and Methods

5.2.1 Study Area

A highly urbanized area of an urban catchment (catchment of San Domenico Creek) located in the municipality of Paola in Calabria Region (Italy) in Mediterranean Climate Region, was selected as test site for modeling the land use conversion scenarios.

In this area the stormwater management is achieved by a combined sewer network consisting of different conduits in terms of section and materials. More specifically, based on the detailed information of a previous study (Palermo, 2018), the concrete conduits have sections of 350x450mm, 400x400mm e 450x450mm, while the circular ones in stoneware material have diameters of 200 mm and 300 mm.

The residential area, here considered, with a total surface of around 7.6 ha, presents a grade of imperviousness of 96.0%. The analysis of land use data, carried out on the base of regional cartography and aerial photographs, illustrated in Table 5.1, shows that the study area consists of 28.9% of rooftops and 67.1% of roads, parking lots and others impervious surfaces; only a small portion, 4.0% of the total surface, is covered by green spaces.

Table 5.1: Land use of the selected area (Palermo et al., 2020a).

Land use	**Area**	
	ha	%
Rooftop	2.2	28.9
Parking lot, roads and other impervious	5.1	67.1
Total Impervious	**7.3**	**96.0**
Green Area	0.3	4.0
Total Pervious	**0.3**	**4.0**
Total Areas	**7.6**	**100.00**

This landscape analysis reveals as the area, almost totally covered by impervious surfaces, can be a suitable site for Low Impact Development (LID) systems implementation for urban stormwater management.

5.2.2 LID Simulation Scenarios

To assess the hydrological effectiveness of LID systems for urban stormwater management, Green Roofs (GRs) and Permeable Pavements (PPs) are the LID systems

selected to model the response of the urban area under different conversions scenarios, described below.

(i) *Scenario 0* is the reference scenario, implemented based on the current land use data, in order to investigate the impact of the LID implementation;

(ii) *Scenario 1* consists in the replacement of 30% of conventional rooftop area with Green Roofs and in the installation of Pemeable Pavements on the 30% of impervious surfaces (excluding roads opened to traffic);

(iii) *Scenario 2*, where 60% of conventional roofs are substituted with Green Roofs and 60% of impervious areas (excluding roads opened to traffic) with Pemeable Pavements;

(iv) *Scenario 3* considers the implementation of Green Roofs on all rooftops, and the replacement of 100% of impervious surfaces (excluding roads opened to traffic) with Pemeable Pavements.

5.2.3 Model Development

To simulate the hydrological response of urban catchment a dynamic rainfall-runoff simulation model PCSWMM (CHI-PCSWMM), based on the EPA-SWMM version 5.1.012 (Rossman, 2015), was used. This choice was carried out based on the results of other studies, which confirm the suitability of SWMM to assess the LID performances and to support their implementation at catchment scale (Palla & Gnecco, 2015; Ahiablame & Shakya, 2016).

The model was built considering topographical data, land use classification and data on the existing stormwater system, already investigated in a previous study (Palermo, 2018). To obtain a detailed model, and improve the previous one, the study area of around 7.6 ha was divided into 26 subcatchments, defined in function of land use and homogeneous properties (the surface slope, area, etc.). More in detail, based on the land use analysis, for each subcatchment, before the modeling implementation, the land use features in terms of pervious and impervious area were defined. In function of this analysis for each subcatchment the Curve Number parameter (-), the Depression Depth value (mm), n Manning coefficient ($s/m^{1/3}$) were chosen, and then considered with the others geometrical data (area, width, slope, etc.) as input subcatchment parameters to implement the model.

The Soil Conservation Service (SCS) Curve Number (CN) method was considered for the infiltration method and the flow routing computations were based on the Dynamic Wave Equations. The drainage network was defined in agreement with the data retrieved from the design plans in terms of conduit length, section and material (Palermo, 2018). Based on this, the implemented model consists of 26 subcatchments, 28 Conduits, 28 Junctions Nodes, and 1 Outfall node. This model is representative of the existing system configuration, i.e. the reference scenario (Scenario 0) of this study.

To simulate the hydrological response of this urban area with the implementation of LID solutions (Scenario 1,2,3), the model, previous defined, was integrated with the use of the LID Control Editor; this is an additional SWMM module developed to simulate the hydrological behaviour of source control solutions as bio-retention cell, rain gardens, green roof, infiltration trench, permeable pavement, rain barrel, rooftop disconnection, vegetative swale (Rossman, 2010).

In this study green roof and permeable pavement modules were selected. To assign the properties for each layer, required by the LID Control section, the stratigraphy features and the physical parameters (based on previous laboratory test measurements) of the green roof and the permeable pavement located at University of Calabria were considered. More detail, the features of these two LID solutions can be found in chapter 4 of this dissertation (linked to Paper II, Palermo et al., 2019b), as well as in the studies carried out by Piro et al., (2019b); Brunetti et al., (2018).

For the hydrodynamic simulation, synthetic Chicago hyetograph was used. The rainfall duration was assumed 30 min and the time-to-peak-ratio 0.4. The hyetograph was defined based on the parameters of the Intensity–Duration-Frequency relationship computed by the analysis of historical records (1945 – 2005) obtained from the Regional Agency for Prevention, Environmental in Calabria Region (Arpacal, 2018) by considering the rain gauge station of Paola.

5.2.4 Hydrological Performance Indexes

The response of each scenario was evaluated in terms of *runoff coefficient* (RC), *runoff reduction* (RR), and *peak flow reduction* (PFR). These values were estimated for each subcatchment and the mean values for each index were calculated in order to analyze the overall result.

The *Runoff Coefficient* for each scenario (RC_0, RC_1, RC_2, RC_3) was expressed as percentage ratio between the total Runoff Depth in mm ($RD_0, RD_1; RD_2; RD_3$) and the total Precipitation Depth in mm (PD).

Table 5.2: Equations used to evaluate the Runoff Coefficient for each scenario (Palermo et al., 2020a)

SCENARIO 0	SCENARIO 1	SCENARIO 2	SCENARIO 3
$RC_0 = \frac{RD_0}{PD} \cdot 100$	$RC_1 = \frac{RD_1}{PD} \cdot 100$	$RC_2 = \frac{RD_2}{PD} \cdot 100$	$RC_3 = \frac{RD_3}{PD} \cdot 100$

While, the *Runoff Reduction* ($RR_{0-1}, RR_{0-2}, RR_{0-3}$) was estimated as the percentage difference between the total Runoff Depth of Scenario 0 (RD_0) and the corresponding total Runoff Depth of the other conversion scenarios ($RD_1; RD_2; RD_3$).

Similarly, the Peak Flow Reduction (PFR_{0-1}, PFR_{0-2}, PFR_{0-3}) was evaluated as the percentage difference between the hydrograph peak of Scenario 0 (PF_0) and the corresponding hydrograph peak for each LID conversion scenarios (PF_1, PF_2, PF_3).

Table 5.3: Equations used to evaluate the surface Runoff Reduction (RR) and Peak Flow reduction (PFR) obtained by comparing Scenario 0 with the other Scenarios (1,2,3) (Palermo et al., 2020a)

SCENARIO 0 vs SCENARIO 1	SCENARIO 0 vs SCENARIO 2	SCENARIO 0 vs SCENARIO 3
$RR_{0-1} = \frac{RD_0 - RD_1}{RD_0} \cdot 100$	$RR_{0-2} = \frac{RD_0 - RD_2}{RD_0} \cdot 100$	$RR_{0-3} = \frac{RD_0 - RD_3}{RD_0} \cdot 100$
$PFR_{0-1} = \frac{PF_0 - PF_1}{PF_0} \cdot 100$	$PFR_{0-2} = \frac{PF_0 - PF_2}{PF_0} \cdot 100$	$PFR_{0-3} = \frac{PF_0 - PF_3}{PF_0} \cdot 100$

5.3 Results and Discussion

5.3.1 Numerical Model

As specified in section 5.2.3, the model was developed by considering topographical data, land use classification and information on the existing stormwater system. The final model configuration (Figure 5.1) presents the entire study area divided into 26 subcatchments, defined in function of land use and homogeneous properties (the surface slope, area, etc.).

The introduction of different percentage of LID units aims at improving the infiltration capability of the selected area reducing the surface runoff.

By analyzing Figure 5.1, and specifically the *Scenario 0* model configuration (Figure 5.1a), it was possible to observe the high imperviousness percentage of this

urbanised area: 22 subcatchments present an imperviousness more than 90%. While, by implementing the different LID scenarios, it was detected a great reduction of imperviousness until to reach the optimal and final condition related to scenario 3 (Figure 5.1d) where the majority of the subcatchments have an imperviousness less than 40%.

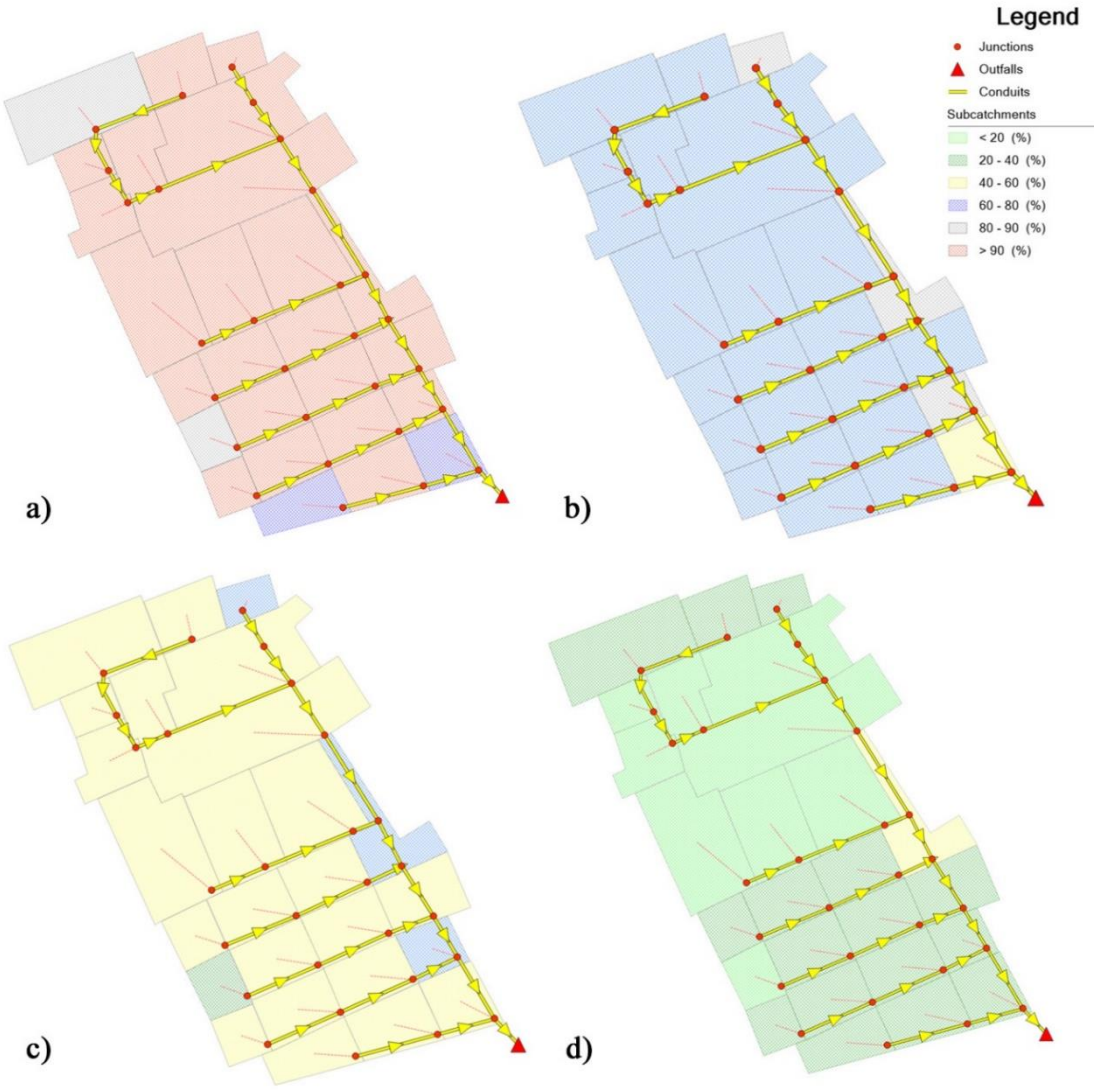

Figure 5.1: PCSWMM final model configuration. (a) Scenario 0; (b) Scenario 1; (c) Scenario 3; (d) Scenario 4.

5.3.2 LIDs hydraulic efficiency at large-scale

To assess the LIDs hydrological effectiveness, the results were evaluated in terms of outflow for the reference condition (Scenario 0) and those ones obtained for the conversions scenarios (Scenarios 1,2,3).

More in detail, first the total Runoff Depth (RD) and the Peak Flow (PF) were estimated at subcatchment scale for each conversion scenario (Figure 5.2). For both cases, the bar-graphs confirm the good performance of the LID systems, by showing how the RD and PF values reduced to the increase of LID percentages in the urban area.

Therefore, based on the data of all subcatchments, the three Hydrological Performance Indexes (RC, RR, PFR) were evaluated at subcatchment scale (Figure 5.3), and then average values calculated in order to analyze the overall result (Table 5.4).

Specifically, by observing Figure 5.3, it is possible to detect the range of variation of the three Hydrological Performance Indexes.

Table 5.4. Rainfall Depth and Average Values of Performance indexes (Palermo et al., 2020a)

	Scenario 0	**Scenario 1**	**Scenario 2**	**Scenario 3**
Rainfall depth (mm)	33.5	33.5	33.5	33.5
Average RC (%)	98.1	72.6	53.0	36.4
		Scenario 0 vs Scenario 1	**Scenario 0 vs Scenario 2**	**Scenario 0 vs Scenario 3**
Average RR (%)		25.9	45.8	62.8
Average PFR (%)		31.4	59.3	83.8

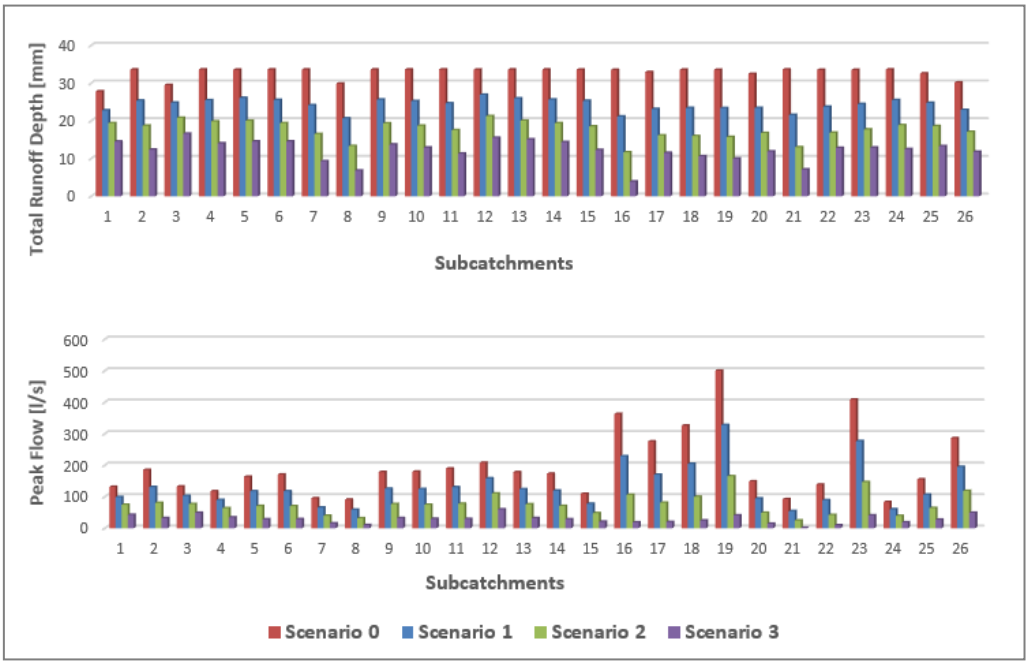

Figure 5.2. Total Runoff Depth (mm) and Peak Flow (l/s) for each subcatchment by comparing all scenarios (Palermo et al., 2020a).

The values reported in Table 5.4 reveal the suitability of the LIDs to improve retention capacity of a highly urbanised area.

The RC average value decreases from 98.1% in the condition of almost total imperviousness to 36.4% in Scenario 3, obtaining also good results for the inter-medium scenarios. RC values of 25.5% and 45.1% less than the Scenario 0 were observed for the Scenario 1 and 2, respectively. While the Runoff Reduction (RR) and Peak Flow Reduction (PFR) present a linear increase of their values with the reduction of the impervious surfaces, simulated from scenario 1 to scenario 3.

More in detail, the implementation of GR and PP on the 30% of the corresponding impervious surface (as specified above) allow a runoff reduction of 25.9 % and a peak reduction of 31.4%. Although the imperviousness change is limited to only this percentage (30%), a good result was achieved by the implementation of the specific GR and PP in Mediterranean climate condition.

As expected, more high performances have been reached in the second and third scenarios, where the percentage of LID reached 60% and 100%, respectively, and the RR and PFR reached values of 45.8% and 59.3% for scenario 2 and 62.8% and 83.8% for the last one.

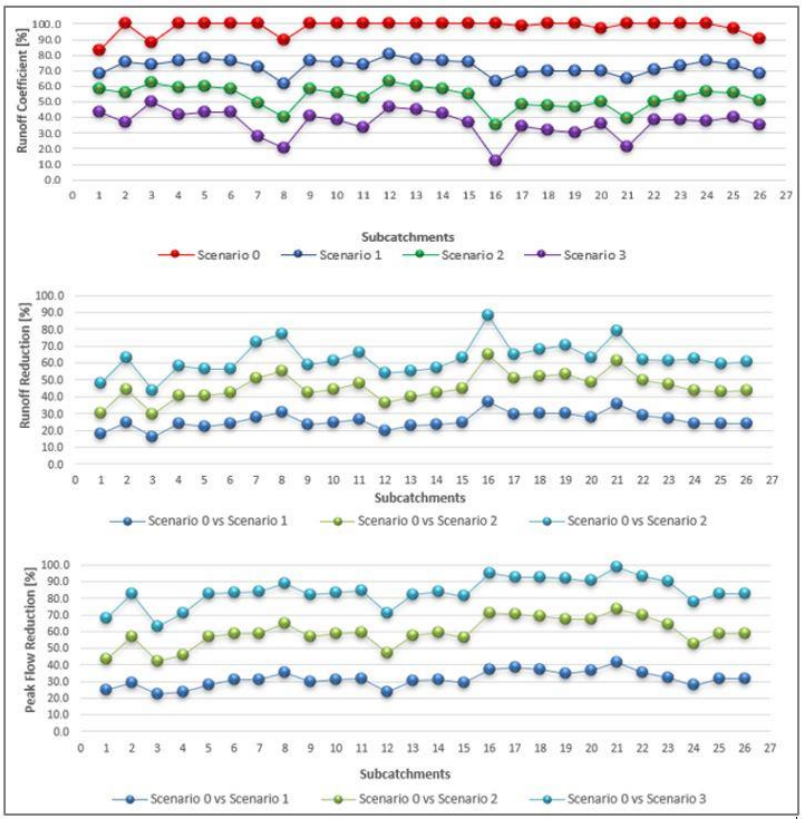

Figure 5.3. Comparison of the Hydrological Performances Indexes evaluated on a subcatchment scale for different conversion scenarios (Palermo et a., 2020a).

All findings, here presented, confirm the suitability of LID solutions for the surface runoff mitigation in terms of volume and hydrographs peak for all three LID conversion scenarios.

By analysing the modeling results emerges the role of LID practices to restore the component of natural hydrological cycle at the urban scale. And, even if, practical and economic considerations are needed to select the optimal LIDs distribution, this study demonstrates that also a small change of imperviousness, considered for example for the Scenario 1, can enhance the hydrological response of an urban catchment.

5.4 Conclusions

To evaluate the hydrological performances of LID systems, in this study the hydrological response of a highly urbanised area located in Southern Italy has been simulated under different LID conversions scenarios.

The selected area was modelled by using PCSWMM. A specific permeable pavement and green roof, developed at University of Calabria, have been considered for the modeling implementation by the LID modules in PCSWMM.

Modeling results confirm the suitability of these LID solutions to reduce surface runoff and, therefore, urban flooding risk. More in detail, the findings reveal that this beneficial effect can be reached by converting also only a small percentage of the impervious surfaces. Considering that practical and economic conditions could limit the implementation of these sustainable practices in urban area, this can be considered a relevant finding.

In conclusion, the LID strategy achieves a sustainable management of urban drainage network, limiting the environmental impact due to urbanization and climate change.

Future investigation will take into account the response of the same area under different rainfall event and by considering others combination of LID systems not only in terms of percentage distribution, but also in terms of different design systems.

5.5 References

Ahiablame, L., & Shakya, R. (2016). Modeling flood reduction effects of low impact development at a watershed scale. Journal of environmental management, 171, 81-91. https://doi.org/10.1016/j.jenvman.2016.01.036

Arpacal, 2018. http://www.cfd.calabria.it/index.php/dati-stazioni/dati-storici

Berndtsson, J. C. (2010). Green roof performance towards management of runoff water quantity and quality: A review. Ecological engineering, 36(4), 351-360. https://doi.org/10.1016/j.ecoleng.2009.12.014

Brunetti, G., Šimůnek, J., Turco, M., & Piro, P. (2018). On the use of global sensitivity analysis for the numerical analysis of permeable pavements. Urban Water Journal, 15(3), 269-275. https://doi.org/10.1080/1573062X.2018.1439975

CHI PCSWMM. Available online: https://www.pcswmm.com/

Fassman, E. A., & Blackbourn, S. (2010). Urban runoff mitigation by a permeable pavement system over impermeable soils. Journal of Hydrologic Engineering, 15(6), 475-485. https://doi.org/10.1061/(ASCE)HE.1943-5584.0000238

Javadinejad, H, Kavianpour, M.R, Pirouz, B, (2014) Performance evaluation of rivers water quality with sustainable development and tourism point of view (Case study: Aras River), First National Conference on Tourism, income and opportunity, Hamadan, Iran

Kuruppu, U., Rahman, A., & Rahman, M. A. (2019). Permeable pavement as a stormwater best management practice: a review and discussion. Environmental Earth Sciences, 78(10), 327. https://doi.org/10.1007/s12665-019-8312-2

Li, D., Bou-Zeid, E., & Oppenheimer, M. (2014). The effectiveness of cool and green roofs as urban heat island mitigation strategies. Environmental Research Letters, 9(5), 055002. http://dx.doi.org/10.1088/1748-9326/9/5/055002

Maiolo, M., Carini, M., Capano, G., & Piro, P. (2017). Synthetic sustainability index (SSI) based on life cycle assessment approach of low impact development in the Mediterranean area. Cogent Engineering, 4(1), 1410272. https://doi.org/10.1080/23311916.2017.1410272

Palermo, M. (2018). Le reti di drenaggio urbano: caratteristiche, problematiche e soluzioni ingegneristiche innovative. Bachelor Thesis. Supervisor Patrizia Piro. Università della Calabria. Italia).

Palermo S.A., Zischg J., Sitzenfrei R., Rauch W., Piro P. (2019a) Parameter Sensitivity of a Microscale Hydrodynamic Model. In: Mannina G. (eds) New Trends in Urban Drainage Modelling. UDM 2018. Green Energy and Technology. Springer, Cham. https://doi.org/10.1007/978-3-319-99867-1_169

Palermo, S. A., Turco, M., Principato, F., & Piro, P. (2019b). Hydrological Effectiveness of an Extensive Green Roof in Mediterranean Climate. Water, 11(7), 1378. https://doi.org/10.3390/w11071378

Palla, A., & Gnecco, I. (2015). Hydrologic modeling of Low Impact Development systems at the urban catchment scale. Journal of hydrology, 528, 361-368. https://doi.org/10.1016/j.jhydrol.2015.06.050

Piro, P., Carbone, M., Morimanno, F., & Palermo, S. A. (2019a). Simple flowmeter device for LID systems: From laboratory procedure to full-scale implementation. Flow Measurement and Instrumentation, 65, 240-249. https://doi.org/10.1016/j.flowmeasinst.2019.01.008

Piro, P., Turco, M., Palermo, S. A., Principato, F., & Brunetti, G. (2019b). A Comprehensive Approach to Stormwater Management Problems in the Next Generation Drainage Networks. In The Internet of Things for Smart Urban Ecosystems (pp. 275-304). Springer, Cham. https://doi.org/10.1007/978-3-319-96550-5_12

Razdar, B, Ghavidel, A, Zoqi, M.J and Pirouz, B (2010) Impact Assessment of Urban Flood, First National Conference Management of urban floods, Tehran. Iran

Razdar, B, Ghavidel, A, and Pirouz, B (2010) the role of Numerical models in improvement the efficiency of surface water management, 13th National Congress on Environmental Health, Kerman, Iran

Rossman, L. A. (2010). Storm water management model user's manual, version 5.0 (p. 276). Cincinnati: National Risk Management Research Laboratory, Office of Research and Development, US Environmental Protection Agency.

Rossman, L. A. (2015). Storm Water Management Model User's Manual Version 5.1. Office of Research and Development. Water Supply and Water Resources Division. US Environmental Protection Agency.

Talarico V.C., Frega F., Palermo S.A., Piro P. (2018). Dall'indice di funzionalità fluviale (IFF) all'indice di qualità morfologica (IQM). Stato dell'arte dell'applicazione su alcuni corsi idrici del parco nazionale della Sila. In: Frega G. (ed.), Tecniche per la difesa del suolo e dall'inquinamento - In Proceedings of 39° Corso di aggiornamento,

Guardia Piemontese (CS), IT, 20-23 June 2018, Edibios, (pp.403-411), ISBN: 978-88-97181-63-7.

Turco, M., Brunetti, G., Carbone, M., & Piro, P. (2018). MODELLING THE HYDRAULIC BEHAVIOUR OF PERMEABLE PAVEMENTS THROUGH A RESERVOIR ELEMENT MODEL. International Multidisciplinary Scientific GeoConference: SGEM: Surveying Geology & mining Ecology Management, 18, 507-514. DOI:10.5593/sgem2018/3.1/S12.066. https://doi.org/10.1007/s12665-019-8312-2

Vijayaraghavan, K. (2016). Green roofs: A critical review on the role of components, benefits, limitations and trends. Renewable and sustainable energy reviews, 57, 740-752. https://doi.org/10.1016/j.rser.2015.12.119

Chapter 6 – On the use of New Mathematical Optimization Approaches for LID Systems

By considering all of the findings, previous achieved by experimental and modeling investigation, it emerged that many aspects related to LIDs design and operation, as well as the choice of the facility and its location can affect the results in terms of hydraulic efficiency. In this regard, a mathematical optimization approach to consider several aspects together could be a suitable tool for designers of LID systems and experts in the field. Therefore, in this chapter the application of Multi-Objective Mathematical Optimization approaches is considered as additional tools for the analysis of essential attributes to optimize the LID, providing a baseline for decision-making. More in detail, the optimization of rainwater harvesting systems by using TOPSIS (Technique for Order Preference by Similarity to Ideal Solution) and Rough Set method as Multi-Objective Optimization approaches was carried out by analyzing different literature case studies. The results obtained by the application of these methods to the Rainwater Harvesting (RWH) system, already published (Paper VIII: Palermo et al., 2020b), are presented in this chapter. Moreover, this chapter is also linked to Paper IX (Pirouz et al., 2020), where the same methodologies was applied for LID sites location by considering hypothetical case studies.

6.1 Introduction

LID systems are important tools in sustainable development and, as widely discussed in section 2.2, they are different types of LID practices such as green roofs, green wall, bioretention cell, permeable pavements, rainwater harvesting systems (RWH), etc. Among these facilities, Rainwater harvesting systems meet the challenges of water saving and surface runoff mitigation. Moreover, the collected rainwater can be re-used for several purposes including green roofs and garden, flushing toilets, etc.

Several studies have been carried out to show the RWH efficiency for water saving and runoff mitigation (Herrmann & Schmida, 2000; Li et al., 2010; Jones and Hunt, 2010; Domènech and Saurí, 2011; Campisano & Modica 2015; Palla et al., 2017; Cipolla et al., 2018; Becciu et al., 2018). However, as observed by Campisano and Modica (2015) the RWH hydrological/hydraulic performance depends of site-specific factors, such as roof type and surface, precipitation regime, demand usage, tank size, number of people in the household, etc.

So far, the optimization of rainwater harvesting systems was mostly limited to optimum size of the tankers according to hydrological and hydraulic analysis and in some cases combined with economic analysis.

Therefore, principal aim of this study is to evaluate the use of mathematical optimization approaches, as an additional tool for the analysis of essential attributes to select and optimize the best LID solution for a project.

To achieve this purpose, Multi-Objective Optimization approaches have been applied to RWH systems.

Thus, based on a deeper literature review, in this analysis some factors, called “attributes” have been selected and considered in the mathematical optimization approach. More in detail, the application of TOPSIS (Technique for Order Preference by Similarity to Ideal Solution) and Rough Set theory (multiple attributes decision-making method) were considered for the purpose. TOPSIS was used to compare algorithms and evaluate the performance of alternatives, while Rough Set method was applied as a machine learning method to optimize the use. Results by Rough Set method provided a baseline for decision making and the minimal decision algorithm were obtained as rules.

6.2 Materials and Methods

In the current study, the Rough Set method applied as a machine learning method to optimize rainwater-harvesting systems. The process is reviewed in details and the result is achieved with analysis of different case studies.

6.2.1 Rough Set Theory

The Rough Set method, introduced by Pawlak (2002) in 1982, can be used as an excellent mathematical tool in analysis of vague description of decisions such as quality of data, means variation or uncertainty that follows from information. The rough sets philosophy is based on assumption that, for every object a certain information (data, knowledge) exists, that can be expressed as attributes (Arabani et al., 2017).

With respect to the available data, the objects with the same description are indiscernible and a set of indiscernible objects, named elementary set, can be provided to build knowledge about a real system. Deal with quantitative or qualitative data depends on the input information and before the analysis, it is necessary to remove the irregularities. With respect to the output data, the relevance of particular attributes and their subsets to the quality of approximation can be acquired (Arabani et al., 2012).

In this regard, the induction-based approach can provide clear rules for decision-makers (DMs) in the form of ``if..., then...". The concept of approximation space in rough set method can be described in a given approximation space as follows:

$$\mathrm{apr} = (\mathrm{U}, \mathrm{A}) \qquad [6.1]$$

where *U* is a finite and non-empty set and *A* is set of attributes in the given space.

Based on the approximation space, the lower and upper approximations of a set can be defined. Let X be a subset of U and the upper and lower approximation of X in A are:

$$\overline{\mathrm{apr}}(\mathrm{A}) = \{\mathrm{x}|\mathrm{x} \in \mathrm{U}, \mathrm{U}/\mathrm{ind}(\mathrm{A}) \subset \mathrm{X}\} \qquad [6.2]$$

$$\underline{\mathrm{apr}}(\mathrm{A}) = \{\mathrm{x}|\mathrm{x} \in \mathrm{U}, \mathrm{U}/\mathrm{ind}(\mathrm{A}) \cap \mathrm{X} \neq \varphi\} \qquad [6.3]$$

where:

$$U/ind(A) = \{(x_i, x_j) \in U \times U, f(x_i, a) = f(x_j, a), \forall a \in A\} \quad [6.4]$$

Eq. [6.2], that is the best upper approximation of X in A, means the minimum composed set in A containing X, and Eq. [6.3], that is the best lower approximation, means the maximum composed set in A contained in X. The graphical illustration of approximations in the rough set method is shown in Fig. 6.1.

The boundary represents as:

$$BN(A) = \overline{apr}(A) - \underline{apr}(A) \quad [6.5]$$

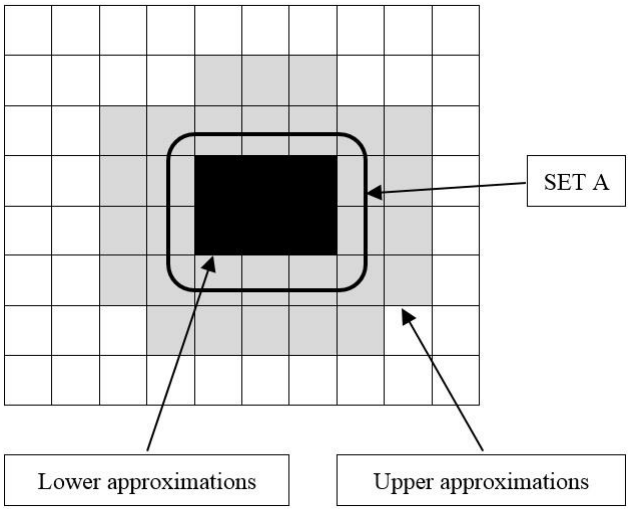

Figure 6.1: Graphical illustration of the rough set approximations (Pirouz et al., 2020).

The reducts and decision rules can be defined as below specified. The reduct RED (B), is a minimal set of attributes $B \subseteq A$ such that $r_B(U) = r_A(U)$, $r_B(U)$ indicates the quality of approximation of U by B.

The equation is:

$$r_B(U) = \frac{\sum card(\underline{B}(X_i))}{card(U)} \quad [6.6]$$

After providing the result of reducts, the decision rules can be derived by using the overlaying of the reducts on the information systems. An expressed decision rule can be as follow:

$$\varphi \Rightarrow \theta \quad [6.7]$$

where φ is the conjunction of elementary conditions and θ is the disjunction of elementary decisions.

6.2.2 TOPSIS method

TOPSIS (Technique for Order Preference by Similarity to Ideal Solution) is a method developed by Hwang and Yoon in 1981 to solve the ranking and compare problems and (Hwang & Yoon, 1981). The ranking in this method is made according to the similarity to ideal solution (Haghshenas et al., 2016; Balioti et al., 2018). The TOPSIS method can be applied to a wide range of multi-attribute decision making with several attributes (İç, 2014; Krohling &Pacheco, 2015; Haghshenas et al., 2017). The graphical illustration of the TOPSIS methodology is presented in Figure 6.2.

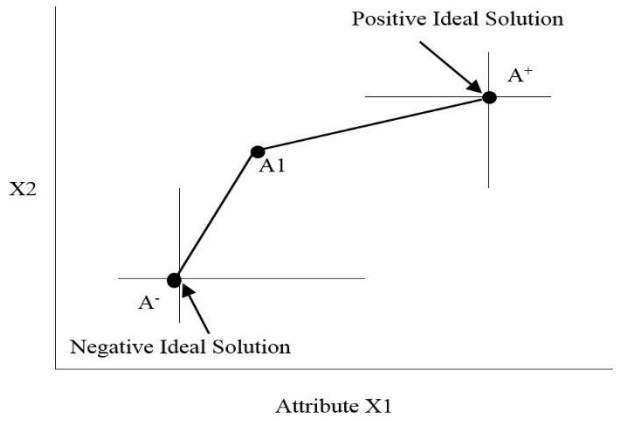

Figure 6.2: Graphical illustration of the TOPSIS methodology, (A+ represents the ideal point, A− represents the Negative-Ideal Point) (Pirouz et al., 2020).

The ranking by TOPSIS is carried out through seven steps

Step 1: Create the matrix

$$(n_{ij})m \times n \qquad [6.8]$$

Step 2: Construct the normalized decision matrix

$$N = n_{ij} = \frac{a_{ij}}{\sqrt{\sum_{i}^{m=1} a_{ij}^2}}, \quad i = 1, 2, \ldots, m \;\; \& \;\; j = 1, 2, \ldots, n \qquad [6.9]$$

Step 3: Construct the weighted normalized decision matrix

$$V = N \times W_n \times n \quad [6.10]$$

Step 4: Determine the solutions (the ideal and negative-ideal solutions)

The ideal solution: $A^+ = \{\langle \max_i (a_{ij} | j \in J_-)\rangle, \langle \min_i (a_{ij} | j \in J_+)\rangle\}$ [6.11]

The negative-ideal solutions:

$$A^- = \{\langle \min_i (a_{ij} | j \in J_-)\rangle, \langle \max_i (a_{ij} | j \in J_+)\rangle\} \quad [6.12]$$

where,

$J_+ = \{j = q, 2, \dots, n | j\}$ Associated with positive impact criteria

$J_- = \{j = q, 2, \dots, n | j\}$ Associated with negative impact criteria

Step 5: Determine the distance of alternatives v_{ij} from the ideal solution d_i^+ and the negative-ideal solutions d_i^-

$$d_i^+ = \sqrt{\sum_{j=1}^{n} (v_{ij} - v_j^+)}\ ,\ i = 1, 2, \dots, m \quad [6.13]$$

$$d_i^- = \sqrt{\sum_{j=1}^{n} (v_{ij} - v_j^-)},\ i = 1, 2, \dots, m \quad [6.14]$$

Step 6: Calculate the closeness to the negative-ideal condition, CL_i^*

$$CL_i^* = \frac{d_i^-}{d_i^- + d_i^+}\ ,\ 0 \le CL_i^* \le 1\ \ \&\ i = 1, 2, \dots, m \quad [6.15]$$

where,

$CL_i^* = 1\ if$ the solution has the best condition and means the highest rank

$CL_i^* = 0\ if$ the solution has the worst condition and means the lowest rank

Step 7: Rank in order to the highest CL_i^* .

6.2.3 Case studies

To carry out the analysis by rough set and TOPSIS a set of data is required such as case studies. The selection of the case studies has been done in a way that considers the main possible attributes/factors confronting in rainwater harvesting systems.

The first and second case studies (*CS1-CS2*) are taken from the study carried out by Herrmann and Schimida (2000) that considers the development and performance of

rainwater utilization systems in Germany, and specifically in Bochum where the mean annual precipitation is 787 mm. More in detail, the data considered there for *CS1* are related to a one-family house (with an effective roof area of 150 m^2, 4 persons, combined demand of 160 l/d, a storage volume of 6 m^3 and an additional retention volume of 15m^3, with a covering efficiency of 98%). The *CS2* case refers to a multi-story building (CS2) (with an effective roof area of 320 m^2, 24 persons, toilet flushing demand of 480 l/d, a storage volume of 14 m3 and an additional retention volume of 35 m^3).

A study carried out by Domènech & Saurí (2011) was considered to select the third (*CS3*) and the fourth (*CS4*) case study. Both case studies are in Sant Cugant del Vallès – Spain. More in detail, CS3 is a single-family house with a rooftop catchment area of 107 m^2, 3 residents, a toilet and laundry usage demand of 27 LCD and 16 LCD, respectively. While CS4 refers to a multi-family building with a rooftop catchment area of 625 m^2, 42 residents, a toilet and laundry usage demand of 30 LCD and 16 LCD, respectively. For *CS3*, the model scenario in which a tank of 13 m^3 can meet 80% of the combined demand of toilet flushing and laundry was selected; while for *CS4* the model scenario is a tank of 31 m^3 covering 59.5% of the combined demand of toilet flushing and laundry.

Case studies *CS5*, *CS6* and *CS7* are considered from the study of Palla et al. (2017). These three case studies are located in Genoa (Italy) with a mean annual precipitation of 1340 mm. More in detail, *CS5* is a 4-flat house with 16 inhabitants, a roof area of 420 m^2, an annual toilet flushing demand of 233.6 m^3/y and a tank capacity of 14 m^3. *CS6* is a 6-flat house with 24 inhabitants, a roof area of 420 m^2, an annual toilet flushing demand of 350.4 m^3/y and a tank capacity of 21 m^3. CS7 is a condominium with 32 inhabitants, a roof area of 680 m^2, an annual toilet flushing demand of 467.2 m^3/y and a tank capacity of 28 m^3. For the three case studies, the modeling results show a water saving efficiency of 0.83, 0.79 and 0.76 for *CS5*, *CS6* and *CS7*, respectively.

The *CS8* case study considers the values of the example of application found in Campisano & Modica (2012), where a 4 people residential house with a daily toilet flushing demand of 0.168 m^3, a roof area of 186 m^2, daily precipitation of 0.0018 m and a size tank of 2.93 m^3, achieving a water saving of 67%, was considered.

The *CS9* case study refers to a real case study at University of Calabria in Southern Italy (Piro et al., 2019b), where a tank of 1.5 m^3 is located at the base of an university building to collect the water for an experimental full-scale green roof implementation and the water is reused to irrigate the same green roof in the dry period.

Finally, three hypothetical cases, *CS10*, *CS11* and *CS12*, have been considered to evaluate remain factors under different conditions. Specifically, *CS10* represent the hypothetical implementation of RWH systems in the old town of Cosenza, *CS11* in the old town of Matera, and *CS12* in the new area of Quattromiglia, in the town of Rende, respectively.

Table 6.1: Case studies (Palermo et al., 2020b).

Locations of Case studies	Case study
Bochum – Germany (Herrmann & Schimida, 2000)	CS1
Bochum – Germany (Herrmann & Schimida, 2000)	CS2
Sant Cugant del Vallès – Spain (Domènech & Saurí, 2011)	CS3
Sant Cugant del Vallès – Spain (Domènech & Saurí, 2011)	CS4
Genoa – Italy (Palla et al., 2017)	CS5
Genoa – Italy (Palla et al., 2017)	CS6
Genoa – Italy (Palla et al., 2017)	CS7
Sicily - Italy (Campisano & Modica, 2012)	CS8
University of Calabria (Rende) – Italy (Piro et al., 2019b)	CS9
Old town of Cosenza - Italy	CS10
Old town of Matera - Italy	CS11
New Area of Quattromiglia (Rende) - Italy	CS12

6.3 Results and Discussion

6.3.1 Application of Rough Set Theory in optimizing rainwater-harvesting systems

In real projects there is an enormous quantity of data that may be considered, and this makes hard the decision-making process. In Rough Set method, all data should be categorized. In this regard, the correlated RWH attributes must be determined. All the information about the case studies in form of determined attributes, classification of attributes and decision level for each of them should be provided.

According to the data gathered in Table 6.1, the main RWH attributes have been determined and are presented in Table 6.2. The attributes have been classified based on 3 classes which denote the suitability conditions for decisions and are high (H), medium (M) and low (L).

Table 6.2: Conditional attributes for ranking decisions of selected case studies (Palermo et al., 2020b).

Conditional Attributes	**Classification of Individual Situations**	**Decision**
(a) Building type	1- One-family building/one-office with garden	H
	2- One-family building/one-office without garden	M
	3- Multi-family building/multi offices with garden	
	4- Multi-family building/multi offices without garden	L
(b) Roof type	1- Slope roof with tiles, corrugated plastic, plastic or metal sheets	H
	2- Flat roof covered with plastic or metal sheet	
	3- Flat roof with concrete or asphalt slabs	
	4-Flat roofs with gravel	M
	5 - Extensive green roof	
	6- Intensive green roof	L
(c) Roof Size (collecting area)	1- Big surface capture (>250)	H
	2- Average surface capture (100 - 250)	M
	3-Small surface capture (<100)	L
(d) The age of the building	1- New building	H
	2- Average age building	M
	3-Old building	L
(e) Average Annual Precipitation	1- > 700 or < 300	H
	2- 300 to 700	M
(f) Number of building residents (based on demand)	1- 1 to 4	H
	2 - 5 to 20	M
	3- more 20	L
(g) Density of city (based on the location of the barrels)	1- Low Density	H
	2- Medium Density	M
	3- High Density	L
(h) Type of urban area	1- New urban area	H
	2- Average age urban area	M
	3- Old urban area	L
(i) Demand usage (m3/y)	1-combined usage	H
	2- one usage (toilet flushing or garden irrigation)	M
	3- laundry	L
	4 - terrace cleaning	
	5- car washing	
(j) Tank size	1 - Big Tank (>20 m^3)	H
	2- Medium Tank (6-20 m^3)	M
	3- Low Tank (< 6 m^3)	L
(k) Economic	1-Very Economic	H
	2- Partly Economic	M
	3-Expensive	L

According to 11 attributes and classes, the selected case studies have been ranked from 1 to 3 and the results are presented in Table 6.3. For instance, in the first case study (*CS1*), since the conditional attribute (a) that is “Building type” is “One-family building”, the highest rank, i.e. 3, has been selected. Since the table represents the correlation between the case studies and conditional attributes it is named "decision rules"

Table 6.3: Data Inspection for analysis of Site Selection Decision Ranking (Palermo et al., 2020b).

Case study	Conditional Attributes											Decision Level
	a	***b***	***c***	***d***	***e***	***f***	***g***	***h***	***i***	***j***	***k***	
CS1	3	3	2	2	3	3	1	2	3	1	2	M
CS2	1	3	3	2	3	1	1	2	2	1	2	M
CS3	3	3	2	2	2	3	1	2	3	2	1	H
CS4	2	3	3	2	2	1	1	2	3	3	1	H
CS5	2	3	3	2	3	2	1	2	2	2	2	M
CS6	2	3	3	2	3	1	1	2	2	3	2	H
CS7	2	3	3	2	3	1	1	2	2	3	2	H
CS8	2	3	2	2	2	3	2	2	2	1	3	M
CS9	2	2	2	2	3	1	2	2	2	1	3	H
CS10	1	3	2	1	3	2	1	1	2	2	1	L
CS11	1	3	1	1	3	2	1	1	3	3	1	L
CS12	1	3	3	3	3	1	1	3	2	3	2	H

All the decisions and attributes have been checked to find out the existence of non-deterministic rules that means that for case studies of similar attributes decisions are different. The number of non-deterministic rules in Table 6.3 was zero. Therefore, the number of conditional attributes is sufficient for determining the decisions. The found reduction in the data is presented in Table 6.4.

Table 6.4. The founded reduction (Palermo et al., 2020b).

Raw	Reduction	Raw	Reduction	Raw	Reduction
1	{a, b, d, j}	13:	{a, b, i, j}	25:	{a, f, j}
2	{a, c, e, j}	14:	{a, b, j, k}	26:	{d, e, g, j}
3	{b, c, e, j}	15:	{a, b, h, j}	27:	{c, f, j}
4:	{a, b, c, j}	16:	{b, c, h, j}	28:	{b, h, i, j}
5:	{b, d, e, j}	17:	{a, e, h, j}	29:	{e, g, h, j}
6:	{a, d, e, j}	18:	{b, e, h, j}	30:	{f, g, h, j}
7:	{b, c, d, j}	19:	{c, e, i, j}	31:	{b, c, i, j}
8:	{a, d, e, f	20:	{a, e, i, j}	32:	{b, d, j, k}
9:	{a, e, f, h}	21:	{d, f, g, j}	33:	{b, h, j, k}
10:	{b, d, f, j}	22:	{b, d, i, j}	34:	{e, j, k}
11:	{a, d, f, k}	23:	{c, e, g, j}	35:	{f, j, k}
12:	{a, f, h, k}	24:	{b, f, h, j}		

After deriving the reducts, the decision rules can be achieved by overlaying the determined reducts on the data. A decision table free of contradiction and determining a minimal decision algorithm can be achieved after elimination of all non-deterministic rules that was zero in this study. The contradictions have been analyzed based on the conditional attributes and the decisions in selected case studies. Moreover, if the attributes do not cause any contradiction they can be removed. In order to check the impact of an attribute on the result, the attributes can be removed one by one. For example, if the conditional attributes (a), (b), (c), and (d) are removed, the decision rules of case studies 1 and 2 might be

contradictory that means the decision levels of these two case studies are subordinate to the mentioned conditional attributes. In this regard, and after elimination of all removable conditional attribute or classes, the minimal decision algorithm has been obtained and is presented in Table 6.5.

Table 6.5: Minimal decision algorithm (Palermo et al., 2020b).

	Rules
Rule 1	(d = 1) => (Decision = L)
Rule 2	(b = 3) & (j = 1) => (Decision = M)
Rule 3	(a = 2) & (j = 2) => (Decision = M)
Rule 4	(f = 1) & (j = 3) => (Decision = H)
Rule 5	(b = 2) => (Decision = H)
Rule 6	(a = 3) & (e = 2) => (Decision = H)

The validation of the rules is presented in Tables 6.6 and 6.7. It must be mentioned that, since the selected case studies are only 12, the accuracy of the rules might not be high. To be able to extend the result of the method to other similar case studies in RWH systems, more field data might be required.

Table 6.6: Confusion Matrix (sum over 10 passes) (Palermo et al., 2020b).

	1	**2**	**3**	**None**
1	2	0	0	0
2	0	2	2	0
3	1	4	1	0

Table 6.7. Average Accuracy (%) (Palermo et al., 2020b).

	Correct	**Incorrect**	**None**
Total	40.00 +- 43.59	60.00 +- 43.59	0.00 +- 0.00
1	20.00 +- 40.00	0.00 +- 0.00	0.00 +- 0.00
2	15.00 +- 32.02	15.00 +- 32.02	0.00 +- 0.00
3	5.00 +- 15.00	45.00 +- 47.17	0.00 +- 0.00

6.3.2 Application of TOPSIS in ranking of rainwater-harvesting systems

In this section, the TOPSIS method has been used to rank the selected case studies and the results are compared with those of a simple ranking. The results of simple ranking

are presented in Tables 6.8 and 6.9. and those obtained by TOPSIS method in Tables 6.10 to 6.12.

Table 6.8: Values of each attribute for each case study (Palermo et al., 2020b).

Case study	Attributes										
	a	**b**	**c**	**d**	**e**	**f**	**g**	**h**	**i**	**j**	**k**
CS1	3	3	150	2	787	4	1	2	58.4	6	2
CS2	1	3	320	2	787	24	1	2	175.2	14	2
CS3	3	3	107	2	612	3	1	2	47.1	13	1
CS4	2	3	625	2	612	42	1	2	705.2	31	1
CS5	2	3	420	2	1086	16	1	2	233.6	14	2
CS6	2	3	420	2	1086	24	1	2	350.4	21	2
CS7	2	3	680	2	1086	32	1	2	467.2	28	2
CS8	2	3	186	2	657	4	2	2	61.3	2.93	3

Table 6.9: Simple ranking of the factors for each case study (Palermo et al., 2020b).

Case study	Rank of Attributes											Sum of ranking	Final rank
	a	**b**	**c**	**d**	**e**	**f**	**g**	**h**	**i**	**j**	**k**		
CS1	1	1	6	1	2	2	4	1	7	6	2	33	6
CS2	3	1	4	1	2	4	4	1	5	4	2	23	4
CS3	1	1	7	1	4	1	1	1	8	5	3	24	5
CS4	2	1	2	1	4	6	1	1	1	1	3	18	2
CS5	2	1	3	1	1	3	3	1	4	4	2	19	3
CS6	2	1	3	1	1	4	3	1	3	3	2	18	2
CS7	2	1	1	1	1	5	3	1	2	2	2	17	1
CS8	2	1	5	1	3	2	2	1	6	7	1	23	4

Table 6.10: TOPSIS matrix without scale (Normalized) (Palermo et al., 2020b).

Case study	Attributes										
	a	**b**	**C**	**d**	**e**	**f**	**g**	**h**	**i**	**j**	**k**
CS1	0.48	0.35	0.13	0.35	0.32	0.11	0.46	0.35	0.06	0.11	0.36
CS2	0.16	0.35	0.27	0.35	0.32	0.26	0.46	0.35	0.18	0.26	0.36
CS3	0.48	0.35	0.09	0.35	0.25	0.25	0.03	0.35	0.05	0.25	0.18
CS4	0.32	0.35	0.53	0.35	0.25	0.59	0.03	0.35	0.73	0.59	0.18
CS5	0.32	0.35	0.36	0.35	0.44	0.26	0.44	0.35	0.24	0.26	0.36
CS6	0.32	0.35	0.36	0.35	0.44	0.40	0.44	0.35	0.36	0.40	0.36
CS7	0.32	0.35	0.58	0.35	0.44	0.53	0.44	0.35	0.48	0.53	0.36
CS8	0.32	0.35	0.16	0.35	0.27	0.06	0.04	0.35	0.06	0.06	0.54

Table 6.11: TOPSIS matrix without scale and equal weighted (Palermo et al., 2020b)

Case study	Attributes										
	a	**b**	**c**	**d**	**e**	**f**	**g**	**h**	**i**	**j**	**k**
CS1	0.044	0.032	0.012	0.032	0.029	0.010	0.041	0.032	0.005	0.010	0.033
CS2	0.015	0.032	0.025	0.032	0.029	0.024	0.041	0.032	0.016	0.024	0.033
CS3	0.044	0.032	0.008	0.032	0.023	0.022	0.003	0.032	0.004	0.022	0.016
CS4	0.029	0.032	0.048	0.032	0.023	0.053	0.003	0.032	0.066	0.053	0.016
CS5	0.029	0.032	0.033	0.032	0.040	0.024	0.040	0.032	0.022	0.024	0.033
CS6	0.029	0.032	0.033	0.032	0.040	0.036	0.040	0.032	0.033	0.036	0.033
CS7	0.029	0.032	0.053	0.032	0.040	0.048	0.040	0.032	0.044	0.048	0.033
CS8	0.029	0.032	0.014	0.032	0.024	0.005	0.003	0.032	0.006	0.005	0.049
V+	**0.044**	**0.032**	**0.053**	**0.032**	**0.040**	**0.053**	**0.003**	**0.032**	**0.066**	**0.053**	**0.049**
V-	**0.015**	**0.032**	**0.008**	**0.032**	**0.023**	**0.005**	**0.041**	**0.032**	**0.004**	**0.005**	**0.016**

Table 6.12 Ranking in TOPSIS based on higher CL and comparison with simple ranking (Palermo et al., 2020b)

Case study	d+	d-	CL	Rank in TOPSIS	Simple Rank Method	Decision Level
CS4	0.040	0.109	0.731	1	2	H
CS7	0.049	0.090	0.645	2	1	H
CS6	0.063	0.064	0.504	**3**	**3**	**H**
CS5	0.077	0.049	0.389	**4**	**4**	**M**
CS3	0.095	0.054	0.363	5	7	H
CS8	0.101	0.053	0.342	**6**	**6**	**M**
CS2	0.088	0.038	0.302	7	5	M
CS1	0.105	0.035	0.250	**8**	**8**	**M**

Despite the fact that in some case studies the difference in ranking methods are minor since in TOPSIS all correlated attributes and the differences among the values are taken into consideration the results could be more accurate.

6.4 Conclusions

There are many benefits in Rainwater harvesting (RWH) systems mainly water saving for non-potable water uses and surface runoff mitigation. Moreover, the collected rainwater can be re-used for several purposes including green roofs and garden, flushing toilets, etc. The analysis showed that, in previous studies the optimization of RWH systems mostly is limited to optimize the size of the tankers according to hydrological and hydraulic analysis and in some cases, this is combined with an economic analysis.

In this study, multi-objective optimization approaches have been considered for comparing algorithms and evaluating the performance of alternatives to identify the ideal solution. For this, a limited set of data extracted from several case studies has been used. The selection of the case studies has been made considering the main possible attributes/factors confronting in rainwater harvesting systems.

The results show that the Rough Set method is a suitable way for analysis of RWH systems and the outcomes can be useful in decision making by decreasing the uncertainties, reducing the cost, and increasing the efficiency. The generated decisions are explicit, and the results are not limited to restrictive assumptions. With consideration of more case studies, more stringent decision rules can be achieved. Moreover, the final ranks of TOPSIS shows the advantages in compared with simple ranking method. According to the results, TOPSIS ranking method showed good agreement with the decision levels in the case studies. This may be due to the consideration of all correlated attributes and of the differences between the values of this ranking method.

Therefore, the Rough Set and TOPSIS methods could be applied as a useful approach in rainwater harvesting systems investigations and provide an additional tool to identify the optimal system and the best site.

The new presented mathematical optimization approaches can improve the previous studies about LIDs. Similar satisfactory results, in fact, were achieved also in Paper IX (Pirouz et. al, 2019) where the same approaches were presented and applied to LID solutions in general, by considering hypothetical case studies.

In conclusion, these methods provide an additional tool for engineers in analysis of essential attributes to select and optimize the best LID system for a project and accordingly define the scenarios and hydrologic or hydraulic modeling. This means that the presented methods would provide a baseline for decision-making and would increase the efficiency of the systems and decrease the project cost by preventing uncertainties.

6.5 References

Arabani, M., Pirouz, M., Pirouz, B. (2012). Geotechnical investigation optimization using rough set theory. 9th International Congress on Civil Engineering (9ICCE), Isfahan, Iran.

Arabani, M., Sasanian, S., Farmand, Y., & Pirouz, M. (2017). Rough-Set Theory in Solving Road Pavement Management Problems (Case study: Ahwaz-Shush Highway). Computational Research Progress in Applied Science & Engineering (CRPASE), 3(2).

Balioti, V., Tzimopoulos, C., & Evangelides, C. (2018). Multi-Criteria Decision Making Using TOPSIS Method Under Fuzzy Environment. Application in Spillway Selection. In Multidisciplinary Digital Publishing Institute Proceedings (Vol. 2, No. 11, p. 637). https://doi.org/10.3390/proceedings2110637

Becciu, G., Raimondi, A., & Dresti, C. (2018). Semi-probabilistic design of rainwater tanks: a case study in Northern Italy. Urban Water Journal, 15(3), 192-199. https://doi.org/10.1080/1573062X.2016.1148177

Campisano, A., & Modica, C. (2012). Optimal sizing of storage tanks for domestic rainwater harvesting in Sicily. Resources, Conservation and Recycling, 63, 9-16. https://doi.org/10.1016/j.resconrec.2012.03.007

Campisano, A., & Modica, C. (2015). Rainwater harvesting as source control option to reduce roof runoff peaks to downstream drainage systems. Journal of Hydroinformatics, 18(1), 23-32. https://doi.org/10.2166/hydro.2015.133

Cipolla, S. S., Altobelli, M., & Maglionico, M. (2018). Decentralized water management: Rainwa-ter harvesting, greywater reuse and green roofs within the GST4Water project. In Multidis-ciplinary Digital Publishing Institute Proceedings, 2(11), p. 673. https://doi.org/10.3390/proceedings2110673

Domènech, L., & Saurí, D. (2011). A comparative appraisal of the use of rainwater harvesting in single and multi-family buildings of the Metropolitan Area of Barcelona (Spain): social experience, drinking water savings and economic costs. Journal of Cleaner production, 19(6-7), 598-608. https://doi.org/10.1016/j.jclepro.2010.11.010

Haghshenas, S. S., Neshaei, M. A. L., Pourkazem, P., & Haghshenas, S. S. (2016). The risk assessment of dam construction projects using fuzzy TOPSIS (case study: Alavian

Earth Dam). Civil Engineering Journal, 2(4), 158-167. http://orcid.org/0000-0003-2859-3920

Haghshenas, S. S., Mikaeil, R., Haghshenas, S. S., Naghadehi, M. Z., & Moghadam, P. S. (2017). Fuzzy and classical MCDM techniques to rank the slope stabilization methods in a rock-fill reservoir dam. Civil Engineering Journal, 3(6), 382-394. 10.28991/cej-2017-00000099

Herrmann, T., & Schmida, U. (2000). Rainwater utilisation in Germany: efficiency, dimensioning, hydraulic and environmental aspects. Urban water, 1(4), 307-316. https://doi.org/10.1016/S1462-0758(00)00024-8

Hwang, C.L., Yoon, K.P. (1981). Multiple attributes decision-making methods and applications. Springer-Verlag, Berlin.

İç, Y. T. (2014). A TOPSIS based design of experiment approach to assess company ranking. Applied Mathematics and Computation, 227, 630-647. https://doi.org/10.1016/j.amc.2013.11.043

Jones, M. P., & Hunt, W. F. (2010). Performance of rainwater harvesting systems in the southeastern United States. Resources, Conservation and Recycling, 54(10), 623-629. https://doi.org/10.1016/j.resconrec.2009.11.002

Krohling, R.A., Pacheco A. G. (2015). A-TOPSIS an approach based on TOPSIS for ranking evolutionary algorithms. Procedia Computer Science, vol. 55, 308–317. https://doi.org/10.1016/j.procs.2015.07.054

Li, Z., Boyle, F., & Reynolds, A. (2010). Rainwater harvesting and greywater treatment systems for domestic application in Ireland. Desalination, 260(1-3), 1-8. https://doi.org/10.1016/j.desal.2010.05.035

Palla, A., Gnecco, I., & La Barbera, P. (2017). The impact of domestic rainwater harvesting systems in storm water runoff mitigation at the urban block scale. Journal of environmental management, 191, 297-305. https://doi.org/10.1016/j.jenvman.2017.01.025

Pawlak, Z. Rough set theory and its applications. (2002). Journal of Telecommunications and Information Technology. vol. 3, 7–10.

Piro P., Turco M., Palermo S.A., Principato F., Brunetti G. (2019b) A Comprehensive Approach to Stormwater Management Problems in the Next Generation Drainage Networks. In: Cicirelli F., Guerrieri A., Mastroianni C., Spezzano G., Vinci A. (eds) The Internet of Things for Smart Urban Ecosystems. Internet of Things

(Technology, Communications and Computing). Springer, Cham. https://doi.org/10.1007/978-3-319-96550-5_12

Chapter 7 – Summary, Conclusions and Future Directions

This Ph.D dissertation is conceived as a cumulative thesis composed of nine papers, already published in international peer-reviewed journals, books and indexed conference proceedings, attached to the appendix, which represent a substantial part of the work. However, this thesis presents not only the findings of the annexed papers, but also additional results, discussion, critical reflections and give a holistic overview of the entire context. In this regard, the structure of this dissertation was conceived in order to provide to the reader a comprehensive analysis of hydrological benefits of Low Impact Development techniques by literature review analysis, experimental investigation, numerical modeling and mathematical approaches. Although, a specific conclusion and outlook is given in each chapter, in this final one an overall view of the entire work in terms of general conclusions and future directions will be discussed.

7.1 Summary and Conclusions

The aim of this thesis was to investigate hydrological benefits of LID techniques by experimental investigation and numerical modeling. LID techniques were analyzed in a comprehensive view to give a new contribution to the scientific community. To achieve this goal, several analyses were carried out by considering different: LID systems, spatial scales, site locations, weather conditions, laboratory techniques, modeling tools (conceptual and mechanistic), numerical analysis, as well as mathematical optimization approaches. In this regard, each case study, discussed during the dissertation, allowed to investigate specific factors which affect the hydrologic/hydraulic behaviour of LID technique and to analyze the LID performances.

More specifically, this dissertation provided contributions by five main aspects:

1. analyzing the state of art of LID systems, by a thorough overview on the principal LID systems components, design features and literature studies, which evaluated the hydrological effectiveness of these solutions, in order to highlight the scientific gaps;
2. assessing the most influential parameters in the development of a detailed hydrodynamic model, based on a real case study in a Continental climate, which integrates conventional drainage infrastructure and LID systems in a sustainable urban stormwater concept;
3. estimating the hydraulic efficiency of a full-scale experimental extensive green roof in Mediterranean climate and the influence of hydrological and physical factors, by empirical analysis, laboratory investigation and mechanistic model implementation;
4. analyzing the performance of LID systems at large-urban scale by considering different land use scenario through a conceptual model;
5. evaluating the use of new mathematical optimization approaches for LID techniques.

More in detail, *Chapter 1* was dedicated to the identification of the stormwater management problem and the innovative solution to solve it. In this regard, the research gaps were identified, the principal aims of the thesis argued, and the structure displayed.

In *Chapter 2* an overview of Low Impact Development (LID) systems was presented, by highlighting design features and analyzing literature studies carried out on

the specific LID systems considered during the thesis. This overview allowed to identified the following key aspects.

- The lack of comprehensive analysis finalized to evaluate the hydrological performance and the physical processes occurring in LID systems, by considering both long-term experimental investigation and numerical modeling.
- The main factors affecting LID hydrological/hydraulic behaviour, can be principally grouped in two main categories site location/weather conditions and the design features.
- The heterogeneity of LIDs' stratigraphy, in terms of materials and components, and consequently the complexity of the physical processes, involved in these systems, require modeling tools able to accurately interpret their hydraulic behaviour.
- The physical parameters, specifically the soil hydraulic properties are not always investigated in a properly way, by limiting the analysis to specific parameters or literature values.
- The analysis of the most influential hydrological parameters is often quite restricted for the missing of full-scale LID implementation, as well as for the unavailability of long-term hydrological monitored data.
- Finally, the missing of tools able to evaluate the optimal solution in terms of LID system and site location by mathematical approaches.

Therefore, based on these considerations in the others Chapters of the thesis these scientific gaps and limiting key factors were considered and overcome, by carrying out a comprehensive analysis of different LID systems in order to investigate the hydrological benefits of these innovative and sustainable solutions at multiple spatial scales, considering experimental full-scale implementation and long-term monitored data as well as modeling large-scale implementation, lab experimental investigations, conceptual and mechanistic models, sensitivity analysis and mathematical optimization approaches.

Therefore, based on these main considerations, in *Chapter 3* a global sensitivity analysis (GSA) was applied to a microscale hydrodynamic model, which combines pipe infrastructure and small-scale source treatments in terms of Rain Gardens (RGs), in order to identify the most influential model parameters. To achieve this purpose, the model creation and simulation, was developed by the Storm Water Management Model (SWMM), while for the GSA the Elementary Effect Test (EET) was considered. More in detail, the uncertainties of 18 model input parameters, (10 for subcatchment and 8 for rain gardens),

are assigned and analyzed by 1,900 simulations. The model's responses are assessed at four main RGs and four model outputs: total inflow, surface level, storage level, and surface runoff at the RGs. GSA's findings showed that an important role is taken by the Depression Storage Impervious, parameter related to the Inflow outcome, followed by the percentage of Impervious Area. While, form the results obtained for the last three model outputs, related to RGs, emerged that the Soil Hydraulic Conductivity and Seepage Rate parameter are the most sensitive parameters. Therefore, in agreement with the studies, discussed in *Chapter 2*, the soil hydraulic properties of infiltration/retention-based LID techniques take an important role for the hydraulic efficiency of the systems in terms of retention and detention of stormwater runoff. Thus, the identification of these properties for LID systems is crucial in order to correctly evaluate the hydraulic performance of such techniques. Moreover, the development of the hydrodynamic model, described in this chapter, allowed also to elaborate the concept of an advanced LID systems, by the modeling implementation of a smart rain barrels, which represents a future research direction.

Starting from the finding achieved in *Chapter 3* in term of most influential parameters and based on the main conclusions achieved in *Chapter* 2, in *Chapter 4* the analysis of a full-scale extensive green roof, located at University of Calabria, was considered in order to assess the hydrological effectiveness of this LID technique in Mediterranean climate. To achieve this aim, the study of some hydrological and physical parameters was taken into account, by monitoring analysis, laboratory investigation on the soil substrate hydraulic properties, and numerical modeling. More in detail, first a field monitoring campaign for one year was conducted, and four hydrological indices (subsurface runoff coefficient, peak flow reduction, peak flow lag-time, and time to start runoff) on an event scale were evaluated, as well as possible correlations between these indicators and hydrological features of storm events were assessed. The findings showed that the subsurface runoff coefficient (SRC) ranges from 17.5% to 83.3% with an average value of 50.4% for the rainfall events with a precipitation depth more than 8 mm, confirming the optimal retention capacity of the experimental green roof in the Mediterranean climate. Moreover, this average value of SRC can be considered during preliminary design choices for the construction of green roofs in Mediterranean climate conditions. Later, to evaluate the influence of the substrate depth on green roof retention capacity, a six-month dataset (January 2016 to June 2016) was considered. Reference evapotranspiration was calculated using the Penman–Monteith equation and in in order to

assess the hydrological response of the green roof by variating the soil substrate depth (6 cm, 9 cm, 12 cm, and 15 cm) using the mechanistic model HYDRUS 1D model, the hydraulic properties of the soil materials were investigated in Laboratory, by the simplified evaporation method. The results obtained in this phase showed the considered substrate depths were able to achieve a runoff volume reduction of 22% to 24% during the selected period for the Mediterranean climate conditions without observing flow over the top surface of the soil. These findings may be explained by the dataset used in these simulations being obtained during winter and spring where evapotranspiration was not predominant. Thus, in the field of extensive green roofs, as the outflow volume reduction achieved by increasing the soil depth was not significant, the ideal depth for soil substrate would be 6 centimetres, while the maximum depth of 15 cm is not recommended for adoption considering the structural overloading.

To follow this study, which considered the evaluation of a single LID units, in *Chapter 5*, the hydrological effectiveness of Low Impact development solutions on the urban stormwater management, at large-urban scale, was examined. The analysis was carried out by considering different land use conversion scenarios including the implementation of LID practices, by developing a predictive conceptual model by PCSWMM. A specific permeable pavement and green roof, developed at University of Calabria, have been considered for the different conversions scenarios: *Scenario 0* (reference scenario), *Scenario 1* (replacement of 30% of rooftop and 30% of impervious surfaces, excluding roads opened to traffic, with green roof and permeable pavement, respectively); *Scenario 2* (where 60% is the related conversion percentage), *Scenario 3*, an ideal scenario, which considers 100% of replacement. The results show that the Runoff Coefficient (RC) average value decreases from 98.1% in the condition of almost total imperviousness to 36.4% in Scenario 3, obtaining also good results for the inter-medium scenarios. While the Runoff Reduction (RR) (%) and Peak Flow Reduction (PFR) (%) present a linear increase of their values with the reduction of the impervious surfaces, simulated from scenario 1 to scenario 3. Globally, the findings confirm the suitability of these LID solutions to reduce surface runoff and, therefore, urban flooding risk. More in detail, the findings reveal that this beneficial effect can be reached by converting also only a small percentage of the impervious surfaces. Considering that practical and economic conditions could limit the implementation of these sustainable practices in urban area, this can be considered a relevant finding.

Finally, as discussed in previous Chapters, since many aspects related to LIDs design and operation, as well as the choice of the facility and its location can affect the results in terms of hydraulic efficiency, thus an optimization approach can be a useful tool for designers and decision makers. In this regard, *Chapter 6* introduced the use of new Mathematical Optimization Approaches for LID techniques. To achieve this goal, TOPSIS (Technique for Order Preference by Similarity to Ideal Solution) and Rough Set method as Multi-Objective Optimization approaches were applied by analyzing different literature case studies. In this chapter, the mathematical approaches were applied to Rainwater Harvesting (RWH) systems. For the analysis, the selection of the case studies has been made considering the main possible attributes/factors confronting in rainwater harvesting systems. The results showed that the Rough Set method is suitable way for analysis of RWH systems. The generated decisions are explicit, with consideration that with more case studies, more stringent decision rules can be achieved. Moreover, TOPSIS ranking method, advantageous method in compared with simple ranking method, exhibited good agreement with the decision levels in the case studies. Therefore, these approaches can be considered as additional tools for the analysis of essential attributes to optimize LIDs, providing a baseline for engineers and decision-making.

7.2 Future Directions

This thesis is not understood as a conclusive act, but as an intermediate step towards new and advanced analysis in the scientific research on Low Impact Development techniques, as well as on others innovative systems for sustainable urban stormwater management.

Despite the interesting findings achieved in this work, since Low Impact Development approaches are Multi-Objectives and many factors affect LID behaviour, some simplifications and assumption were made during the work, therefore there is space for improvements, by considering all aspects not yet taken into account.

Overall, based on the research results, several further investigations are recommended.

From the Literature Review it emerged that some LID practices, like green wall systems are not still widely investigated from a hydraulic perspective. In this regard, future

research will extend the analysis to this facility, and to others LID solutions not yet investigated, by considering experimental investigations and numerical modeling.

Moreover, as introduced in some Chapters, an innovation in the field of Urban drainage is look at the single LID techniques as smart objects, optimizing them with ICT technologies, based on the IoT (Internet of Things) paradigm. In this regard, future research challenge will be to investigate the use of IoT from the single LID unit optimization to the large scale optimization, as well as investigate the integrated use of more than one LID solutions, with the aim to optimize their operation in Real Time Control maximizing the hydraulic efficiency. This concept can be extended also to the conventional drainage network, and, in this regard, some results are already achieved, with the final aim to reach a smart urban stormwater management.

Acknowledgements

The author would like to thank the CHI for the disposal of PCSWMM in the University Grant Program, used during the development of the different conceptual models considered during the thesis (Chapter 3 and 5).

The research presented in Chapter 2 was carried out during six months spent at the University of Innsbruck, for the international mobility programme of PhD students. Moreover, the “smart campus” and “smart rain barrels”, considered in this research were funded by the Climate and Energy Fund within the Smart Cities program (project number 858782).

In Chapters 4 and 5, the data from experimental sites, located at University of Calabria were considered, therefore the research was based on the experimental installation funded by the Italian National Operative Project (PON) PON01_02543 “Integrated and sustainable management service for the water–energy cycle in urban drainage systems”, Research and Competitiveness for the convergence regions 2007/2013, I Axis “Support to structural changes” operative objective 4.1.1.1. “Scientific-technological generators of transformation processes of the productive system and creation of new sectors” Action II: “Interventions to support industrial research”.

The overview on the green wall system (presented in part in Chapter 2), as well as the study on the new mathematical optimization approaches presented in Chapter 6 was co-funded by the “Innovative Building Envelope through Smart Technology (I-Best)” Project funded by the Italian National Operational Program "Enterprise and Competitiveness" 2014-2020 ERDF – I AXIS “Innovation” - Action 1.1.3 – “Support for the economic enhancement of innovation through experimentation and the adoption of innovative solutions in processes, products and organizational formulas, as well as through the financing of the industrialization of research results”.

Moreover, in the annexed papers can be found in details each Acknowledgements related to each research.

Appendix – Papers

Paper I

Parameter Sensitivity of a Microscale Hydrodynamic Model

Palermo S.A., Zischg J., Sitzenfrei R., Rauch W., Piro P. (2019a)

Published in: Mannina G. (eds) New Trends in Urban Drainage Modelling. UDM 2018. Green Energy and Technology. Springer, Cham.
https://doi.org/10.1007/978-3-319-99867-1_169

Parameter Sensitivity of a Microscale Hydrodynamic Model

Stefania Anna Palermo[1,2(✉)], Jonatan Zischg[2], Robert Sitzenfrei[2], Wolfgang Rauch[2], and Patrizia Piro[1]

[1] Department of Civil Engineering, University of Calabria, Rende, CS, Italy
stefania.palermo@unical.it
[2] Department of Infrastructure Engineering, University of Innsbruck, Innsbruck, Austria

Abstract. Here we present the results of a global sensitivity analysis (GSA) applied for a microscale hydrodynamic model, which combines pipe infrastructure and small scale source treatments in terms of raingardens (RGs). The aim is to identify the most influential model parameters to support the decision for future measurement installation sites and smart water control. For the model creation and simulation, the Storm Water Management Model (SWMM) is used. For the GSA method the Elementary Effect Test (EET) is applied, were uncertainties to 18 model input parameters, comprising 10 sub-catchment and 8 Low Impact Development (LID) parameters, are assigned and analysed by 1,900 simulations. The model's responses are evaluated at four main RGs and for two model outputs: *Inflow* and *Surface runoff* at the RGs. First results show that the most sensitive factors are the *Depression Storage Impervious* and the *Soil Hydraulic Conductivity* for the *Inflow* and *Surface Runoff* at RGs, respectively.

Keywords: Elementary Effect Test · LID · Sensitivity · SWMM Uncertainty

1 Introduction

The emerging challenges due to ongoing urbanization and climate change require a transition from traditional drainage infrastructure towards a sustainable, smart and resilient urban water management.

One promising strategy is the implementation of decentralized stormwater controls, also known as e.g. Green Infrastructure (GI) or Low Impact Development (LID), which provide several benefits at multiple scales (Zischg et al. 2018, Maiolo et al. 2017). Different studies have analyzed those beneficial effects and many numerical and physical models were developed to prove GI feasibility and performance (Garofalo et al. 2016). By implementing multiple small scale units in urban areas, a complex system of temporal storage facilities for managing stormwater runoff is created.

For the system optimization with regard of flood mitigation, pollutant reduction, sustainable irrigation, or recreational aspects, smart water control is needed. This can

G. Mannina (Ed.): UDM 2018, GREEN, pp. 982–987, 2019.
https://doi.org/10.1007/978-3-319-99867-1_169

be achieved by equipping the existing drainage systems with low-cost sensors and controllers, in order to have a highly adaptive new green and grey stormwater system.

This work provides a first step towards the sustainable operation of the newly set up "Smart Campus" at the University of Innsbruck, where recently LID systems and multiple sensors have been implemented. The first objective of this study is to present the development of a detailed micro-scale hydrodynamic model. Secondly, the most influencing model parameters are identified through a sensitivity analysis, including the uncertainties of subcatchment and LID parameters.

2 Materials and Methods

2.1 Case Study Description

The case study area is the University Campus Innsbruck, in Tyrol, Austria (47° 15'50.87"N 11°20'40.17"E), where 12 Rain Gardens (RGs), 1 Green Roof (GR) and 3 Gravel Roofs were implemented to enable a more sustainable water management strategy and to make the Campus more attractive and resilient to flooding risk.

To connect impervious surface areas (e.g. pavements, streets) to those LIDs a new drainage system, consisting of a network of open channels (OCs) with a parabolic cross-section and PVC conduits (DN200) was built. This system supports the existing underground drainage network, composed of around 420 m of conduits (DN200÷DN600), which collect the rainwater only from the roofs. Thus, the total drainage system can be divided into two independent systems: one related to the RGs; and the second one concerning the old drainage network.

Four RGs with an area of 65 m^2 each are located at the centre of the main square and receive the rainwater collected only by the OCs system. The others RGs (ranging from 16 m^2 to 43 m^2) intercept the stormwater runoff from different areas. Even if the RGs differ from each other regarding the area and the storage depth, they have identical stratigraphy, and consist of the following horizontal layers (from top to bottom): (1) a surface vegetated layer vegetated with a berm height of 26 cm; (2) a soil layer with a thickness of 30 cm, (3) a storage layer with varying depths and (4) an underdrain.

2.2 Model Development

A detailed hydrodynamic model was developed considering the entire Campus drainage system. The dynamic rainfall-runoff simulation model PCSWMM (CHI PCSWMM), based on the EPA-SWMM version 5.1.012 (Rossman 2015), was used. The model was built considering topographical data, land use classification, new and existing stormwater system, RG details, taken from construction plans and site measurements.

To obtain a detailed microscale model, the study area of 3.02 ha was divided into 252 subcatchments, which were precisely defined depending on changes of the surface slope and the land use. The drainage systems consists of 139 Junctions, 139 Conduits and 13 LID Controls (12 RG and 1 GR). The subcatchment width that describes the overland flow characteristic is generally an important and sensitive model parameter,

especially for large subcatchments. For our microscale model, knowing all geometrical features of the system, it was calculated as the fraction between the subcatchment area and the flow length. The Soil Conservation Service (SCS) Curve Number (CN) method was considered for the infiltration method and the flow routing computations were based on the Dynamic Wave Equations.

2.3 Sensitivity Analysis

Taking into account that the implementation of the LID structures strongly influences the hydraulic performance of the drainage system and that most model input parameters are uncertain, a Global Sensitivity Analysis (GSA) was carried out. More specific, the Morris screening method (Morris 1991), also known as Elementary Effect Test (EET), was used (Saltelli et al. 2008).

Two sensitivity measures, the standard deviation of the EET (σ) and the mean of EET (μ) are calculated. The sampling strategy defines r trajectories in the input space (here assumed equal to 100). This strategy selects the starting point randomly over a uniform grid of the parameter space and the subsequent points by moving one factor at a time (OAT) by a fixed amount Δ, so that each trajectory allows for evaluating one Elementary Effect (EE) per factor (Pianosi et al. 2016).

To consider the spatial variability of the model results ("*prediction function*"), the outcome of the four main circular RGs was evaluated at different horizontal layers for the presented case study (see Sect. 2.1).

Starting from the assumption the site-specific subcatchment parameters, *slope*, *width* and *area* are measured physical features; the following 18 input parameters were selected for the GSA (see Table 1). For each parameter, the range of variability was chosen based on of their physical attributes and by considering reported values in the SWMM Manual (Rossman 2015).

As previously mentioned, the four main circular RGs were considered for the sensitivity analysis of this study. The effect of the variability of each parameters was analysed by considering two different model outputs for the four RGs. The first one is the *LID Total Inflow*, which considers the total runoff intercepted in each RG and takes into account the influence of the subcatchment parameters; the other one is the *LID Surface Runoff* to evaluate the hydrological performance of the RGs. To summarize the four main RGs with similar physical characteristics, but different intercepted surfaces, the mean values of these outputs are built. For the hydrodynamic simulation, design storm event with a return period of one year (1.13 mm/min) was used.

For carrying out the GSA 1,900 model runs are performed through a Matlab Script which uses SWMM and integrates the SAFE-toolbox (Pianosi et al. 2015).

3 Results and Discussion

First results of the EET Sensitivity Analysis are reported in Fig. 1, where the Mean of EEs versus their standard deviation (left side) and the Convergence plots (right side) are shown. In the graphs on the left side - where each input factor corresponds with one point - the point located at the more right side along the horizontal axis is the more

Table 1. Input parameters for GSA, meaning and corresponding range of variability taken from User SWMM Manual

	N	Name of parameter	Meaning	Value range
Subcatchemnet Parameters	1	Imperv (%)	*Percent of impervious area*	90–100
	2	Perv (%)	*Percent of pervious area*	0–10
	3	Depression storage - Imperv (mm)	*Depth of depression storage on impervious area*	1.27–2.54
	4	Depression storage -Perv (mm)	*Depth of depression storage on pervious area*	2.54–5.08
	5	N-Imperv	*Manning's roughness coefficient for impervious area*	0.012–0.014
	6	N-Perv	*Manning's roughness coefficient for pervious area*	0.13–0.24
	7	CN-Imperv	*SCS runoff curve number for impervious area*	90–98
	8	CN-Perv	*SCS runoff curve number for pervious area*	30–61
	9	Drying Time (days)	*Time for a fully saturated soil to be completely dry*	2–14
	10	OpenChannel Roughness	*Manning's roughness coefficient for Open Channel*	0.022–0.026
RG Parameters	11	Vegetative Volume (fraction)	*Fraction of volume within the surface storage depth filled with vegetation*	0.1–0.2
	12	Porosity (volume fraction)	*The volume of pore space relative to total volume of soil*	0.42–0.437
	13	Field Capacity (volume fraction)	*Volume of pore water relative to total volume after the soil has been allowed to drain fully*	0.062–0.105
	14	Wilting Point (volume fraction)	*Volume of pore water relative to total volume for a well dried soil where only bound water remain*	0.024–0.047
	15	Conductivity (mm/hr)	*Hydraulic conductivity for the fully saturated soil*	30–180
	16	Conductivity Slope	*Slope of the curve of log(conductivity) versus soil moisture content (dimensionless)*	30–60
	17	Seepage rate (mm/hr)	*The rate at which water seeps into the native soil below the layer*	30–180
	18	Drain coefficient (mm/hr)	*The drain coefficient C which determines the rate of flow through a drain*	3–6

influential one, while the higher up referring to the vertical axis is that one presents the larger degree of interactions with other factors. In the graphs on the right side, the sensitivity indexes are estimated using an increasing sample size by considering one line per factor, while the dashed lines represent confidence bounds (Pianosi et al. 2016).

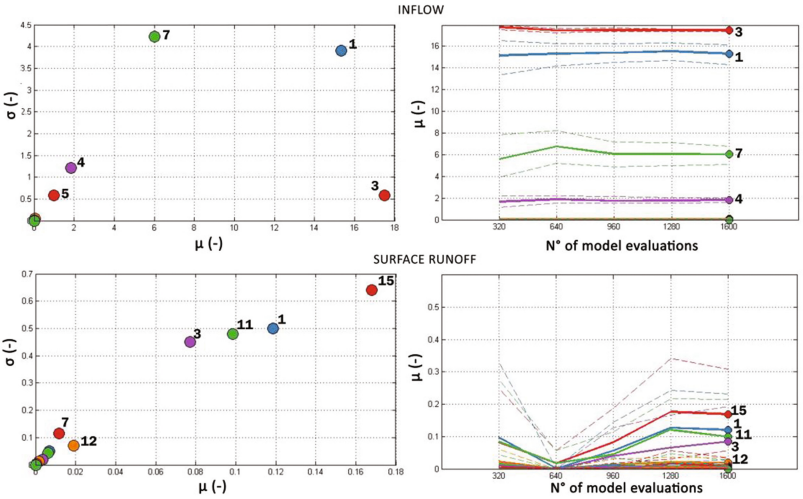

Fig. 1. Results of GSA for the 2 model outputs in terms of: mean of EEs vs their standard deviation (left side) and the Convergence plots (right side). The number of each parameter are the same reported in Table 1.

Being the μ of EEs a measure on the global sensitivity, the findings show that the most influential factor for the *LID Total Inflow* output is the *Depression Storage Impervious* (3), the second one is the *% Impervious Area* (1). Even if, the higher σ is reached by the *CN-Impervious* (7), the factor 1 presents also a high σ, and this means that these two factors (7 and 1) have a huge degree of interaction with the other factors.

By considering the results obtained for the *LID Surface Runoff* outcome, it can be seen that the *Soil Hydraulic Conductivity* (15) is the most sensitive parameter and it presents also the greater degree of interaction with the other factors. The *% Impervious Area* (1), the *Vegetative Volume* (11), and the *Depression Storage Impervious* (3) follow this result. The plots on the right side - where each μ index is estimated using an increasing sample size (one line per factor) - confirm previous findings in terms of most influential factors, also providing other details about the number of model evaluations needed to reach the convergence.

4 Conclusions

In this study, the development of a microscale model for enhancing the implementation of tools, devices and methods related to the smart campus project, i.e. smart water management case study at the University Innsbruck was presented.

Moreover, a global sensitivity analysis (GSA) of the model was carried out in order to identify the most influential parameters. The model's performances were analysed at four RGs and for two model outputs (Inflow and Surface Runoff at the RG).

First results showed that an important role is taken by the *Depression Storage Impervious* parameter related to the *Inflow* outcome and that the *Soil Hydraulic Conductivity* is the more sensitive factor for the RG hydraulic performance.

Acknowledgments. The authors would like to thank the CHI for the disposal of PCSWMM in the University Grant Program.

This research was funded by the Climate and Energy Fund within the Smart Cities program (project number 858782)

References

CHI PCSWMM. https://www.pcswmm.com/. Accessed 20 Mar 2018

Garofalo, G., Palermo, S., Principato, F., Theodosiou, T., Piro, P.: The influence of hydrologic parameters on the hydraulic efficiency of an extensive green roof in mediterranean area. Water **8**(2), 44 (2016)

Maiolo, M., Carini, M., Capano, G., Piro, P.: Synthetic sustainability index (SSI) based on life cycle assessment approach of low impact development in the Mediterranean area. Cogent Eng. **4**(1), 1410272 (2017)

Morris, M.D.: Factorial sampling plans for preliminary computational experiments. Technometrics **33**(2), 161–174 (1991)

Pianosi, F., Sarrazin, F., Wagener, T.: A Matlab toolbox for global sensitivity analysis. Environ. Modell. Softw. **70**, 80–85 (2015)

Pianosi, F., Beven, K., Freer, J., Hall, J.W., Rougier, J., Stephenson, D.B., Wagener, T.: Sensitivity analysis of environmental models: a systematic review with practical workflow. Environ. Modell. Softw. **79**, 214–232 (2016)

Rossman, L.A.: Storm Water Management Model - User's Manual, Version 5.1. Cincinnati: National Risk Management Research Laboratory, Office of Research and Development, US Environmental Protection Agency (2015)

Saltelli, A., Ratto, M., Andres, T., Campolongo, F., Cariboni, J., Gatelli, D., Saisana, M., Tarantola, S.: Global Sensitivity Analysis. The Primer. Wiley, Hoboken (2008)

Zischg, J., Zeisl, P., Winkler, D., Rauch, W., Sitzenfrei, R.: On the sensitivity of geospatial low impact development locations to the centralized sewer network. Water Sci. Technol. wst2018060 (2018)

Paper II

Hydrological Effectiveness of an Extensive Green Roof in Mediterranean Climate

Palermo, S. A., Turco, M., Principato, F., & Piro, P. (2019b)

Published in: Water, 11(7), 1378.
https://doi.org/10.3390/w11071378

water

MDPI

Article

Hydrological Effectiveness of an Extensive Green Roof in Mediterranean Climate

Stefania Anna Palermo [1,*], Michele Turco [2], Francesca Principato [1] and Patrizia Piro [1]

[1] Department of Civil Engineering, University of Calabria, 87036 Rende (CS), Italy
[2] Department of Environmental and Chemical Engineering, University of Calabria, 87036 Rende (CS), Italy
* Correspondence: stefania.palermo@unical.it

Received: 16 May 2019; Accepted: 2 July 2019; Published: 4 July 2019

Abstract: In urban water management, green roofs provide a sustainable solution for flood risk mitigation. Numerous studies have investigated green roof hydrologic effectiveness and the parameters that influence their operation; many have been conducted on the pilot scale, whereas only some of these have been executed on full-scale rooftop installations. Several models have been developed, but only a few have investigated the influence of green roof physical parameters on performance. From this broader context, this paper presents the results of a monitoring analysis of an extensive green roof located at the University of Calabria, Italy, in the Mediterranean climate region. To obtain this goal, the subsurface runoff coefficient, peak flow reduction, peak flow lag-time, and time to the start of runoff were evaluated at an event scale by considering a set of data collected between October 2015 and September 2016 consisting of 62 storm events. The mean value of subsurface runoff was 32.0% when considering the whole dataset, and 50.4% for 35 rainfall events (principally major than 8.0 mm); these results indicate the good hydraulic performance of this specific green roof in a Mediterranean climate, which is in agreement with other studies. A modeling approach was used to evaluate the influence of the substrate depth on green roof retention. The soil hydraulics features were first measured using a simplified evaporation method, and then modeled using HYDRUS-1D software (PC-Progress s.r.o., Prague, Czech Republic) by considering different values of soil depth (6 cm, 9 cm, 12 cm, and 15 cm) for six months under Mediterranean climate conditions. The results showed how the specific soil substrate was able to achieve a runoff volume reduction ranging from 22% to 24% by increasing the soil depth.

Keywords: green roof; rainfall runoff; subsurface runoff coefficient; retention; soil depth; HYDRUS-1D model; urban hydrology

1. Introduction

The combined effect of climate change and land-use alterations, due to ongoing urbanization, produces several environmentally adverse effects. The constant loss of natural areas, which significantly affects the natural hydrological cycle, and the increase in the frequency of extreme weather events have resulted in a considerable increase in runoff volumes that overload the drainage systems and produce floods [1–4].

In this scenario, the use of sustainable solutions as an alternative to conventional techniques has become a general goal of urban water management. To move in this sustainable direction, low impact developments (LIDs) such as green roofs (GRs) are a possible eco-solution that contributes to restoring the pre-development natural hydrological response [5–8].

GRs, by exploiting otherwise unused spaces, are particularly beneficial in densely built urban areas [9]. They represent a source of storm water runoff mitigation by reducing the total runoff volume, peak flow rate, and delaying peak discharge time into the combined sewer systems [10,11]. GRs, which

incorporate both the natural environment and engineered systems, offer a wide range of other benefits, including an enhancement of water quality, reduction in the building energy demand, attenuation of urban heat islands, decrease in air pollution and noise levels in urban spaces, increase in the building's aesthetic value, and wildlife and biodiversity growth [12–17].

Many studies agree on the classification of GRs into two main categories: extensive and intensive, which differ from each other regarding the depth of soil layer and vegetation. Generally, extensive GRs have a thin soil layer of less than approximately 15 cm, whereas intensive soil layers exceed this value; shallow rooting and drought-resistant plants are used for the extensive GR, whereas deeper rooting plants are used for the intensive GRs. Therefore, due to its characteristics, the extensive GR is lighter, cheaper, and requires less maintenance than the intensive one [18–20].

Several studies have analyzed GRs retention performance worldwide; many of these have been conducted on a pilot scale, generally consisting of different test beds or similar modules [11,18,19]; others have been conducted on a full-scale rooftop [10,20,21]. However, not all of these have analyzed the GR behavior for a continuous monitoring period, evaluating each parameter on an event scale.

The hydraulic behavior of GRs has also been analyzed from a modeling point of view. Numerical models have been developed using software such as the Environmental Protection Agency (EPA)'s Storm Water Management Model (SWMM) [19,22–24], Soil, Water, Atmosphere, and Plant (SWAP) model [25], and HYDRUS model [26–29].

From the analysis of these studies, some indicators (runoff volume reduction, peak flow reduction, peak flow lag-time, etc.) have been used to estimate GR hydraulic effectiveness. Another useful lumped parameter that is crucial for designing purposes is the subsurface runoff coefficient (SRC), which is calculated as the ratio between the total runoff depth delivered from the GR and the total rainfall depth, i.e., the inverse value of the GR retention capacity. From a literature review completed by Garofalo et al. [30], the SRC presented a large variability in mean value, ranging from 0.30 to 0.90. This wide range can be explained by analyzing, for each study, the climate conditions of the GR site, the GR's size (full-scale or pilot system), period of data analysis, the time step resolution, and the hydraulic and physical features.

Factors that typically influence GR water retention capacity can be grouped in two main categories: weather conditions (length of the antecedent dry weather period, season/climate, characteristics of rainfall event) and the GR's physical features (number of layers and materials, substrate depth, its hydraulic characteristics, type of vegetation, percentage of roof covered, roof geometry, and green roof age). Being unable to intervene in the weather conditions of the site where the installation is located, the choice of the physical characteristics of the substrate is crucial. In this regard, many studies have observed that the hydraulic behavior of a GR is influenced by the substrate depth and type [31–33]. Some of these studies were conducted in the laboratory by considering constant rainfall data and not real data recorded by a rain gauge, whereas others considered the results of modeling simulations based on literature hydraulic soil properties and not real substrate hydraulic properties.

From this broader context, the first objective of this study was to present the field hydrological monitoring results of a specific extensive GR that has been installed at the University of Calabria, Italy, in a Mediterranean climate. To complete this analysis, first, one year of rainfall data (October 2015 to September 2016) recorded by a rain gauge located on the experimental site was selected. Secondly, the corresponding runoff from the GR was evaluated and compared with the runoff from an impervious roof, which was located at the same site. Thirdly, to analyze the green roof's hydraulic efficiency, the response in terms of the SRC, peak flow reduction (PFR), peak flow lag-time (PFL), and time to start of runoff (TSR) were determined on an event scale. The second objective of the study was to evaluate the influence of the soil depth on the retention capacity of a substrate soil for an extensive green roof in Mediterranean climate by considering the measured soil hydraulic properties and varying the thickness (from 9 to 15 cm) by means of the HYDRUS-1D model.

2. Materials and Methods

2.1. Experimental Site

The experimental green roof (Figure 1) was built in 2012 on the terrace of the Department of Mechanical, Energy and Management Engineering (DIMEG), at the University of Calabria, Italy, located 221 m above sea level in the Vermicelli Catchment. The University is in the south of Italy in the vicinity of Cosenza (39°18′ N 16°15′ E), under a Mediterranean climate condition, which is characterized by an average annual precipitation of 881.2 mm/year and a mean annual temperature of 15.5 °C [27].

Figure 1. The experimental green roof (GR) located at the University of Calabria, Italy. A map of Italy, with the location of the green roof (left), the GR experimental site (middle), and an axonometric detail stratigraphy (right). All the figures were captured or created by the Urban Hydraulic and Hydrology Laboratory, University of Calabria, Italy.

The green roof (GR) was built according to Italian regulation UNI 11235, and from top to bottom consisted of: (1) a surface layer, vegetated with three native Mediterranean species; (2) a commercial soil substrate, called "Terra Mediterranea" (Harpo spa, Trieste, Italy), with a maximum depth of 8 cm composed of a mineral terrain; (3) a permeable geotextile with a weight of 105 g/m^2 to prevent fine soil particles from moving into the underlying layers; (4) a drainage layer in polystyrene foam with a water storage capacity of 11 L/m^2 and a drainage capacity of 0.46 L·s^{-1}m^{-2}; (5) an anti-root layer consisting of a waterproof bituminous membrane with an anti-root additive, specific for green roof installation; and (6) an additional recovery waterproof membrane in elastobituminous membrane. In detail, as discussed in depth by Brunetti et al. [27], the soil substrate consists of a mineral soil with 74% gravel, 22% sand, and 4% silt and clay; it presents a measured bulk density of 0.86 g·cm^{-3} and 8% organic matter, which was determined in the laboratory using the Walkley–Black method. Among the three native Mediterranean species, two are herbaceous plants that are suited for well-drained soils (*Dianthus gratianopolitanus* and *Cerastium tomentosum*), and one is a succulent plant (*Carpobrotus edulis*), which is characterized by a high drought tolerance. More detail on the specific soil substrate hydraulic properties are reported in the results section, where the measurements recorded in the laboratory are provided.

To evaluate the hydraulic efficiency of this specific stratigraphy, the outflow collected from the GR, which is characterized by an area of 50 m^2 and a slope of 1%, was compared with that discharged by an impervious roof (IR) located on the same site, which presented an area of 40 m^2. The different areas of the GR and IR were considered during the outflow comparison analysis.

The GR water supply is guaranteed only by reusing the green roof's outflow, which was collected in a specific storage tank and distributed through a drip irrigation system. This irrigation system is activated during drought periods, generally occurring in summer when the precipitation volume for the specific climate condition is low and very high temperatures are recorded in accordance with low

values of soil moisture measured in the soil substrate. By analyzing the whole dataset, the irrigation, actioned only during the driest days, did not affect the runoff results.

Rainfall depth was measured every minute using a tipping bucket rain gauge with a resolution of 0.254 mm, which was located on the roof. The outflow rates were collected by a flow meter device that was installed at the base of the building, consisting of a vertically developed system, formed by a polyvinyl chloride (PVC) pipe with a sharp-crested weir [34]. The water level in the device was measured by a pressure transducer (Ge Druck PTX1830, GE Measurement & Control Solutions, Groby Leicester, UK), with a measurement range of 75 cm and an accuracy of 0.1% of the full scale, and was continuously recorded in the SQLITE database system with a resolution of 1 min.

2.2. Data Analysis

For this study, rainfall and runoff data with one-minute time resolution that were recorded at the experimental site between October 2015 and September 2016 were considered.

In the first phase, from all the data collected, only the events with a precipitation depth greater than 2 mm were selected. This assumption was supported by an analysis of the recorded rainfall events. We found that the 51 events (total volume around 28 mm) with rainfall depths less than 2 mm are unlikely to produce runoff volume for the specific site, confirming the assumption of Voyde et al. [10]. Individual events were also defined as being separated by continuous dry periods of at least six hours [10,11,35].

To consider the hydrological features of each storm event, the precipitation depth (PD), rainfall duration (D), rainfall intensity (i), antecedent dry weather period (ADWP, defined as the dry weather period between two independent rainfall events), and event return period (RP, defined as the average recurrence interval between events equaling or exceeding a specific magnitude [36]), were evaluated at the event scale. To use a more rigorously probabilistic method, the characteristics of the selected storm events were evaluated by considering the local precipitation pattern. For the evaluation of the return period (RP) event, the experimental rainfall events were compared with the historical records obtained from the Regional Agency Prevention Environment in Calabria Region, Italy (ARPACAL) [37]. To consider all the rainfall events here with a duration of more than one day, the intensity–duration–frequency (IDF) relationships were computed by analyzing the historical records of the annual maximum series for rainfall durations of 1, 3, 6, 12, and 24 hours (1923–2012) and for rainfall durations of 1, 2, 3, 4, and 5 days (1935–1999) according to data from the rain gauge station in Cosenza.

In the second phase, for each selected rainfall event and by using the data collected from the flux meter devices, the corresponding total outflow rate in terms of runoff depth (RD) from the GR and IR were evaluated. We chose to show the results in terms of runoff depth (mm) and not in terms of runoff flow (L/s or m^3/s) to obtain two comparable values, despite the two different areas of the GR and IR.

Finally, in order to determine the green roof (GR) hydraulic effectiveness, the precipitation hyetographs and corresponding hydrographs of GR and impervious roof (IR) on an event scale were analyzed and the hydrological indicators, reported below, were estimated.

(1) Subsurface runoff coefficient (SRC) was expressed as a percentage ratio between the total RD from GR (RD_{GR}) and the total precipitation depth (PD):

$$SRC(\%) = \frac{RD_{GR}}{PD} \times 100 \quad (1)$$

(2) Peak flow reduction (PFR) was calculated as the percentage difference between the hydrographs peak of the IR (PF_{IR}) and hydrographs peak of the GR (PF_{GR}):

$$\mathrm{PFR}(\%) = \frac{\mathrm{PF_{IR}} - \mathrm{PF_{GR}}}{\mathrm{PF_{IR}}} \times 100 \quad (2)$$

(3) Peak flow lag-time (PFL) was determined as the time difference between the peak of precipitation hyetograph (t_P) and the peak of GR hydrograph $\left(t_{P_{GR}}\right)$:

$$PFL(min) = t_{P_{GR}} - t_P \quad (3)$$

(4) Time to start of runoff (TSR) was evaluated, according to Stovin et al. [11], as the time difference between the start of rainfall (t_0) and the time at which the total runoff exceeded 0.01 mm $(t_{RD>0.01\ mm})$:

$$TSR(min) = t_{RD>0.01\ mm} - t_0 \quad (4)$$

2.3. Soil hydraulic Properties

To evaluate the influence of the substrate depth on green roof retention capacity, a six-month dataset (January 2016 to June 2016) was selected from a weather station that measured the precipitation, velocity and direction of wind, air humidity, air temperature, atmospheric pressure, and global solar radiation. The weather station is located at the University of Calabria, next to the experimental site (the Green Roof) cited in this work. Data from the station were collected online and were processed and stored in an SQL database. Reference evapotranspiration was calculated using the Penman–Monteith equation [38]. An average value of albedo of 0.23 was assumed considering that the albedo for vegetated areas was 0.23 in a similar study conducted on a green roof [39].

In order to assess the hydrological response of the green roof by variating the soil substrate depth using the HYDRUS model, the hydraulic properties of the soil materials were investigated.

There are many methods to assess the hydraulic properties of soils in different conditions [40,41]. Among these, the simplified evaporation method [42] is one of the most popular. This method is based on measuring both soil moisture and pressure head during a soil drying cycle under the effect of evaporation. The method was developed by Wind [43], who introduced an iterative graphical procedure to estimate, first, the water retention curve from the average soil moisture and pressure head readings, and to define hydraulic conductivities from measured pressure head profile and variations in the water content distribution. Afterwards, several authors proposed simplifications to this method [44–46].

In this work, the hydraulic properties of the soil substrates were measured in the Urban Hydraulics and Hydrology Laboratory, University of Calabria, Italy using a simplified evaporation method proposed by Schindler et al. [45,46] using the HYPROP® device (METER Group AG, Munich, Germany) [47]. With this method, two tensiometers are placed at two depths of a soil sample sitting in a sample ring. The plane in the middle between the two tensiometers is identical to the horizontal symmetry plane of the column. The sample is saturated with water, basally closed, and set on a balance. The soil surface is open to the ambient atmosphere so that the soil water can evaporate. HYPROP® (METER Group AG, Munich, Germany) measures the water tension in two horizons of the soil sample over the evaporation process by means of two vertical tension shafts. The changing mass of the sample over time is assessed by weighing. The medial water content is calculated based on the mass change. This results in one measuring value per point in time for the retention curve.

The soil substrate of the green roof for the laboratory analysis was packed using a stainless-steel sampling ring with a volume of 250 mL. Then, the soil sample was saturated from the bottom before starting the evaporation test. The measurement unit and the tensiometers were degassed using a vacuum pump to reduce the potential nucleation sites in the demineralized water. At the end of the experiment, the sample was placed in an oven at 105 °C for 24 h; then, the dry weight was measured. For a complete description of the system, please refer to the UMS [47].

The numerical optimization procedure, HYPROP-FIT [48], was used to simultaneously fit the retention and hydraulic conductivity functions to the experimental data obtained using the evaporation method. Fitting was accomplished using a non-linear optimization algorithm that minimizes the sum of the weighted squared residuals between model predictions and measurements.

The unimodal van Genuchten–Mualem model [49] was evaluated for the description of soil hydraulic properties:

$$\Theta = \begin{cases} \frac{1}{(1+(\alpha|h|)^n)^m} & \text{if } h \le 0 \\ 1 & \text{if } h > 0 \end{cases} \quad (5)$$

$$\Theta = \frac{\theta - \theta_r}{\theta_s - \theta_r} \quad (6)$$

$$K = \begin{cases} K_s \Theta^L \left[\left(1 - \left(1 - \Theta^{\frac{1}{m}} \right) \right)^m \right]^2 & \text{if } h < 0 \\ K_s & \text{if } h > 0 \end{cases} \quad (7)$$

$$m = 1 - \frac{1}{n} \quad (8)$$

where Θ is the effective saturation; α is a parameter related to the inverse of the air-entry pressure head (L^{-1}); θ_s and θ_r are the saturated and residual water contents, respectively (–); n and m are pore-size distribution indices; K_s is the saturated hydraulic conductivity ($L \cdot T^{-1}$); and L is the tortuosity and pore-connectivity parameter.

2.4. Simulation Procedure

Based on the hydraulic properties measured by the simplified evaporation method proposed by Schindler et al. [45,46] using the HYPROP® device (METER Group AG, Munich, Germany) [47], we analyzed the runoff volume from a specific substrate for an extensive green roof by considering increasing values of soil depth using the HYDRUS-1D model. In detail, the cumulative runoff volume from the green roof, in response to a continuous period of six months of rainfall events, was evaluated by varying the depth of the soil from time to time, not exceeding the maximum soil thickness of 15 cm generally attributed to an extensive green roof (6 cm, 9 cm, 12 cm, and 15 cm).

To run a simulation by varying the soil substrate, the HYDRUS-1D model [50] was used. HYDRUS-1D is a one-dimensional finite element model that is used for simulating the movement of water, heat, and multiple solutes in variably saturated porous media. HYDRUS-1D implements multiple uniform (single-porosity) and nonequilibrium (dual-porosity and dual-permeability) water flow models [50].

The studied green roof was interpreted as a one-dimensional, single-porosity, porous medium system, which could be described by the Richards equation in the following form:

$$\frac{\partial \theta}{\partial z} = \frac{\partial}{\partial z} \left[K(h) \frac{\partial h}{\partial z} + 1 \right] - S \quad (9)$$

where θ is the volumetric water content, h is the soil water pressure head (L), $K(h)$ is the unsaturated hydraulic conductivity (LT^{-1}), z is the soil depth (L), and S is a sink term ($L^3L^{-3}T^{-1}$), which is defined as a volume of water removed from a unit volume of soil per unit of time due to plant water uptake. Feddes et al. [51] defined S as:

$$S(h) = a(h) \times S_p \quad (10)$$

where $a(h)$ is a dimensionless water stress response function that depends on the soil pressure head h and has a range of values between 0–1, and S_p is the potential root water uptake rate.

Feddes et al. [51] proposed a water stress response function, in which water uptake is assumed to be zero close to soil saturation and for pressure heads higher than the wilting point. Water uptake is assumed to be optimal between two specific pressure heads, which depend on a particular plant. Feddes parameters were assumed according to the HYDRUS database considering the vegetation as grass.

2.5. Numerical Domain and Boundary Conditions

The numerical domain representing the stratigraphy of the green roof consisted of one layer. An atmospheric boundary condition was applied at the soil surface using the precipitation and meteorological conditions measured. A seepage face boundary condition was specified at the bottom of the layer. A seepage face boundary acts as a zero-pressure head boundary when the bottom boundary node is saturated, and as a no-flux boundary when it is unsaturated.

The initial pressure head was assumed to be constant in the entire domain and was set to −100 cm.

3. Results and Discussion

3.1. Rainfall Events

The whole studied period was characterized by 62 rainy events and one snowy event (19 January 2016), which was not considered in this study (Table 1), for a total precipitation depth (PD) of 1256.3 mm ranging from 2.0 mm to 120.1 mm with a mean value of 20.3 mm. For the whole dataset and the specific climate conditions, more than half (51.6%) of the rainfall events had a precipitation depth less than 10 mm, while 24.2% had a precipitation depth between 10–30 mm, 16.1% had a precipitation depth between 30–50 mm, 3.2% had a precipitation depth between 50–70 mm, 1.6% (one event) had a precipitation depth between 70–90 mm, one event had a precipitation depth between 90–110 mm, and one had a precipitation depth greater than 110 mm. Our analysis is representative of the specific precipitation pattern where the experimental site is located, and therefore is affected by the Mediterranean climate condition characterized by hot and dry summers and cool and wet winters [30].

Table 1. Hydrological characteristics of each rainfall event collected from October 2015 to September 2016 on the experimental site. PD: precipitation depth, D: rainfall duration, Mean i: mean rainfall intensity, Max i: maximum rainfall intensity, ADWP: antecedent dry weather period, and RP: return period.

No.	Date	PD	D	Mean i	Max i	ADWP	RP
	(dd/mm/yyyy; hh:mm)	(mm)	(hh:mm)	(mm/h)	(mm/h)	(hh:mm:ss)	(years)
1	07/10/2015; 07:47	42.2	15:05	2.8	121.9	-	<1
2	09/10/2015; 19:21	24.1	16:32	1.5	167.6	43:40	<1
3	10/10/2015; 23:25	48.3	17:11	2.8	106.7	11:33	<1
4	15/10/2015; 08:01	6.4	04:24	1.4	15.2	90:45	<1
5	21/10/2015; 14:51	120.1	42:55	2.8	45.7	146:25	<20
6	29/10/2015; 13:10	63.3	35:32	1.8	61.0	147:25	<2
7	21/11/2015; 23:26	37.1	10:37	3.5	30.5	526:45	<1
8	23/11/2015; 16:30	13.0	04:19	3.0	15.2	30:28	<1
9	24/11/2015; 17:24	97.3	61:31	1.6	76.2	20:34	<3
10	28/11/2015; 08:49	2.8	01:53	1.5	15.2	25:54	<1
11	10/12/2015; 13:05	8.4	02:48	3.0	15.2	290:22	<1
12	03/01/2016; 06:04	66.3	36:28	1.8	76.2	566:10	<2
13	05/01/2016; 02:51	3.3	08:15	0.4	30.5	08:19	<1
14	06/01/2016; 05:45	24.6	24:08	1.0	30.5	18:37	<1
15	07/01/2016; 19:36	9.9	08:58	1.1	15.2	13:43	<1
16	12/01/2016; 19:02	6.1	08:43	0.7	30.5	110:28	<1
17	15/01/2016; 21:39	24.9	25:51	1.0	15.2	58:22	<1
18	11/02/2016; 08:01	23.4	04:54	4.8	30.5	519:58	<1
19	12/02/2016; 06:25	18.8	07:07	2.6	45.7	17:30	<1
20	12/02/2016; 23:22	74.9	35:24	2.1	76.2	09:49	<3
21	18/02/2016; 05:26	45.2	18:25	2.5	45.7	90:40	<1
22	20/02/2016; 12:15	4.6	00:48	5.7	30.5	36:24	<1
23	23/02/2016; 22:11	3.1	02:55	1.0	15.2	81:07	<1
24	26/02/2016; 03:52	10.9	19:30	0.6	30.5	50:46	<1

Table 1. *Cont.*

No.	Date	PD	D	Mean i	Max i	ADWP	RP
	(dd/mm/yyyy; hh:mm)	(mm)	(hh:mm)	(mm/h)	(mm/h)	(hh:mm:ss)	(years)
25	01/03/2016; 00:00	4.1	01:21	3.0	15.2	72:37	<1
26	01/03/2016; 07:19	31.0	15:33	2.0	45.7	05:58	<1
27	03/03/2016; 06:13	40.9	18:14	2.2	61.0	31:21	<1
28	07/03/2016; 06:13	7.4	14:36	0.5	15.2	77:46	<1
29	09/03/2016; 14:42	4.8	06:51	0.7	15.2	41:52	<1
30	12/03/2016; 06:27	6.1	08:03	0.8	15.2	56:54	<1
31	15/03/2016; 08:06	9.1	01:49	5.0	30.5	65:36	<1
32	16/03/2016; 14:38	27.9	20:10	1.4	30.5	29:33	<1
33	23/03/2016; 07:43	34.3	22:30	1.5	91.4	140:55	<1
34	24/03/2016; 23:08	2.8	01:15	2.2	15.2	16:55	<1
35	08/04/2016; 08:33	5.3	00:54	5.9	30.5	344:10	<1
36	08/04/2016; 21:12	2.3	02:12	1.0	15.2	11:46	<1
37	09/04/2016; 20:39	15.7	08:36	1.8	30.5	21:13	<1
38	23/04/2016; 18:12	8.1	00:36	13.5	61.0	325:01	<1
39	24/04/2016; 04:00	11.2	11:12	1.0	106.7	09:13	<1
40	25/04/2016; 04:38	2.5	02:00	1.3	15.2	13:27	<1
41	25/04/2016; 12:45	8.1	05:36	1.5	76.2	06:07	<1
42	28/04/2016; 21:44	14.7	08:36	1.7	15.2	75:25	<1
43	01/05/2016; 11:00	3.3	07:50	0.4	15.2	52:40	<1
44	02/05/2016; 06:28	23.9	24:54	1.0	15.2	11:40	<1
45	04/05/2016; 03:49	5.3	04:00	1.3	15.2	20:25	<1
46	12/05/2016; 03:47	3.6	09:36	0.4	30.5	188:01	<1
47	14/05/2016; 19:09	35.6	21:42	1.6	61.0	53:48	<1
48	20/05/2016; 09:15	2.5	02:48	0.9	15.2	112:27	<1
49	13/06/2016; 01:01	2.8	03:30	0.8	15.2	564:57	<1
50	19/06/2016; 11:34	2.5	06:00	0.4	15.2	151:06	<1
51	24/06/2016; 03:34	7.9	01:42	4.6	15.2	106:03	<1
52	26/07/2016; 14:43	2.0	00:12	10.2	45.7	777:28	<1
53	07/08/2016; 13:28	8.4	10:24	0.8	15.2	286:34	<1
54	11/08/2016; 22:29	2.3	00:12	11.5	30.5	391:36	<1
55	23/08/2016; 14:51	22.4	22:06	1.0	76.2	280:10	<1
56	31/08/2016; 23:31	6.9	06:54	1.0	30.5	178:37	<1
57	06/09/2016; 03:44	36.3	07:12	5.0	76.2	117:21	<1
58	08/09/2016; 03:50	13.7	07:18	1.9	15.2	40:52:48	<1
59	13/09/2016; 15:29	12.5	02:42	4.6	91.4	124:24	<1
60	17/09/2016; 04:22	7.9	05:48	1.4	45.7	82:10	<1
61	18/09/2016; 23:19	38.9	20:48	1.9	61.0	37:10	<1
62	22/09/2016; 05:49	2.3	00:42	3.3	15.2	57:40	<1
	Mean	20.3	11:47	2.5	40.8	129:27	
	Minimum	2.0	00:12	0.4	15.2	05:58	
	Maximum	120.1	61:31	13.5	167.6	777:28	
	Sum	1256.3					

October 2015, with 340.4 mm of precipitation depth (24.2% of the total considered period), was the wettest month, whereas July 2016, with only 2.0 mm, was the driest month in this experimental period.

By comparing all the 62 monitored storms events in terms of total rainfall depth and duration with the relevant intensity–duration–frequency (IDF) curves, which considered the event return periods found using the historical data collected from the rain gauge station in Cosenza, it emerges that most of the rainfall events fall below the one-year return period threshold. This finding is important for the analysis of the precipitation events, and for the subsequent evaluations of the hydraulic efficiency of the green roof.

3.2. Green Roof Hydrologic Effectiveness

To evaluate the hydrological performance of the experimental green roof, the runoff volume—which was generated in response to the 62 rainfall events recorded at the experimental site—and the hydrological indicators, were both analyzed.

Table 2 reports the results obtained in terms of total runoff depth (RD) and subsurface runoff coefficient (SRC) for each event. For peak flow reduction (PFR), peak flow lag-time (PFL), and time to start runoff (TSR), only the results for rainfall events with a precipitation depth (PD) greater than 8 mm are shown. In detail, the choice to evaluate the PFR, PFL, and TSR indexes for only for some events was based on the evaluations conducted on rainfall events with precipitation depths less than 8 mm, which were almost completely preserved by the green roof. In this regard, having found a minimal runoff for these events, it was difficult to identify a demarcated hydrograph peak as well as the start of the hydrograph, which was considerably delayed. The same situation was found for event 53, which, despite having a rainfall depth of 8.4 mm, had a minimal runoff volume that was probably affected by the long event duration and the high temperature of the period (August), and therefore was not suitable for the analysis. Table 2 also reports the mean, minimum, and maximum values for each hydrological indicator.

Table 2. Hydrological performance indicators for GR at event scale. *PD*—precipitation depth, *RD*—runoff depth, *SRC*—subsurface runoff coefficient, *PFR*—peak flow reduction, *PFL*—peak flow lag-time, *TSR*—time to start runoff.

No.	Date	PD	RD	SRC	PFR	PFL	TSR
	(dd/mm/yyyy; hh:mm)	(mm)	(mm)	(%)	(%)	(min)	(min)
1	07/10/2015; 07:47	42.2	20.0	47.4	65.4	6.0	17.0
2	09/10/2015; 19:21	24.1	10.8	44.8	17.9	5.0	23.0
3	10/10/2015; 23:25	48.3	31.0	64.2	13.3	2.0	10.0
4	15/10/2015; 08:01	6.4	0.4	6.3	-	-	-
5	21/10/2015; 14:51	120.1	100.0	83.3	28.3	9.0	30.0
6	29/10/2015; 13:10	63.3	46.4	73.3	52.6	531.0	51.0
7	21/11/2015; 23:26	37.1	13.0	35.0	83.0	468.0	200.0
8	23/11/2015; 16:30	13.0	4.2	32.3	82.0	197.0	60.0
9	24/11/2015; 17:24	97.3	79.5	81.7	44.3	207.0	10.0
10	28/11/2015; 08:49	2.8	0.4	14.3	-	-	-
11	10/12/2015; 13:05	8.4	1.6	19.0	95.2	168.0	15.0
12	03/01/2016; 06:04	66.3	32.7	49.3	75.5	1647.0	54.0
13	05/01/2016; 02:51	3.3	0.3	9.1	-	-	-
14	06/01/2016; 05:45	24.6	12.9	52.4	51.3	57.0	5.0
15	07/01/2016; 19:36	9.9	6.4	64.6	36.6	369.0	3.0
16	12/01/2016; 19:02	6.1	1.1	18.0	-	-	-
17	15/01/2016; 21:39	24.9	13.2	53.0	29.6	1447.0	24.0
18	11/02/2016; 08:01	23.4	4.1	17.5	79.7	18.0	42.0
19	12/02/2016; 06:25	18.8	11.1	59.0	27.6	58.0	102.0
20	12/02/2016; 23:22	74.9	56.0	74.8	22.5	8.0	5.0
21	18/02/2016; 05:26	45.2	30.4	67.3	33.6	55.0	39.0
22	20/02/2016; 12:15	4.6	0.9	19.6	-	-	-
23	23/02/2016; 22:11	3.1	0.1	3.2	-	-	-
24	26/02/2016; 03:52	10.9	4.6	42.2	73.6	13.0	42.0
25	01/03/2016; 00:00	4.1	0.7	17.1	-	-	-
26	01/03/2016; 07:19	31.0	19.9	64.2	32.1	49.0	73.0
27	03/03/2016; 06:13	40.9	29.4	71.9	41.3	1280.0	154.0
28	07/03/2016; 06:13	7.4	2.1	28.4	-	-	-
29	09/03/2016; 14:42	4.8	0.9	18.8	-	-	-
30	12/03/2016; 06:27	6.1	1.6	26.2	-	-	-
31	15/03/2016; 08:06	9.1	3.8	41.8	44.9	124.0	3.0

Table 2. *Cont.*

No.	Date	PD	RD	SRC	PFR	PFL	TSR
	(dd/mm/yyyy; hh:mm)	(mm)	(mm)	(%)	(%)	(min)	(min)
32	16/03/2016; 14:38	27.9	19.4	69.5	41.6	897.0	73.0
33	23/03/2016; 07:43	34.3	16.1	46.9	74.5	9.0	26.0
34	24/03/2016; 23:08	2.8	0.1	3.6	-	-	-
35	08/04/2016; 08:33	5.3	0.3	5.7	-	-	-
36	08/04/2016; 21:12	2.3	0.0	0.0	-	-	-
37	09/04/2016; 20:39	15.7	5.8	36.9	86.5	8.0	11.0
38	23/04/2016; 18:12	8.1	1.8	22.2	92.9	11.0	15.0
39	24/04/2016; 04:00	11.2	2.9	25.9	62.1	4.0	10.0
40	25/04/2016; 04:38	2.5	0.2	8.0	-	-	-
41	25/04/2016; 12:45	8.1	4.2	51.9	73.3	1.0	4.0
42	28/04/2016; 21:44	14.7	5.8	39.5	*	521.0	108.0
43	01/05/2016; 11:00	3.3	0.3	9.1	-	-	-
44	02/05/2016; 06:28	23.9	16.9	70.7	72.8	1253.0	399.0
45	04/05/2016; 03:49	5.3	1.3	24.5	-	-	-
46	12/05/2016; 03:47	3.6	0.0	0.0	-	-	-
47	14/05/2016; 19:09	35.6	23.3	65.4	38.3	512.0	132.0
48	20/05/2016; 09:15	2.5	0.0	0.0	-	-	-
49	13/06/2016; 01:01	2.8	0.0	0.0	-	-	-
50	19/06/2016; 11:34	2.5	0.0	0.0	-	-	-
51	24/06/2016; 03:34	7.9	0.2	2.5	-	-	-
52	26/07/2016; 14:43	2.0	0.0	0.0	-	-	-
53	07/08/2016; 13:28	8.4	0.2	2.4	-	-	-
54	11/08/2016; 22:29	2.3	0.0	0.0	-	-	-
55	23/08/2016; 14:51	22.4	7.2	32.1	93.0	5.0	1.0
56	31/08/2016; 23:31	6.9	0.0	0.0	-	-	-
57	06/09/2016; 03:44	36.3	13.4	36.9	*	34.0	28.0
58	08/09/2016; 03:50	13.7	5.1	37.2	74.2	324.0	5.0
59	13/09/2016; 15:29	12.5	4.4	35.2	89.5	8.0	3.0
60	17/09/2016; 04:22	7.9	0.4	5.1	-	-	-
61	18/09/2016; 23:19	38.9	20.9	53.7	19.0	16.0	45.0
62	22/09/2016; 05:49	2.3	0.0	0.0	-	-	-
	Mean (**)	20.3	11.1	32.0			
	Minimum (**)	2.0	0.0	0.0			
	Maximum (**)	120.1	100.00	83.3			
	Sum (**)	1256.3	689.7				
	Mean (***)	32.5	19.4	50.4	56.0	294.9	52.1
	Minimum (***)	8.1	1.6	17.5	13.3	1	1
	Maximum (***)	120.1	100	83.3	95.2	1647	399
	Sum (***)	1137.0	678.2				

* Due to an interruption of the sensor signal, it was not possible to evaluate the runoff from the conventional roof (IR); thus, the result in terms of PFR was not evaluated; ** Values evaluated considering the whole dataset (62 rainfall events); *** Values estimated by excluding the storm events with rainfall depth less than 8 mm and the rainfall event 53.

By analyzing the results in Table 2, we found that the SRC exhibits a high variability, ranging from 0% to 83.3% with a mean value of 32.0% when the whole dataset (62 storms event) was considered; meanwhile, it ranges from 17.5% to 83.3% with a mean value of 50.4% for storm events with rainfall depths more than 8 mm (26 events) and excluding event 53, too. In this regard, this increase of the mean value of SRC is due to the exclusion by the average evaluation of 27 storm events, which were almost totally retained by the green roof, and are the same events that are not considered also for the other indexes (PFR, PFL and TSR). This first result, in accordance with a previous study carried out for an extensive green roof in Mediterranean climate [23] and fully falling within the range of the variation mentioned in Section 1 (30–90%), confirms the good response of the specific GR, but simultaneously

highlights how the SRC index is strongly influenced by weather conditions. For example, by comparing two events with different rainfall depths, such as Event 9 (PD = 97.3 mm) and Event 18 (PD = 23.4 mm), the SRC values were 81.7% and 17.5%, respectively. Two events with similar rainfall depths, such as Event 7 (PD = 37.1 mm) and Event 27 (PD = 40.9 mm), produced SRC values of 35.0% and 71.9%, respectively. These differences in SRC given similar precipitation can be understood by observing the antecedent dry weather period (ADWP) of the two events, which affects the initial soil moisture condition and therefore the soil retention capacity. Event 7, with a retention of 65.0% (SRC = 35.0%), occurred after more than 20 continuous dry days, whereas when Event 27 happened, at the beginning of the event, the soil substrate had a reduced retention capacity due to the short ADWP (just over one day); therefore, this results in a higher SRC than Event 7.

A similar conclusion can be reached by observing the other three indices (PFR, PFL, and TSR) in Table 2. We found that PFR, PFL, and TSR—with mean values of 56.0%, 294.9 min, and 52.1 min, respectively—were highly variable, and principally associated with the climate condition before the beginning of the storm events, and therefore, with the initial humidity of the soil.

By considering the results in Figure 2, which shows the regression plots (significance level equal of 0.5) estimated for selected hydrological parameters, we noted a linear strong relationship (R^2 = 0.95) between RD and PD (Figure 2a) and a logarithmic relationship (R^2 = 0.77) between SRC and PD (Figure 2b). By analyzing the Figure 2a, we found that RD tended to be 0 to 10 mm for PD values lower than 20 mm, whereas Figure 2b shows SRC values ranging between ~75–85% for PD greater than 70 mm, and a significant variation in the SRC value for PD less than 10 mm, principally depending on the ADWP.

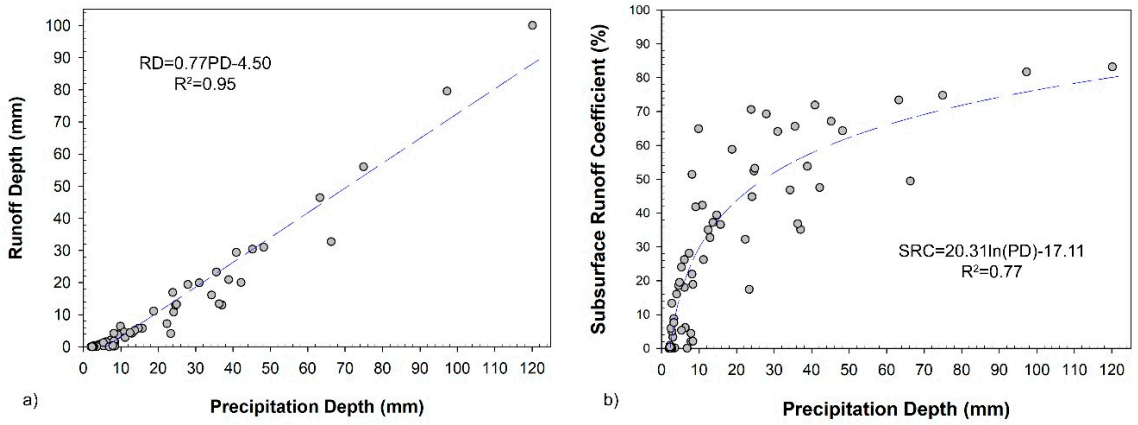

Figure 2. Regression plots (significance level = 0.05) for selected key parameters, by using all the rainfall events: (**a**) runoff depth (RD) as a function of precipitation depth (PD) and (**b**) subsurface runoff coefficient (SRC) as a function of precipitation depth (PD).

All these findings confirm the findings reported in the literature [3,11], which identified ADWP as a significant determinant of hydrological performance. This specific hydrological parameter, which ranged from around 6 hours to more than 777 hours in this study (Table 1), significantly affects the substrate moisture conditions and thus the green roof hydrological response in terms of SRC, PFR, PFL, and TSR indexes.

All the results that were analytically evaluated in terms of runoff volume, rainfall intensity, and hydrological indexes, provided excellent feedback, as shown in Figure 3, where hyetographs and corresponding hydrographs of the GR (black line) and the IR (grey color) are shown for eight selected rainfall events. These storms events were selected to cover a wide range of precipitation depths, durations, and antecedent dry weather conditions. The events shown in Figure 3 confirm the hydrological efficiency of the experimental green roof in terms of runoff volume reduction and peak hydrograph mitigation compared to the conventional roof, and the delay in peak flow compared with the hyetograph.

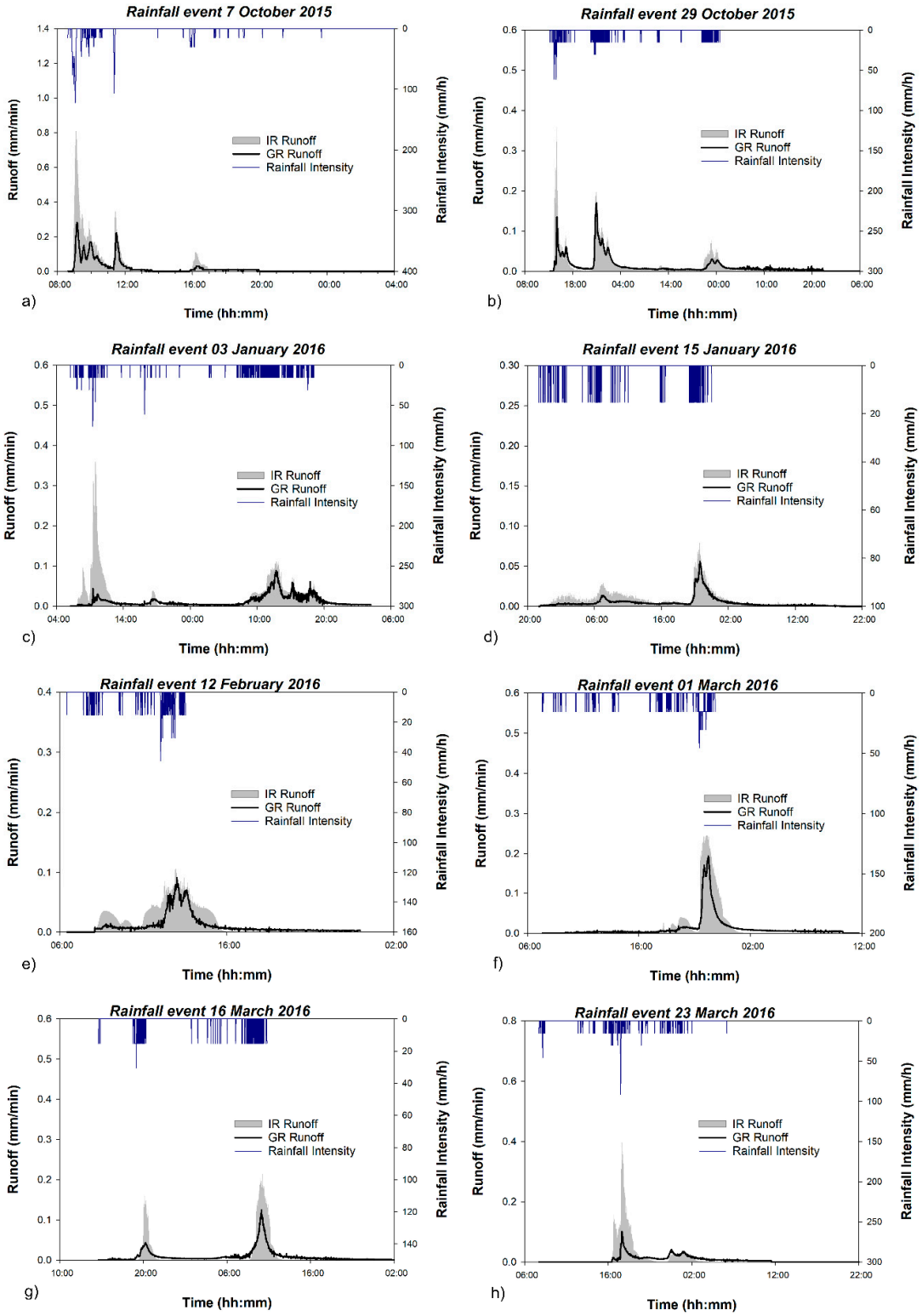

Figure 3. Hyetographs and corresponding green roof (GR) and impervious roof (IR) runoff hydrographs for eight selected rainfall events: (**a**) 7 October 2015 (total precipitation depth (PD) = 42.2 mm and total green roof runoff depth (GR-RD) = 20.0 mm); (**b**) 29 October 2015 (PD = 63.3 mm and GR-RD = 46.4 mm); (**c**) 03 January 2016 (PD = 66.3 mm and GR-RD = 32.7 mm); (**d**) 15 January 2016 (PD = 24.9 mm and GR-RD = 13.2 mm); (**e**) 12 February 2016 (PD = 18.8 mm and GR-RD = 11.1 mm); (**f**) 01 March 2016 (PD = 31.0 mm and GR-RD = 19.9 mm); (**g**) 16 March 2016 (PD = 27.9 mm and GR-RD = 19.4 mm); (**h**) 23 March 2016 (PD = 34.3 mm and GR-RD = 16.1 mm).

3.3. Soil Hydraulic Properties

The soil hydraulic properties of the soil substrate measured with the evaporation method are shown in Figure 4. The measured soil water retention curve (SWRC) is well described across the entire water content range (blue points of the left-side curve), whereas the measured points of the hydraulic conductivity function (blue points of the central and right-side curve) are concentrated in the dry range between 10–30% of the volumetric water content. The measured data were imported into HYPROP-FIT (METER Group AG, Munich, Germany) software to fit the analytical hydraulic property functions.

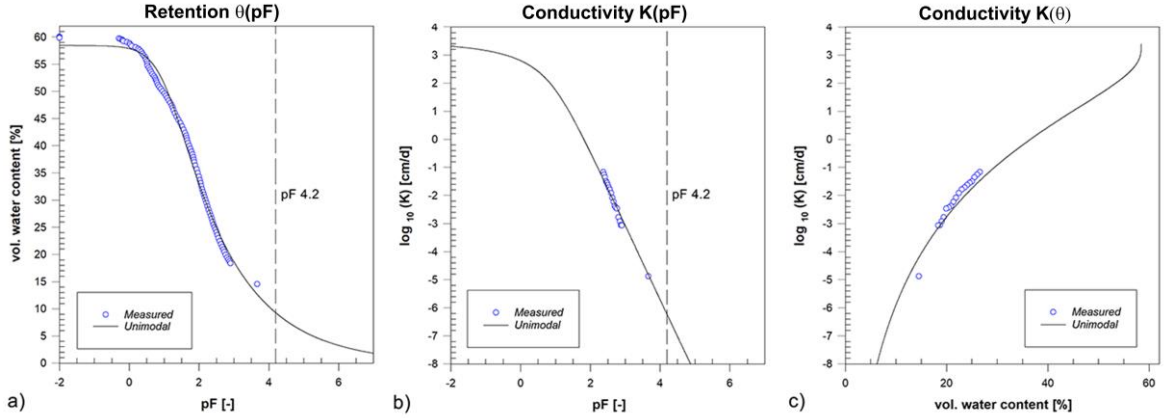

Figure 4. (**a**) The soil water retention curve showing the volumetric water content (θ) versus pF (decimal log of tension, expressed as pressure head in the unit of cm); (**b**) the conductivity curves showing the log of the hydraulic conductivity (K) versus pF, and (**c**) the log of hydraulic conductivity versus volumetric water content (θ).

The unimodal van Genuchten Mualem model (VGM) [49] was fitted (Figure 4, black line). The root mean square error (RMSE) values for retention and conductivity functions were 0.01 cm^3cm^{-3} and 0.16 log K, cm/day, respectively.

The hydraulic properties obtained by fitting the van Genuchten Mualem model and their limit of confidence are described in Table 3, where α is a parameter related to the inverse of the air-entry pressure head (L^{-1}); θ_s and θ_r are the saturated and residual water contents, respectively; n is a pore-size distribution index; K_s is the saturated hydraulic conductivity (LT^{-1}); and l is the tortuosity and pore-connectivity parameter.

Table 3. Estimated soil hydraulic parameters. θ_r, residual water content; θ_s, saturated water content; α, inverse of the air-entry pressure head; n, pore-size distribution index; and l, tortuosity.

Parameter	Value	Lower Limit	Upper Limit	Unit of Measure
θ_r	0.00	0	0.07	cm^3cm^{-3}
θ_s	0.58	0.57	0.59	cm^3cm^{-3}
α	0.09	0.07	0.11	cm^{-1}
n	1.25	1.20	1.32	-
K_s	3000	0.00	4000	cm day^{-1}
l	0.5	-	-	-

The model used indicates a soil characterized by a very high permeability, which corresponds well with the textural composition of the GR substrate. This characteristic is well suited for green roof substrates, which must guarantee fast drainage and avoid water ponding on the surface, even during intense precipitation. Narrow confidence intervals for parameters indicate high confidence in their estimation, whereas a huge range in the estimation of K_s indicates that the evaporation method is not accurate for the determination of the hydraulic conductivity near saturation, and this is reflected in

the estimation of K_s. To improve the accuracy in the estimation of the hydraulic conductivity near saturation, other methods and devices should be used such as Ksat [52] based on the Darcy experiment.

3.4. Green Roof Hydraulic Behavior for Different Soil Depths

As stated above, the hydraulic parameters of the soil substrate were used in HYDRUS-1D to describe the hydrological behavior of the green roof with different soil depths.

Cumulative inflow and outflow fluxes of the green roof are reported in Figure 5. By increasing the soil substrate depth, the green roof was able to reduce the total runoff volume from 22% to 24% in response to the same total precipitation during the considered period.

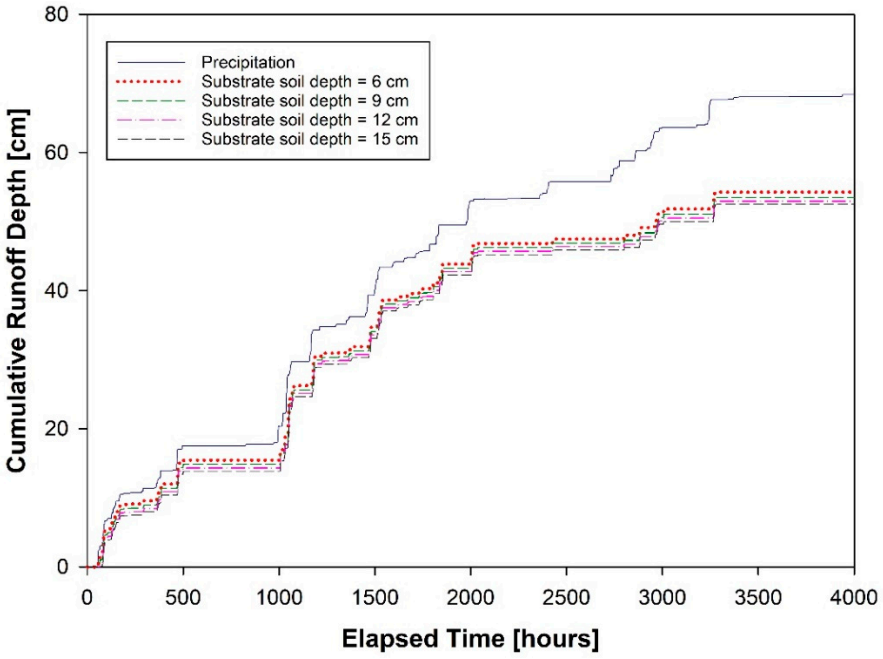

Figure 5. Cumulative rainfall and cumulative modeled runoff for different values of soil depth (H) by considering a six-month dataset (January–June 2016).

The steep gradients in the cumulative outflow indicate that the green roof responded quickly to precipitation. This aspect is directly related to the limited thickness of the substrate, which reduces the possible delay.

During simulations, mass balance errors were always below 1%, which is generally considered acceptable at these low levels.

As shown in Figure 5, the outflow volume reduction achieved by doubling the soil substrate depth under the same climate conditions was not significant. This result, which confirms the findings of Feitosa and Wilkinson [32], can be justified by observing that the six-month dataset used for these simulations was obtained in winter and spring, where evapotranspiration is not predominant. Based on these findings, since the adoption of a deeper soil depth does not contribute to a significant increase in the retention capacity, it would only represent a structural overloading, while a substrate depth of six centimeters would be an ideal soil depth for extensive green roofs.

4. Conclusions

Green roofs may be a solution for minimizing the impact of urbanization on the hydrologic cycle. Given the important role they play in the mitigation of urban flooding, several studies have focused on the analysis of their hydraulic behavior.

In this study, we conducted a field monitoring campaign for one year on a full-scale extensive green roof. We evaluated hydrological indices (subsurface runoff coefficient, peak flow reduction, peak

flow lag-time, and time to start runoff) on an event scale, and we found possible correlations between these indicators and hydrological features of storm events. The findings showed that the subsurface runoff coefficient (SRC) ranges from 17.5% to 83.3% with an average value of 50.4% for the rainfall events with a precipitation depth more than 8 mm (35 rainfall events) and by excluding Event 53, which presents an average value of 32.0% for the whole dataset (62 rainfall events). This result, which is evaluated by considering an event scale analysis, falls in the range (around 30–90%) evaluated in literature [30] under different climate conditions and temporally scales. In addition, as the subsurface runoff coefficient is an extremely useful index to quantify the hydraulic efficiency of a green roof, this finding confirms the optimal retention capacity of the experimental green roof in the Mediterranean climate. Therefore, the average value of the subsurface runoff that was obtained in this study for the specific green roof can be taken into account during preliminary design choices for the construction of green roofs in Mediterranean climate conditions.

Finally, to evaluate the influence of soil thickness on the hydraulic behavior of a green roof, the HYDRUS 1D model was used to consider green roofs with soil depths of 6 cm, 9 cm, 12 cm, and 15 cm. The results obtained in this phase show how the considered substrate depths for green roofs were able to achieve a runoff volume reduction of 22% to 24% during the selected period for the Mediterranean climate conditions without observing flow over the top surface of the soil. These findings are in accordance with the literature [32], which may be explained by the dataset used in these simulations being obtained during winter and spring where evapotranspiration, one of the key factors reducing storm water in the hydrological cycle, was not predominant. Thus, in the field of extensive green roofs, as the outflow volume reduction achieved by increasing the soil depth was not significant, the ideal depth for soil substrate would be six centimeters.

Finally, since the outflow volume reduction achieved by doubling the soil substrate depth under the same climate conditions is not significant, the maximum depth of 15 cm is not recommended for adoption considering the structural overloading.

Author Contributions: The authors contributions in the realization of the paper have been as follows. Conceptualization, S.A.P., M.T., F.P, and P.P.; methodology, S.A.P. and M.T.; data curation, S.A.P., M.T., and F.P.; formal analysis, S.A.P. and M.T.; investigation, S.A.P. and M.T.; writing—original draft preparation, S.A.P., M.T. and F.P.; writing—review, S.A.P. and M.T.; editing, S.A.P., M.T, and F.P.; supervision: P.P.

Funding: The study was co-funded by the Italian National Operative Project (PON) PON01_02543 "Integrated and sustainable management service for the water–energy cycle in urban drainage systems", Research and Competitiveness for the convergence regions 2007/2013, I Axis "Support to structural changes" operative objective 4.1.1.1. "Scientific-technological generators of transformation processes of the productive system and creation of new sectors" Action II: "Interventions to support industrial research".

Acknowledgments: We acknowledge the support by the Italian National Operative Project (PON) PON01_02543 "Integrated and sustainable management service for the water–energy cycle in urban drainage systems", Research and Competitiveness for the convergence regions 2007/2013, I Axis "Support to structural changes" operative objective 4.1.1.1. "Scientific-technological generators of transformation processes of the productive system and creation of new sectors" Action II: "Interventions to support industrial research".

Conflicts of Interest: The authors declare no conflict of interest.

References

1. Starzec, M.; Dziopak, J.; Słyś, D.; Pochwat, K.; Kordana, S. Dimensioning of Required Volumes of Interconnected Detention Tanks Taking into Account the Direction and Speed of Rain Movement. *Water* **2018**, *10*, 1826. [CrossRef]
2. Kordana, S. The identification of key factors determining the sustainability of stormwater systems. *E3S Web Conf.* **2018**, *45*, 00033. [CrossRef]
3. Piro, P.; Turco, M.; Palermo, S.A.; Principato, F.; Brunetti, G. A Comprehensive Approach to Stormwater Management Problems in the Next Generation Drainage Networks. In *The Internet of Things for Smart Urban Ecosystems. Internet of Things (Technology, Communications and Computing)*; Cicirelli, F., Guerrieri, A., Mastroianni, C., Spezzano, G., Vinci, A., Eds.; Springer: Cham, Switzerland, 2019. [CrossRef]

4. Pumo, D.; Arnone, E.; Francipane, A.; Caracciolo, D.; Noto, L.V. Potential implications of climate 363 change and urbanization on watershed hydrology. *J. Hydrol.* **2017**, *554*, 80–99. [CrossRef]
5. Palermo, S.A.; Zischg, J.; Sitzenfrei, R.; Rauch, W.; Piro, P. Parameter Sensitivity of a Microscale Hydrodynamic Model. In *New Trends in Urban Drainage Modelling. UDM 2018*; Green Energy and Technology; Mannina, G., Ed.; Springer: Cham, Switzerland, 2019; pp. 982–987.
6. Bhaskar, A.S.; Hogan, D.M.; Archfield, S.A. Urban base flow with low impact development. *Hydrol. Process.* **2016**, *30*, 3156–3171. [CrossRef]
7. Brunetti, G.; Šimůnek, J.; Turco, M.; Piro, P. On the use of global sensitivity analysis for the numerical analysis of permeable pavements. *Urban Water J.* **2018**, *15*, 269–275. [CrossRef]
8. Turco, M.; Brunetti, G.; Carbone, M.; Piro, P. Modelling the hydraulic behaviour of permeable pavements through a reservoir element model. *Int. Multidiscip. Sci. GeoConf. SGEM* **2018**, *18*, 507–514. [CrossRef]
9. Wang, X.; Tian, Y.; Zhao, X. The influence of dual-substrate-layer extensive green roofs on rainwater runoff quantity and quality. *Sci. Total Environ.* **2017**, *592*, 465–476. [CrossRef] [PubMed]
10. Voyde, E.; Fassman, E.; Simcock, R. Hydrology of an extensive living roof under sub-tropical climate conditions in Auckland, New Zealand. *J. Hydrol.* **2010**, *394*, 384–395. [CrossRef]
11. Stovin, V.; Vesuviano, G.; Kasmin, H. The hydrological performance of a green roof test bed under UK climatic conditions. *J. Hydrol.* **2012**, *414*, 148–161. [CrossRef]
12. Vijayaraghavan, K. Green roofs: A critical review on the role of components, benefits, limitations and trends. *Renew. Sustain. Energy Rev.* **2016**, *57*, 740–752. [CrossRef]
13. Pęczkowski, G.; Kowalczyk, T.; Szawernoga, K.; Orzepowski, W.; Żmuda, R.; Pokładek, R. Hydrological Performance and Runoff Water Quality of Experimental Green Roofs. *Water* **2018**, *10*, 1185. [CrossRef]
14. Bevilacqua, P.; Mazzeo, D.; Arcuri, N. Thermal inertia assessment of an experimental extensive green roof in summer conditions. *Build. Environ.* **2018**, *131*, 264–276. [CrossRef]
15. Santamouris, M. Cooling the cities–a review of reflective and green roof mitigation technologies to fight heat island and improve comfort in urban environments. *Solar Energy* **2014**, *103*, 682–703. [CrossRef]
16. Rowe, D.B. Green roofs as a means of pollution abatement. *Environ. Pollut.* **2011**, *159*, 2100–2110. [CrossRef] [PubMed]
17. Yang, H.S.; Kang, J.; Choi, M.S. Acoustic effects of green roof systems on a low-profiled structure at street level. *Build. Environ.* **2012**, *50*, 44–55. [CrossRef]
18. Buccola, N.; Spolek, G. A pilot-scale evaluation of green roof runoff retention, detention, and quality. *Water Air Soil Pollut.* **2011**, *216*, 83–92. [CrossRef]
19. Krebs, G.; Kuoppamäki, K.; Kokkonen, T.; Koivusalo, H. Simulation of green roof test bed runoff. *Hydrol. Process.* **2016**, *30*, 250–262. [CrossRef]
20. Carson, T.B.; Marasco, D.E.; Culligan, P.J.; McGillis, W.R. Hydrological performance of extensive green roofs in New York City: Observations and multi-year modeling of three full-scale systems. *Environ. Res. Lett.* **2013**, *8*, 024036. [CrossRef]
21. Fassman-Beck, E.; Voyde, E.; Simcock, R.; Hong, Y.S. 4 Living roofs in 3 locations: Does configuration affect runoff mitigation? *J. Hydrol.* **2013**, *490*, 11–20. [CrossRef]
22. Peng, Z.; Stovin, V. Independent validation of the SWMM green roof module. *J. Hydrol. Eng.* **2017**, *22*, 04017037. [CrossRef]
23. Cipolla, S.S.; Maglionico, M.; Stojkov, I. A long-term hydrological modelling of an extensive green roof by means of SWMM. *Ecol. Eng.* **2016**, *95*, 876–887. [CrossRef]
24. Principato, F.; Ferrante, A.P.; Frega, F.; Bartolo, M.; Piro, P. Mitigation of Urban Surface Runoff through LID Solutions: Case Study in Mediterranean Area. In *New Trends in Urban Drainage Modelling. UDM 2018*; Green Energy and Technology; Mannina, G., Ed.; Springer: Cham, Switzerland, 2019; pp. 665–670.
25. Metselaar, K. Water retention and evapotranspiration of green roofs and possible natural vegetation types. *Resour. Conserv. Recycl.* **2012**, *64*, 49–55. [CrossRef]
26. Palla, A.; Gnecco, I.; Lanza, L.G. Compared performance of a conceptual and a mechanistic hydrologic models of a green roof. *Hydrol. Process.* **2012**, *26*, 73. [CrossRef]
27. Brunetti, G.; Šimůnek, J.; Piro, P. A Comprehensive Analysis of the Variably Saturated 461 Hydraulic Behavior of a Green Roof in a Mediterranean Climate. *Vadose Zone J.* **2016**, *15*. [CrossRef]
28. Hilten, R.N.; Lawrence, T.M.; Tollner, E.W. Modeling stormwater runoff from green roofs with HYDRUS-1D. *J. Hydrol.* **2008**, *358*, 288–293. [CrossRef]

29. Li, Y.; Babcock, R.W., Jr. Modeling hydrologic performance of a green roof system with HYDRUS-2D. *J. Environ. Eng.* **2015**, *141*, 04015036. [CrossRef]
30. Garofalo, G.; Palermo, S.; Principato, F.; Theodosiou, T.; Piro, P. The influence of hydrologic parameters on the hydraulic efficiency of an extensive green roof in mediterranean area. *Water* **2016**, *8*, 44. [CrossRef]
31. Liu, R.; Fassman-Beck, E. Hydrologic response of engineered media in living roofs and bioretention to large rainfalls: Experiments and modeling. *Hydrol. Process.* **2017**, *31*, 556–572. [CrossRef]
32. Feitosa, R.C.; Wilkinson, S. Modelling green roof stormwater response for different soil depths. *Landsc. Urban Plan.* **2016**, *153*, 170–179. [CrossRef]
33. Soulis, K.X.; Ntoulas, N.; Nektarios, P.A.; Kargas, G. Runoff reduction from extensive green roofs having different substrate depth and plant cover. *Ecol. Eng.* **2017**, *102*, 80–89. [CrossRef]
34. Piro, P.; Carbone, M.; Morimanno, F.; Palermo, S.A. Simple flowmeter device for LID systems: From laboratory procedure to full-scale implementation. *Flow Meas. Instrum.* **2019**, *65*, 240–249. [CrossRef]
35. Getter, K.L.; Rowe, D.B.; Andresen, J.A. Quantifying the effect of slope on extensive green roof stormwater retention. *Ecol. Eng.* **2007**, *31*, 225–231. [CrossRef]
36. Shiau, J.T. Return period of bivariate distributed extreme hydrological events. *Stoch. Environ. Res. Risk Assess.* **2003**, *17*, 42–57. [CrossRef]
37. Arpacal. 2019. Available online: http://www.cfd.calabria.it/index.php/dati-stazioni/dati-storici (accessed on 24 January 2019).
38. Allen, R.G.; Pereira, L.S.; Raes, D.; Smith, M. *FAO Irrigation and Drainage Paper No. 56: Crop Evapotranspiration*; FAO: Rome, Italy, 1998.
39. Lazzarin, R.M.; Castellotti, F.; Busato, F. Experimental measurements and numerical modelling of a green roof. *Energy Build.* **2005**, *37*, 1260–1267. [CrossRef]
40. Arya, L.M. Wind and hot-air methods. In *Methods of Soil Analysis*; Part 4. Physical Methods; Dane, J.H., Topp, G.C., Eds.; SSSA: Madison, WI, USA, 2002; pp. 916–926.
41. Dane, J.H.; Hopmans, J.W. Pressure plate extractor. In *Methods of Soil Analysis*; Part 4. Physical Methods; Dane, J.H., Topp, G.C., Eds.; SSSA: Madison, WI, USA, 2002; pp. 688–690.
42. Schindler, U. Ein Schnellverfahren zur Messung der Wasserleitfähigkeit im teilgesättigten Boden an Stechzylinderproben. *Arch. Für Acker-Und Pflanzenbau Und Bodenkd.* **1980**, *24*, 1–7.
43. Wind, G.P. Capillary conductivity data estimated by a simple method. Available online: https://library.wur.nl/WebQuery/wurpubs/fulltext/350954 (accessed on 3 July 2019).
44. Peters, A.; Durner, W. Simplified evaporation method for determining soil hydraulic properties. *J. Hydrol.* **2008**, *356*, 147–162. [CrossRef]
45. Schindler, U.; Durner, W.; von Unold, G.; Mueller, L.; Wieland, R. The evaporation method: Extending the measurement range of soil hydraulic properties using the air-entry pressure of the ceramic cup. *J. Plant Nutr. Soil Sci.* **2010**, *173*, 563–572. [CrossRef]
46. Schindler, U.; Durner, W.; von Unold, G.; Muller, L. Evaporation Method for Measuring Unsaturated Hydraulic Properties of Soils: Extending the Measurement Range. *Soil Sci. Soc. Am. J.* **2010**, *74*, 1071–1083. [CrossRef]
47. UMS GmbH. *UMS (2015): Manual HYPROP, Version 2015-01*; UMS GmbH: München, Germany, 8137; Volume 37.
48. Pertassek, T.; Peters, A.; Durner, W. *HYPROP-FIT Software User's Manual, V.3.0*; UMS GmbH: München, Germany, 2015.
49. Van Genuchten, M.T. A closed-form equation for predicting the hydraulic conductivity of unsaturated soils 1. *Soil Sci. Soc. Am. J.* **1980**, *44*, 892–898. [CrossRef]
50. Šimůnek, J.; van Genuchten, M.T.; Šejna, M. Recent Developments and Applications of the HYDRUS Computer Software Packages. *Vadose Zone J.* **2016**, *15*. [CrossRef]
51. Feddes, R.A.; Kowalik, P.J.; Zaradny, H. *Simulation of Field Water Use and Crop Yield*; PUDOC: Wageningen, The Netherlands, 1978.
52. UMS GmbH. *KSAT: Operation Manual*; Umwelt Monitoring System; GmbH: Munich, Germany, 2012.

Paper III

Simple flowmeter device for LID systems: From laboratory procedure to full-scale implementation

Piro, P., Carbone, M., Morimanno, F., & **Palermo, S. A.** (2019a)

Published in: Flow Measurement and Instrumentation, 65, 240-249.
https://doi.org/10.1016/j.flowmeasinst.2019.01.008

Flow Measurement and Instrumentation 65 (2019) 240–249

Contents lists available at ScienceDirect

Flow Measurement and Instrumentation

journal homepage: www.elsevier.com/locate/flowmeasinst

Simple flowmeter device for LID systems: From laboratory procedure to full-scale implementation☆

Patrizia Piro, Marco Carbone, Francesco Morimanno, Stefania Anna Palermo*

Department of Civil Engineering, University of Calabria, Rende, CS 87036, Italy

ARTICLE INFO

Keywords:
Flow measurement
Rectangular sharp-crested weir
Discharge coefficient
Discharge equation
Evolutionary polynomial regression
Green roof

ABSTRACT

Low impact development (LID) systems provide sustainable solutions for flood risk mitigation. Given their relevant role in urban water management, accurate estimation of the outflow rate of such systems is crucial to assess their retention efficiency and the corresponding volumes discharged into the drainage network. Thus, the selection of an appropriate flowmeter device is necessary. Thus far, various flowmeter devices have been designed and calibrated for pipes, open channels, rivers, and irrigation systems, while only scarce and general information has been presented for the devices used in LID systems. The main objective of this study is to propose a new, simple, and easily replicable flowmeter device, which can be positioned in confined spaces, such as drain wells, for measuring a large outflow rate range of LID systems. To identify the most influential parameters on the discharge coefficient, the evolutionary polynomial regression multi-objective and multi-case strategy approaches were used for data mining. The results demonstrate that the ratio between the upstream head (h) on the weir crest and the weir width (b), namely the (h/d) parameter, significantly affects the discharge coefficient. Therefore, neglecting the Reynolds and Weber condition and h/d coefficient (where d is the weir height), a simple and accurate relationship of the discharge coefficient was obtained. Finally, to implement the laboratory findings to a full-scale green roof, the runoff collected by the developed device for a continuous period of three months was analysed. The findings demonstrate that the plotted hydrographs do not exhibit fluctuations and effectively interpret the small flow, at both the continuous and event scales.

1. Introduction

Continual urbanisation and climate change have severely modified natural catchments, leading to significant alteration of the hydrological cycle, thereby increasing urban flooding risks [1,2]. In response to this issue, several strategies, known as 'best management practices' and 'low impact development' (LID), have been adopted [3]. Among these, permeable pavements, green roofs, and rain gardens provide innovative solutions, mainly based on ground infiltration and temporal storage, which provide significant reductions in runoff volume [4,5]. In order to estimate the hydraulic benefits of these solutions, an appropriate evaluation of the outflow rate is important. Therefore, the selection of a specific flowmeter device for LID systems, which can also estimate the minimum flow rates released following small rain events, is necessary.

The accuracy and precision of the device strongly affect the flow measurement; thus, several studies have focused on the detailed design of flowmeter devices, particularly for the flow measurement of pipes, open channels, rivers, and irrigation systems [6–9]. A common configuration for measuring the flow rate, generally used in hydraulic laboratories and irrigation practices, involves placing a side weir, namely an overflow structure, laterally to a channel [6]. Weirs are one of the oldest and simplest hydraulic structures used for flow measurement, energy dissipation, flow depth regulation, flood passages, and other purposes [7]. Numerous weir types exist: the broad-crested, short-crested, and sharp-crested weirs. Specifically, the sharp-crested weir is used in hydraulic laboratories, industry, and irrigation pilot schemes, where high accuracy is required [8]. Therefore, in the past several years, there has been increasing interest in rectangular weirs and the potentialities these devices offer in terms of the simplicity of outflow modelling [9,10]. In fact, compared to those with orifice openings, these devices exhibit a discharge law that is influenced by fewer interpretation errors. Moreover, as they do not exhibit a high influence of viscous phenomena, such as V-shaped devices, they can measure both the smallest flow rates and the peak flow occurring during extreme

☆ The authors contributed equally to this work.

* Corresponding author.
E-mail addresses: patrizia.piro@unical.it (P. Piro), marco.carbone@unical.it (M. Carbone), francescomorimanno@libero.it (F. Morimanno), stefania.palermo@unical.it (S.A. Palermo).

https://doi.org/10.1016/j.flowmeasinst.2019.01.008
Received 1 March 2018; Received in revised form 31 December 2018; Accepted 6 January 2019
Available online 08 January 2019
0955-5986/

Nomenclature

d	Weir height [mm]
b	Weir width [mm]
L	Thickness of weir crest [mm]
θ	Crest bevelled angle [°]
h	Upstream head over weir [mm]
B	Channel or tank width [mm]
C_d	Discharge coefficient of weir [dimensionless]
Q	Flow rate discharge by weir [l/s]

rainfall events.

In estimating the flow from rectangular weirs, the discharge coefficient plays a significant role. Several studies have been carried out to determine the discharge coefficient for the sharp-crested weir [8,11–16]. The theoretical formulation of the discharge coefficient, as presented in Section 2.1.3, is strongly affected by the geometric configuration of the weir and a numerical analysis adopted.

In the studies, as previously mentioned, no specific devices for LID systems were identified. Moreover, as discussed later, the studies on LID systems, specifically green roofs, only provided general information on the flowmeter device used. In more detail, Bliss et al. [17] considered a channel with a trapezoidal area and used a Greyline LIT25 ultrasonic sensor to measure the water levels released by extensive green roofs. Voyde et al. [18] rated the runoff from each green roof plot by a restricted orifice device equipped with a Global Water WL16USB pressure transducer. Stovin et al. [19] collected the outflow from a green roof test bed in a tank via a gutter, and monitored the water levels by means of a pressure transducer. Moreover, Carson et al. [20] obtained continuous measurements of green roof runoff using a weir device consisting of a runoff chamber with an outlet weir, and a Senix TSPC-30S1 ultrasonic sensor. Hakimdavar et al. [21] installed a tipping bucket placed beneath the drain of the green roof test box. Versini et al. [22] recorded the outflow from each green roof plot by means of a custom-made PVC tipping bucket with a resolution of 0.01 mm. Moreover, Zhang et al. [23] used PVC pipes with a U-shape, connected to the green roof outlet on one side, and fitted with a 0.5 m Odyssey capacitance water level sensor on the other.

Although these studies carried out on green roofs introduced certain devices for outflow estimation, no details on the construction and calibration phases, which are useful for reproducing the devices, were provided. Moreover, only few studies were conducted on full-scale implementations; however, the spaces in which the measures were detected were often confined within a manhole. Thus, research on and definition of a device that is easily reproducible for geometrical and material features, and can be used for different LID systems as well as positioned in limited spaces, could provide suitable support to experts in the field of sustainable urban drainage.

Therefore, the main objective of this study is to propose an innovative and simple flowmeter device. The device, developed in the laboratory, was created to measure the outflow rates from several full-scale LID systems, including an extensive green roof located in the Urban Hydraulics Park at the University of Calabria. A prototype was developed with a rectangular sharp-crested weir in a thin wall, and laboratory volumetric tests with a wide range of hydraulic loads were carried out to define the outflow scale. A monomial discharge law derived from dimensional analysis of the discharge equation for a rectangular weir was analysed. Thereafter, to identify the most influential parameters on the discharge coefficient, the evolutionary polynomial regression multi-objective genetic algorithm (EPR-MOGA) and multi-case strategy (MCS-EPR) were used for data mining. Furthermore, in order to obtain a direct and continuous estimation of the water level, a pressure transducer was selected, calibrated, and implemented. Finally, the flowmeter device was reproduced and implemented in the LID systems installed at the University of Calabria. To demonstrate the actual performance of the proposed device, the outflow rates collected from an experimental green roof for a continuous monitored period of three months are presented.

2. Materials and methods

2.1. Laboratory phases

The first part of the study was performed in the laboratory, and consisted of three main phases, which are described in detail in the following subsections. Thus, according to this section, a useful guide is proposed to experts in the field of sustainable urban drainage for reproduction in the laboratory, followed by installation in full-scale implementation, using the same flowmeter device that is suitable for the estimation of outflow from LID systems.

2.1.1. Construction phase

In order to define a new and simple flowmeter device that can be placed in manholes located at the base of LID systems, the main aspects considered during the design and construction phases were: feasibility, easy implementation, versatility, simple on-site installation and removal for maintenance, lightness, and adequate size for reliable flow measurement (that is, a device suitable for measuring the smallest flow rates released from an LID system, and that, in the function of its configuration, can minimise the cinematic viscosity and surface tension effects on the efflux).

To fulfil all these characteristics, a ‘measuring pipe’ consisting of a vertical PVC pipe DN200 with a rectangular weir was developed. The selection of a device with a rectangular weir depends on the high variability of flow rates from an LID system, which, given their retention capacities, are generally small, but could also be greater when extreme rainfall events occur. Moreover, the use of a vertical pipe is

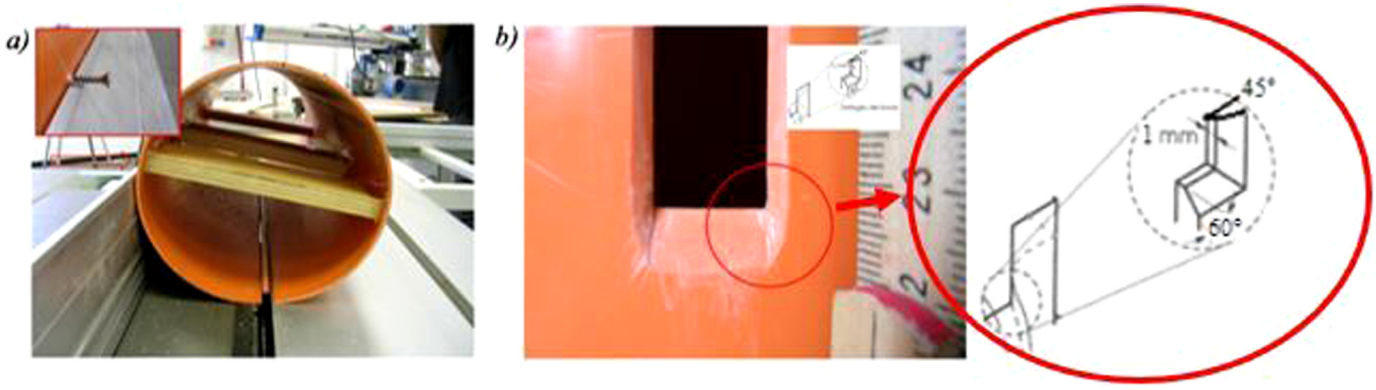

Fig. 1. a) Guided cutting of weir; b) re-finishing of edges.

suitable for obtaining effective variability of the fluid vein, and owing to its shape, it is possible to place it easily in manholes. Furthermore, PVC material is a common material that can be processed effectively.

As a prototype diameter, a DN200 instead of a DN250 was considered for obtaining major water level variations, thereby enabling easier reading of the water level by a piezometer and/or pressure transducer.

On this basis, during the construction phase, the PVC pipe (DN200) was first stiffened with wooden planks (Fig. 1a) and cut with a circular saw bench for a weir width (b) of 12 mm. To prevent the risk of the small opening clogging, toothed gratings were implemented in the intake pipe and calm zone. The opening of 12 mm was placed 22 cm from the bottom (Fig. 2b); thus, the calm zone performed a sedimentation function in addition to the hydraulic function. Furthermore, the data collected on the experimental sites following the device installation confirmed the non-existence of a clogging problem, as the coarser particles (> 12 mm) that escaped from the LID systems never blocked the small opening. The geometric features of the weir and calm zone were defined to minimise the viscosity and surface tension effects on the efflux.

Moreover, the selection of the diameter and weir width depended on preliminary considerations conducted to determine the maximum flow rate. The areas of the experimental LID systems installed at the University of Calabria, a rain intensity, for the laboratory tests, of 98 mm/h (mean value between 80 mm/h and 116 mm/h and rain events with two- and five-years return periods, respectively), and an evaluation on the infiltration conditions of the LID systems, according to the literature values, were considered. Based on these observations, a peak flow rate of 1.5 l/s was estimated.

In order to achieve sharp detachment of the fluid vein and also lower flow rates, the vertical walls and threshold were shaped at 45 °C and 60 °C, respectively (Fig. 1b). Previous laboratory tests demonstrated that an edge thickness greater than $1 \div 2$ mm gives rise to adhesion phenomena of the fluid vein, with instabilities for low flow rates.

To obtain correct water level measurements, it is relevant to consider the energy dissipation by the incoming current, in the case of both a piezometer and pressure sensor. Thus, a system consisting of a concentric DN100 pipe, approximately 50 cm long (Fig. 2b), with openings at the bottom, was placed within the DN200 pipe to inject and dissipate the water energy mass. Moreover, to collect the water from the surface and infiltration systems with ease, the dissipation system was connected to the top by means of a special piece (diameter reducer DN200-DN100), thereby obtaining a total device length of 58 cm (Fig. 2b). The maximum length of the device was previously defined based on the depths of the manholes in which the device would be located following the laboratory phase. Furthermore, rectangular openings were made at the bottom to allow energy dissipation in the opposite direction to the weir (Figs. 2a and 2b).

For the water level measurement, during this laboratory phase, a piezometer with a graduated scale was placed laterally and below the overflow threshold. Thereafter, to fix the zero reference point of the piezometer, the measuring pipe was placed on a level surface and filled up to the weir.

Finally, in order to allow for possible maintenance and inspection of the device, its top and bottom were designed to be removable.

2.1.2. Experimental setup

Direct flow measurement tests based on the volumetric method were performed in the laboratory to obtain the device outflow scale. This method required that all of the flow originating from the weir device was diverted into a graduated reservoir, by determining the time necessary to fill five reference volumes, defined by splitting the entire reservoir volume into equal parts.

Two reservoir volumes were used to consider different flow rate ranges. The first, with graduation levels equal to 0.40, 0.80, 1.20, 1.60, and 2.00 l, was used for small flow rates up to approximately 0.155 l/s, while the second, with graduations of 4.00, 8.00, 12.00, 16.00, and 17.80 l, was used for higher flow rates.

Moreover, a pumping system was used to guarantee a constant flow into the weir device during the test.

A schematic representation of the system used for the previously mentioned volumetric method is illustrated in Fig. 3a.

The reservoir dimensions were substantially larger than the rectangular weir base, a section of which is illustrated in Fig. 3, according to the details previously described. The geometric parameters of the rectangular sharp-crested weir were: weir height d (220 mm); weir width b (12 mm); weir crest thickness L (1 mm); crest bevelled angle θ (60°); and upstream head over weir h.

The discharged flow rate and relative water level were measured when the fluid vein was effectively detached from the weir; that is, when the head was sufficiently high for free flow and the water nappe was at atmospheric pressure [24].

For this reason, the pairs of the flow and water level values referring to an imperfectly aerated jet were not examined. Complete separation of the fluid vein was observed at 21 mm (Fig. 4b). This value guarantees the condition of a sharp-crested or thin-plated weir; that is, the upstream head (h) on the weir crest must be at least 15 times the thickness

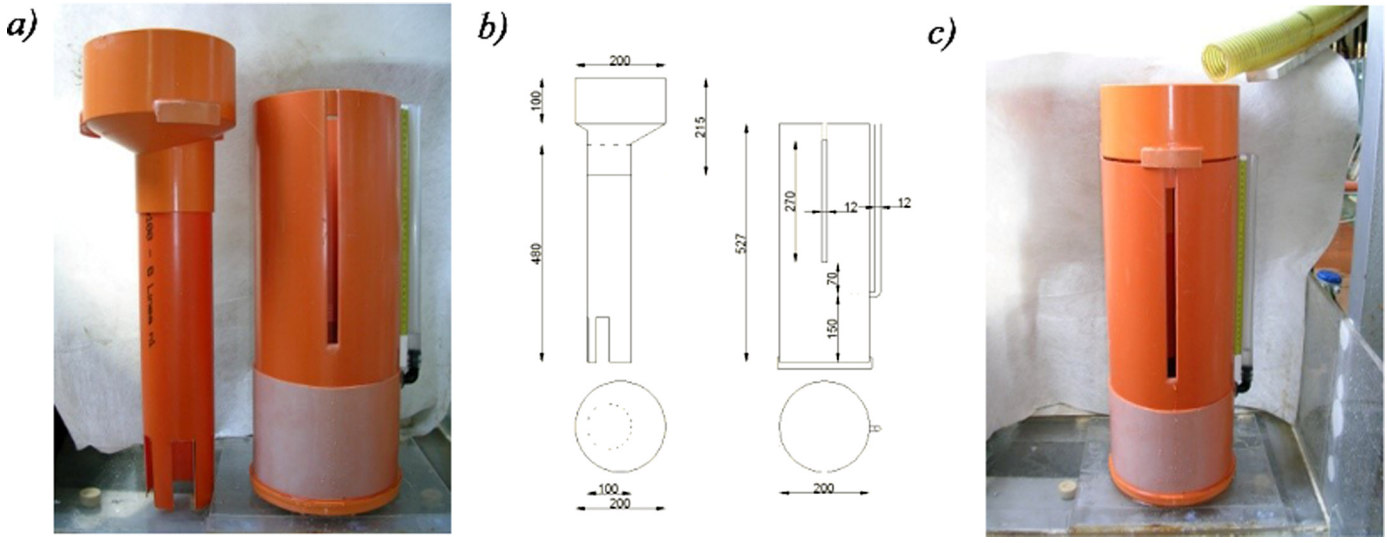

Fig. 2. a) Energy sink and measuring tube not yet assembled; b) final dimensions of two elements; c) device prototype in vertical position, ready for laboratory tests.

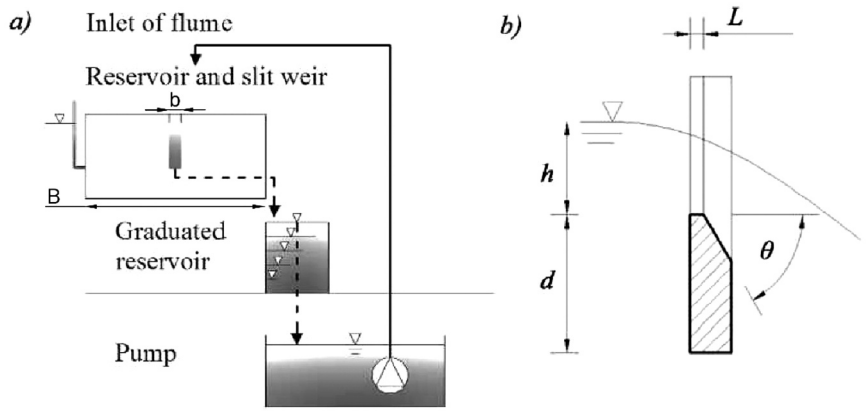

Fig. 3. a) Schematic representation of system used for tests; b) rectangular sharp-crested weir section with indication of geometric parameters.

of the weir crest itself (L) [8,25].

Complete detachment of the effluent vein was identified at an h value of 21 mm (h_{min}). Trials were carried out by increasing the head by approximately 5–6 mm at a time for a total of 31 tests. The mean discharged flow estimation was obtained by dividing the volume collected for the time (Appendix A).

Table 1 summarises the trial conditions. For each upstream head value on the weir, the procedure was repeated four times.

2.1.3. Theoretical considerations and numerical analysis

As discussed previously, several studies have been conducted on the estimation of the flow through a measuring channel. All of the results, from De Marchi [26] to Zahiri et al. [6], exhibit the consensus that the flow rate discharged by a rectangular weir can be expressed according to Eq. (1), which is derived from considerations on the flow energy [25]:

$$Q = \frac{2}{3} C_d \sqrt{2g}\, b h^{3/2}, \tag{1}$$

where Q is the flow rate discharged by the weir; C_d is the discharge coefficient; g is the gravitational acceleration; h is the upstream head over the weir; and b is the weir width.

The discharge coefficient is strongly affected by the geometric configuration of the weir and, as can be detected in certain studies, can be expressed as a function of the h/d ratio [11,14,27], Reynolds number (Re) [16], and b/B ratios [8,28]. Therefore, C_d can be expressed as [9]:

$$C_d = f(Re, We, h/b, b/B, h/d), \tag{2}$$

in which, in addition to h, b, and d, as discussed above, B is the channel or tank width, while Re and We are the Reynolds and Weber numbers, respectively.

In order to proceed with the evaluation of the discharge coefficient equation best representing the outflow from the sharp-crested weir, by considering the observed values of the flow (Q) and upstream head over the weir (h), the corresponding experimental values of C_d were evaluated by means of the following equation, derived from Eq. (1):

$$C_d = \frac{3Q}{2\sqrt{2g}\, b h^{3/2}}. \tag{3}$$

Thereafter, to obtain an analytical expression that correlates the C_d coefficient to one or more parameters, the C_d values as a function of h/b, h/d, Re, and We were analysed. Moreover, as $B >> b$, the parameter b/B was omitted, with the effect of the wall on the outflow considered as negligible [9]. The parameter h/d was taken into account because, for high values of head on the weir, the ratio h/d ranges from 0.10 to 0.78 (Table 1).

Although the effects owing to viscosity (ν) and surface tension (σ) in thin walls could be considered negligible, they were investigated to consider the properties of the Re and We parameters. For the dimensionless Reynolds and Weber numbers, Eqs. (4) and (5) were used. Moreover, working with effective approximation, in the hypothesis of the hydrostatic regime in the calm zone, the Torricellian velocity ($\sqrt{2gh}$) was considered for the Reynolds number determination (4). The hypotheses of the hydrostatic regime have exhibited strong confirmation in experimental evidence.

$$Re = \frac{\sqrt{2gh}\, b}{\upsilon} \tag{4}$$

Table 1
Variation range of experimental data.

b [mm]	h_{min} [mm]	h_{max} [mm]	h_{min}/b	h_{max}/b	h_{min}/d	h_{max}/d	Q_{min} [l/s]	Q_{max} [l/s]
12	21	171	1.75	14.25	0.10	0.78	0.082	1.82

Fig. 4. a) Fluid vein adhering to weir (water level: 13 mm); b) fluid vein detached from weir and well aerated (water level: 21 mm); and c) fluid vein corresponding to maximum water level on weir (171 mm).

$$We = \frac{2ghb\rho}{\sigma}, \quad (5)$$

where g is the gravitational acceleration (9.81 m/s^2); ν is the fluid viscosity ($1.27 \cdot 10^{-6}$ m^2/s); σ is the surface tension (0.0074 kg/m); and ρ is the fluid density (102 kg s^2/m^4).

Thus, based on these considerations, Eq. (2) can be reduced to the following:

$$C_d = f(Re, We, h/b, h/d). \quad (6)$$

This work considered a data-mining approach [29] to achieve additional knowledge regarding the relationship between the available aggregate information and hydraulic features, assumed as input/output data from the system on hand. The analysis was performed by EPR MOGA-XL, developed in the MATLAB environment. This analysis exploited two recent variants of EPR, namely the EPR-MOGA and MCS-EPR.

This approach encompasses a multi-objective optimisation strategy, in which the accuracy of data reproduction and parsimony of model structures are simultaneously maximised [30]. The parsimony feature refers to the number of variables and/or additive terms involved in the analytic equations, and its minimisation is assumed to result in more general phenomena descriptions, while allowing for physical readability at the same time [31]. The version of EPR MOGA-XL employed uses a MOGA optimisation strategy based on the Pareto dominance criteria [32,33], and at the end of the modelling phase, a set of model solutions is produced (the Pareto front of optimal models).

The Pareto front is the set of all Pareto-efficient allocations, conventionally depicted graphically (in a chart with accuracy and parsimony). It is an area of multiple criteria decision-making that is concerned with mathematical optimisation problems involving more than one objective function to be optimised simultaneously.

The main advantages of the EPR-MOGA are: (1) it allows for developing a Pareto set of models with different accuracy and parsimony in only one modelling run; (2) the similarities between the returned relationships lead to discussing and evaluating the phenomenon; and (3) the set of models is aimed at supporting the user in the selection of a suitable expression.

More specifically, in the study, EPR MOGA-XL modelling was performed using the control option 'penalisation of complex structures', which enables a trade-off between the data fitting quality (sum of squared errors, SSE) and model complexity (the number of input combinations) [30]. Moreover, the multi-objective optimisation strategy for the evolutionary search of EPR was used.

Thus, the selected options were carried out in the following two steps.

- *Min(Xi,SSE)*, where Xi is the i-th model parameter: MOGA optimisation strategy using two objective functions [30]; minimisation of the input number (in this case, also maximisation of the model parsimony) and minimisation of SSE (maximisation of model accuracy).
- *Min(aj,SSE)*, where aj is the j-th model coefficient: Optimisation strategy based on the MOGA, using two objective functions [30]; minimisation of number of terms (maximisation of model parsimony) and minimisation of SSE (maximisation of model accuracy on training data).

2.2. Full-scale implementation

The flowmeter device, which is the object of this study, was placed at the base of the Department of Mechanical, Energy and Management Engineering building, on which an experimental green roof was constructed. The site, located in southern Italy, is characterised by Mediterranean climate conditions, according to the Köppen climate classification [34]. This green roof is part of the Urban Hydraulic Park located at the University of Calabria, which also includes an extensive green roof, a bioretention system, and a sedimentation tank connected to a treatment unit [35,36].

The experimental green roof, with an area of 50 m^2 and a slope of 1%, vegetated with native Mediterranean plants, is characterised from top to bottom as follows: a soil substrate with mineral terrain; a permeable geotextile; a drainage layer in polystyrene foam (with a storage capacity of 11 l/m^2 and drainage capacity of 0.46 l/(s m^2)); an anti-root layer; and a waterproof membrane.

Weather data, including precipitation, wind velocity, air humidity, air temperature, barometric pressure, and solar radiation, were collected by a weather station located at the experimental site [37]. The rainfall depth was measured using a tipping bucket rain gauge, with a resolution of 0.254 mm and an acquisition frequency of 1 min.

For direct and continuous estimation of the water level in the flowmeter device, instead of the piezometer used in the previous laboratory phase, a pressure transducer (Ge Druck PTX1830) was selected. This transducer, with a measurement range of 75 cm and an accuracy of 0.1% of the full scale, was calibrated in the laboratory by using a water column to identify the relationship between the output signal in mA, obtained through a digital bench multimeter, and the water tension h, measured by a graduated rod. The water levels thus measured were continuously recorded in a SQLITE database system with a resolution of 1 min [36].

In order to analyse the outflow rates from this green roof, a continuous three-month dataset (rainfall and runoff) with a one-minute time resolution, recorded at the experimental site from October 2015 to December 2015, was considered. The entire studied period was characterised by a total precipitation depth of 447.50 mm, with October being the rainiest month and December the driest.

3. Results and discussion

3.1. Laboratory results

By following the procedure described in Section 2.1.3, the application of the first step *Min(Xi,SSE)* simultaneously led to the model structures in the output. The different models, denoted by 1–5, are displayed in Table 2. These models were derived from the EPR-MOGA analysis; that is, from an evolutionary type of optimisation strategy, where the selection of models is based on the criteria of parsimony

Table 2
SSE and COD for different models in output at first step.

			SSE	COD %
Model 1	$C_d = const$	$C_d = 0.73$	$1.97 \cdot 10^{-4}$	0.51
Model 2	$C_d = f(Re)$	$C_d = a_0 - a_1 \cdot Re$	$3.82 \cdot 10^{-5}$	80.47
Model 3	$C_d = f(Re;h/b)$	$C_d = a_0 + a_1 \cdot \frac{1}{Re^{1.5}} - a_2 \cdot \frac{1}{h/b}$	$3.54 \cdot 10^{-5}$	81.91
Model 4	$C_d = f(Re;We;h/d)$	$C_d = a_0 + a_1 \cdot \frac{1}{Re^{1.5}} - a_2 \cdot \frac{(h/d)^{0.5}}{We^{1.5}}$	$3.57 \cdot 10^{-5}$	81.74
Model 5	$C_d = f(Re;We;h/b)$	$C_d = a_0 - a_1 \cdot \frac{1}{Re^2} + a_2 \cdot \frac{Re^{0.5} \cdot We^{0.5}}{(h/b)^{1.5}}$	$3.58 \cdot 10^{-5}$	81.73

(number of model parameters) and accuracy (model coefficient of determination (COD)).

$$COD = 1 - \frac{\sum_N (\hat{y} - y_{exp})^2}{\sum_N (y_{exp} - avg(y_{exp}))^2}, \quad (7)$$

where N is the number of samples, $\hat{y}$ is the value predicted by the model, y_{exp} represents the corresponding observations, and $avg(y_{exp})$ is the average value of the observations (evaluated on N samples).

As mentioned previously, the Pareto front allows for evaluating the optimal solution (among the models identified by EPR with the same parsimony, the model with the highest accuracy is selected). On this basis, the best model is graphically deduced on the knee point of the Pareto front (Fig. 5a), in which the values (*1-COD*) are indicated on the abscissas, while the numbers of input parameters (Xi) present in each model are reported on the ordinates.

Furthermore, it is possible to detect that models 2 and 3 exhibit an optimal compromise between precision (minimum value (*1-COD*)) and simple structure (minimum number of inputs *Xi*).

By analysing Table 2, it can be noted that model 2 is a function only of the *Re* parameter, and it yields a COD coefficient that is not very different from the other more complex models (3, 4, and 5), while model 1 can be rejected because the COD is close to 0 and, therefore, it is not precise (*1-COD* equal to 1).

Based on the previous analysis, displayed in Table 2, the following analysis focused on processing the discharge coefficient C_d as function of the *Re* and *h/b* parameters.

In order to proceed with this second step, as described in detail in Section 2.1.3, the optimisation strategy of the number of terms was applied. This final application simultaneously led to the model structures in the output displayed in Table 3.

The results presented in Table 3 agree with the EPR-MOGA XL procedure, in which the parsimony was first analysed (therefore, the number of parameters in play), and then, the efficiency was evaluated for the same parsimony. The results in Table 3 indicate a model with a constant C_d and another with one variable (*h/b*), which is in agreement with typical hydraulic results.

According to this procedure, the discharge coefficient equation can be expressed as:

$$C_d = 0.77988 - 0.017232\left(\frac{h}{b}\right)^{0.5}. \quad (8)$$

Thus, by using the second strategy, the discharge coefficient is a function of the *h/b* parameter, instead of the *Re* number.

Table 3
SSE and COD for different models in output at second step.

			SSE	COD %
Model 1	$C_d = const$	$C_d = 0.73$	$1.96 \cdot 10^{-4}$	0.25
Model 2	$C_d = f\left(Re; \frac{h}{b}\right)$	$C_d = a_0 - a_1 \cdot \left(\frac{h}{b}\right)^{0.5}$	$3.86 \cdot 10^{-5}$	80.26

Having obtained the theoretical relationship of the discharge coefficient (Fig. 5b and Eq. (8)), the *theoretical flow rate* can be expressed through the *discharge law* (9).

$$Q_{theoretical} = \frac{2}{3}\left[0.77988 - 0.017232\left(\frac{h}{b}\right)^{0.5}\right]\sqrt{2g}\, b h^{1.5} \quad (9)$$

In Fig. 6, the observed data (the data measured during the laboratory tests) and theoretical data (the data obtained using Eqs. 8 and 9) are compared in terms of both the C_d coefficient and Q. By analysing the figures, it can be observed that Eqs. (8) and (9) effectively interpolated the C_d and Q obtained for the observed data. A high correlation with $R^2 = 99.97\%$ was achieved when comparing the Q obtained using Eq. (9) and that observed during the laboratory tests.

Moreover, analysing Fig. 7, it can be observed that the residuals are randomly arranged around the null value of the ordered axis, and the relative error is less than 2%. The residuals (10) were calculated as the difference between the experimental value (Q_i) and corresponding theoretical predicted value (Q_i*), while the relative flow rate was defined as the ratio presented in (11).

$$e_i = Q_i - Q_i^* \quad (10)$$

$$E_r = \frac{Q_i - Q_i^*}{Q_i^*} 100 \quad (11)$$

Moreover, approximately 77% of the 31 experimental points exhibited an error of less than 1%, while the remaining 23% had an error of less than 2%. These findings are comparable to those in the experimental studies of Aydin et al. [9].

3.2. Runoff results from full-scale implementation

By considering the water level data recorded from the green roof located at the University of Calabria, and by applying the flow Eq. (8), as discussed previously, the corresponding runoff data were obtained for a continuous period of three months (1 October 2015–31 December

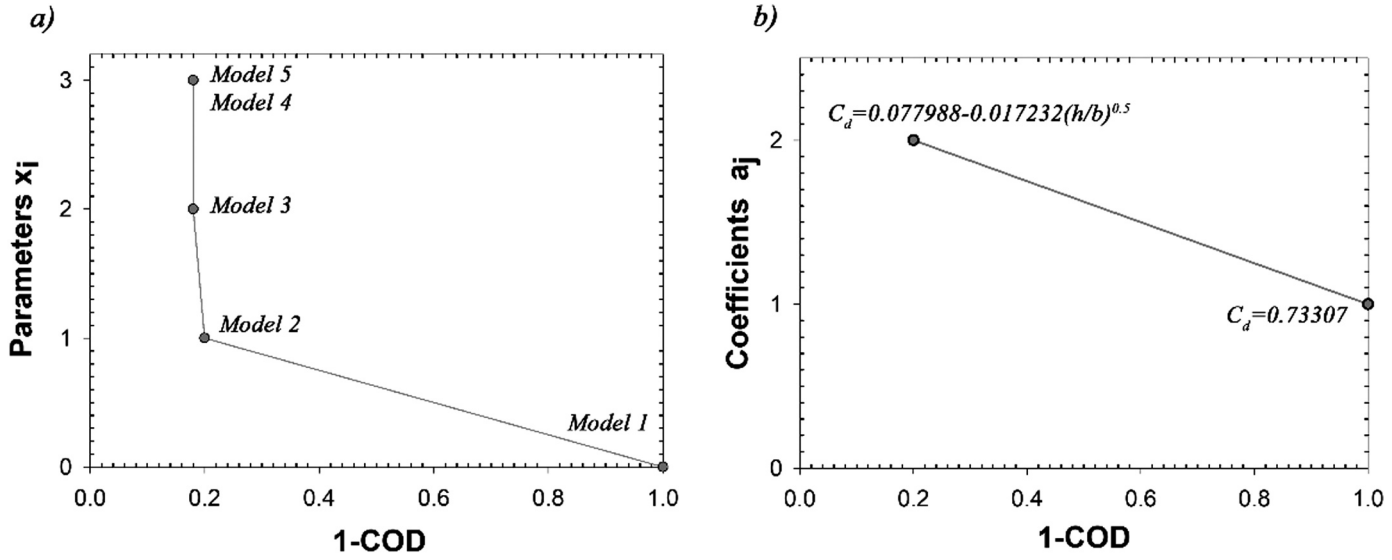

Fig. 5. a) Pareto front for first strategy; b) Pareto front for second strategy.

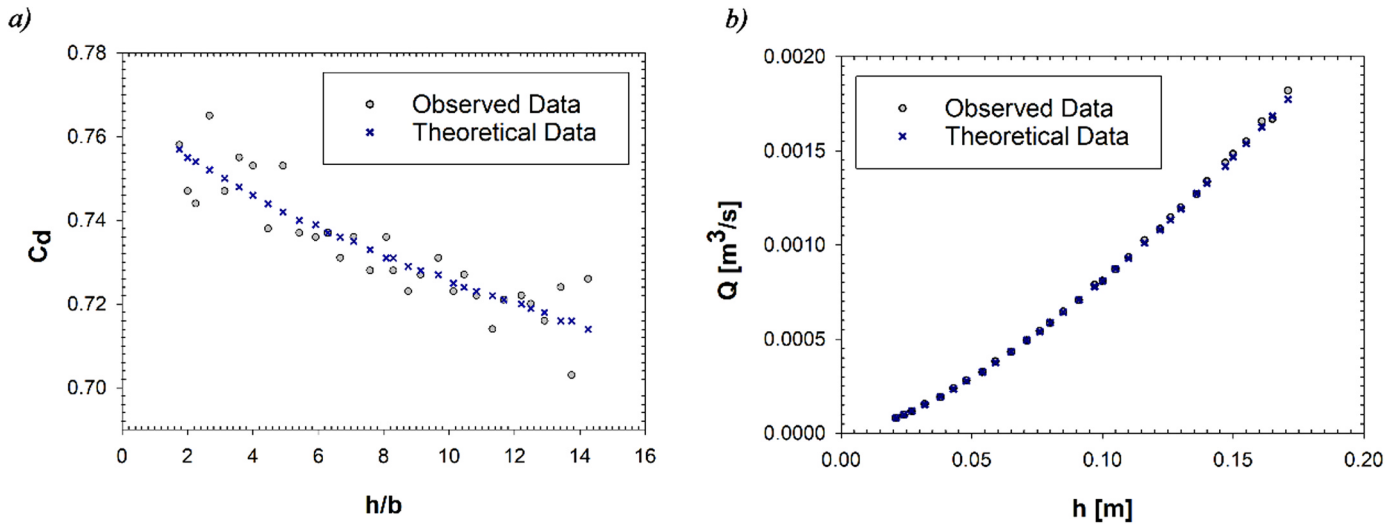

Fig. 6. a) Best fit of discharge coefficient (C_d) data for sharp-crested weir; b) best fit of flow (Q) data for sharp-crested weir.

2015).

In order to obtain an estimation of the ability of the flowmeter device to record each runoff type, from the small events to the largest ones, the green roof runoff hydrographs were evaluated from the three-month scale to the event scale (Fig. 8).

The total runoff evaluated for the quarterly scale (Fig. 8a) was 269.87 mm; consequently, the specific green roof exhibited a subsurface runoff coefficient (SRC), which is evaluated as the percentage ratio between the runoff depth and total rainfall depth, of 60.30%. These results confirm the effective hydrological performances of this specific green roof in terms of runoff volume reduction.

By observing the performance on a weekly scale (23–30 November 2015 – Fig. 8b), in response to the 115.57 mm precipitation depth, the total runoff recorded was 84.39 mm, with an SRC value of approximately 73%.

From Fig. 8a, it is possible to detect that the flowmeter device also recorded small rain events, specifically those from the end of November 2015 to the middle of December 2015. In particular, December 2015 was the driest month in the year; thus, from 28 November 2015 to 3 January 2016, only two small rain events occurred. The rain event of 28 November 2015, with a 2.8 mm rainfall depth, was almost totally retained by the green roof, exhibiting an SRC value of approximately 13%; for the rainfall event that occurred on 12 December 2015, characterised by a precipitation depth of 8.4 mm, the green roof exhibited an SRC of approximately 18%.

For individual rainfall events, only one of which was separated by continuous dry periods of at least 6 h [19] and a rain depth greater than 2 mm [18], the event of 21–23 October 2015 (Fig. 8c) was considered. This event exhibited a total precipitation depth of approximately 120 mm, which was the maximum value for a single rain event recorded in this specific three-month dataset, and the corresponding recorded runoff depth was 100 mm. This result indicates that the experimental green roof can also partially retain significant events in Mediterranean climate conditions.

Following this generic analysis of the hydraulic performance of the specific green roof, by considering three different temporal scales, from the hydrographs in Fig. 8, it can observed that with both the flowmeter device and Eq. (9) applied to the full-scale implementation, a high level of precision was achieved in the data conversion. The plotted hydrographs do not present fluctuations, and effectively interpret the small flow on both the continuous scale and event scale.

Based on these considerations, the developed flowmeter device and validated equation can provide useful and accurate tools for recording the runoff data from the experimental green roof installations, and could easily be replicated by experts in the field, as with the laboratory phases for the other real-scale LID implementations.

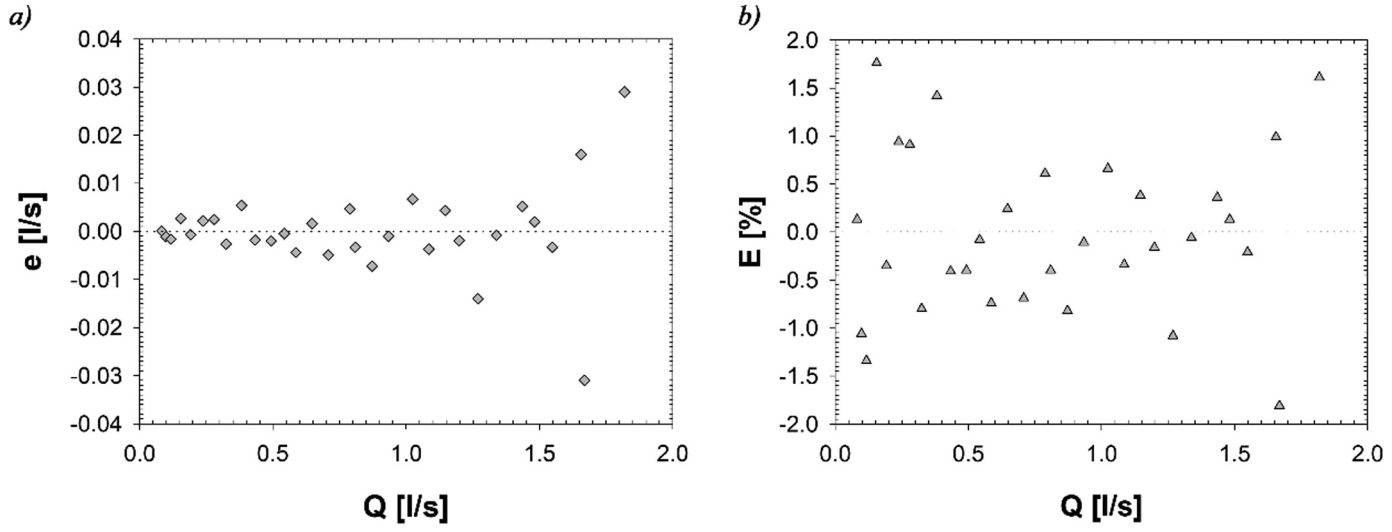

Fig. 7. a) Absolute error; b) relative error.

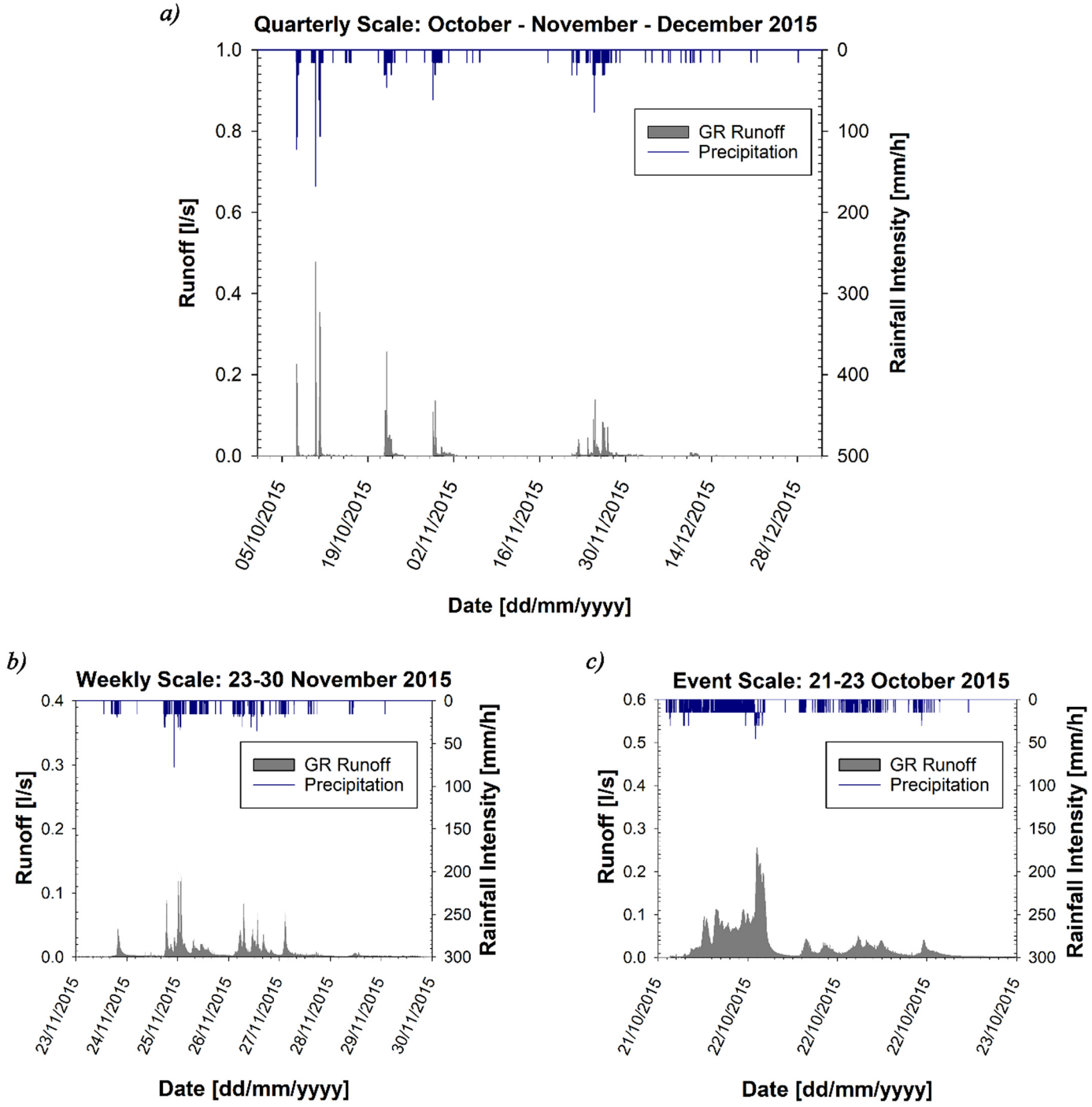

Fig. 8. Hyetographs and corresponding green roof runoff hydrographs for: a) quarterly scale; b) weekly scale; c) event scale.

4. Conclusions

An experimental study was carried out on a rectangular sharp-crested weir with a numerical analysis of the observed data. Modelling was performed in two phases, and finally, a simple and accurate equation for the discharge coefficient, only according to the h/b parameter, was obtained.

With $B >> b$ and the ratio $h/d < 1$, the modelling confirmed that the outflow was not influenced by the boundary conditions imposed by the tank side and bottom walls. Moreover, according to the modelling procedure used, it is clear that, in the case of the thin weir, with high h/b ratio values, the contributions offered by the viscosity and surface tension were negligible. This final observation confirms that the outflow coefficient formulation, as a function of only the h/b ratio, could be highly advantageous, as in this case, the physical process of the outflow is not taken into account.

Considering the high theoretical values of the discharge coefficient (C_d), the achieved results demonstrate that the flow rate followed a thin-walled weir law with a high correlation of $R^2 = 99.97\%$. The theoretical discharge law tests the effectiveness of the interpolation of the experimental points, and the relative errors are very low.

Finally, based on the analysis of the runoff results recorded from the specific flowmeter device installed at the base of the experimental green roof at the University of Calabria, the specific device and

determined relationship effectively estimate not only the outflow for different temporal scales, but also for various rainfall depths, from the minimum registered outflow value to the largest one.

Acknowledgements

The study was co-funded by the Italian National Operative Project (PON) - Research and Competitiveness for the convergence regions 2007/2013 - I Axis "Support to structural changes" operative objective 4.1.1.1. "Scientific-technological generators of transformation processes of the productive system and creation of new sectors" Action II: "Interventions to support industrial research".

Appendix A. Measurement values for the 31 Lab Tests

No.	h [mm]	Qmean [l/s]
1	21	0.082
2	24	0.098
3	27	0.117
4	32	0.155
5	37.5	0.192
6	43	0.238
7	48	0.280
8	53.5	0.324
9	59	0.382
10	65	0.433
11	71	0.493
12	75.5	0.542
13	80	0.586
14	85	0.647
15	91	0.708
16	97	0.788
17	99.5	0.809
18	105	0.872
19	109.5	0.934
20	116	1.024
21	121.5	1.085
22	125.5	1.146
23	130	1.199
24	136	1.269
25	140	1.338
26	146.5	1.435
27	150	1.482
28	155	1.549
29	161	1.656
30	165	1.669
31	171	1.819

References

[1] M. Guan, N. Sillanpää, H. Koivusalo, Modelling and assessment of hydrological changes in a developing urban catchment, Hydrol. Process. 29 (13) (2015) 2880–2894, https://doi.org/10.1002/hyp.10410.
[2] M. Carbone, G. Garofalo, G. Nigro, P. Piro, A conceptual model for predicting hydraulic behaviour of a green roof, Procedia Eng. 70 (2014) 266–274, https://doi.org/10.1016/j.proeng.2014.02.030.
[3] T.D. Fletcher, W. Shuster, W.F. Hunt, R. Ashley, D. Butler, S. Arthur, P.S. Mikkelsen, SUDS, LID, BMPs, WSUD and more–The evolution and application of terminology surrounding urban drainage, Urban Water J. 12 (7) (2015) 525–542, https://doi.org/10.1080/1573062X.2014.916314.
[4] J. Zischg, M.L. Goncalves, T.K. Bacchin, G. Leonhardt, M. Viklander, A. van Timmeren, R. Sitzenfrei, Info-Gap robustness pathway method for transitioning of urban drainage systems under deep uncertainties, Water Sci. Technol. 76 (5) (2017) 1272–1281, https://doi.org/10.2166/wst.2017.320.
[5] G. Garofalo, S. Palermo, F. Principato, T. Theodosiou, P. Piro, The influence of hydrologic parameters on the hydraulic efficiency of an extensive green roof in mediterranean area, Water 8 (2) (2016) 44, https://doi.org/10.3390/w8020044.
[6] A. Zahiri, X. Tang, S. Bagheri, Flow discharge computation over compound sharp-crested side weirs, ISH J. Hydraul. Eng. 23 (3) (2017) 341–345, https://doi.org/10.1080/09715010.2017.1328647.
[7] S.M. Borghei, M.R. Jalili, M.A.S.O.U.D. Ghodsian, Discharge coefficient for sharp-crested side weir in subcritical flow, J. Hydraul. Eng. 125 (10) (1999) 1051–1056, https://doi.org/10.1061/(ASCE)0733-9429(1999)125:10(1051).
[8] S. Bagheri, M. Heidarpour, Flow over rectangular sharp-crested weirs, Irrig. Sci. 28 (2) (2010) 173, https://doi.org/10.1007/s00271-009-0172-1.
[9] I. Aydin, A.B. Altan-Sakarya, C. Sisman, Discharge formula for rectangular sharp-crested weirs, Flow Meas. Instrum. 22 (2) (2011) 144–151, https://doi.org/10.1016/j.flowmeasinst.2011.01.003.
[10] A.S. Ramamurthy, J. Qu, C. Zhai, D. Vo, Multislit weir characteristics, J. Irrig. Drain. Eng. 133 (2) (2007) 198–200, https://doi.org/10.1061/(ASCE)0733-9437(2007)133:2(198).
[11] H. Rouse, Discharge characteristics of the free overfall: use of crest section as a control provides easy means of measuring discharge, Civil Eng. 6 (4) (1936) 257–260.
[12] C.E. Kindsvater, R.W. Carter, Discharge characteristics of rectangular thin-plate weirs, Trans. Am. Soc. Civil Eng. 124 (1) (1959) 772–801.
[13] A.S. Ramamurthy, U.S. Tim, M.V.J. Rao, Flow over sharp-crested plate weirs, J. Irrig. Drain. Eng. 113 (2) (1987) 163–172, https://doi.org/10.1061/(ASCE)0733-9437(1987)113:2(163).
[14] P.K. Swamee, Generalized rectangular weir equations, J. Hydraul. Eng. 114 (8) (1988) 945–949, https://doi.org/10.1061/(ASCE)0733-9429(1988)114:8(945).
[15] M.C. Johnson, Discharge coefficient analysis for flat-topped and sharp-crested weirs, Irrig. Sci. 19 (3) (2000) 133–137, https://doi.org/10.1007/s002719900009.
[16] I. Aydin, A.B. Altan-Sakarya, A.M. Ger, Performance of slit weir, J. Hydraul. Eng. 132 (9) (2006) 987–989, https://doi.org/10.1061/(ASCE)0733-9429(2006)132:9(987).
[17] D.J. Bliss, R.D. Neufeld, R.J. Ries, Storm water runoff mitigation using a green roof, Environ. Eng. Sci. 26 (2) (2009) 407–418, https://doi.org/10.1089/ees.2007.0186.
[18] E. Voyde, E. Fassman, R. Simcock, Hydrology of an extensive living roof under sub-tropical climate conditions in Auckland, New Zealand, J. Hydrol. 394 (3–4) (2010) 384–395, https://doi.org/10.1016/j.jhydrol.2010.09.013.
[19] V. Stovin, G. Vesuviano, H. Kasmin, The hydrological performance of a green roof test bed under UK climatic conditions, J. Hydrol. 414 (2012) 148–161, https://doi.org/10.1016/j.jhydrol.2011.10.022.
[20] T.B. Carson, D.E. Marasco, P.J. Culligan, W.R. McGillis, Hydrological performance of extensive green roofs in New York City: observations and multi-year modeling of three full-scale systems, Environ. Res. Lett. 8 (2) (2013) 024036, https://doi.org/10.1088/1748-9326/8/2/024036.
[21] R. Hakimdavar, P.J. Culligan, M. Finazzi, S. Barontini, R. Ranzi, Scale dynamics of extensive green roofs: quantifying the effect of drainage area and rainfall characteristics on observed and modeled green roof hydrologic performance, Ecol. Eng. 73 (2014) 494–508, https://doi.org/10.1016/j.ecoleng.2014.09.080.
[22] P.A. Versini, D. Ramier, E. Berthier, B. De Gouvello, Assessment of the hydrological

impacts of green roof: from building scale to basin scale, J. Hydrol. 524 (2015) 562–575, https://doi.org/10.1016/j.jhydrol.2015.03.020.
[23] Z. Zhang, C. Szota, T.D. Fletcher, N.S. Williams, J. Werdin, C. Farrell, Influence of plant composition and water use strategies on green roof stormwater retention, Sci. Total Environ. 625 (2018) 775–781, https://doi.org/10.1016/j.scitotenv.2017.12.231.
[24] E.J. Finnemore, J.B. Franzini, Fluid Mechanics with Engineering Applications, 10th ed., McGraw-Hill, New York, 2002.
[25] M.G. Bos, Discharge measurement structures. International Institute for Land Reclamation and Improvement, ILRI, Wageningen, 1989.
[26] De Marchi, G., Essay on the performance of lateral weirs, L'Energia Elettrica, Milan, Italy, 11, 1934, pp. 849–860.
[27] T. Rehbock, Discussion of precise weir measurements by EW Schoder and KB Turner, Trans. ASCE 93 (1929) 1143–1162.
[28] R.H. French, R.H. French, Open-channel Hydraulics, McGraw-Hill, New York, 1985.
[29] M. Rezania, A.A. Javadi, O. Giustolisi, Evaluation of liquefaction potential based on CPT results using evolutionary polynomial regression, Comput. Geotech. 37 (1–2) (2010) 82–92, https://doi.org/10.1016/j.compgeo.2009.07.006.
[30] O. Giustolisi, D.A. Savic, A symbolic data-driven technique based on evolutionary polynomial regression, J. Hydroinform. 8 (3) (2006) 207–222, https://doi.org/10.2166/hydro.2006.020.
[31] M. Carbone, L. Berardi, D. Laucelli, P. Piro, Data-mining approach to investigate sedimentation features in combined sewer overflows, J. Hydroinform. 14 (3) (2012) 613–627, https://doi.org/10.2166/hydro.2011.003.
[32] O. Giustolisi, D.A. Savic, Advances in data-driven analyses and modelling using EPR-MOGA, J. Hydroinform. 11 (3–4) (2009) 225–236, https://doi.org/10.2166/hydro.2009.017.
[33] D. Laucelli, O. Giustolisi, Scour depth modelling by a multi-objective evolutionary paradigm, Environ. Model. Softw. 26 (4) (2011) 498–509, https://doi.org/10.1016/j.envsoft.2010.10.013.
[34] P. Bevilacqua, D. Mazzeo, N. Arcuri, Assessment of the thermal inertia of an experimental extensive green roof in summer conditions, Build. Environ. (2017), https://doi.org/10.1016/j.buildenv.2017.11.033.
[35] M. Maiolo, M. Carini, G. Capano, P. Piro, Synthetic sustainability index (SSI) based on life cycle assessment approach of low impact development in the Mediterranean area, Cogent Eng. 4 (1) (2017) 1410272, https://doi.org/10.1080/23311916.2017.1410272.
[36] G. Brunetti, J. Šimůnek, M. Turco, P. Piro, On the use of surrogate-based modeling for the numerical analysis of Low Impact Development techniques, J. Hydrol. 548 (2017) 263–277, https://doi.org/10.1016/j.jhydrol.2017.03.013.
[37] M. Carbone, F. Principato, G. Garofalo, P. Piro, Comparison of evapotranspiration computation by FAO-56 and hargreaves methods, J. Irrig. Drain. Eng. 142 (8) (2016) 06016007, https://doi.org/10.1061/(ASCE)IR.1943-4774.0001032.

Paper IV

Smart Rain Barrels: Advanced LID Management Through Measurement and Control

Oberascher M., Zischg J., **Palermo S.A.**, Kinzel C., Rauch W., Sitzenfrei R. (2019)

Published in: Mannina G. (eds) New Trends in Urban Drainage Modelling. UDM 2018. Green Energy and Technology. Springer, Cham.
https://doi.org/10.1007/978-3-319-99867-1_134

Smart Rain Barrels: Advanced LID Management Through Measurement and Control

Martin Oberascher[1(✉)], Jonatan Zischg[1], Stefania Anna Palermo[1,2], Carolina Kinzel[1], Wolfgang Rauch[1], and Robert Sitzenfrei[1]

[1] Unit of Environmental Engineering, Department of Infrastructure Engineering, University of Innsbruck, Innsbruck, Austria
martin.oberascher@uibk.ac.at
[2] Department of Civil Engineering, University of Calabria, Rende, Italy

Abstract. Rain barrels are micro-scale applications which are used as temporary storage and for rainwater harvesting. They can be easily implemented into existing stormwater infrastructure. Recent advances in the field of Internet of Things (IoT) have opened up new possibilities for real-time monitoring and control of such structures, that enable the reduction of urban flooding or combined sewer overflows. The special feature of our smart rain barrel is its integration into a pilot project for smart cities, where every water inflow and outflow of the university campus in Innsbruck (Austria) is measured. Weather forecasts and time-controlled filling levels of different Low Impact Developments (LID) structures and the connected sewer system are used for real-time control (RTC). In a first step, the smart rain barrels are implemented into a SWMM-model with the objective of reducing the peak runoff rate by using the filling level in the main conduit as the control variable for real-time control. Results show that depending on the installation site and the storage volume of the rain barrel, a flood volume reduction of 18–40% can be achieved although only a simplified automatic control system has been implemented.

Keywords: LID · Smart cities · Real-time monitoring and control
Peak flow reduction

1 Introduction

Low Impact Development (LID) practices are used to control runoff volumes, peak runoff rates, flow frequency/duration and to improve the water quality in receiving waters by increasing the intercepted runoff, water treatment, evaporation, infiltration and storage volume. In many cases, LIDs are micro-scale applications, including rain barrels and cisterns, which can be used as temporary storage and for rainwater harvesting (Prince George's County 1991). In Australia, on-site detention systems, consisting of controlled water tanks and placed on individual properties, have already been used since the 1990 s to reduce stormwater runoff in the sewer system (O'Loughlin, Beecham et al. 1995) and were later completed with storage volumes for non-potable water usage (van der Sterren et al. 2009). Further research on controlled water tanks

G. Mannina (Ed.): UDM 2018, GREEN, pp. 777–782, 2019.
https://doi.org/10.1007/978-3-319-99867-1_134

show that discharge rates and water demands can be reduced by an average of 18% and 10% respectively by using daily time-steps for the analyses (Melville-Shreeve et al. 2016). In particular, rain barrels require little space and can therefore be easily integrated into existing infrastructure. Nowadays, due to the technological advances of the Internet of Things (IoT), even in LID devices the water flow water can be measured, communicated and analysed in real-time, and as a result, the overall state of the water systems is known at any time. This information can be used for real-time control (RTC) which allows for an adaption of existing infrastructure to changing needs (Kerkez 2018).

In this paper, IoT and rain barrels are linked together, resulting in a smart rain barrel, which is real-time monitored and real-time controlled. The idea of a smart rain barrel is nothing new, as the large number of different publicly available products shows (RainGrid n.d., Sieker n.d.). Unlike these products, however, our smart rain barrels are integrated into a pilot project for smart cities, where LIDs will communicate among each other and are connected with the RTC system. Within the Smart Water Control project, every water inflow and outflow from the university campus in Innsbruck (Austria) is measured in real-time, including filling levels of different LIDs and the central sewer system. In combination with weather forecasts, these data are used for RTC of the smart rain barrels to optimize the efficiency of the above-mentioned LID aims. In a first step, a simplified smart rain barrel model is implemented in the existing stormwater infrastructure, by using only the filling depth in the sewer system as the control variable for RTC. The objective of this paper is to investigate the potential of peak runoff reduction and to estimate the future suitability of optimizing smart rain barrels.

2 Materials and Methods

2.1 Concept of the Smart Rain Barrel (SRB)

The conceptual idea of the SRB is shown in Fig. 1(a). The SRB is equipped with a controllable valve and a water level measurement and is placed within a network of SBRs. The SRBs communicate with each other without a central database (IoT concept); instead, data is transmitted wirelessly and directly between the SRBs via Long Range Wide Area Network (LoRaWAN). The aims of the presented control strategy are the reduction of peak runoff rate and the reduction of potable water consumption for irrigation.

An important factor that influences the control of the SRB is the weather forecast with predicted amount and duration of precipitation. Depending on the weather forecast, three states of the control strategy can be distinguished: (i) the predicted rainfall exceeds the available storage volume, (ii) the predicted rainfall is less than the available storage volume, and (iii) dry weather period. If the predicted inflow to the rain barrel exceeds the total storage volume, the SRB empties completely just before the rainfall event. However, if the calculated inflow is less than the storage volume, the SRB is only partially emptied to ensure a fully filled barrel at the end of the rain event, e.g. for irrigation purposes. And for dry weather periods, the SRB reduces potable water

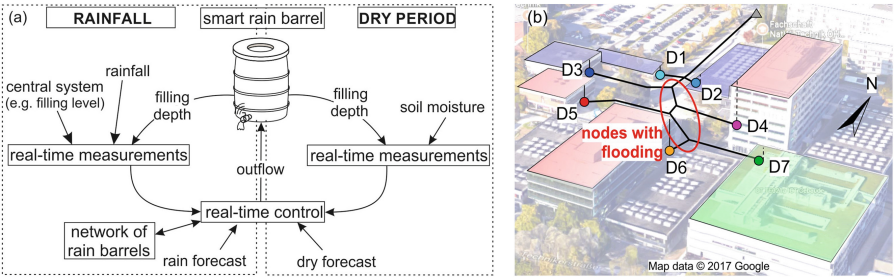

Fig. 1. (a) Concept of a SRB: Different strategies for rainfall events or dry periods and (b) placement of 7 SRBs (D1 to D7) and their intercepted roof areas. The red coloured areas represent conventional roofs, the blue coloured areas are gravel roofs, and the green area corresponds to a green roof.

consumption by using the stored water for irrigation. To reduce the uncertainties of the weather forecast, rainfall is measured in real-time and compared with the weather forecast to change the strategy if necessary. To find the ideal time for using the storage volume of the SRB, minimizing system flooding and discharges to receiving waters, the outflow of the SRB is real-time controlled by using data of the central drainage system. Furthermore, in dry weather periods, soil moisture is measured and plants are irrigated with the stored water to reduce the potable water consumption. As an example of the effects of the SRB, the impact of the rain barrel control on the reduction of stormwater runoff with a simple control strategy is presented.

2.2 Case Study

The SRBs are implemented into the existing stormwater system at the university campus in Innsbruck (Austria). The Campus area is equipped with different measuring devices including water meters, rain gauges, ultrasonic sensors and soil moisture sensors. These devices measure water flows (e.g. water supply, rainfall, groundwater, sewer system etc.) to and from the campus area in real-time. These data are used for the development of RTC strategies such as SRBs.

The campus area can be divided into two different and currently independent systems. On the one hand, surface areas (e.g. pavements, streets, green spaces), that drain into decentralized LIDs (e.g. raingarden and infiltration trenches), on the other hand, roof areas which are connected to the central stormwater system. The latter system is used for the implementation of our SRBs. The SRBs can also be used to connect the central and decentral systems, either by discharging into the LIDs and fully utilizing their capacities, or by directly discharging to the central system. Figure 1(b) shows the campus area, object of this study, consisting of one green roof (green colour), three gravel roofs (blue colour) and three flat roofs without LIDs (red colour), with a total area of 0.71 ha. The main stormwater conduit has a total length of 270 m and consists of pipes with diameters from 200 mm to 500 mm, which exceeds the design capacities. To show the advantages of the SRBs under design conditions, the diameters were artificially reduced to 200 mm and 300 mm to observe flooding when

applying the design rain events. D1 to D7 indicate the locations of the implemented SRBs, which are independently investigated. This study is a modelling study to support the development of a prototypes of SRBs (e.g. choice of sizes and locations) which is currently under construction and will be situated at the campus area in the near future.

2.3 Numerical Model

For the hydrodynamic simulation, the EPA Storm Water Management Model SWMM (Gironás et al. 2010) was used. In a first step, a simplified model for the SRBs was created, using the filling level in the sewer system for RTC. The objective was to reduce the peak runoff rate in the sewer system. The SRBs were implemented as additional storage volume and placed between the roof subcatchments and the inlet of the sewer system. The SRBs were controlled by rules consisting of a conditional clause (e.g. filling level of the sewer systems) and an action clause (e.g. different outflows from the rain barrel). In the model, the outlet from the SRBs was closed when the filling level at the closest manhole was higher than a predefined height. As an initial assumption, a filling level of 60% at the manhole was used for peak runoff reduction in the drainage system. When the storage volume of the SRB was full, the overflow was routed into the drainage system. To evaluate the reduction of peak runoff and the effect of the SRB's location, each building was individually equipped with a SRB (see Fig. 1 (b)). Furthermore, the additional storage of the SRBs was modified in a range from 0.1 to 6 m^3. For the simulation, a 14-year rain series from a nearby weather station was used and an exact rain forecast was assumed. The 16 rain events that caused flooding were extracted from the rain series and aggregated to reduce the simulation time. They were separated by an additional day without precipitation, which was used for emptying the SRBs. The rain data were available in 5 min steps and the rain events had maximum intensities from 3.3 to 11.5 mm in 5 min and a maximum total precipitation of 13 to 38 mm. The total flood volume of the reference state was 214 m^3 and was used for comparison of the different locations and SRB sizes.

3 Results and Discussion

Figure 2 shows the simulation results for the implementation of SRBs of different sizes and at different locations as compared to the reference (actual) state without SRBs. The flood volume reduction depends on the barrel size and its location (same colour coding as in Fig. 1(b)). It can be seen that the location of the SRB has a major impact on the reduction of the flooding volume. For example, SRBs located at D1 or D2 have no effect, while SRBs situated at all other locations clearly decrease the total flood volume of up to approximately 97 m^3 which corresponds to a reduction rate of 40%. The variations of the results can be explained by the fact that flooding primarily occurs in the marked area (see red circled area in Fig. 1(b)), implying that not all SRB locations are efficient. Additional storage volumes at D1 or D2 are located downstream of the primary flooding area, so that the peak runoff rate that causes flooding is not reduced. All other nodes are located in upstream direction of the flooding area, resulting in a decrease of the flood volume by 18–40%.

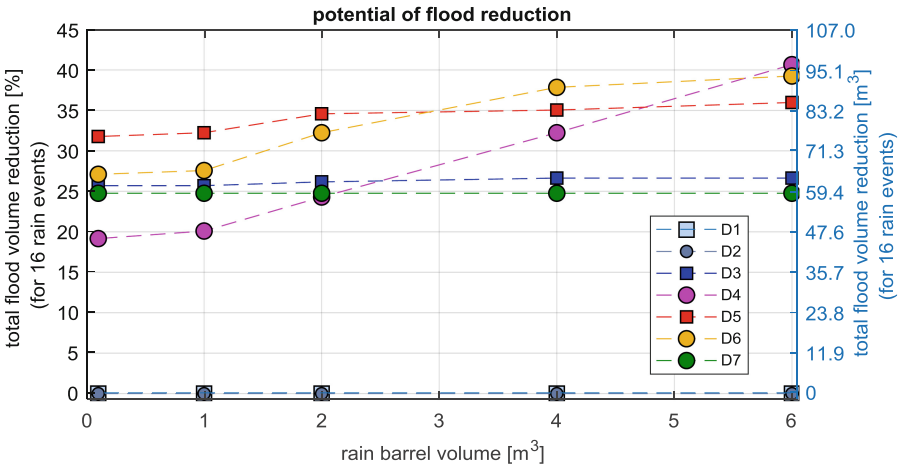

Fig. 2. Results of the simulation showing the potential of flood reduction when implementing SRBs of different size at different locations compared to the reference state

It is particularly interesting to note that the size of SRBs located at a gravel roof (D3) or a green roof (D7) does not have any influence on the flood volume reduction, while for conventional roofs the flood volume reduction is greatly dependent on the available volume. Another important point is, that there is hardly any difference between rain barrels with storage volumes less than 1 m^3 noticeable. By a more detailed exclamation, the effectiveness of storage volumes less than 1 m^3 is mainly influenced by two main factors. The first factor is the relation between filling time of the SRB and the chosen report time steps in SWMM. For example, if the SRB is filled in 10 s the report time step must be small enough to show effects in the flood reduction. The other point is, that the control strategy with the fixed filling level in the sewer system as input parameter is not suitable for minimising the flood volume. For example, in the worst case the SRB is already fully filled bevor flooding occurs. Although, the primary purpose of the SRB is not flood prevention, it can be seen that the accumulated flood reduction can reach up to 40% compared to the reference state. However, this reduction rates are not realistic because of SRB volumes of 6 m^3.

4 Conclusions

This paper presented a concept for using real-time controlled smart rain barrels integrated into a smart city pilot project using weather forecasts and real-time measurements of rain, soil moisture and filling levels recorded in the LIDs and the sewer system. The smart rain barrels were implemented into a SWMM-model for a first evaluation of their effectiveness. In the current model setup, a simplified automatic control by using the filling level in the sewer system as the only control variable was applied. First results showed that accumulated flood volume reductions of 18 – 40% can be achieved and that the location of the smart rain barrel and the storage size are

important factors to reduce flooding. However, the main purpose of a smart rain barrel is to reduce potable water consumption and not necessarily to increase flood robustness. If the uncertainty of the weather forecast is increased, the choice of appropriate weights for the two contradicting objectives of flood reduction and water savings for irrigation becomes more important. Based on the presented evaluations, smart rain barrels are installed and operated on campus. A further advantage of the proposed concept is that the structures can communicate with each other even without a central database (Internet of Things concept). Similar to the decentralised smart rain barrels, we want to achieve a decentralised real-time control system, which is desirable in the context of smart cities, and therefore the Internet of Things concept is most appropriate. The smart rain barrels can also be used to connect the central and decentral systems, either by discharging into the LIDs and fully utilizing their capacities, or by directly discharging to the central system.

Acknowledgements. This research was funded by the Climate and Energy Fund within the Smart Cities program (project number 858782).

References

Gironás, J., Roesner, L.A., Rossman, L.A., Davis, J.: A new applications manual for the Storm Water Management Model (SWMM). Environ. Model Softw. **25**(6), 813–814 (2010)

Kerkez, B.: Building smarter water systems. Bridge Spring **2018**, 7 (2018)

Melville-Shreeve, P., Cadwalder, O., Eisenstein, W., Ward, S., Butler, D.: Rainwater harvesting for drought management and stormwater control in the San Francisco Bay Area. In: 9th International Conference NOVATECH, Lyon (2016)

O'Loughlin, G., Beecham, S., Lees, S., Rose, L., Nicholas, D.: On-site stormwater detention systems in Sydney. Water Sci. Technol. **32**(1), 7 (1995)

Prince George's County: Low-Impact Develompent Design Strategies: An Integrated Design Approach, Prince George's County, Maryland (1991)

RainGrid. (n.d.). Stormwater Smartgrids. https://www.raingrid.com/stormwater-smartgrids/. Accessed 26 Mar 2018

Sieker. (n.d.). Smart Cistern - Efficient rainwater usage based on precipitation forecast. http://www.sieker.de/en/products-and-services/product/smart-cistern-40.html. Accessed 26 Mar 2018

van der Sterren, M., Rahman, A., Shrestha, S., Barker, G., Ryan, G.: An overview of on-site retention and detention policies for urban stormwater management in the Greater Western Sydney Region in Australia. Water Int. **34**(3), 362–372 (2009)

Paper V

A Comprehensive Approach to Stormwater Management Problems in the Next Generation Drainage Networks

Piro P., Turco M., **Palermo S.A.**, Principato F., Brunetti G. (2019b)

Published in: Cicirelli F., Guerrieri A., Mastroianni C., Spezzano G., Vinci A. (eds) The Internet of Things for Smart Urban Ecosystems. Internet of Things (Technology, Communications and Computing). Springer, Cham.
https://doi.org/10.1007/978-3-319-96550-5_12

A Comprehensive Approach to Stormwater Management Problems in the Next Generation Drainage Networks

Patrizia Piro, Michele Turco, Stefania Anna Palermo, Francesca Principato and Giuseppe Brunetti

Abstract In an urban environment, sewer flooding and combined sewer overflows (CSOs) are a potential risk to human life, economic assets and the environment. In this way, traditional urban drainage techniques seem to be inadequate for the purpose so to mitigate such phenomena, new techniques such as Real Time Control (RTC) of urban drainage systems and Low Impact Development (LID) techniques represent a valid and cost-effective solution. This chapter lists some of the recent experiences in the field of Urban Hydrology consisting in a series of facilities, fully equipped with sensors and other electronical component, to prevent flooding in urban areas. A series of innovative numerical analysis (in Urban Hydrology research) have been proposed to define properties of the hydrological/hydraulic models used to reproduce the natural processes involved.

1 Introduction

During the last few decades, the area of impervious surfaces in urban areas has exponentially increased as a consequence of demographic growth. This long-term process has altered the natural hydrological cycle by reducing the infiltration and evaporation capacity of urban catchments, while increasing surface runoff and reducing groundwater recharge. Moreover, the frequency of extreme rainfall events, characterized by high intensity and short duration, is expected to increase in the near future as a consequence of global warming [34, 38]. In addition, these processes have led to an increase in the frequency and magnitude of two undesired phenomena which negatively affect human life, economic assets and the environment: (i) local flooding and (ii) combined sewer overflows (CSOs) [44, 47]. Urban flooding occurs when the urban drainage system (UDS) overload during extreme rainfall events, causing untreated combined sewage and storm water to back up into basements and to over-

P. Piro · M. Turco (✉) · S. A. Palermo · F. Principato · G. Brunetti
Department of Civil Engineering, University of Calabria, Rende, CS 87036, Italy
e-mail: michele.turco@unical.it

F. Cicirelli et al. (eds.), *The Internet of Things for Smart Urban Ecosystems*,
Internet of Things, https://doi.org/10.1007/978-3-319-96550-5_12

flow from manholes onto surface streets. This phenomenon is generally worsened by obstructions in conduits and manholes due to an infrequent maintenance.

CSO [42, 43] takes place when the wastewater treatment plant (WWTP) is not able to treat the wastewater delivered by the UDS. Specifically, the sewage and wet weather flows that exceed the WWTP treatment capacity. Specifically, the sewage and wet weather flows are conveyed through the UDS to the WWTP until the maximum treatment capacity is reached. The exceedance of the water flows is discharged directly into the receiving water bodies, such as rivers or lakes, without receiving any treatment. As a consequence, CSO is one of the major contributors to water pollution experienced in rivers, lakes, etc.

This work proposes two innovative alternatives to manage stormwater in urban areas:

1. Direct management by using offline storage facilities with decentralized Real Time Control (RTC) system;
2. Pervasive management by using Low Impact Development techniques (LID).

The offline storage facilities such as storage tanks, which have the goal to temporarily accumulate stormwater volumes, are widely used, even though they are often overly expensive due to the high construction and maintenance costs. In contrast, approaches aiming at temporarily accumulating stormwater volumes directly in the existing UDSs have also been developed thus avoiding large investments [5, 7, 52]. These approaches are supported by the fact that the UDSs are typically designed by taking into account a set of safety factors. In particular, conduits are intentionally designed to be larger than required in the case of typical network working conditions. Basically, the UDS is managed by a real-time control (RTC) system which requires the network to be embedded with sensors and actuators permitting the network to be real-time monitored and regulated so as to adapt to the different rainfall events [1, 19].

Previous studies in literature was focused on RTC based on a centralized approach. In the study of Pleau et al. [45] a sewer networks global optimal control (GOC) scheme with a two-level architecture has been designed. The upper level was composed of a central station, which computed flow set points, whereas the lower level was composed of local stations, which are used for monitoring, flow computation, data validation and feedback control. The real-time computer was dedicated to all RTC operations and supports a supervisory software, a GOC software, a non-linear hydrologic–hydraulic model and a non-linear programming algorithm. The site was controlled automatically under a flow set point computed by the GOC scheme. The optimization problem was defined by a multi-objective (cost) function and a set of equality and inequality constraints, based on the following control objectives: minimizing overflows, minimizing set point variations and maximizing the use of WWTP capacity. In Fu et al. [23] a multi-objective optimization genetic algorithm was proposed which is used to derive the Pareto optimal solutions, which can illustrate the whole trade-off relationships between objectives. In Schütze et al. [52] a global optimal predictive real time control system has been implemented, which involves solution of a multi-objective optimization problem. The control objectives

were the minimization of overflows, the maximization of the use of the treatment plant capacity, the minimization of accumulated volumes and, finally, the minimization of variations of the setpoints. The real time control system was implemented at a central station and used flow monitoring and water level data, rainfall intensity data, radar rainfall images and 2 h rain predictions. Set-points were translated into moveable gate positions at local stations by Programmable Logic Controllers (PLC). In this work we illustrate the Distributed Real-Time Control (DRTC) system already proposed in previous studies [16, 24, 25]. A multi-agent paradigm and specifically a gossip-based algorithm has been exploited. The UDS was equipped with electronically moveable gates and a set of water level sensors spread across the network. All the gates are locally controlled by Proportional Integrative Derivative (PID) controllers which are globally orchestrated by the mentioned gossip-based algorithm thus achieving an optimal hydrodynamic behaviour in terms of CSO and flooding reduction. The case study is the UDS of the city of Cosenza (Italy), which is modelled by using the StormWater Management Model (SWMM) simulation software. SWMM is an open-source computer model widely used by the hydraulic engineering community for simulation of hydrodynamic water and pollutant transport in sewer systems. It is provided by US EPA [50] and permits an accurate simulation of the hydrological and hydraulic behaviour of the UDS during both dry and wet weather conditions. SWMM simulation software has been customized in order to allow it to be integrated with an external real-time control module. Experiments, conducted using a set of selected extreme rainfall, show a substantial reduction of both CSO and flooding when the proposed approach is exploited.

The other innovative approach presented here consist of implementation of pervasive technique. This approach to land development known as low-impact development (LID) has gained increasing popularity. LID systems consist of a series of facilities whose purpose is to reproduce the site's pre-developed hydrological processes using design techniques that infiltrate, filter, store, evaporate, and detain runoff close to its source. Low-impact development practices consist of bioretention cells, infiltration wells or trenches, stormwater wetlands, wet ponds, level spreaders, permeable pavements, swales, green roofs, vegetated filter and buffer strips, sand filters, smaller culverts, and water harvesting systems. In recent years, researchers have focused their attention on applying and developing empirical, conceptual, and physically based models for LID analysis. In their review, Li and Babcock [36] reported that there were >600 studies published worldwide involving green roofs, with a significant portion of them related to modeling.

Benefits of LIDs in terms of runoff reduction and pollutants removal have been widely discussed in the literature [14, 26, 29, 32]

For example, Kamali et al. [32] investigated the performance of a permeable pavement under sediment loadings during its life span by evaluating the temporal and spatial clogging trends of this facility and by finding its vulnerability to sediment loadings during rainfalls. Zhang and Guo [68] developed an analytical model to evaluate the long-term average hydrologic performance of green roofs. Local precipitation characteristics were described using probabilistic methods, and the hydrological behavior of the system was described using mass balance equations. Carbone

et al. [15] proposed a conceptual model to predict the hydraulic behaviour of a full-scale physical model of a vegetated roof, located at University of Calabria, Italy. The model idealized the vegetated roof as a system consisting of three individual components in series. A mass balance equation was applied to each block, taking into account the specific physical phenomena occurring in each module. The model was validated using dataset observed from the monitoring campaign carried out on the prototype of a full-scale vegetated roof. She and Pang [53] developed a physical model that combined an infiltration module (based on the Green–Ampt equation) and a saturation module (SWMM). The model calculates the water content in a green roof in a stepwise manner from the initiation of precipitation until saturation. In simulating the hydraulic response of green roofs to precipitation, an infiltration module is used before field capacity is reached and when no drainage is produced, while a saturation module is used after field capacity is reached and when drainage is produced. However, because runoff and infiltration can occur simultaneously during heavy precipitation, this stepwise approach may not be appropriate for a wide range of precipitation events.

Carbone et al. [12] developed a physically-based model using the explicit Finite Volume Method (FVM) for the infiltration process during rainfall events in green roof substrates. The model solves a modified version of the Richards equation which considers neglected the soil water diffusivity.

In another work, Huang et al. [29] proposed a numerical model for permeable pavements and also proved its applicability by applying it to simulate both hydraulics and water quality. The results of this study demonstrated a good agreement between field measurements and modeled results for three types of pavement in terms of hydraulics and water quality variables including peak flow, time to peak, outflow volume and TSS removal rates. The sustainable management of water resources requires the identification of procedures to optimize the use and the management of resources [17, 37]. As pointed out by several authors (e.g., [22, 65]), there is a strong demand for predictive models that can be applied across a range of locations and conditions to predict the general performance of a range of stormwater treatment measures. In addition, the heterogeneity of the materials that compose LIDs (concrete, gravel, soils, etc.) and their strongly unsaturated hydraulic behaviour, pose significant modelling challenges. In this way, several studies demonstrated that physically-based models can provide a rigorous description of various relevant processes such as variably-saturated water flow, evaporation and root water uptake, solute transport, heat transport, and carbon sequestration [10].

Although analytical and conceptual models represent a viable alternative to the numerical analysis of green roofs, their use suffers from several limitations. Conceptualization of the physical processes involved often leads to simplification of the system and a reduction in numerical parameters. While in a physical model each parameter has its own meaning, in conceptual models, lumped parameters often incorporate different components of the described process. These lumped parameters are case sensitive and need to be calibrated against experimental data, implying a lack of generality of the model itself. These drawbacks could represent a barrier

to the use of modeling tools among practitioners who need reliable and generally applicable models.

For these reasons, in this work some techniques/procedures on how to interpret the hydraulic behaviour of several LIDs (green roof, permeable pavement) part of the "Urban Hydraulic Park" of the University of Calabria, south Italy, have been presented. It will suggest experimental and mathematical procedures for model calibration, which consists of: (a) experimental design (system construction, and number and character of measured transient flow data); (b) methods for independently evaluating of material hydraulic properties; (c) additional analysis of material hydraulic parameters using the transient flow data; and (d) model validation.

2 Real Time Control Approach

In urban areas with Combined Sewer Systems, stormwater and wastewater are collected in the same conveyance pipes. During heavy rainfall events, due to eventual obstructions in the pipes or to a poor maintenance, the surface runoff may overburden existing storm-water management facilities and cause flooding or combined sewage overflow into receptive water bodies.

Since the current drainage systems will fail to control and manage a constantly increasing runoff volume, and given the potential risk to human life, economic assets and the environment, an efficient adaptation strategy able to improve the flood resilience for the future urban environment is needed.

In this context, the main objective of this section is to illustrate a Distributed Real Time Control (DRTC) approach, proposed in previous studies [16, 24, 25], as a solution to mitigate CSO and reduce flooding at catchment scale. To illustrate the advantages of the flood alleviation strategy focused on DRTC, the drainage network of the city of Cosenza (south Italy), was chosen as a testbed. The proposal consists in instrumenting the existing urban drainage network with sensors and a series of movable gates that, by monitoring water level and the filling degree in each conduit, self-adjust in real time to optimize the storage capacity of the pipelines and reduce the CSO. In the following subsections will be described the components of the DRTC system and the approach used, then will be provided details regarding the implementation in the network and some results.

2.1 Components and Implementation of the DRTC System

In order to achieve the proposed goals and be controlled in Real Time, an urban drainage network needs to be instrumented with a series of components, whose conceptual organization is basically structured in control loops which can be implemented by hardware components including sensors, actuators, controllers and telemetry systems (Fig. 1). Sensors, by monitoring the process evolution, collect

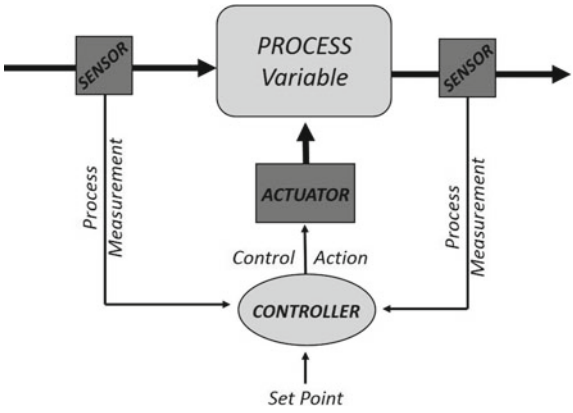

Fig. 1 Control Loop Scheme. Simple arrows indicate data flows, bold arrows the actions. Bold letters indicate hardware components and italic letters indicate transferred information

information about the current state of the system, actuators modify the monitored process and influence it, controllers adjust actuators with a certain objective and the telemetry system supports the data transmission among the different devices.

With regard to urban drainage networks, most of the time RTC implementations are based on water level measurements. The selection of the correct equipment, together with the choice of an adequate communication system and the proper software to be used, is thus crucial for a durable and reliable installation of RTC systems in UDSs. More in detail, to improve the performance of existing drainage networks and balancing water level throughout the conduits of the network, so as to reduce water level in the more overloaded conduits, the drainage network needs to be implemented with the following equipment:

(i) Water level sensors, which measure the water level in each conduit and the flow on the outfall;
(ii) Moveable gates, functioning as actuators, which can be real-time regulated electronically;
(iii) Computational nodes, which can host and execute the distributed control algorithm.

Sensors, which monitor water level and, hence, the degree of filling in each conduit, are positioned into pipes to evaluate flow depths and to monitor surcharge conditions during rain events. Since the mechanism cannot work properly if the increase of water level is not correctly perceived, it is important to correctly position the water level sensor, because if it is placed in the "underloaded" part the gate-agent would perceive a decreased water level instead of an increased one. In the proposed approach, this issues is addressed by deploying more than one sensor per conduit and taking the maximum sensed value as the water level value for the conduit.

Using the information acquired by the sensors, electronically Moveable Gates—-functioning as actuators—can self-regulate to intelligently manage the storage capacity of the pipelines. The moveable gates are made up of mobile plates rotating around a horizontal hinge placed on the bottom of the conduit, as shown in Fig. 2. The gates

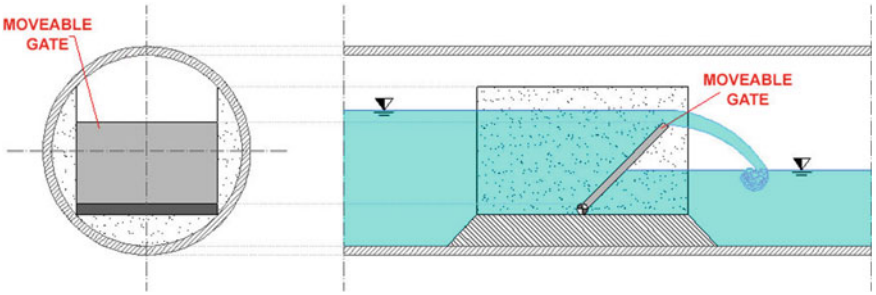

Fig. 2 The down-hinged movable gate

are dynamically regulated in order to utilize the full storage capacity of the pipeline by accumulating the excess stormwater volume in the less overloaded conduits thus preventing CSO.

The gate is completely closed when the plate rotates in a perpendicular position with respect to the flow direction. Conversely, the gate is fully open when the plate is parallel to the flow. When the gate is closed, the opening area is null and no flow rate is delivered from the node. An intermediate position of the gate corresponds to a partial opening degree. The gates, as actuators, are the regulators elements of the RTC system that are used to adjust flows and water levels in the controlled system.

The manipulation of actuators in RTC systems is performed by control units (controller). A certain number of computing nodes are spread throughout the drainage network in order to cover all the points of interest. In particular, these devices read data received from local sensors through wireless connection, and collectively elaborate the acquired information in order to provide—according to the objectives—output adjustments to actuators and thus supply the gates with an "intelligent" behaviour (Fig. 3).

The gates are located at the points of the network where subnetworks are connected to the main channel. Figure 4a shows the logical places for inserting the gates, while Fig. 4b shows the gates insertion in a case of a realistic network.

Each computational node has a partial view of the network as it can read only from sensors which are located in its spatial neighbourhood and can actuate only gates it can physically reach. Thus, these devices dynamically regulate the gates according to the information acquired by the sensors in the neighbour areas. On the basis of the previous considerations the idea proposed lies in using a distributed agent-based architecture [66]. The agent paradigm has several important characteristics:

- Autonomy: Each agent is self-aware and has a self-behaviour. It perceives the environment, interacts with others and plans its execution autonomously;
- Local views: No agent has a full global view of the whole environment but it behaves solely on the basis of local information;
- Decentralization: There is no "master" agent controlling the others, but the system is made up of interacting "peer" agents.

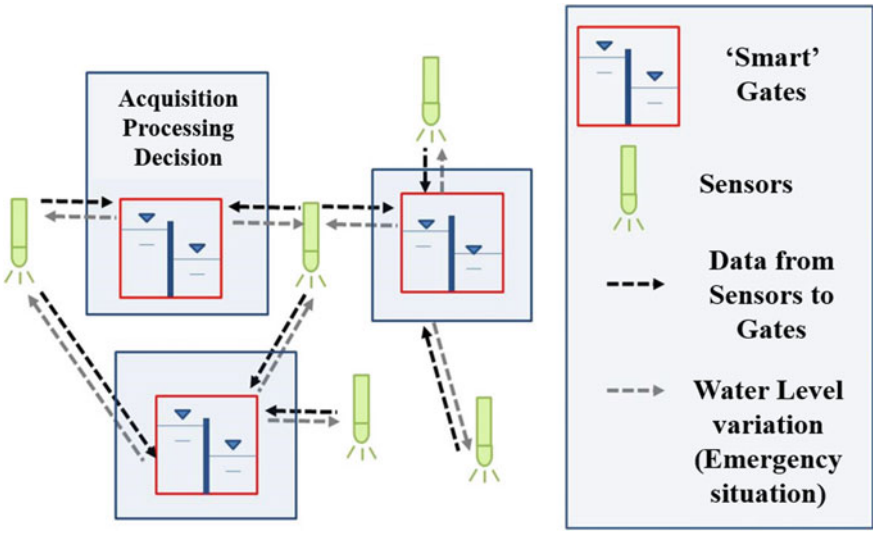

Fig. 3 Schematisation of the DRTC system

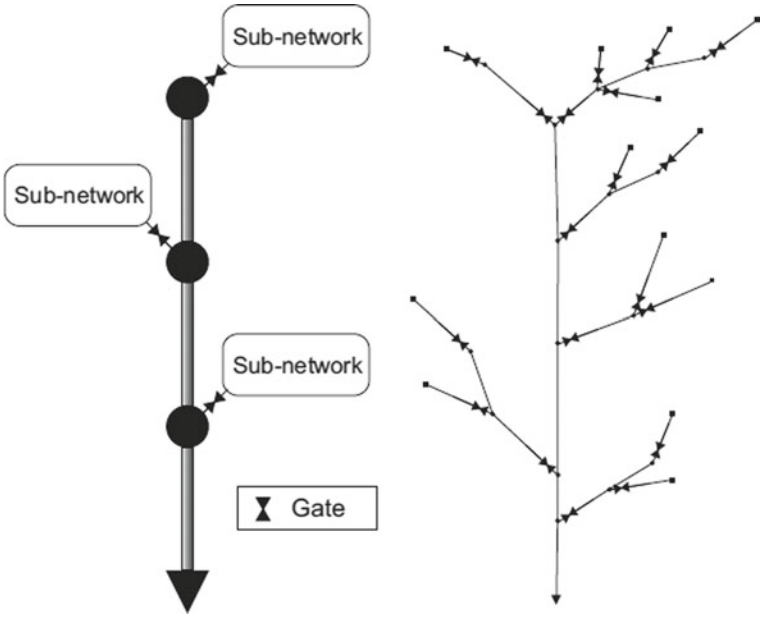

Fig. 4 Gate position

From the point of view of software architecture, the approach requires one agent per gate. Each gate-agent runs on one of the computational nodes covering the specific gate, it can perceive the local water level and communicate with the neighbouring

gate-agents in order to elaborate a proper actuation strategy for its gate. In addition to the gate-agents, another agent, called outfall agent, is logically associated with the outlet node, it behaves the same as other agents except for the actuation part, indeed, it is not associated with any gate. For each generated network, an optimization algorithm, executed on computing nodes in a distributed fashion, leads to balance—in real-time—the water level perceived by the agents and aims to distribute equally the degree of filling of the conduits, thus preventing overcharge phenomena as far as possible. The proposed goal has been achieved by means of agents continuously executing two tasks:

1. Figuring out collectively the average of the water level in the generated network;
2. Each agent triggers its specific gate in order to bring the water level closer to that average.

Task 1 is accomplished by exploiting a Gossip-based aggregation [30] for dealing with the global aspect of the drainage network, while Task 2 is accomplished exploiting locally a PID controller [4]. Once an agent knows the global water level through the "gossip-based aggregation", there remains the problem of appropriately tuning its gate so as to reach that "desired" level. This issue is addressed using the PID logic which, sending Proportional Integral and Derivative control action signals to actuators, can be used when you do not know an exact mathematical model of the system you want to control. A PID controller is a control loop feedback mechanism where an error value is computed as the difference between a measured output of a process and the desired value (setpoint). In the case studies proposed by Giordano et al. [24] and Garofalo et al. [25], each gate of the drainage network is controlled by a PID implemented by the gate-agent.

Once established the optimization computational operations to be carried out, the drainage network of Cosenza was simulated using a customized version of SWMM software, built for permitting it to Real-Time communicate with a separate Java controller which implements the algorithm described before. Further hardware and software details of this approach, which allows a dynamic management of the drainage network, are given elsewhere [24, 25].

2.2 Case Study: The Drainage Network of Cosenza

The test site chosen for the proposed approach and the hydrological modelling of the conversion scenarios was the Liguori catchment, a highly urbanized catchment in Cosenza. The catchment has a population of 50.000 inhabitants and a total surface area of 414 ha, of which almost one-half (48%) is densely urbanized and highly impervious, while the other 52% (202 ha) is pervious, occupied by natural areas (Fig. 5a).

The catchment is drained by a combined sewer system that collects sanitary sewage and stormwater runoff in a single pipe system, conveying the entire water flow directly to the wastewater treatment plant (WWTP). During the most intense

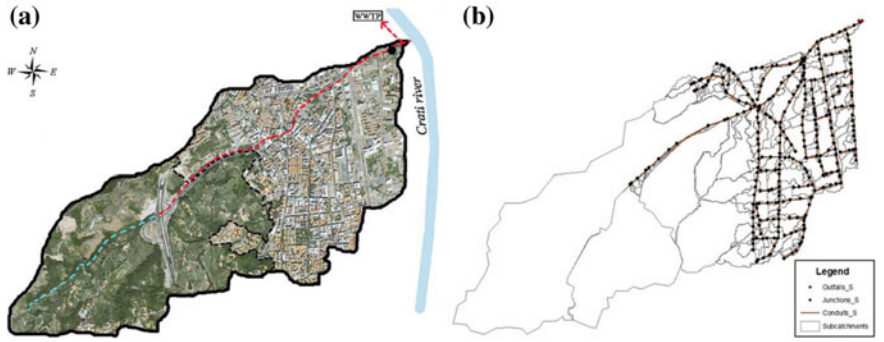

Fig. 5 **a** The Liguori catchment of Cosenza; **b** SWMM model of the drainage network of Cosenza

rainfall events, wet-weather flows occasionally exceed the capacity of the sewer system and the excess flows escape from the sewer system, via an overflow structure, as a combined sewer overflow (CSOs) [43]. Such overflows are directly discharged, without receiving any treatment, into the receiving water body, the Crati River.

In order to simulate the response of the LC drainage network to storm events, the sewer dataset and the physiographic characteristics of the sub-catchments, were imported into EPA-SWMM software [50] for the next hydraulic modelling of the drainage system. The software SWMM, provided by EPA, is an open-source computer model that allows a dynamic rainfall-runoff simulation for predicting hydrological and hydraulic behaviour of urban drainage systems and watersheds.

More in detail, in SWMM, the Liguori Catchment area was simplified in 296 subcatchments, of which 258 are mostly urbanized (%Imp > 0.7) and 23 average urbanized (0.3 < %Imp < 0.7). The urban drainage network modelled in SWMM (Fig. 5b), instead, consists of 324 conduits with different shapes and sizes and a slope varying from 0.5 to 6%. Some pipes are circular and egg-shaped with diameters varying from 0.3 to 1.5 m and others are polycentric pipes. Finally, there are in total 326 nodes (with Outfall and Junctions functions) which represent the catch basins. The model used in this study was previously calibrated on the basis of several measurement campaigns [42]. Calibration parameters taken into consideration in flow modelling were surface roughness of the conduit (n), the impervious (N-Imperv) and pervious (N-Perv) surfaces in the catchment, and the depths of surface depressions on impervious (Dstore-Imperv) and pervious (Dstore-Perv) areas.

As previously said, for the purposes of the proposed studies, the drainage network was simulated using a customized version of SWMM built for the purpose for permitting it to communicate in real time with a separate Java controller which implements the algorithm described before. More in detail, in this version, the moveable gates are modelled as a transverse weir with the opening area equal to the conduit section area.

2.3 Experiences and Results

In the following section, the finding obtained from the DRTC application to the case study, will be described and discussed.

At first Giordano et al. [24] used and applied a totally decentralized RTC approach to a drainage network. In this study the experiments were carried out using a simplified network, which consists in a main channel of 1 m diameter and a total of 35 pipes inside the sub-networks, instrumented with a series of moveable gates and sensors which monitor water level and, hence, the degree of filling in each conduit, during severe rainy events. The water level in the pipes is balance by a combination of a Gossip-based algorithm, which ensures a global correct behaviour, and a PID controller used for each gate, so as to maintain locally its related water level as close as possible to the "suggested" value computed by the algorithm. The results have demonstrated that when the RTC is applied, the filling degree of conduits are much closer to each other as the load on the entire network is more balanced. This means that the network does properly exploit the residual water capacity of the undercharged conduits and the latter implies an improvement in the behavior of the critical conduit that reaches the overcharge condition later. The proposal provides positive effects on the overall hydraulic performance of the network as it is able to prevent (or delay) flooding events that would occur in the original (not instrumented) network. Following works, instead, focused on extending the algorithm and validating the DRTC approach in real drainage networks.

In the study carried out by Carbone et al. [16], the DRTC investigations have been extended to the real drainage network of Cosenza. To evaluate the effect of the moveable gates on reducing the storage capacity of the conduits, a part of the drainage network of Cosenza was investigated by comparing two scenarios of the CSS in SWMM: the existing configuration (Scenario 0) and a new one (Scenario 1) where six sluice gates were placed in the secondary conduits of the system. To investigate the response of the new configuration of the drainage system, three extreme events (dated March 1st, June 16th, October 8th) occurred in 2011 and which put in crisis the system, were analysed.

Specially, in Scenario 0 were identified 2 most overloaded pipes in the main conduit and used in this study to demonstrate the beneficial influence of gates in alleviating the most critical sections of the system. Two example results obtained for the Conduit 2 are reported in Fig. 6.

Figures show the distribution of storage capacity for two of the analysed events and for both considered scenarios; as it can be noticed the storage capacity in Scenario 0 varies up to 100%; this mean that in some time points the selected conduits get completely full. Instead the filling degree is lower when sluice gates are used to control stormwater volumes. In Table 1 is reported the average storage capacity reduction for each event; the reduction varies from 22 to 77% showing lower value for the event with higher rainfall volume. However, as the authors have pointed out, the beneficial effect may be dependent upon the storm characteristics (such as hydrographs, intensity and duration).

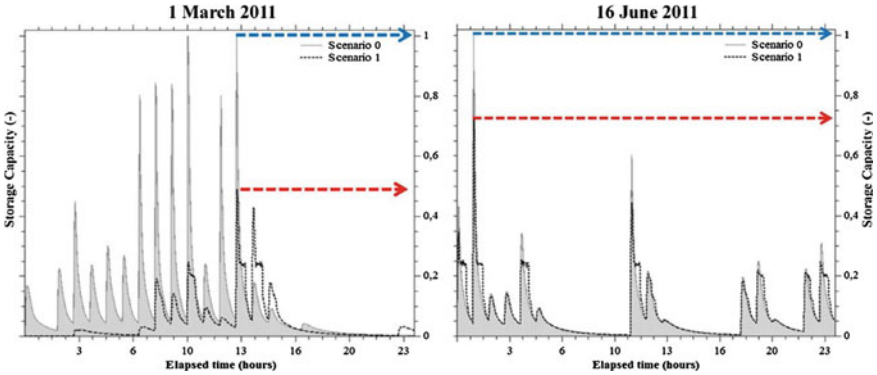

Fig. 6 Temporal distribution of storage capacity for Conduits 2

Table 1 Selected rainfall events

Rainfall event	Rainfall volume (mm)	Average storage capacity reduction (%)
1 March 2011	97.40	22
16 June 2011	20.10	60
8 October 2011	48.60	77

The findings show that a series of devices inside the urban drainage systems are actually able to control the flow rate to drop the storage capacity to a reasonable value.

In Garofalo et al. [25], later, different scenarios have been analysed to evaluate the performance of the DRTC as a function of the number of the moveable gates placed in the system. As for the previous studies, the scenario without DRTC, which corresponds to the actual UDS, is called Scenario 0. The other scenarios, controlled by the DRTC, and differ according to the number of secondary pipes equipped with moveable gates: 91 for Scenario 1 (S1), 107 for Scenario 2 (S2), 214 for Scenario 3 (S3) and 322 for Scenario 4 (S4). The response of the UDS for all these scenarios is modelled for 15 independent rainfall events recorded in the weather station in Cosenza during the years 2010–2015.

In this work, for each selected rainfall event, were evaluated both CSO reduction (computed as the relative percentage difference between the CSO volume in the scenarios with DRTC and the Scenario 0), and the local flooding reduction (as the relative percent difference between the total flooding volumes from the conversion scenarios and the reference one). Referring to the Scenarios 1 and 4, was observed a CSO reduction which varies respectively between 2.7 and 83% (S1), and from 13 to 99% (S4), according to the rainfall events. The consistently higher CSO drop in the S4, demonstrates the beneficial effect provided by using a larger number of moveable gates. At the local level, thanks to the DRTC, the temporary stormwater detention provided in the less overloaded conduits, utterly prevents the UDS from

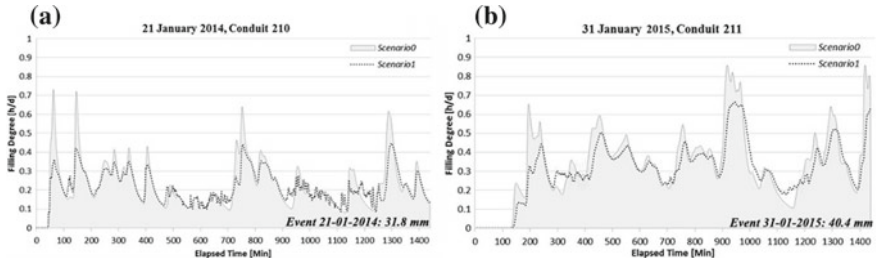

Fig. 7 Temporal distribution of Filling Degree (h/d) of two conduits during two rainfall events

local flooding in S1, where a drop of 100% is obtained for all the events. Otherwise, the S4 the risk of flooding is solely mitigated, with reductions varying from 2.4 to 13.4% for all the events, except for one event (dated 23 Nov. 2013), where a drop of 100% is obtained. As highlighted by the authors, the reasons why S4 offers a limited flooding reduction are strongly related to the high number of gates adopted. The high number of gates involved, able to exploit all the possible storage capacity of the network, makes the Scenario 4 the best choice in order to prevent the CSO, but it performs quite badly in terms of flooding reduction with respect to the other controlling scenarios. The reason for this behaviour lies in the fact that when the whole storage capacity is exploited, no additional water can be stored temporarily, and so a growth in incoming water flows produces unavoidable flooding phenomena. Therefore, these findings suggest that S2 and S3 are the most convenient solutions, since they offer the highest overall performance in terms of reduction of local flooding and perform well also with respect to the CSO reduction. Summing up, this study clearly demonstrated that the DRTC produced beneficial effects on the management of the UDS by substantially mitigating the risk of flooding and CSO.

More recently, Principato et al. [46], evaluated the potential of an integrated and sustainable approach for a better management of the drainage network. The main objective of this study was to assess the mitigation of CSO's impact when dynamic (RTC) and static (LID) measures are simultaneously adopted to cope with greater stormwater volumes. With this purpose different conversion scenarios have been applied on a portion of the Liguori Catchment (LC) of Cosenza: Scenario1, emulates the behavior of the drainage network regulated by moveable gates controlled in Real Time, while Scenario2 investigate the hydrologic response of the network considering Green Roofs (GRs) implementation, in replace of impervious rooftops, in a portion of the LC. A last scenario (Scenario3) has also been developed to analyze the combined effect of RTC and GRs implementation, in the same portion of LC considered for the Scenario2. As a confirm of the studies already analyzed, also these model results revealed that the RTC of urban drainage system, equipped with a series of gates, provides beneficial effects to the overall hydraulic performance of the network. Results reported in Fig. 7, show that the filling degree of two selected conduits is lower when smart gates are used to control stormwater volumes: the peak reduction is around 29% for conduit 210 and 19% for conduit 211.

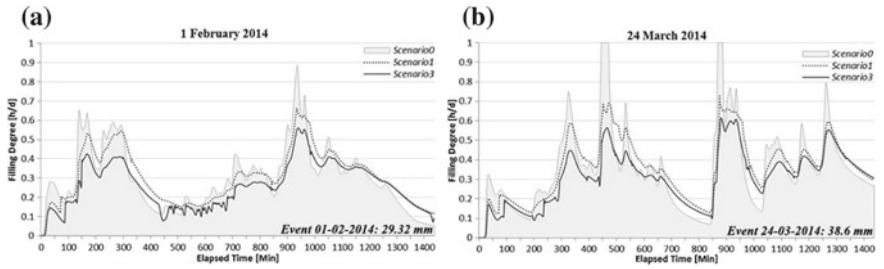

Fig. 8 Temporal distribution of Filling Degree (h/d) of the last conduit of the network during two rainfall events

A novelty, compared to the studies already analyzed, are the results obtained from Scenario3, which prove the importance of an integrated approach on the overall hydraulic performance of the network, as a valid solution for controlling flooding in urban areas. In particular Fig. 8, which refers to the last conduit of the network, reveals that the coupling of distributed (RTC) and source control (LID) solutions, leads a further reduction of the filling degree also compared to Scenario1, for the most part of the event chosen.

In conclusion, the use of smart moveable gates provides beneficial effects to the overall hydraulic performance of the network during critical rainfall-runoff events, offering an alternative and valid solution for controlling flooding in urban areas. The advantage of this system is to utilize the full storage capacity of the pipeline by accumulating the excess volumes of rainwater that otherwise would be spilled out in the pipes with a low water level. The advantage is also from the economic point of view because it takes advantage of the existing sewer system.

3 LID Approach

Despite the hydrological benefits of LIDs are already studied in literature, these techniques are not yet widespread probably because modelling tools often used simplified methodologies, based on empirical and conceptual equations, which do not take into account hydrological processes in a physical way. In addition, the hydraulic properties of LIDs materials have not been investigated in a comprehensive manner, limiting the investigation only to specific properties [59]. In this way, Brunetti et al. [8, 9] proposed an innovative approach to investigate the hydraulic behaviour of several LIDs using a mechanistic model coupled with specific numerical analysis to explore the hydraulic properties of LIDs techniques. The LID systems considered in this chapter are all implemented in the "Urban Hydraulic Park," which includes a permeable pavement, a stormwater filter, and a sedimentation tank connected to a treatment unit.

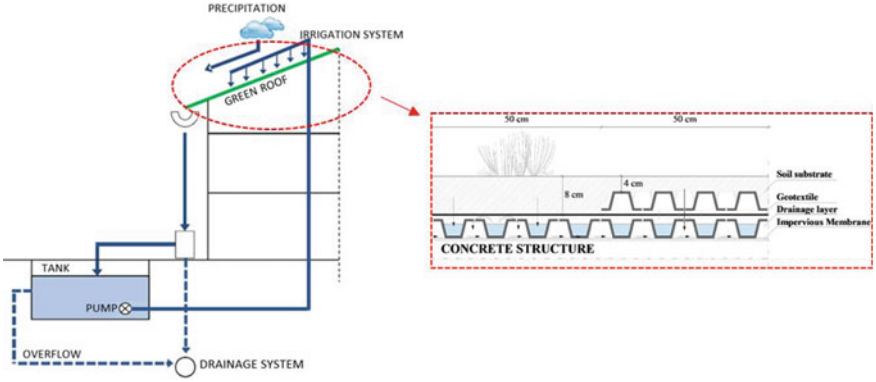

Fig. 9 Schematic representation of the RWH system to collect the rainwater from green roof (left) and the inset of a cross-section of the GR (right)

3.1 Green Roof Experience

To analyse the green roof and LIDs hydraulic behaviour, as discussed in the Introduction sectin, different models from the conceptual and analytical to the mechanistic ones have been developed and widely used, but very few studies have focused on a comprehensive analysis of the hydrological behavior of a green roof. Starting from this assumption Brunetti et al. [8] carried out an accurate and comprehensive analysis of Variably Saturated Hydraulic behavior of the experimental green roof installed at University of Calabria by using HYDRUS 3D. The experimental green roof (GR), considered in the study, was built on a fifth-floor terrace of the Department of Mechanical, Energy and Management Engineering (DIMEG) at the University of Calabria (Italy), in Mediterranean climate region. The area of an existing roof was parcelled into four sectors: two sectors are vegetated with the same native Mediterranean species (Carpobrotus edulis, Dianthus gratianopolitanus, and Cerastium tomentosum), but present different drainage layers; a third sector is mostly characterized by spontaneous vegetation; while the last sector is the original roof, considered as the reference compartment for experimental data analysis.

The water supply of GR is guaranteed by reusing the green roof's outflow, collected in a specific storage tank and distributes through a drip irrigation system during drought periods. The Rainwater Harvesting (RWH) system (Fig. 9, left), designed ad hoc for the site specific, consists of: (1) a system for collecting rainwater from the experimental site; (2) a storage tank of 1.5 m^3 with a pump to relaunch the irrigation system; (3) a connection system with the water supply to ensure the full satisfaction of irrigated demand in any condition. When the storage capacity of the tank is reached, the overflow is directly discharged into the sewer system. The drip irrigation system is currently actioned by an electric valve at predetermined time, and the irrigation rate is recorded by a water counter with a frequency of 1 min.

3.1.1 Modeling Theory

To investigate the hydraulic behaviour of the GR and finally to evaluate a possible optimization strategy of the specific green roof, it is necessary to proceed first of all with a detailed description of its stratigraphy (Fig. 9 on the right). Thus, the GR considered in the study, characterized by an area of 50 m^2, an average slope of 1% and vegetated, as described before, with native species, consists from top to bottom of: a soil substrate, with a maximum depth of 8 cm, composed of a mineral soil consisting of a hetero-disperse Particle Size Distribution (74% gravel, 22% sand, and 4% silt and clay); a permeable geotextile; a drainage layer in polystyrene foam with a storage capacity of 11 L/m^2 and a drainage capacity of 0.46 Ls^{-1} m^{-2}; an anti-root layer and a waterproof membrane.

A weather station located directly at the site collect precipitation, velocity and direction of wind, air humidity, air temperature, atmospheric pressure, and global solar radiation [11]. Rainfall data are measured every minute by using a tipping bucket rain gauge with a resolution of 0.254 mm. While the outflow from each sector is recorded at the base of the building by a flowmeter device composed of a PVC pipe with a sharp-crested weir and a pressure transducer (Ge Druck PTX1830) to estimate the water level inside the pipe.

In the work of Brunetti et al. [8] two-months rainfall data from 2015-09-01 and 2014-10-30 were used and the Penman-Monteith equation [2] was implemented to estimate the hourly reference evapotranspiration. To model the water flow in unsaturated soils by the Richards equation, and, thus, estimate the water retention function $\theta(h)$ and hydraulic conductivity function $K(h)$, the evaluation of unsaturated hydraulic properties of GR substrate was carried out by implementing a simplified evaporation method with the extended measurement range (down to –9,000 cm) [60]. While to simultaneously fit $\theta(h)$ and $K(h)$ to the experimental data obtained by the evaporation method, HYPROP-FIT [41] numerical optimization procedure was used. For the description of soil hydraulic properties, first of all the unimodal van Genuchten–Mualem (VGM) model [62] was implemented; next, since the unimodal VGM model couldn't always describe the full complexity of measured data, the bimodal model of Durner [20] was taken into account. Results of the experiments are reported in Table 2.

To describe the complex physical features of the experimental green roof, HYDRUS-3D software [54], which solves the Richards equation for multi-dimensional unsaturated flow, was used implementing the parameters obtained with the evaporation method. Finally, to evaluate the agreement between measured and modeled hydrographs the Nash-Sutcliffe Efficiency (NSE) index [40] was evaluate.

The results concerning the estimated soil hydraulic parameters with their confidence intervals, reported in this study revealed that the bimodal function presents a more accurate description of the retention curve. While the findings obtained during the validation process showed that: the unimodal and bimodal models are both able to accurately describe the GR hydraulic behavior; a higher precision is achieved by the bimodal model; both model slightly overestimate the outflow.

Table 2 Estimated soil hydraulic parameters and their confidence intervals (CIs) for the unimodal and bimodal hydraulic functions

Parameter	Unimodal	CIs	Bimodal	CIs
Residual water content, θ_r (–)	0	0.05	0.070	0.007
Saturated water content, θ_s (–)	0.551	0.01	0.562	0.003
Air-entry pressure head index for the first pore system, α_1 (1/cm)	0.13	0.03	0.843	0.07
Pore-size distribution index for the first pore system, n_1 (–)	1.25	0.06	1.24	0.04
Saturated hydraulic conductivity, K_S (cm/day)	4700	3500	12,600	3700
Air-entry pressure index for the secondary pore system α_2 (1/cm)	–	–	0.01	0.001
Pore-size distribution index for the secondary pore system n_2 (–)	–	–	1.97	0.08
Weight coefficient w_2 (–)	–	–	0.422	0.01
Tortuosity and pore connectivity parameter, L (–)	0.53	0.02	0.5	–

In addition, starting from the assumption that critical rainfall events occur in a very short time [8, 13] have investigated the hydrological response of the GR to single precipitation events. The results obtained for four rainfall events with different total precipitation volume (V_{prec}) in terms of peak flow reduction P_{red} (%) and volume reduction V_{red} (%), for both modeled and measured outflow, are shown in Table 3 and Fig. 10. By the analysis of this results the authors concluded that the green roof hydraulic performance was affected primarily by the antecedent substrate moisture and secondly by the precipitation pattern.

Table 3 Analysis of the hydrological performance of the green roof during single precipitation events

Rainfall events	V_{prec} (mm)	Modeled outflow		Measured outflow	
		P_{red} (%)	V_{red} (%)	P_{red} (%)	V_{red} (%)
9 September 2015	100	5	12	7	16
7 October 2015	42	40	27	60	31
10 October 2015	69	5	5	45	9
21 October 2015	120	5	17	7	17

3.1.2 Future Perspective: GR and RHW from a Smart and Innovative Point of View

The integration of GR and RWH system, like in the case of the experimental site of University of Calabria, allows considerable benefits in terms of rational management of water resource. Furthermore, different studies have considered the RWH systems as a good strategy to limit environmental impacts that the on-going urbanization produce on the drainage network and receiving water bodies [48].

However, so far, these techniques (GR and RWH) have been studied from a purely hydrological-hydraulic point of view, there are no studies that consider these ones as smart objects for an integrated management of the water resource and urban drainage system.

In light of this, an innovation in the field of Urban drainage is look at the single techniques GR and RWH as smart objects, optimizing them with ICT technologies, based on the IoT (Internet of Things) paradigm.

A new aspect, in fact, could lie in the integration of GRs and RWH techniques through a complex network equipped with: sensors, which allow rapid quantitative assessments from a hydraulic, energy and environmental point of view; regulators or actuators, able to modify the processes in progress; transducers that allow the conversion of the data detected in command; control units that report the variables to the pre-established threshold values.

According on what was previously discussed about Green Roof experimental site of University of Calabria, the rainwater collected in the storage tank is re-introduced through the irrigation system at fixed time and in quantity set by the operator of the experimental site. The optimization of this system could be achieved by considering the smart automation through the estimation of water content and the evaluation on the wheatear situation. More in detail, when the water content, monitored by specific sensors dislocated within the layers of the green roof, falls below a threshold value that causes the plant water stress, the smart system sends a command to activate the irrigation withdrawing the water from the storage tank in the needed rates to re-reach

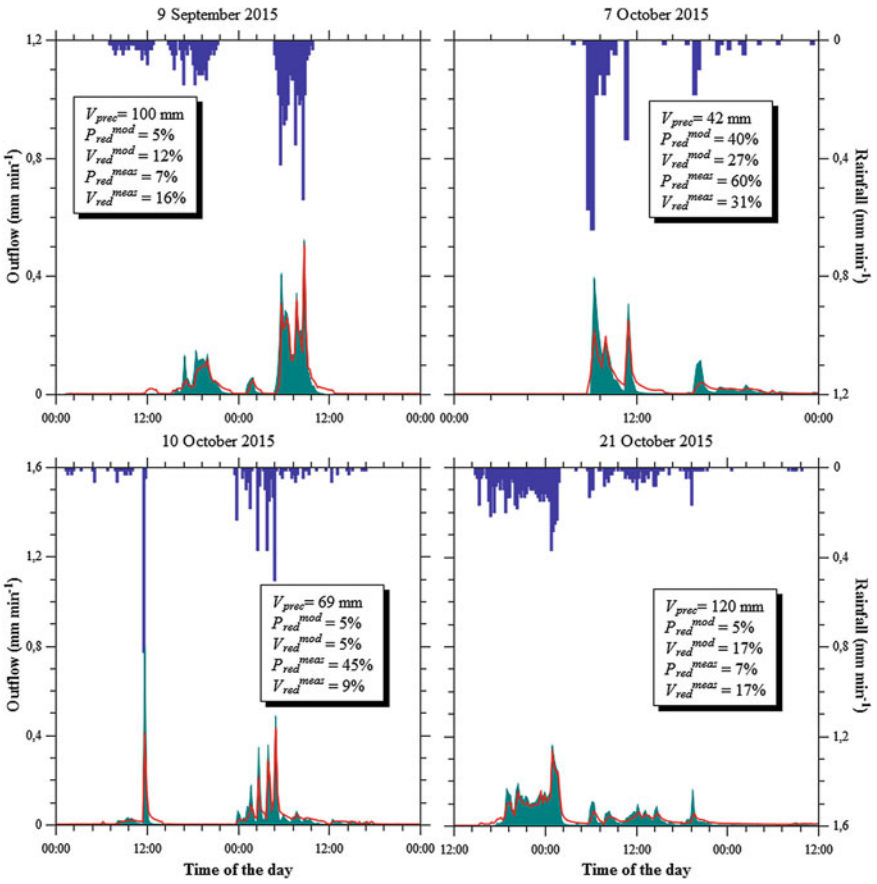

Fig. 10 Rainfall (blue area) and modeled (cyan area) and measured (red line) outflow for four selected rainfall events in the analysis of the hydrological performance of the green roof during single precipitation events; Pred meas and Pred mod are the measured and modeled peak flow reductions, respectively, and Vred meas and Vred mod are the measured and modeled volume reductions, respectively

the appropriate water content. The Weather Station located at the experimental site offers also the opportunity to make preventive estimates, based on the rainfall regime and solar radiation recorded on the site, so as to better calibrate the operation of the irrigation system.

Through these innovative strategies, in fact, not only a hydraulic benefit would be obtained, optimizing the reuse of the rainwater and reducing the flow to the drainage system, but also a thermo-energetic one. The activation of the irrigation system could also be carried out following the temperature measurements in the rooms below in order to improve the summer thermal comfort of the building.

Furthermore, if we consider the possibility of reusing water for other domestic uses (WC flushing, machine washing, ect.), it is possible to achieve total system hydraulic efficiency with minimum runoff discharge in the sewer system. In this case, the collected rainwater could be reused totally, avoiding that, in autumn and winter season, when irrigation demand is lower and precipitations increase, the storage tank exceeds the maximum value and the overflow is directly sent in the drainage network.

This innovation could be extended to the integration of others LID techniques (green wall, permeable pavement, etc.) with RWH systems in order to maximize the hydraulic, environmental and energy efficiency of these solutions. Furthermore, it would be appropriate to develop of an optimization algorithm that not only includes local actions for the building-scale system, but also evaluates the efficiency on the district and basin scale to favour smart and eco-sustainable neighbourhoods. The smart system, so thought, could be classified in function of its Hydraulic Efficiency Class, i.e. the rainwater rate spilled in the urban sewer system.

3.2 Permeable Pavement Experience

Lack of studies in literature focused on the description of the hydraulic behavior of a permeable pavement in a comprehensive manner suggested that research is particularly needed in the development and identification of accurate modeling tools for the analysis of LID practices, especially for permeable pavements.

In their work, Brunetti et al. [9] explored the suitability of the HYDRUS mechanistic model to correctly describe unsaturated flow in typical permeable pavement, installed at the experimental site of the University of Calabria. Multiple uniform and nonequilibrium flow models included in HYDRUS-1D, such as single and dual-porosity models, are used to define the hydraulic behavior of the permeable pavement. The problem was addressed by combing a Global Sensitivity Analysis (GSA), used to prioritize the hydraulic parameters and identify those that are non-influential, with a Monte Carlo filtering approach, used to investigate the parameter space and identify behavioral regions. Results from these analysis are then used in the calibration process conducted with the Particle Swarm Optimization (PSO) algorithm. Finally, the calibrated model was validated on an independent set of measurements.

The studied permeable pavement has an area of 154 m^2, an average slope of 2%, and a total depth of the profile of 0.98 m. Figure 11 shows a schematic of the permeable pavement, consisting of 5 layers.

The surface wear layer consists of porous concrete blocks characterized by high permeability (8 cm depth). Base (35 cm depth), sub-base (45 cm depth) and bedding layers (5 cm depth) were constructed by following the suggestions of the Interlocking Concrete Pavement Institute (ICPI), which recommends certain ASTM stone gradations.

A weather station located directly at the site measures precipitation, wind velocity and direction, air humidity, air temperature, atmospheric pressure, and global solar radiation. Rain data are measured by a tipping bucket rain gauge with a resolution

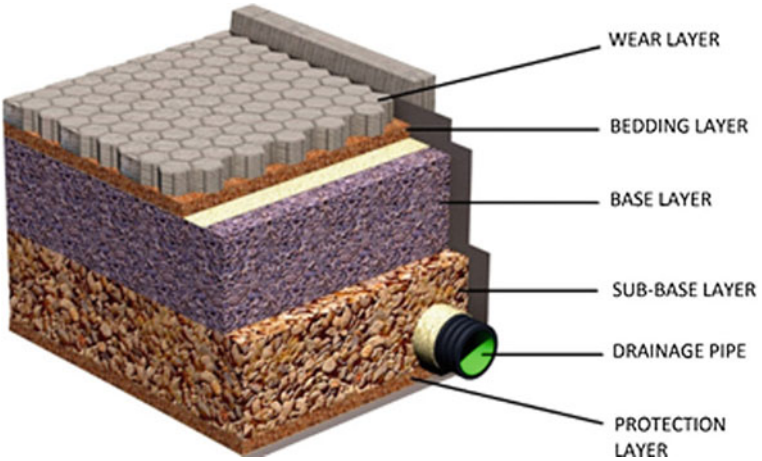

Fig. 11 A Schematic of permeable pavement

of 0.254 mm and an acquisition frequency of one minute. Climatic data are acquired with a frequency of 5 min. Data are processed and stored in the SQL database.

Outflow from the pavement is measured by two flux meters, composed of a PVC pipe with a sharp-crested weir and a pressure transducer. The pressure transducers were calibrated in the laboratory by using a hydrostatic water column, linking the electric current intensity with the water level inside the column. The exponential head-discharge equations for the two PVC flux meters were obtained by fitting the experimental data with a coefficient of determination $R2 = 0.999$ for both devices. No measurements of pressure heads or volumetric water contents inside the pavement were taken.

Two month-long data sets were selected for further analysis. The first data set, which started on 2014-01-15 and ended on 2014-02-15, was used for parameter optimization and sensitivity analysis. Total precipitation and total potential evapotranspiration for the first data set were 274 and 43 mm, respectively. The second data set, which started on 2014-03-01 and ended on 2014-03-31, was used for model validation. Total precipitation and total potential evapotranspiration for the second data set were 175 mm and 81 mm, respectively. The second data set was selected so that it had significantly different meteorological data than during the first period. The optimization set is characterized by multiple rain events with few dry periods. The validation set has fewer rain events, which are concentrated at the beginning and end of the time period and separated by a relatively long dry period between. Surface runoff was not observed during these time periods.

Potential evaporation was calculated using the Penman-Monteith equation [2]. The permeable pavement was installed in 2013 and has been constantly exposed to atmospheric conditions and traffic since then that has altered the surface roughness and color. For these reasons, an albedo of 0.25 was used as suggested by Levinson and Akbari [35] for weathered gray cement.

3.2.1 Modeling Theory

Water flow simulations were conducted using the HYDRUS-1D software [57]. HYDRUS-1D is a one-dimensional finite element model for simulating the movement of water, heat, and multiple solutes in variably-saturated porous media. HYDRUS-1D implements multiple uniform (single-porosity) and nonequilibrium (dual-porosity and dual-permeability) water flow models [56].

Two different conceptual models have been used to study the unsaturated water flow in the pavement structure. Scenario I assumed that water flow in all five soil layers of the permeable pavement can be described using the classical single-porosity approach (SPM) described using the one-dimensional Richards equation:

$$\frac{\partial \theta}{\partial z} = \frac{\partial}{\partial z}\left[K(h)\left(\frac{\partial h}{\partial z} + 1\right)\right] \tag{1}$$

where θ is the volumetric water content [–], h is the soil water pressure head [L], K(h) is the unsaturated hydraulic conductivity [LT^{-1}], t is time [T], and z is the soil depth [L]. The soil hydraulic properties are described by the van Genuchten–Mualem relation [62].

Scenario II assumes a single-porosity model for the wear layer, the bedding layer, and the protection layer, and a dual-porosity model for the base and sub-base layers. This configuration was selected in order to consider the occurrence of preferential flow in the coarse layers of the pavement that are composed of crushed stones, with particle size diameters ranging from 2.5 to 37 mm in the base layer and from 20 to 75 mm in the sub-base layer. Crushed stones were washed before installation in order to remove fine particles. From a physical point of view, the structure of the base and sub-base materials closely resembles fractured aquifers [6].

In this way, the classical approach to model water flow in fractured porous media is the so-called "dual-porosity" or "mobile-immobile water" (MIM) approach [6, 63, 64]. This approach assumes that flow occurs only in the mobile fracture domain, while water in the matrix domain is immobile with a coefficient Γ_w that represents the mass transfer between two domains, which is assumed to be proportional to the difference in effective saturations of the two regions [55, 56].

$$\Gamma_w = \omega \cdot (S_\theta^m - S_\theta^{im}) \tag{2}$$

In this, Scenario II thus includes 20 parameters (additionally also ω and θs of the immobile domain for the base and subbase layers).

3.2.2 Global Sensitivity Analysis

A sensitivity analysis (SA) can identify the most influential parameters and their interactions and how these parameters affect the output [51].

Most SAs performed in the literature of environmental sciences are the so-called 'one-at-a-time' (OAT) sensitivity analyses, performed by changing the value of parameters one-at-a-time while keeping the others constant [18, 28, 49].

One of the most widespread algorithms for the GSA is the variance-based Sobol' method [58]. Variance-based methods aim to quantify the amount of variance that each parameter contributes to the unconditional variance of the model output. For the Sobol' method, these amounts are represented by Sobol's sensitivity indices (SI's). These indices give quantitative information about the variance associated with a single parameter or related to interactions of multiple parameters. For a more complete explanation about the Sobol' method, please refer to Sobol' [58].

In order to assess the accuracy of estimations of the sensitivity indices, the bootstrap confidence intervals (BCIs) [21] were estimated. The rationale of the bootstrap method is to replace the unknown distribution with its empirical distribution and to compute the sensitivity indices using a Monte Carlo simulation approach where samples are generated by resampling the original sample used for the sensitivity analysis. In our case, the q samples used for the model evaluation were sampled 1000 times with replacement, whereby Sobol's indices were calculated for each resampling. In this way, 95% confidence intervals are constructed by using the percentile method and the moment method [3].

The sensitivity analysis was conducted using the programming language Python and in particular, the Sensitivity Analysis Library (SALib) [61]. An elaborated script overwrites the input file containing the parameters for different materials at each iteration. The script then executes HYDRUS-1D, which usually runs less than one second.

As stated before, the GSA was also coupled with a basic Monte Carlo filtering in order to identify behavioral regions in the parameter space and to reduce the uncertainty in the following parameter estimation step by using the same sample and runs of the GSA. Potential solutions are divided into two groups depending on the value of the objective function calculated: behavioral, solutions with $NSE > 0.0$, and non-behavioral, solutions with $NSE \leq 0.0$. Particle Swarm Optimization Inverse modeling is a procedure to estimate unknown parameters of the model from experimental data. In this work a global search method based on Particle Swarm Optimization (PSO) [33] have been used. PSO has been used in multiple studies involving inverse modeling with complex environmental models [27, 31, 67]. In PSO, collections of "particles" explore the search space, looking for a global or near-global optimum.

For the optimization process, a modified version of the PySwarm Python Library has been used.

3.2.3 Experimental Results

Results from SA indicated that only two parameters exhibit a significant direct influence on the output's variance, the pore-size distribution index n1 and the air-entry pressure parameter a1. The third most influential parameter, the saturated hydraulic conductivity Ks1, has the effect, which is only half of the second most influential

parameter, a1. Ten parameters have a first-order index lower than 1%, which indicates that their main effect on the output variance is negligible.

In addition, SA showed that almost 75% of variance in simulated outflow is caused by n1, either by the variation of the parameter itself (30%) or by interactions with other parameters. Together with a1 (51%) and Ks1 (42%), it is the most influential parameter for simulated flow. It can be noted that the saturated hydraulic conductivity, Ks1, has a relatively low main effect but a relatively high total effect. That indicates that this parameter has a limited direct effect on the variance of the objective function, but it has an effect in interactions with other parameters.

The effect of the sub-base layer on the output is less significant, while the wear layer strongly conditions the output.

A Monte Carlo Filtering procedure was applied to the runs of the GSA. The threshold value of NSE = 0.0 produced a filtered sample composed of 1,452 behavioral solutions.

Also, for Scenario II, parameters a1 and n1 exhibit the highest main effects on the output's variance (about 35%). For both scenarios, modeling results are most sensitive to the wear layer, which strongly influences the output's variance. However, in Scenario II, the influence of the wear layer is partially reduced and redistributed to other layers. It is evident that the adoption of the dual-porosity model for the unsaturated hydraulic properties significantly affects the influence of the base and sub-base layers on the model's output. The dynamics of sensitivity indices between the two scenarios suggest that the physical description of unsaturated flow in the sub-base layer is an important element in numerical simulations.

A Monte Carlo Filtering procedure was again applied to the runs of the GSA. The filtered sample now consisted of 28,107 behavioral solutions. The filtered sample of behavioral solutions for Scenario II was considerably larger than for Scenario I. This indicates that the implementation of the dual-porosity model leads to higher values of the objective function.

Figure 12 compares measured and modeled hydrographs for the two scenarios. The PSO for Scenarios I and II resulted in NSE values of 0.43 and 0.81, respectively. Both NSE values of the objective function are higher than zero and thus admissible [39]. However, the implementation of the dual-porosity model for the base and sub-base layers in Scenario II provides a more accurate description of the hydraulic behavior of the permeable pavement.

In order to evaluate the reliability of the estimated parameters, the model has been validated on another independent set of experimental data. Figure 13 shows a comparison between measured and modeled hydrographs for the two scenarios during the validation period.

The value of the objective functions is NSE = 0.43 for Scenario I and NSE = 0.86 for Scenario II. For Scenario I, the value of the objective function remains the same, which confirms the reliability of the calibrated model. Although the simulated hydrograph provides an overall sufficiently accurate description of the hydraulic behavior of the pavement, it is less accurate during rainfall events, which may be a time period of main interest. For Scenario II, the value of the objective function

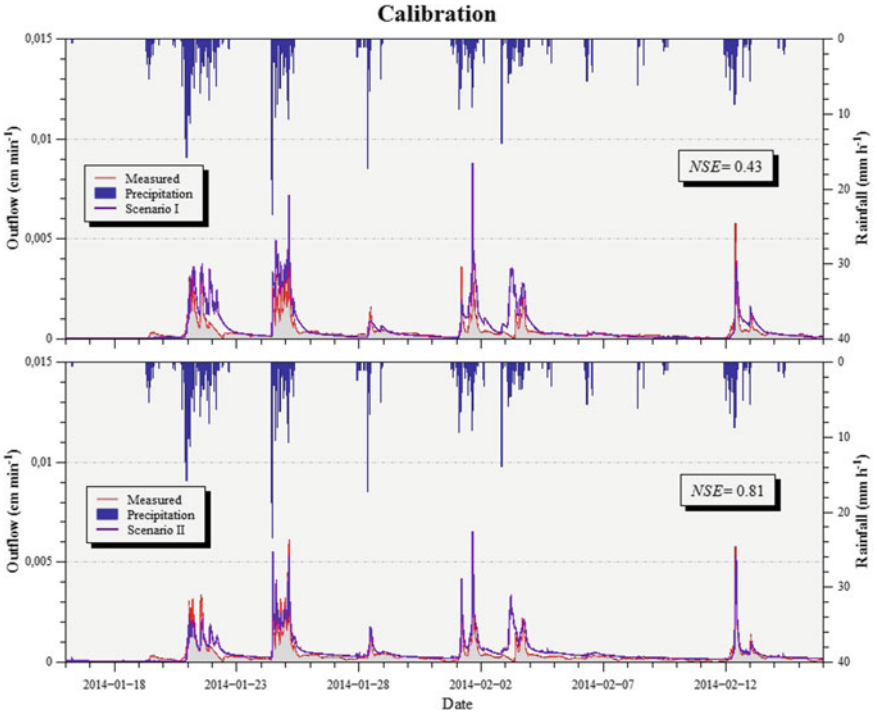

Fig. 12 Comparison between the modeled and measured hydrographs for Scenarios I (top) and II (bottom) for the optimization process

actually increased and reached the value NSE = 0.86, which is very high and reflects the accuracy of the modeled hydrograph.

4 Conclusion

The aim of this chapter was to presents the recent experiences in the Urban Hydrology field able to manage stormwater in a correct way. The cited works have shown how the smart management of the drainage networks and the application of urban regeneration facilities such as green roof or permeable pavement can help in knowledge of flooding phenomena. In particular, findings from Garofalo et al. [25] showed how DRTC algorithm proposed was able to balance the hydraulic capacity of the conduits within the system by utilizing the storage capacity of the less overwhelmed conduits during intense rainfall events. In other words, the DRTC algorithm was able to control the water level within the UDS successfully, ensuring a full utilization of the actual storage capacity of the system. The findings clearly demonstrated that the DRTC produced beneficial effects on the management of the UDS by substantially

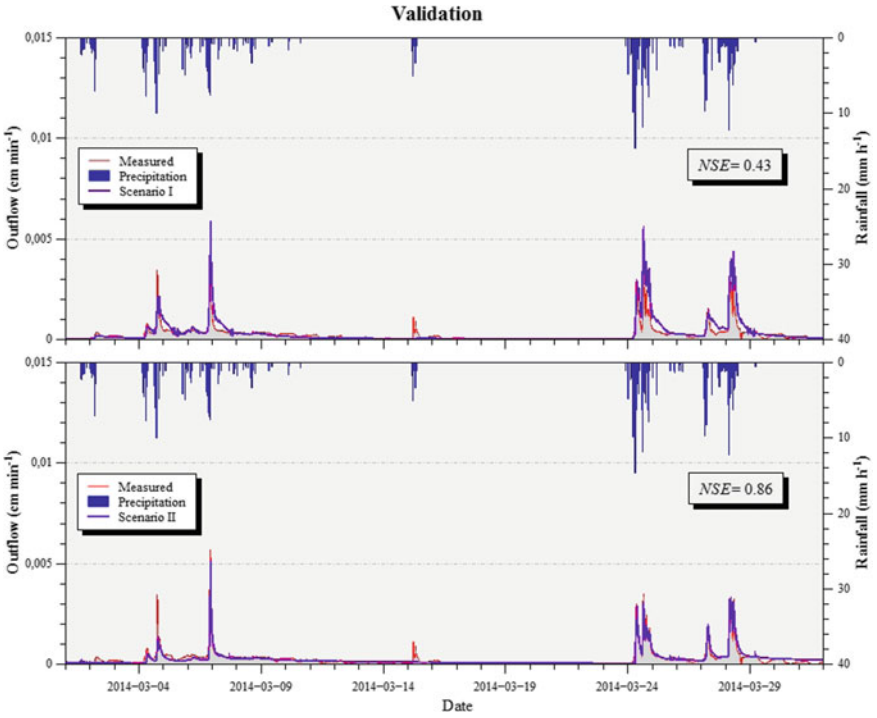

Fig. 13 Comparison between the modeled and measured hydrograph for the two scenarios for the validation period

mitigating the risk of flooding and CSO. Results from Brunetti et al. [8, 9] showed that the implementation of a model aimed at soil systems, together with accurate experimental and numerical procedures, has been able to accurately describe the hydraulic behaviour of systems of multiple layered materials that are not really soils. Future perspectives are oriented in the smart optimization of LID and RWH systems by the IoT advanced innovations in order to maximize the hydraulic efficiency of these techniques and mitigate the urban flooding risk.

References

1. S. Achleitner, M. Möderl, W. Rauch, CITY DRAIN ©—an open source approach for simulation of integrated urban drainage systems. Environ. Model. Softw. **22**, 1184–1195 (2007). https://doi.org/10.1016/j.envsoft.2006.06.013
2. R.G. Allen, L.S. Pereira, D. Raes, M. Smith, FAO Irrigation and Drainage Paper No. 56: Crop Evapotranspiration, FAO. Rome (1998)
3. G.E.B. Archer, A. Saltelli, I.M. Sobol, Sensitivity measures, ANOVA-like techniques and the use of bootstrap. J. Stat. Comput. Simul. **58**, 99–120 (1997). https://doi.org/10.1080/00949659708811825

4. K. Astrom, PID controllers: theory, design and tuning. Instrum. Soc. Am. (1995). ISBN 1556175167
5. P.M. Bach, W. Rauch, P.S. Mikkelsen, D.T. McCarthy, A. Deletic, A critical review of integrated urban water modelling—urban drainage and beyond. Environ. Model. Softw. (2014). https://doi.org/10.1016/j.envsoft.2013.12.018
6. G. Barenblatt, I. Zheltov, I. Kochina, Basic concepts in the theory of seepage of homogeneous liquids in fissured rocks [strata]. J. Appl. Math. Mech. **24**, 1286–1303 (1960). https://doi.org/10.1016/0021-8928(60)90107-6
7. T. Beeneken, V. Erbe, A. Messmer, C. Reder, R. Rohlfing, M. Scheer, M. Schuetze, B. Schumacher, M. Weilandt, M. Weyand, Real time control (RTC) of urban drainage systems—a discussion of the additional efforts compared to conventionally operated systems. Urban Water J. **10**, 293–299 (2013). https://doi.org/10.1080/1573062X.2013.790980
8. G. Brunetti, J. Simunek, P. Piro, A comprehensive analysis of the variably-saturated hydraulic behavior of a green roof in a mediterranean climate. Vadose Zo. J. **15** (in press) (2016a). https://doi.org/10.2136/vzj2016.04.0032
9. G. Brunetti, J. Šimůnek, P. Piro, A comprehensive numerical analysis of the hydraulic behavior of a permeable pavement. J. Hydrol. **540**, 1146–1161 (2016). https://doi.org/10.1016/j.jhydrol.2016.07.030
10. G. Brunetti, J. Šimůnek, M. Turco, P. Piro, On the use of surrogate-based modeling for the numerical analysis of low impact development techniques. J. Hydrol. **548**, 263–277 (2017). https://doi.org/10.1016/j.jhydrol.2017.03.013
11. M. Carbone, F. Principato, G. Garofalo, P. Piro, Comparison of evapotranspiration computation by FAO-56 and Hargreaves methods. J. Irrig. Drain. Eng. **142**(8), 06016007 (2016). https://doi.org/10.1061/(ASCE)IR.1943-4774.0001032
12. M. Carbone, G. Brunetti, P. Piro, Modelling the hydraulic behaviour of growing media with the explicit finite volume solution. Water (Switzerland) **7**, 568–591 (2015). https://doi.org/10.3390/w7020568
13. M. Carbone, M. Turco, G. Brunetti, P. Piro, A cumulative rainfall function for subhourly design storm in mediterranean urban areas. Adv. Meteorol. **2015**, 1–10 (2015). https://doi.org/10.1155/2015/528564
14. M. Carbone, M. Turco, G. Nigro, P. Piro, Modeling of hydraulic behaviour of green roof in catchment scale, in *14th SGEM GeoConference on Water Resources. Forest, Marine and Ocean Ecosystems* (2014a), pp. 471–478. https://doi.org/10.5593/sgem2014/b31/s12.061
15. M. Carbone, F. Principato, G. Nigro, P. Piro, Proposal of a conceptual model as tool for the hydraulic design of vegetated roof, in *Applied Mechanics and Materials*, vol. 641 (Trans Tech Publications, 2014b), pp. 326–331. https://doi.org/10.4028/www.scientific.net/AMM.641-642.326
16. M. Carbone, G. Garofalo, P. Piro, Decentralized real time control in combined sewer system by using smart objects. Procedia Eng. 473–478 (2014c). https://doi.org/10.1016/j.proeng.2014.11.237
17. M. Carini, M. Maiolo, D. Pantusa, F. Chiaravalloti, G. Capano, Modelling and optimization of least-cost water distribution networks with multiple supply sources and user. Ricerche Mat. **2017** (2017). https://doi.org/10.1007/s11587-017-0343-y
18. B. Cheviron, Y. Coquet, Sensitivity analysis of transient-MIM HYDRUS-1D: case study related to pesticide fate in soils. Vadose Zo. J. **8**, 1064 (2009). https://doi.org/10.2136/vzj2009.0023
19. G. Dirckx, M. Schütze, S. Kroll, C. Thoeye, G. De Gueldre, B. Van De Steene, Cost-efficiency of RTC for CSO impact mitigation. Urban Water J. **8**, 367–377 (2011). https://doi.org/10.1080/1573062X.2011.630092
20. W. Durner, Hydraulic conductivity estimation for soils with heterogeneous pore structure. Water Resour. Res. **30**, 211–223 (1994). https://doi.org/10.1029/93WR02676
21. B. Efron, R. Tibshirani, Bootstrap methods for standard errors, confidence intervals, and other measures of statistical accuracy. Stat. Sci. **1**, 54–75 (1986)
22. A.H. Elliott, S.A. Trowsdale, A review of models for low impact urban stormwater drainage. Environ. Model. & Softw. **22**, 394–405 (2007). https://doi.org/10.1016/j.envsoft.2005.12.005

23. G. Fu, D. Butler, S.-T. Khu, Multiple objective optimal control of integrated urban wastewater systems. Environ. Model Softw. **23**, 225–234 (2008). https://doi.org/10.1016/j.envsoft.2007.06.003
24. A. Giordano, G. Spezzano, A. Vinci, G. Garofalo, P. Piro, A cyber-physical system for distributed real-time control of urban drainage networks in smart cities, in *International Conference on Internet and Distributed Computing Systems* (Springer, Cham, 2014), pp. 87–98. https://doi.org/10.1007/978-3-319-11692-1_8
25. G. Garofalo, A. Giordano, P. Piro, G. Spezzano, A. Vinci, A distributed real-time approach for mitigating CSO and flooding in urban drainage systems. J. Netw. Comput. Appl. **78**, 30–42 (2017). https://doi.org/10.1016/j.jnca.2016.11.004
26. G. Garofalo, S. Palermo, F. Principato, T. Theodosiou, P. Piro, The influence of hydrologic parameters on the hydraulic efficiency of an extensive green roof in mediterranean area. Water **8**(2), 44 (2016). https://doi.org/10.3390/w8020044
27. M.K. Gill, Y.H. Kaheil, A. Khalil, M. McKee, L. Bastidas, Multiobjective particle swarm optimization for parameter estimation in hydrology. Water Resour. Res. **42**, n/a–n/a (2006). https://doi.org/10.1029/2005wr004528
28. T. Houska, S. Multsch, P. Kraft, H.-G. Frede, L. Breuer, Monte Carlo based calibration and uncertainty analysis of a coupled plant growth and hydrological model. Biogeosci. Discuss. **10**, 19509–19540 (2013). https://doi.org/10.5194/bgd-10-19509-2013
29. J. Huang, J. He, C. Valeo, A. Chu, Temporal evolution modeling of hydraulic and water quality performance of permeable pavements. J. Hydrol. **533**, 15–27 (2016). https://doi.org/10.1016/j.jhydrol.2015.11.042
30. M. Jelasity, A. Montresor, O. Babaoglu, Gossip-based aggregation in large dynamic networks. ACM Trans. Comput. Syst. **23**, 219–252 (2005). https://doi.org/10.1145/1082469.1082470
31. Y. Jiang, C. Liu, C. Huang, X. Wu, Improved particle swarm algorithm for hydrological parameter optimization. Appl. Math. Comput. **217**, 3207–3215 (2010). https://doi.org/10.1016/j.amc.2010.08.053
32. M. Kamali, M. Delkash, M. Tajrishy, Evaluation of permeable pavement responses to urban surface runoff. J. Environ. Manag. **187**, 43–53 (2017). https://doi.org/10.1016/j.jenvman.2016.11.027
33. J. Kennedy, R. Eberhart, Particle swarm optimization. Eng. Technol. 1942–1948 (1995)
34. Z.W. Kundzewicz, M. Radziejewski, I. Pińskwar, Precipitation extremes in the changing climate of Europe. Clim. Res. **31**, 51–58 (2006). https://doi.org/10.3354/cr031051
35. R. Levinson, H. Akbari, Effects of composition and exposure on the solar reflectance of portland cement concrete. Cem. Concr. Res. **32**, 1679–1698 (2002). https://doi.org/10.1016/S0008-8846(02)00835-9
36. Y. Li, R.W. Babcock, *Green roof hydrologic performance and modeling: A review* (Technol, Water Sci, 2014). https://doi.org/10.2166/wst.2013.770
37. M. Maiolo, D. Pantusa, An optimization procedure for the sustainable management of water resources. Water Sci. Technol.: Water Supply **16**(1), 61–69 (2016). https://doi.org/10.2166/ws.2015.114
38. S.K. Min, X. Zhang, F.W. Zwiers, G.C. Hegerl, Human contribution to more-intense precipitation extremes. Nature **470**, 378–381 (2011). https://doi.org/10.1038/nature09763
39. D.N. Moriasi, J.G. Arnold, M.W. Van Liew, R.L. Binger, R.D. Harmel, T.L. Veith, Model evaluation guidelines for systematic quantification of accuracy in watershed simulations. Trans. ASABE **50**, 885–900 (2007). https://doi.org/10.13031/2013.23153
40. J.E. Nash, J.V. Sutcliffe, River flow forecasting through conceptual models Part I—A discussion of principles. J. Hydrol. **10**, 282–290 (1970). https://doi.org/10.1016/0022-1694(70)90255-6
41. T. Pertassek, A. Peters, W. Durner, HYPROP-FIT Software User's Manual, V.3.0 (2015)
42. P. Piro, M. Carbone, A modelling approach to assessing variations of total suspended solids (TSS) mass fluxes during storm events. Hydrol. Process. **28**, 2419–2426 (2014). https://doi.org/10.1002/hyp.9809
43. P. Piro, M. Carbone, G. Garofalo, Distributed vs. concentrated storage options for controlling CSO volumes and pollutant loads. Water Pract. Technol. **5**, wpt2010071–wpt2010071 (2010a). https://doi.org/10.2166/wpt.2010.071

44. P. Piro, M. Carbone, G. Garofalo, J. Sansalone, Size distribution of wet weather and dry weather particulate matter entrained in combined flows from an urbanizing sewershed. Water Air Soil Pollut. **206**, 83–94 (2010). https://doi.org/10.1007/s11270-009-0088-7
45. M. Pleau, H. Colas, P. Lavallée, G. Pelletier, R. Bonin, Global optimal real-time control of the Quebec urban drainage system. Environ. Model. Softw. (2005). https://doi.org/10.1016/j.envsoft.2004.02.009
46. F. Principato, S.A. Palermo, G. Nigro, G. Garofalo, Sustainable strategies and RTC to mitigate CSO's impact: different scenarios in the highly urbanized catchment of Cosenza, Italy, in *Proceedings of the 14th IWA/IAHR International Conference on Urban Drainage, ICUD2017*, Prague, CZ, 10–15 Sept 2017, Oral Presentation, pp. 587–589
47. A. Raimondi, G. Becciu, On pre-filling probability of flood control detention facilities. Urban Water J. **12**, 344–351 (2015). https://doi.org/10.1080/1573062X.2014.901398
48. A. Raimondi, G. Becciu, Probabilistic modeling of rainwater tanks. Procedia Eng. **89**, 1493–1499 (2014). https://doi.org/10.1016/j.proeng.2014.11.437
49. M. Rezaei, P. Seuntjens, I. Joris, W. Boënne, S. Van Hoey, P. Campling, W.M. Cornelis, Sensitivity of water stress in a two-layered sandy grassland soil to variations in groundwater depth and soil hydraulic parameters. Hydrol. Earth Syst. Sci. Discuss. **12**, 6881–6920 (2015). https://doi.org/10.5194/hessd-12-6881-2015
50. L.A. Rossman, Storm water management model quality assurance report: dynamic wave flow routing. Storm Water Manag. Model Qual. Assur. Rep. 1–115 (2006)
51. A. Saltelli,, S. Tarantola, M. Saisana, M. Nardo, What is sensitivity analysis?, in *II Convegno Della Rete Dei Nuclei Di Valutazione E Verifica*, Napoli 26, 27 Gennaio 2005, Centro Congressi Universitá Federico II, Via Partenope 36 (2005)
52. M. Schütze, A. Campisano, H. Colas, W. Schilling, P.A. Vanrolleghem, Real time control of urban wastewater systems—where do we stand today? J. Hydrol. **299**, 335–348 (2004). https://doi.org/10.1016/j.jhydrol.2004.08.010
53. N. She, J. Pang, Physically based green roof model. J. Hydrol. Eng. **15**, 458–464 (2010). https://doi.org/10.1061/(ASCE)HE.1943-5584.0000138
54. J. Šimůnek, M.T. van Genuchten, M. Šejna, Recent developments and applications of the HYDRUS Computer Software Pac. Vadose Zo. J. **15**, 25 (2016). https://doi.org/10.2136/vzj2016.04.0033
55. J. Simunek, N.J. Jarvis, M.T. van Genuchten, A. Gardenas, Review and comparison of models for describing non-equilibrium and preferential flow and transport in the vadose zone. J. Hydrol. **272**, 14–35 (2003). https://doi.org/10.1016/S0022-1694(02)00252-4
56. J. Šimůnek, M.T. van Genuchten, Modeling nonequilibrium flow and transport processes using HYDRUS. Vadose Zo. J. **7**, 782 (2008). https://doi.org/10.2136/vzj2007.0074
57. J. Šimůnek, M.T. van Genuchten, M. Šejna, Development and applications of the HYDRUS and STANMOD software packages and related codes. Vadose Zo. J. **7**, 587 (2008). https://doi.org/10.2136/vzj2007.0077
58. I. Sobol', Global sensitivity indices for nonlinear mathematical models and their Monte Carlo estimates. Math. Comput. Simul. **55**, 271–280 (2001). https://doi.org/10.1016/S0378-4754(00)00270-6
59. M. Turco, R. Kodešová, G. Brunetti, A. Nikodem, M. Fér, P. Piro, Unsaturated hydraulic behaviour of a permeable pavement: laboratory investigation and numerical analysis by using the HYDRUS-2D model. J. Hydrol. **554**, 780–791 (2017). https://doi.org/10.1016/j.jhydrol.2017.10.005
60. UMS GmbH, UMS (2015): Manual HYPROP, Version 2015-01 (2015)
61. W. Usher, Xantares, D. Hadka, bernardoct, Fernando, J. Herman, C. Mutel, SALib: New documentation, doc strings and installation requirements (2015). https://doi.org/10.5281/zenodo.31316
62. M.T. van Genuchten, A closed-form equation for predicting the hydraulic conductivity of unsaturated soils. Soil Sci. Soc. Am. J. **44**, 892 (1980). https://doi.org/10.2136/sssaj1980.03615995004400050002x

63. M.T. Van Genuchten, P.J. Wierenga, Mass transfer studies in sorbing porous media I. Analytical solutions. Soil Sci. Soc. Am. J. **40**, 473–480 (1976). https://doi.org/10.2136/sssaj1976.03615995004000040011x
64. J.E. Warren, P.J. Root, The behavior of naturally fractured reservoirs. Soc. Pet. Eng. J. **3**, 245–255 (1963). https://doi.org/10.2118/426-PA
65. T.H.F. Wong, T.D. Fletcher, H.P. Duncan, G.A. Jenkins, Modelling urban stormwater treatment—a unified approach. Ecol. Eng. **27**, 58–70 (2006). https://doi.org/10.1016/j.ecoleng.2005.10.014
66. M. Wooldridge, *An Introduction to MultiAgent Systems*, 2nd edn. (Wiley, 2009), ISBN-10 0470519460, ISBN-13 978-0470519462
67. M. Zambrano-Bigiarini, R. Rojas, A model-independent Particle Swarm Optimisation software for model calibration. Environ. Model Softw. **43**, 5–25 (2013). https://doi.org/10.1016/j.envsoft.2013.01.004
68. S. Zhang, Y. Guo, Analytical probabilistic model for evaluating the hydrologic performance of green roofs. J. Hydrol. Eng. **18**, 19–28 (2013). https://doi.org/10.1061/(ASCE)HE.1943-5584.0000593

Paper VI

On the LID systems effectiveness for urban stormwater management: case study in Southern Italy

S. A. Palermo, V. C. Talarico and M. Turco. (2020a)

Published in: IOP Conference Series: Earth and Environmental Science (Vol. 410, No. 1, p. 012012). IOP Publishing.
https://doi.org/10.1088/1755-1315/410/1/012012

On the LID systems effectiveness for urban stormwater management: case study in Southern Italy

On the LID systems effectiveness for urban stormwater management: case study in Southern Italy

S A Palermo[1], V C Talarico[1] and M Turco[2]

[1] Department of Civil Engineering, University of Calabria, Italy
[2] Department of Environmental and Chemical Engineering, University of Calabria, Italy

E-mail address: stefania.palermo@unical.it

Abstract. Here we present the hydrological effectiveness of Low Impact development (LID) solutions at urban catchment scale, by modelling a highly urbanised area located in South Italy. For the model creation and simulation, PCSWMM based on the Storm Water Management Model (SWMM) was used. The analysis was carried out by considering different land use conversion scenarios including the implementation of LID practices. Therefore, a specific permeable pavement and green roof developed and implemented at full scale at University of Calabria were chosen as source-control measures. The simulations were run by using as input a synthetic hyetograph of 30 min with return period of 10 years. Three hydrological performance indexes, Runoff Coefficient (RC), Runoff Reduction (RR) and Peak Flow Reduction (PFR) were evaluated at subcatchment scale and, a mean value was estimated for an overall evaluation. Main findings show that RR and PFR linearly increase with the reduction of imperviousness due to the modelling of a major percentage of LID solutions, while the RC decreases. In addition, first detailed results reveal the suitability of LID solutions to reduce surface runoff also for the scenario 1 which considers the conversion of only 30% of specific impervious surface in green roofs and permeable pavements.

Keywords: Rainfall-Runoff, Green Roof, Permeable Pavement, PCSWMM, Hydrodynamic Modelling

1. Introduction

Climate change and on-going urbanization can be considered the main factors which lead several environmental impacts from the watershed scale to urban catchment scale, as increase of flooding risk, water pollution, urban heat island, air pollution, biodiversity, problems related to water bodies alteration, and so on [1-3].

In this context, to enhance the environmental quality and restore the exosystemic balance affected by urbanization and climate change, sustainable solutions and assessment methodologies at different spatial scale (urban, peri-urban, watershed, and so on) are become a priority, and in this direction several studies have been carried out [4-6].

Focusing on urban environment, the highly imperviousness led a drastic change in the natural hydrological cycle components with consequences in terms of reduction of infiltration and evapotranspiration and increase of runoff volumes. Therefore, during extreme stormwater events such volumes can overload the sewer systems causing local floods [7].

In this scenario, is relevant to find solutions to reduce the impacts [8]. A promising strategy is the implementation of decentralized stormwater controls, also known as LID (Low Impact Development) systems which provide several benefits at multiple scales [9-11]. These techniques allow a management of stormwater directly at the source by a nature-based approach.

Green roofs and permeable pavements, largely investigated, have been considered among the most efficient strategies in terms of urban flooding risk mitigation, water quality enhancement, and urban heat islands reduction [12-18].

Based on this framework, main objective of this study is to analyse how the implementation of Low Impact Development systems (LIDs) can contribute to mitigate the effect of climate change and urbanization in terms of surface runoff reduction and, consequently urban flooding risk mitigation.

To achieve this, the hydrological response of a small selected urban area - located in Southern Italy - was investigated under different land use conversion scenarios, by considering the modelling implementation of Green Roofs and Permeable Pavements integrated in the existing drainage network, by using PCSWMM [19].

2. Materials and Methods

2.1. Study Area

A highly urbanized area of an urban catchment (catchment of San Domenico Creek) located in the municipality of Paola in Calabria Region (Italy) in Mediterranean Climate Region, was selected as test site for modelling the land use conversion scenarios.

In this area the stormwater management is achieved by a combined sewer network consisting of different conduits in terms of section and materials. More specifically, based on the detailed information of a previous study [20], the concrete conduits present sections of 350x450mm, 400x400mm e 450x450mm, while the circular ones in stoneware material have diameters of 200 mm and 300 mm.

The residential area, here considered, with a total surface of around 7.6 ha, presents a grade of imperviousness of 96.0%. The analysis of land use data, carried out on the base of regional cartography and aerial photographs, illustrated in Table 1, shows that the study area consists of 28.9% of rooftops and 67.1% of roads, parking lots and others impervious surfaces; only a small portion of around 4.0% of the total surface is covered by green spaces.

This landscape analysis reveals as the area, almost totally covered by impervious surfaces, can be a suitable site for LID systems implementation for urban stormwater management.

Table 1. Land use of the selected area.

Land use	**Area**	
	ha	%
Rooftop	2.2	28.9
Parking lot, roads and other impervious	5.1	67.1
Total Impervious	**7.3**	**96.0**
Green Area	0.3	4.0
Total Pervious	**0.3**	**4.0**
Total Areas	**7.6**	**100.00**

2.2. LID Simulation Scenarios

To assess the hydrological effectiveness of LID systems for urban stormwater management, Green Roofs (GRs) and Permeable Pavements (PPs) are the LID systems selected to model the response of the urban area under different conversions scenarios:

(i) *Scenario 0* is the reference scenario, implemented based on the current land use data, in order to investigate the impact of the LID implementation;
(ii) *Scenario 1* consists in the replacement of 30% of conventional rooftop area with Green Roofs and in the installation of Pemeable Pavements on the 30% of impervious surfaces (excluding roads opened to traffic);
(iii) *Scenario 2*, where 60% of conventional roofs are substituted with Green Roofs and 60% of impervious areas (excluding roads opened to traffic) with Pemeable Pavements;
(iv) *Scenario 3* considers the implementation of Green Roofs on all rooftops, and the replacement of 100% of impervious surfaces (excluding roads opened to traffic) with Pemeable Pavements.

2.3. Model development

To simulate the hydrological response of urban catchment a dynamic rainfall-runoff simulation model PCSWMM (CHI-PCSWMM), based on the EPA-SWMM version 5.1.012 [21], was used. This choice was carried out based on the results of other studies, which confirm the suitability of SWMM to assess the LID performances and to support their implementation at catchment scale [22,23].

The model was built considering topographical data, land use classification and data on the existing stormwater system, already investigated in a previous study [20].

To obtain a detailed model, and improve the previous one, the study area of around 7.6 ha was divided into 26 subcatchments, defined in function of land use and homogeneous properties (the surface slope, area, etc.). More in detail, based on the land use analysis, for each subcatchment, before the modelling implementation, the land use features in terms of pervious and impervious area were defined. In function of this analysis for each subcatchment the Curve Number parameter (-), the Depression Depth value (mm), n Manning coefficient ($s/m^{1/3}$) were defined, and then considered with the others geometrical data (area, width, slope, etc.) as input subcatchment parameters to implement the model.

The Soil Conservation Service (SCS) Curve Number (CN) method was considered for the infiltration method and the flow routing computations were based on the Dynamic Wave Equations.

The drainage network was defined in agreement with the data retrieved from the design plans in terms of conduit length, section and material.

Based on this, the implemented model consists of 26 subcatchments, 28 Conduits, 28 Junctions Nodes, and 1 Outfall node. This model is representative of the existing system configuration, i.e. the reference scenario (Scenario 0) of this study.

To simulate the hydrological response of this urban area with the implementation of LID solutions (Scenario 1,2,3), the model, previous defined, was integrated with the use of the LID Control Editor; this is an additional SWMM module developed to simulate the hydrological behaviour of source control solutions as bio-retention cell, rain gardens, green roof, infiltration trench, permeable pavement, rain barrel, rooftop disconnection, vegetative swale [21].

In this study green roof and permeable pavement modules were selected. To assign the properties for each layer, required by the LID Control section, the stratigraphy features and the physical parameters (based on previous laboratory test measurements) of the green roof and the permeable pavement located at University of Calabria were considered. More detail, the features of these two LID solutions can be found in [7,24,25].

For the hydrodynamic simulation, synthetic Chicago hyetograph was used. The rainfall duration was assumed 30 min and the time-to-peak-ratio 0.4. The hyetograph was defined based on the parameters of the Intensity–Duration-Frequency relationship computed by the analysis of historical records (1945 – 2005) obtained from the Regional Agency for Prevention, Environmental in Calabria Region [26] by considering the rain gauge station of Paola.

The hydrodynamic model here presented, as stated above, was used to simulate the response of an urban catchments under different conversion scenarios with the aims to evaluate the hydrological effectiveness of LID systems for stormwater management.

2.4. Hydrological Performance Indexes

The response of each scenario was evaluated in terms of runoff coefficient (RC), runoff reduction (RR), and peak flow reduction (PFR). These values were estimated for each subcatchment and the mean values for each index were calculated in order to analyse the overall result.

More in detail:

The *Runoff Coefficient* for each scenario (RC_0, RC_1, RC_2, RC_3) was expressed as percentage ratio between the total Runoff Depth in mm ($RD_0, RD_1; RD_2; RD_3$) and the total Precipitation Depth in mm (PD).

Table 2. Equations used to evaluate the Runoff Coefficient for each scenario.

SCENARIO 0	SCENARIO 1	SCENARIO 2	SCENARIO 3
$RC_0 = \frac{RD_0}{PD} \cdot 100$	$RC_1 = \frac{RD_1}{PD} \cdot 100$	$RC_2 = \frac{RD_2}{PD} \cdot 100$	$RC_3 = \frac{RD_3}{PD} \cdot 100$

While, the *Runoff Reduction* ($RR_{0\text{-}1}, RR_{0\text{-}2}, RR_{0\text{-}3}$) was estimated as the percentage difference between the total Runoff Depth of Scenario 0 (RD_0) and the corresponding total Runoff Depth of the other conversion scenarios ($RD_1; RD_2; RD_3$).

Similarly, the Peak Flow Reduction ($PFR_{0\text{-}1}$, $PFR_{0\text{-}2}$, $PFR_{0\text{-}3}$) was evaluated as the percentage difference between the hydrograph peak of Scenario 0 (PF_0) and the corresponding hydrograph peak for each LID conversion scenarios (PF_1, PF_2, PF_3).

Table 3. Equations used to evaluate the surface Runoff Reduction (RR) and Peak Flow reduction (PFR) obtained by comparing Scenario 0 with the other Scenarios (1,2,3).

SCENARIO 0 vs SCENARIO 1	SCENARIO 0 vs SCENARIO 2	SCENARIO 0 vs SCENARIO 3
$RR_{0-1} = \frac{RD_0 - RD_1}{RD_0} \cdot 100$	$RR_{0-2} = \frac{RD_0 - RD_2}{RD_0} \cdot 100$	$RR_{0-3} = \frac{RD_0 - RD_3}{RD_0} \cdot 100$
$PFR_{0-1} = \frac{PF_0 - PF_1}{PF_0} \cdot 100$	$PFR_{0-2} = \frac{PF_0 - PF_2}{PF_0} \cdot 100$	$PFR_{0-3} = \frac{PF_0 - PF_3}{PF_0} \cdot 100$

3. Results and Discussion

The introduction of different percentage of LID units aims at improving the infiltration capability of the selected area reducing the surface runoff. By analysing the *Scenario 0* model configuration, it was possible to observe the high imperviousness percentage of this urbanised area: 22 subcatchments present an imperviousness more than 90%. While, by implementing the different LID scenarios, it was detected a great reduction of imperviousness until to reach the optimal and final condition related to scenario 3, where most of the subcatchments have an imperviousness less than 40%.

To assess the LID hydrological effectiveness, the results were evaluated in terms of outflow for the reference condition (Scenario 0) and those one obtained for the conversions scenarios (Scenarios 1,2,3).

More in detail, first the total Runoff Depth (RD) and the Peak Flow (PF) were estimated at subcatchment scale for each conversion scenario (Figure 1). For both cases, the bargraphs confirm the good performance of the LID systems, by showing how the RD and PF values reduced to the increase of LID percentages in the urban area.

Therefore, based on the data of all subcatchments, the three Hydrological Performance Indexes (RC, RR, PFR) were evaluated at subcatchment scale (Figure 2), and then average values calculated in order to analyse the overall result (Table 4).

Specifically, by observing Figure 2, it is possible to detect the range of variation of the three Hydrological Performance Indexes.

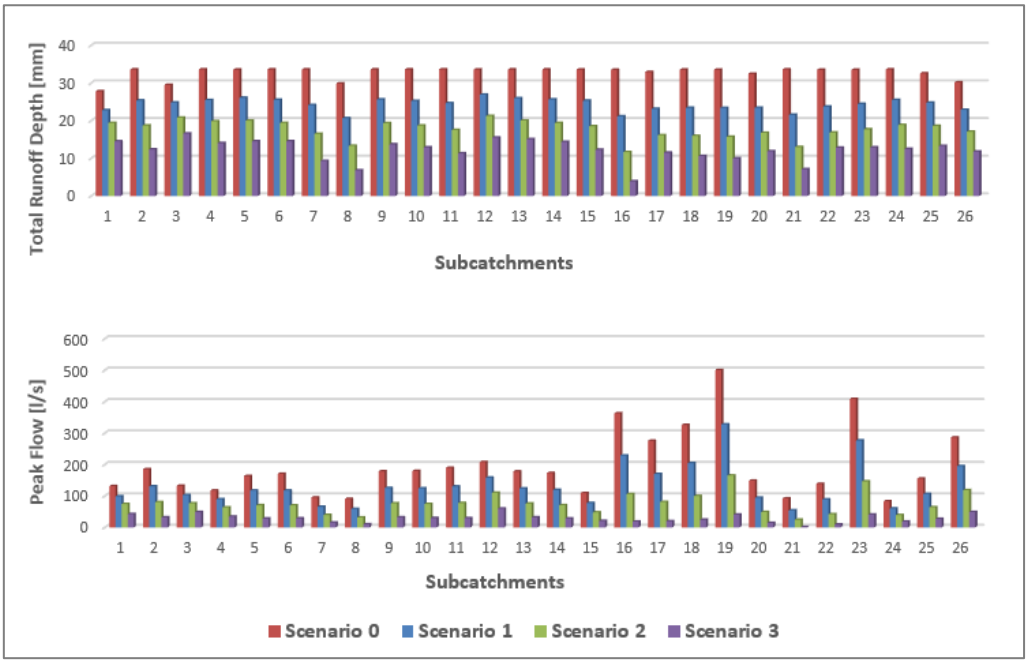

Figure 1. Total Runoff Depth [mm] and Peak Flow [l/s] for each subcatchment by comparing all scenarios.

Table 4. Rainfall Depth and Average Values of Performance indexes

	Scenario 0	**Scenario 1**	**Scenario 2**	**Scenario 3**
Rainfall depth [mm]	33.5	33.5	33.5	33.5
Average RC [%]	98.1	72.6	53.0	36.4

	Scenario 0 vs Scenario 1	**Scenario 0 vs Scenario 2**	**Scenario 0 vs Scenario 3**
Average RR [%]	25.9	45.8	62.8
Average PFR [%]	31.4	59.3	83.8

The values reported in Table 4 reveal the suitability of the LIDs to improve retention capacity of a highly urbanised basin.

The RC average value decreases from 98.1% in the condition of almost total imperviousness to 36.4% in Scenario 3, obtaining also good results for the inter-medium scenarios. RC values of 25.5% and 45.1% less than the Scenario 0 were observed for the Scenario 1 and 2 respectively.

While the Runoff Reduction (RR) [%] and Peak Flow Reduction (PFR) [%] present a linear increase of their values with the reduction of the impervious surfaces, simulated from scenario 1 to scenario 3.

More in detail, the implementation of GR and PP on the 30% of the corresponding impervious surface (as specified above) allow a runoff reduction of 25.9 % and a peak reduction of 31.4%. Although the imperviousness change is limited to only this percentage (30%), a good result was the same achieved by the implementation of the specific GR and PP in Mediterranean climate condition.

As expected, more high performances have been reached in the second and third scenarios, where the percentage of LID reached 60% and 100%, respectively, and the RR and PFR reached values of 45.8% and 54.3% for scenario 2 and 62.8% and 83.8% for the last one.

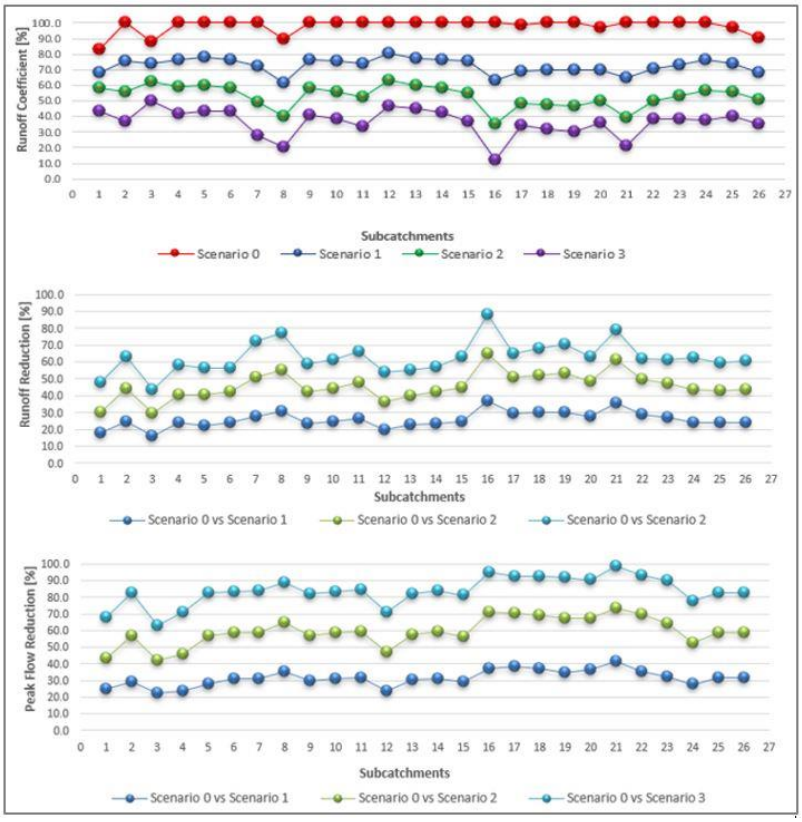

Figure 2. Comparison of the Hydrological Performances Indexes evaluated at subcatchment scale for different conversion scenarios.

All findings, here presented, confirm the suitability of LID solutions for the surface runoff mitigation in terms of volume and hydrographs peak for all three LID conversion scenarios.

By analysing the modelling results emerges the role of LID practices to restore the component of natural hydrological cycle at the urban scale. And, even if, practical and economic considerations are needed to select the optimal LIDs distribution, this study demonstrates that also a small change of imperviousness, considered for example for the Scenario 1, can enhance the hydrological response of an urban catchment.

4. Conclusions

To evaluate the hydrological performances of LID systems, in this study the hydrological response of a highly urbanised area locate din Southern Italy has been simulated under different conversions scenarios. The selected area was modelled by using PCSWMM. A specific permeable pavement and green roof, developed at University of Calabria, have been considered for the modelling implementation by the LID modules in PCSWMM. Modelling results confirm the suitability of these LID solutions to reduce surface runoff and, therefore, urban flooding risk. The findings reveal that this beneficial effect can be reached by converting also only a small percentage of the impervious surfaces. Considering that practical and economic conditions could limit the implementation of these sustainable practices in urban area, this can be considered a relevant finding.

In conclusion, the LID strategy achieves a sustainable management of urban drainage network, limiting the environmental impact due to urbanization and climate change.

Future investigation will take into account the response of the same area under different rainfall event and by considering others combination of LID systems not only in terms of percentage distribution, but also in terms of different design systems.

References

[1] Antrop, M. (2004). Landscape change and the urbanization process in Europe. *Landscape and urban planning*, *67*(1-4), 9-26.
[2] Violin, C. R., Cada, P., Sudduth, E. B., Hassett, B. A., Penrose, D. L., & Bernhardt, E. S. (2011). Effects of urbanization and urban stream restoration on the physical and biological structure of stream ecosystems. *Ecological Applications*, *21*(6), 1932-1949.
[3] Long, H., Liu, Y., Hou, X., Li, T., & Li, Y. (2014). Effects of land use transitions due to rapid urbanization on ecosystem services: Implications for urban planning in the new developing area of China. *Habitat International*, *44*, 536-544.
[4] Razdar, B, Ghavidel, A, and Pirouz, B (2010) the role of Numerical models in improvement the efficiency of surface water management, 13th National Congress on Environmental Health, Kerman, Iran
[5] Javadinejad, H, Kavianpour, M.R, Pirouz, B, (2014) Performance evaluation of rivers water quality with sustainable development and tourism point of view (Case study: Aras River), *First National Conference on Tourism, income and opportunity*, Hamadan, Iran
[6] Talarico V.C., Frega F., Palermo S.A., Piro P. (2018). Dall′indice di funzionalità fluviale (IFF) all′indice di qualità morfologica (IQM). Stato dell′arte dell′applicazione su alcuni corsi idrici del parco nazionale della Sila. In: Frega G. (ed.), Tecniche per la difesa del suolo e dall'inquinamento - *In Proceedings of 39° Corso di aggiornamento, Guardia Piemontese* (CS), IT, 20-23 June 2018, Edibios, (pp.403-411), ISBN: 978-88-97181-63-7.
[7] Piro, P., Carbone, M., Morimanno, F., & Palermo, S. A. (2019). Simple flowmeter device for LID systems: From laboratory procedure to full-scale implementation. *Flow Measurement and Instrumentation*, *65*, 240-249.
[8] Razdar, B, Ghavidel, A, Zoqi, M.J and Pirouz, B (2010) Impact Assessment of Urban Flood, First National Conference Management of urban floods, Tehran. Iran
[9] Fletcher, T. D., Shuster, W., Hunt, W. F., Ashley, R., Butler, D., Arthur, S., ... & Mikkelsen, P. S. (2015). SUDS, LID, BMPs, WSUD and more–The evolution and application of terminology surrounding urban drainage. *Urban Water Journal*, *12*(7), 525-542.
[10] Zischg, J., Zeisl, P., Winkler, D., Rauch, W., & Sitzenfrei, R. (2018). On the sensitivity of geospatial low impact development locations to the centralized sewer network. *Water Science and Technology*, *77*(7), 1851-1860.
[11] Palermo S.A., Zischg J., Sitzenfrei R., Rauch W., Piro P. (2019) Parameter Sensitivity of a Microscale Hydrodynamic Model. In: Mannina G. (eds) New Trends in Urban Drainage Modelling. UDM 2018. *Green Energy and Technology*. Springer, Cham.
[12] Fassman, E. A., & Blackbourn, S. (2010). Urban runoff mitigation by a permeable pavement system over impermeable soils. *Journal of Hydrologic Engineering*, *15*(6), 475-485.
[13] Berndtsson, J. C. (2010). Green roof performance towards management of runoff water quantity and quality: A review. *Ecological engineering*, *36*(4), 351-360.
[14] Li, D., Bou-Zeid, E., & Oppenheimer, M. (2014). The effectiveness of cool and green roofs as urban heat island mitigation strategies. *Environmental Research Letters*, *9*(5), 055002.
[15] Vijayaraghavan, K. (2016). Green roofs: A critical review on the role of components, benefits, limitations and trends. *Renewable and sustainable energy reviews*, *57*, 740-752.
[16] Maiolo, M., Carini, M., Capano, G., & Piro, P. (2017). Synthetic sustainability index (SSI) based on life cycle assessment approach of low impact development in the Mediterranean area. *Cogent Engineering*, *4*(1), 1410272.

[17] Turco, M., Brunetti, G., Carbone, M., & Piro, P. (2018). MODELLING THE HYDRAULIC BEHAVIOUR OF PERMEABLE PAVEMENTS THROUGH A RESERVOIR ELEMENT MODEL. *International Multidisciplinary Scientific GeoConference: SGEM: Surveying Geology & mining Ecology Management*, *18*, 507-514.
[18] Kuruppu, U., Rahman, A., & Rahman, M. A. (2019). Permeable pavement as a stormwater best management practice: a review and discussion. *Environmental Earth Sciences*, 78(10), 327.
[19] CHI PCSWMM. Available online: https://www.pcswmm.com/
[20] Palermo, M. (2018). Le reti di drenaggio urbano: caratteristiche, problematiche e soluzioni ingegneristiche innovative. *Bachelor Thesis*. Supervisor Patrizia Piro. Università della Calabria. Italia).
[21] Rossman, L. A. (2010). *Storm water management model user's manual, version 5.0* (p. 276). Cincinnati: National Risk Management Research Laboratory, Office of Research and Development, US Environmental Protection Agency.
[22] Palla, A., & Gnecco, I. (2015). Hydrologic modeling of Low Impact Development systems at the urban catchment scale. *Journal of hydrology*, *528*, 361-368.
[23] Ahiablame, L., & Shakya, R. (2016). Modeling flood reduction effects of low impact development at a watershed scale. *Journal of environmental management*, *171*, 81-91.
[24] Brunetti, G., Šimůnek, J., Turco, M., & Piro, P. (2018). On the use of global sensitivity analysis for the numerical analysis of permeable pavements. *Urban Water Journal*, *15*(3), 269-275.
[25] Piro, P., Turco, M., Palermo, S. A., Principato, F., & Brunetti, G. (2019). A Comprehensive Approach to Stormwater Management Problems in the Next Generation Drainage Networks. In *The Internet of Things for Smart Urban Ecosystems* (pp. 275-304). Springer, Cham.
[26] Arpacal, 2018. http://www.cfd.calabria.it/index.php/dati-stazioni/dati-storici

Acknowledgments

The first author would like to thank the CHI for the disposal of PCSWMM in the University Grant Program

This work considers the experimental permeable pavement and green roof funded by the Italian Operational Project (PON)—Research and Competitiveness for the convergence regions 2007/2013 — I Axis “Support to structural changes” operative objective 4.1.1.1. “Scientific-technological generators of transformation processes of the productive system and creation of new sectors” Action II: “Interventions to support industrial research”.

The authors would also to thank the Sila National Park Agency to have funded the research for the "Evaluation of the Morphological Quality Index (IQM) on some water bodies in the Sila National Park".

Paper VII

Green wall systems: where do we stand?

S. A. Palermo and M. Turco (2020)

Published in: IOP Conference Series: Earth and Environmental Science (Vol. 410, No. 1, p. 012013). IOP Publishing.
https://doi.org/10.1088/1755-1315/410/1/012013

Green Wall systems: where do we stand?

Green Wall systems: where do we stand?

S A Palermo[1] and M Turco[2]

[1] Department of Civil Engineering, University of Calabria, Italy
[2] Department of Environmental and Chemical Engineering, University of Calabria, Italy

E-mail address: stefania.palermo@unical.it

Abstract. In the last few years, the increase of impervious surfaces, due to ongoing urbanization and climate change led several environmental impacts such as: urban heat island effect, air pollution, urban flooding, deterioration of water discharged in the receiving water bodies, and so on. In this context, a sustainable strategy is required, and an innovative solution can be found in the implementation of low impact development (LID) systems as green walls. These sustainable solutions, by reintroducing vegetation in urban area, can partially restore the pre-urbanization situation and mitigate these drastic environmental impacts. To investigate the state of art of these techniques, a deeper overview on the green wall systems was carried out. This analysis was finalized to evaluate the current developed systems in terms of classification, components and benefits in order to establish where do we stand in terms of evolution of these systems and where we are going in terms of new trends and possible future directions.

Keywords: Climate Change, Review, Vertical Greening System, Green Facades, Living Wall

1. Introduction

The combined effect of uncontrolled urbanization and climate change is one of the most challenging problems of our time [1,2]. The drastically increase of urban heat island effect, air and water pollution, urban flooding, loss of ecosystems as well as human health and well-being can be considered the main environmental issues at global scale produced by these challenges. Only an innovative, sustainable, and ecologically based approach can meet all these impacts, which even if are different from each-other are strongly correlated.

Therefore, there is a growing attention of the governments to promote actions to develop sustainable cities and societies [3]. In this regard, a promising strategy is the implementation of nature-based solutions, also known as Low Impact Development systems (LID) or Green Infrastructures (GI), which reintroducing vegetation in areas highly urbanized, can restore the pre-development conditions and mitigate the impacts due to climate change and urbanization, providing several benefits at multiple scale [4-7].

Among these systems, green wall techniques, generally mentioned also as vertical greening/greenery systems, vertical garden, bio-walls, and so on, [8] can be considered as a sustainable strategy, that by using spaces otherwise unused, able to obtain beneficial effects from the building to the urban scale. Specifically, at building scale, by optimizing the benefits of plants species, they can be considered passive design solutions which improve thermal comfort both in winter and summer, thereby reducing

energy demand for heating and cooling [9,10]. In addition, the implementation of a green wall increases the value of the real estate and allow sound insulation; while at urban scale, these systems can enhance air quality, urban biodiversity, mitigate urban heat island effect [11,12]. They represent also a control source of stormwater management at urban catchment scale [13]. Moreover, from a social point of view, the implementation of vegetation on facades improve cities image and wellbeing, favouring the fruition of them [14].

Given their effectiveness from many points of view, several studies have been carried on these ecologically solutions. In this regard, here we present an overview on the papers published on green wall systems in order to: analyze the current state of art in terms of developed systems (components, materials and features), design and construction methods, systems benefits; evaluate the main differences, and establish where do we stand in terms of evolution of these techniques and where we are going in terms of new trends and possible future directions.

2. Green Wall systems: types and components

The green wall system represents one of the low impact development (LID) solutions able to increase the green spaces in urban area, aiming at enhancing the aesthetic value of the building and leading several benefits in terms of reduction of the environmental impacts caused by urbanization and climate change.

Since with the term "green wall system", we refer to each form of vegetation for facades, the first applications can be found 2500 years ago in the hanging Gardens of Babylon; similar examples were also in the Roman Empire. Many applications occurred over the centuries, until the 19th century, when these techniques were used in several European and North America cities, as ornamental elements and for thermal purposes [8,15,16].

Nowadays, with "green wall" we refer to a vegetative system which is, generally, developed along the façade of a building, consisting of different components, and it can be directly attached on the wall or supported by a structure [8,16].

To better identify the characteristics of the different green wall systems typologies, it is necessary to introduce the general functional elements of this technique, consisting of: (i) supporting elements; (ii) growing media; (iii) vegetation; (iv) drainage; and (v) irrigation. Based on the features of these elements and on the presence or absence of some of these, the green wall systems can be subdivided into two macro-categories: *Green Facades* (hereafter named GFs) (Fig. 1) and *Living Walls* (hereafter named LWs) (Fig.2) [8].

The *Green Facades (GFs)* are characterized by a low systemic technology, few constituent elements, and a limited level of integration between plants and walls. They are light, easy to install and, generally, aimed at supporting the natural development of plants, mainly climbing plants, that can have evergreen foliage or deciduous, and reach until 25 m of height, taking, however, some years for the full coverage of the wall [8].

In addition, as it is possible to observe in Figure 1, in function of the presence or absence of the supporting structure, the green facades can be differentiated into *direct GFs* and *indirect GFs* systems. In the first case the plants are directly attached to the wall; while the indirect GFs present a structural support for the growth of vegetation, generally consisting of continuous or modular guides (tensile cables, stainless steel, grids, etc.). This support structure leads several benefits: to prevent the falling of vegetation, to create an air gap between the surface of the building and the vegetation, to increase the system resistance to the environmental actions as rain, wind, snow, and so on. Moreover, for both systems, in case of very tall buildings or lack space at the base of the building, it is possible to use special boxes (Fig. 1b and 1d), placed at intermediate heights [8,15,16].

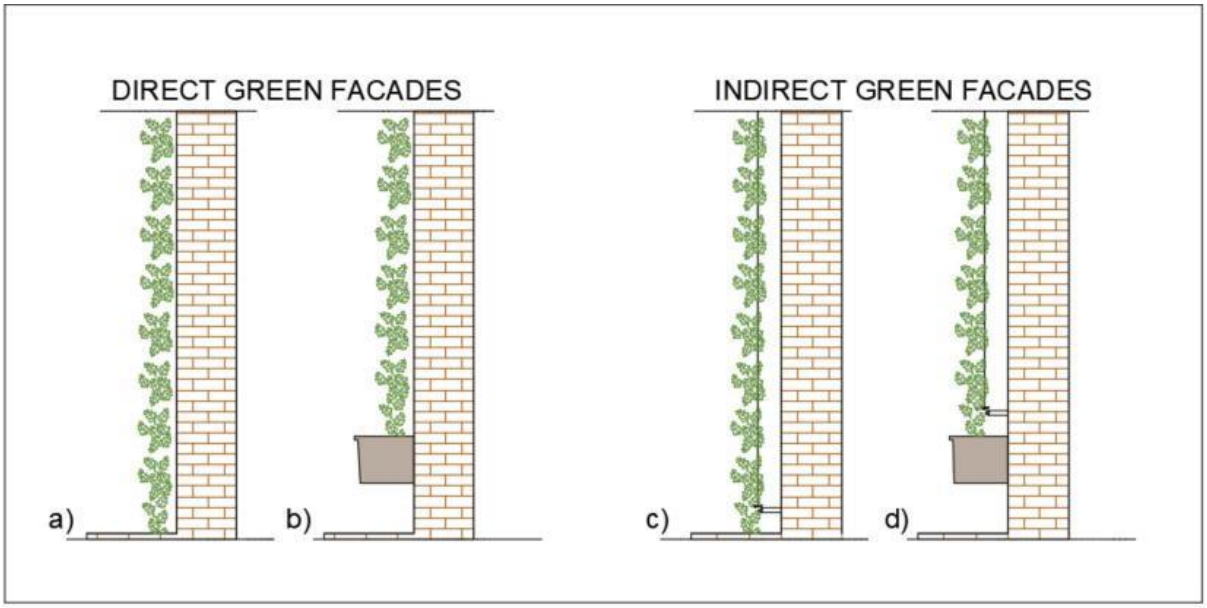

Figure 1. Different types of Green Facades: (a) Direct Green Facade with vegetation planted into the soil; (b) Direct Green Facade with plants rooted in the box; (c) Indirect Green Facade with vegetation planted into the soil; (d) Indirect Green Facades with plants rooted in the box.

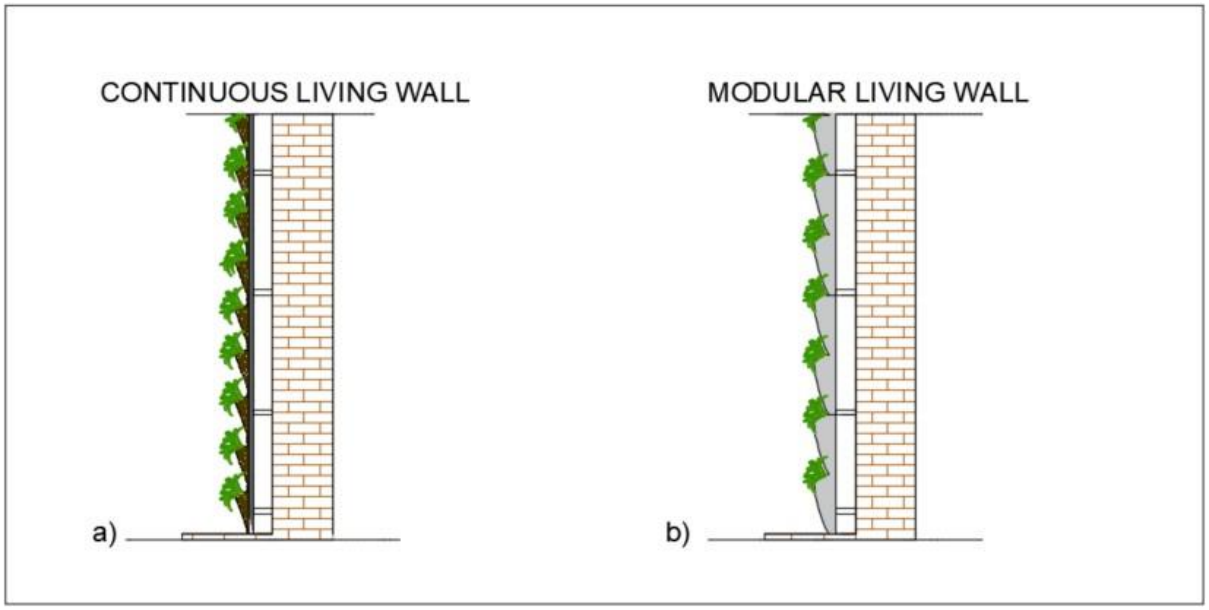

Figure 2. Different types of Living Walls: (a) Continuous Living Wall; (b) Modular Living Wall.

The *Living Walls (LWs)*, allowing the rapid coverage by vegetation of high building, represent a more recent innovation than the green facades. These types of green wall can use a wide variety of plants species (grasses, perennial plants, shrub, succulent, and so on), selected according to the climate condition, the drought tolerance, the root development, and specifically combined to achieve aesthetic effects [8].

Based on their application method, the LW systems can be *continuous* (Fig. 2a) or *modular* (Fig. 2b). More in detail, the *continuous LWs* do not require a substrate of soil, but the plants grow in lightweight and absorbent screens, as a fabric layer (i.e. felt), cut to form pockets. This layer is connected to different layers (permeable, flexible and root proof screens), supported by a base panel, directly attached to a

supporting structure, consisting of a frame indirectly fixed to the wall. These types of systems are mainly based on hydroponic technique [8,16,17]. The water supply is generally guaranteed by an irrigation system installed at the top of the structure, while the permeable layer ensures the uniform distribution of water and nutrients [8]. On the other hand, the *modular LWs* are characterized by pre-vegetated panels with specific supporting elements (vessels, trays, flexible bags, planter tiles) in which the plants grow. The growing media consists in an organic and/or inorganic substrate, which present a good retention capacity, and where the roots can proliferate. The irrigation system, according to the configuration of the supporting elements, is generally installed between the panels, and the water is drained through the panels for the entire facade and collected on the bottom [8,15].

Due to its specific feature the Modular LWs provide greater seeding depth than the continuous ones, and, allow easy maintenance in terms of replacing plant species [11,18].

By comparing the two main categories (GFs and LWs), in terms of installations cost, it is detected that although the LWs require much more materials than the GFs and, therefore, the costs are higher, they offer several benefits during the maintenance process. In fact, in case of unexpected problems, the LWs panels can be easily replaced or it is possible to provide a more rapid renewal of vegetation [8,19-22]. While, the direct GFs present the advantage to not require a supporting structure, but the disadvantage to employ a long period to cover the entire wall. The use of a supporting structure offers the benefits to have a space between the system and the wall, which could be used for insulation or maintenance purposes [8,23].

3. Green Wall Benefits: an overview

Green wall systems represent sustainable solutions to restore the environmental quality of urban areas by re-introducing vegetation. Due to their features, these systems provide several benefits at multiple scale.

Thus, in agreement with the European energy saving directions, that promote a rational and sustainable development starting by the building sector [24], several studies have proved the potential benefits of the green wall systems in terms of reduction of internal building temperatures and energy consumption, and mitigation of urban heat island effect [25]. In fact, since the plants function as a solar filter and prevent the adsorption of heat radiation, the use of greening systems produces a strong effect on the thermal performance of buildings and on the urban environment [19].

In this regard, Eumorfopoulou and Kontoleon [26] have evaluated the thermal analysis of two equal building floors (one with bare surface and one plant-covered surface). The findings have shown the importance of the contribution on the thermal behaviour of plant-covered wall sections in densely populated urban areas in Mediterranean region during the cooling period.

The same authors, the year after, presented another work on how the wall orientation, the wall plant foliage percentage, and the type of wall configuration can affect the thermal behaviour of typical building located in the northern Greek region during the summer period [20]. The results, obtained by using a validated thermal-network model, were: a superior thermal comfort conditions within the building zone that included a plant-covered wall; an increase of thermal benefits when there was more percentage of plant foliage; benefits in terms of energy conservation of a plant-covered wall, which allowed to improve the microclimate around the built environment by neutralizing the solar impact.

During the same year, Cheng et al. [27] used an experimental approach to assess the effect of vegetation on the thermal performance of a vertical greening system, obtaining that the vegetated cladding reduced interior temperatures and delayed the transfer of solar heat. Therefore, the implementation of the green system decreased power consumption in air-conditioning compared with a building with bare concrete.

While in another work, Wong et al. [9] showed the potential thermal benefits of eight vertical greenery systems, located in HortPark, to reduce the surface temperature of buildings facades in the tropical climate, and decrease the cooling load and energy cost.

In 2011, Jim and He [28] evaluated the thermodynamic transmission process of the vertical greenery ecosystem, by designing a field experiment and developing a thermodynamics transmission model. The results showed that: the green wall radiation transmission was strongly correlated with canopy transmittance and reflectance; the thermal shielding effectiveness depended on the orientation; due to the presence of the vertical greenery ecosystem and, therefore, its more intensive evapotranspiration effect, the south wall could transfer much more heat flux.

The same year, Perini et al. [19] analyzed the possible reduction of the wind velocity and (air and surface) temperature by three different green wall systems in the Netherlands: (1) direct façade greening (Delft); (2) Indirect façade greening system (Rotterdam); Living wall system (Benthuizen). The findings showed not difference in the air temperature and wind profiles starting from 1 m in front of the façades until inside the foliage. Moreover, the investigated systems could be considered effective natural sunscreens; a low wind velocity was monitored inside the air cavity of the Living Wall and inside the foliage of the direct and indirect systems. In addition, due the reduction of wind velocity, the exterior surface resistance could be equalized to the interior one and, therefore, affect the total thermal resistance with results in terms of energy savings.

Mazzali et al. [29] monitored three Living Wall field tests in different climate context located in Mediterranean temperate region (at latitudes corresponding to Northern and Central Italy) to investigate the potential effects of the energy behaviour on building envelopes. The analysis revealed a temperature difference between the bare wall and the covered wall ranging between a minimum of 12 °C (for the living wall located in Lonigo) and a maximum of 20 °C (for the living wall located in Pisa), during sunny days. In addition, the analysis on the heat flux showed how these systems can significantly contribute to cooling energy reduction.

Coma et al. [30], by comparing the thermal performance of two experimental vertical greenery systems (a double -skin green facade with deciduous creeper plants and a designed green wall with evergreen species), obtained a high potential energy savings for green wall (58.9%) and double-skin green facade (33.8%) in comparison to a reference system during the cooling season, and no extra energy consumption for evergreen system during heating periods.

In the Jubilee Campus of University of Nottingham, by an experimental and numerical investigation on the thermal regulation feature of green wall systems located at the University, Cuce [25] obtained an average of 2.5°C temperature reduction in internal wall for green walls with around 10 cm thickness climbing vegetation of Hedera helix

To investigate the potential benefits of green walls as passive tool for energy saving, Perez et al. [31] investigated a double-skin green facade implemented in an experimental site in Mediterranean continental climate. The experimental findings showed the high potential of the green system as a passive system in comparison to the reference conventional site, obtaining an energy saving up to 34% with a leaf area index of 3.5-4. In addition, the results showed that, since the shadow effect of green facades on the East and West orientations was representative, this should be considered as well as that one of South orientation.

Another study, carried out by Tudiwer and Korjenic [32], analyzed the influence of two greened façades on the thermal resistance of the walls, by developing a method to evaluate the U-value at greened facades. The results showed: a lower temperature on the surface without vegetation in the winter, even for south orientation; the greening reduced the fluctuation rate of the surface temperature and the heat flux; the difference of the thermal between vegetated and not vegetated sections in winter ranged between 0.31 m^2K/W and 0.68 m^2K/W.

In Mediterranean climate, Perini et al. [10] evaluated the cooling potential during the summer season of a vertical greening system built in Genoa (Italy). The findings showed that a green layer can decrease outdoor and surface temperature, improving thermal comfort and the building surfaces heating and, thus contributing also to urban heat island mitigation. In addition, the presence of vertical greening system allowed a reduction of cooling demand of 26% during summer.

In another study, Galagoda et al. [33] quantified the thermal performance, the relative humidity and the CO2 concentration for three types of green infrastructures: living walls, indirect green façades and

direct green façades located in Colombo metropolitan in Sri Lanka. Comparing the results with the bare wall, they obtained a maximum temperature reduction of 8.0 °C - 0.28 °C for the living wall, 7.86 °C - 1.34 °C for the indirect green facades, and 6.64 °C - 1.34 °C for the direct green facades. In addition, the study showed an averaged relative humidity increase of 1.6%–1.81% and a CO2 reduction of 0.63% near green walls. Then, the authors demonstrated the capability of these systems on micro climatic changes and human thermal comfort. The green walls were able to reduce 2.4 °C at indoors compared to bare wall building; an energy saving of 10.97 MW was obtained; and, finally, a positive perception of 79% of people, a thermal comfort by 58% of inhabitants, a visually comfort of 89.5%, a satisfied about the light penetration level of the vertical greening systems of 61% occupants, were reached.

As it was possible observed, the benefits in terms of energy saving (for reduction of air conditioning demand) is strongly correlated to the economic sustainability of the green wall system. In this regard, Rosasco and Perini [34] carried out a Cost-Benefits Analysis on the vertical greening system, installed at Genoa (Italy), in order to evaluate its economic sustainability. The findings revealed that the system can be economically sustainable when a tax reduction on installation costs is considered. In addition, by a sensitivity analysis they found how the optimal choice of the materials and technological solutions during the design phase is relevant to reduce the installation and maintenance costs.

In addition, from the overview carried out, it is emerged that the vertical greenery system can be also considered a Key element to mitigate the noise pollution. In this regard, Wong et al. [35] evaluated the acoustics impacts of eight different vertical greenery systems installed in HortPark, Singapore on the on the insertion loss of building walls. Furthermore, they determined the sound absorption coefficient of a vertical greenery system developed in the reverberation chamber of National University of Singapore. The results of first part of the study showed a higher attenuation at low to middle frequencies due to the absorbing effect of substrate; while at higher frequencies, a smaller attenuation was observed due to scattering from vegetation. During the second part of the study, they determined the sound absorption coefficient which resulted one of the highest values compared with other materials and obtained that this coefficient increased with the frequencies and with greater greenery coverage.

To evaluate the benefits of these systems in terms of mitigation of impacts due to climate change, another environmental aspect was considered. The green walls systems, like green roofs or rain gardens, are low impact development solution that can be considered sustainable tools able to restore the pre-urbanization hydrological natural cycle and, thus mitigate urban flooding risk. In literature, the benefits of these solutions in terms of runoff mitigation were not widely investigated as well as the other LID solutions (green roof or rain garden). In this regard, Lau and Mah [13] studied the green wall hydrological effectiveness, by developing a USEPA SWMM model, that considers the green wall system as a portion of urban drainage system. More in detail, the study is based on a modelling implementation of a modular green wall system on the commercial building in Central City, Kota Samarahan. They carried out four simulation models, characterized of different conditions (soil texture classes: sand, loamy sand, sandy loam and loam) and precipitation input. The findings confirmed that green wall systems can be effectively considered for reducing surface runoff.

Moreover, to better investigate the environmental impacts of green wall techniques, a comparative life cycle analysis (LCA) was carried out by Ottelé et al. [17] for Mediterranean and Temperate climate condition. They considered different facades: a conventional bare wall (brick), a direct green façade, an indirect green façade, a living wall system based on planter boxes and another living wall system based on felt layers. The results revealed that, due to the reduction in energy demand for heating, even if additional resources needed, the direct greening system, the indirect greening system (with hard wood, coated steel or HDPE as supporting system) and the living wall system based on planter boxes represented a good environmentally choice.

Finally, starting by the concept of "reconciliation ecology", Francis e Lorimer [12] evaluated the reconciliation potential of living roofs and walls, by observing that: the successful implementation of these ecological engineering techniques is strongly related to the participation of urban citizens; and these systems are important solutions to enhance urban biodiversity.

In conclusion, based on the analysis carried out, the green wall system can contribute significant environmental, social and economic benefits for the built environment. From the overview, it is highlighted the difficulty to compare studies which consider different construction system, climate, plants species, and other parameters (as orientation, thickness, etc.). However, the analysis allowed to evaluate the scientific gap on the green wall system in terms of the performance evaluations and investigate the new trends and future directions.

4. New trends and future directions in green wall technology

In the last few years, new several applications encouraged the growth of green wall techniques as tool for energy saving and this was deeper demonstrated in the previous overview.

However, as green infrastructures, these systems, like green roofs or rain gardens, can be valuable engineering solutions to reduce the stormwater discharged into the drainage systems, mitigating thus the urban flooding risk. But, from the literature review, it is emerged that green walls were little investigated as elements able to reduce the runoff in urban environment. For example, Studies on the laboratory analysis of the retention capacity of green walls soil substrates, were not find, as well as experimental and numerical investigations on the hydraulic efficiency of these systems at urban scale. Based on this background, future scientific trends could focus on the investigation of the hydraulic performance of green walls both by developing experimental lab analysis and modelling the flow inside the porous media and evaluating the hydrological efficiency of these systems from the building scale to the catchment. In addition, another innovative element, in the field of water management, could be the optimal integration of a green wall system with a rainwater harvesting system. The rainwater harvesting system could provide the irrigation to the green wall, by reusing the water discharged from the system itself. In addition, given the potential of vegetation, these systems could be further investigated as tool to mitigate water pollution.

Finally, a further green wall optimization at multiple scales could be achieved, by developing smart façade systems, i.e. façades that dynamically respond to the demands and conditions received by the external environment. In this direction, for example it could be possible to optimize the green wall irrigation, monitoring the soil humidity and the inside and outside building temperature.

Therefore, it is expected that the research on green walls will increase, by focusing the attention also on the benefits and implications not still deeper investigated.

In this regard, the study, here presented, is a part of the analysis carried out during the project "Innovative Building Envelope through Smart Technology (I-Best)", developing at University of Calabria (Italy) in Mediterranean climate. This project involves, as one of the objectives, the experimental analysis, the modelling development and the full scale implementation of an innovative modular green wall system, aimed at decreasing urban flooding risk, achieving water saving, reducing water pollution, enhancing biodiversity, and mitigating other environmental impacts due to climate change.

Acknowledgments

The study was funded by the "Innovative Building Envelope through Smart Technology (I-Best)" Project funded by the Italian National Operational Program "Enterprise and Competitiveness" 2014-2020 ERDF – I AXIS "Innovation" - Action 1.1.3 – "Support for the economic enhancement of innovation through experimentation and the adoption of innovative solutions in processes, products and organizational formulas, as well as through the financing of the industrialization of research results".

References

[1] Piro, P., Carbone, M., Morimanno, F., & Palermo, S. A. (2019). Simple flowmeter device for LID systems: From laboratory procedure to full-scale implementation. *Flow Measurement and Instrumentation*, 65, 240-249. https://doi.org/10.1016/j.flowmeasinst.2019.01.008

[2] Maiolo, M., Carini, M., Capano, G., & Piro, P. (2017). Synthetic sustainability index (SSI) based on life cycle assessment approach of low impact development in the Mediterranean area. *Cogent Engineering*, 4(1), 1410272. https://doi.org/10.1080/23311916.2017.1410272

[3] Mazzeo, D., Baglivo, C., Matera, N., Congedo, P. M., & Oliveti, G. (2019). A novel energy economic-environmental multi-criteria decision-making in the optimization of a hybrid renewable system. *Sustainable Cities and Society*, 101780. https://doi.org/10.1016/j.scs.2019.101780

[4] Palermo S.A., Zischg J., Sitzenfrei R., Rauch W., Piro P. (2019) Parameter Sensitivity of a Microscale Hydrodynamic Model. In: Mannina G. (eds) New Trends in Urban Drainage Modelling. UDM 2018. *Green Energy and Technology*. Springer, Cham. https://doi.org/10.1007/978-3-319-99867-1_169

[5] Zischg, J., Zeisl, P., Winkler, D., Rauch, W., & Sitzenfrei, R. (2018). On the sensitivity of geospatial low impact development locations to the centralized sewer network. *Water science and technology*, 77(7), 1851-1860. https://doi.org/10.2166/wst.2018.060

[6] Turco M., Brunetti G., Porti M., Grossi G., Maiolo M., Piro P. (2019) Metals Potential Removal Efficiency of Permeable Pavement. In: Mannina G. (eds) New Trends in Urban Drainage Modelling. UDM 2018. *Green Energy and Technology*. Springer, Cham https://doi.org/10.1007/978-3-319-99867-1_29

[7] Piro P., Turco M., Palermo S.A., Principato F., Brunetti G. (2019) A Comprehensive Approach to Stormwater Management Problems in the Next Generation Drainage Networks. In: Cicirelli F., Guerrieri A., Mastroianni C., Spezzano G., Vinci A. (eds) The Internet of Things for Smart Urban Ecosystems. *Internet of Things (Technology, Communications and Computing).* Springer, Cham. https://doi.org/10.1007/978-3-319-96550-5_12

[8] Manso, M., & Castro-Gomes, J. (2015). Green wall systems: a review of their characteristics. *Renewable and Sustainable Energy Reviews*, 41, 863-871. https://doi.org/10.1016/j.rser.2014.07.203

[9] Wong, N. H., Tan, A. Y. K., Chen, Y., Sekar, K., Tan, P. Y., Chan, D.,& Wong, N. C. (2010). Thermal evaluation of vertical greenery systems for building walls. *Building and environment*, 45(3), 663-672. https://doi.org/10.1016/j.buildenv.2009.08.005

[10] Perini, K., Bazzocchi, F., Croci, L., Magliocco, A., & Cattaneo, E. (2017). The use of vertical greening systems to reduce the energy demand for air conditioning. Field monitoring in Mediterranean climate. *Energy and Buildings*, 143, 35-42. https://doi.org/10.1016/j.enbuild.2017.03.036

[11] Hadba, L., Mendonça, P., & Silva, L. T. (2017). Green walls: an efficient solution for hygrothermal, noise and air pollution control in the buildings. In *Living and Sustainability: An Environmental Critique of Design and Building Practices, Locally and Globally*. AMPS, Architecture_MPS. London South Bank University.

[12] Francis, R. A., & Lorimer, J. (2011). Urban reconciliation ecology: the potential of living roofs and walls. *Journal of environmental management*, 92(6), 1429-1437. https://doi.org/10.1016/j.jenvman.2011.01.012

[13] Lau, J. T., & Mah, D. Y. S. (2018). Green Wall for Retention of Stormwater. *Pertanika Journal of Science and Technology*, 1, 283.

[14] Sheweka, S., & Magdy, A. N. (2011). The living walls as an approach for a healthy urban environment. *Energy Procedia*, 6, 592-599. https://doi.org/10.1016/j.egypro.2011.05.068

[15] Dunnett, N., & Kingsbury, N. (2008). Planting green roofs and living walls. Portland, OR: Timber press.

[16] Baran Y., Gültekin A.B. (2018) Green Wall Systems: A Literature Review. In: Fırat S., Kinuthia J., Abu-Tair A. (eds) *Proceedings of 3rd International Sustainable Buildings Symposium* (ISBS 2017). ISBS 2017. Lecture Notes in Civil Engineering, vol 7. Springer, Cham. https://doi.org/10.1007/978-3-319-64349-6_8
[17] Ottelé, M., Perini, K., Fraaij, A. L. A., Haas, E. M., & Raiteri, R. (2011). Comparative life cycle analysis for green façades and living wall systems. *Energy and Buildings*, 43(12), 3419-3429. https://doi.org/10.1016/j.enbuild.2011.09.010
[18] Amorim, F., & Mendonça, P. (2017). Advantages and Constraints of Living Green Façade Systems. *International Journal of Environmental Science and Development*, 8(2), 124-129.
[19] Perini, K., Ottelé, M., Fraaij, A. L. A., Haas, E. M., & Raiteri, R. (2011). Vertical greening systems and the effect on air flow and temperature on the building envelope. *Building and Environment*, 46(11), 2287-2294.https://doi.org/10.1016/j.buildenv.2011.05.009
[20] Kontoleon, K. J., & Eumorfopoulou, E. A. (2010). The effect of the orientation and proportion of a plant-covered wall layer on the thermal performance of a building zone. *Building and environment*, 45(5), 1287-1303. https://doi.org/10.1016/j.buildenv.2009.11.013
[21] Raji, B., Tenpierik, M. J., & van den Dobbelsteen, A. (2015). The impact of greening systems on building energy performance: A literature review. *Renewable and Sustainable Energy Reviews*, 45, 610-623. https://doi.org/10.1016/j.rser.2015.02.011
[22] Besir, A. B., & Cuce, E. (2018). Green roofs and facades: A comprehensive review. *Renewable and Sustainable Energy Reviews*, 82, 915-939. https://doi.org/10.1016/j.rser.2017.09.106
[23] Omrany, H., Ghaffarianhoseini, A., Ghaffarianhoseini, A., Raahemifar, K., & Tookey, J. (2016). Application of passive wall systems for improving the energy efficiency in buildings: A comprehensive review. *Renewable and sustainable energy reviews*, 62, 1252-1269. https://doi.org/10.1016/j.rser.2016.04.010
[24] Bruno, R., Bevilacqua, P., Cuconati, T., & Arcuri, N. (2019). Energy evaluations of an innovative multi-storey wooden near Zero Energy Building designed for Mediterranean areas. *Applied energy*, 238, 929-941. https://doi.org/10.1016/j.apenergy.2018.12.035
[25] Cuce, E. (2017). Thermal regulation impact of green walls: An experimental and numerical investigation. *Applied energy*, 194, 247-254. https://doi.org/10.1016/j.apenergy.2016.09.079
[26] Eumorfopoulou, E. A., & Kontoleon, K. J. (2009). Experimental approach to the contribution of plant-covered walls to the thermal behaviour of building envelopes. *Building and Environment*, 44(5), 1024-1038. https://doi.org/10.1016/j.buildenv.2008.07.004
[27] Cheng, C. Y., Cheung, K. K., & Chu, L. M. (2010). Thermal performance of a vegetated cladding system on facade walls. *Building and environment*, 45(8), 1779-1787. https://doi.org/10.1016/j.buildenv.2010.02.005
[28] Jim, C. Y., & He, H. (2011). Estimating heat flux transmission of vertical greenery ecosystem. *Ecological Engineering*, 37(8), 1112-1122. https://doi.org/10.1016/j.ecoleng.2011.02.005
[29] Mazzali, U., Peron, F., Romagnoni, P., Pulselli, R. M., & Bastianoni, S. (2013). Experimental investigation on the energy performance of living walls in a temperate climate. *Building and Environment*, 64, 57-66. https://doi.org/10.1016/j.buildenv.2013.03.005
[30] Coma, J., Pérez, G., de Gracia, A., Burés, S., Urrestarazu, M., & Cabeza, L. F. (2017). Vertical greenery systems for energy savings in buildings: A comparative study between green walls and green facades. *Building and environment*, 111, 228-237. https://doi.org/10.1016/j.buildenv.2016.11.014
[31] Pérez, G., Coma, J., Sol, S., & Cabeza, L. F. (2017). Green facade for energy savings in buildings: The influence of leaf area index and facade orientation on the shadow effect. *Applied energy*, 187, 424-437. https://doi.org/10.1016/j.apenergy.2016.11.055
[32] Tudiwer, D., & Korjenic, A. (2017). The effect of living wall systems on the thermal resistance of the façade. *Energy and Buildings*, 135, 10-19. https://doi.org/10.1016/j.enbuild.2016.11.023

[33] Galagoda, R. U., Jayasinghe, G. Y., Halwatura, R. U., & Rupasinghe, H. T. (2018). The impact of urban green infrastructure as a sustainable approach towards tropical micro-climatic changes and human thermal comfort. *Urban forestry & urban greening*, 34, 1-9. https://doi.org/10.1016/j.ufug.2018.05.008

[34] Rosasco, P., & Perini, K. (2018). Evaluating the economic sustainability of a vertical greening system: A Cost-Benefit Analysis of a pilot project in mediterranean area. *Building and Environment*, 142, 524-533. https://doi.org/10.1016/j.buildenv.2018.06.017

[35] Wong, N. H., Tan, A. Y. K., Tan, P. Y., Chiang, K., & Wong, N. C. (2010). Acoustics evaluation of vertical greenery systems for building walls. *Building and Environment*, 45(2), 411-420. https://doi.org/10.1016/j.buildenv.2009.06.017

Paper VIII

Optimizing rainwater harvesting systems for non-potable water uses and surface runoff mitigation

Palermo, S. A., Talarico, V. C., & Pirouz, B. (2020b)

Published in: Sergeyev Y., Kvasov D. (eds) Numerical Computations: Theory and Algorithms. NUMTA 2019. Lecture Notes in Computer Science, vol 11973. Springer, Cham.
https://doi.org/10.1007/978-3-030-39081-5_49

Optimizing Rainwater Harvesting Systems for Non-potable Water Uses and Surface Runoff Mitigation

Stefania Anna Palermo[1(✉)], Vito Cataldo Talarico[1], and Behrouz Pirouz[2]

[1] Department of Civil Engineering, University of Calabria, Rende, CS, Italy
{stefania.palermo, vitocataldo.talarico}@unical.it
[2] Department of Mechanical, Energy and Management Engineering, University of Calabria, Rende, CS, Italy
behrouz.pirouz@unical.it

Abstract. Rainwater harvesting systems represent sustainable solutions that meet the challenges of water saving and surface runoff mitigation. The collected rainwater can be re-used for several purposes such as irrigation of green roofs and garden, flushing toilets, etc. Optimizing the water usage in each such use is a significant goal. To achieve this goal, we have considered TOPSIS (Technique for Order Preference by Similarity to Ideal Solution) and Rough Set method as Multi-Objective Optimization approaches by analyzing different case studies. TOPSIS was used to compare algorithms and evaluate the performance of alternatives, while Rough Set method was applied as a machine learning method to optimize rainwater-harvesting systems. Results by Rough Set method provided a baseline for decision-making and the minimal decision algorithm were obtained as six rules. In addition, The TOPSIS method ranked all case studies, and because we used several correlated attributes, the findings are more accurate from other simple ranking method. Therefore, the numerical optimization of rainwater harvesting systems will improve the knowledge from previous studies in the field, and provide an additional tool to identify the optimal rainwater reuse in order to save water and reduce the surface runoff discharged into the sewer system.

Keywords: Rainwater harvesting · Water supply · Flood risk mitigation

1 Introduction

There are many benefits in Rainwater harvesting (RWH) systems mainly water saving for non-potable water uses and surface runoff mitigation. Moreover, the collected rainwater can be re-used for several purposes including green roofs and garden, flushing toilets, etc. In previous studies, the optimization of rainwater harvesting systems was mostly limited to optimum size of the tankers according to hydrological and hydraulic analysis and in some cases combined with economic analysis.

However, the design of RWH systems depends on many elements and even optimizing different water usages is significant. Therefore, in this paper, Multi-Objective Optimization approaches have been applied, and ranking methods such as TOPSIS

Y. D. Sergeyev and D. E. Kvasov (Eds.): NUMTA 2019, LNCS 11973, pp. 570–582, 2020.
https://doi.org/10.1007/978-3-030-39081-5_49

(Technique for Order Preference by Similarity to Ideal Solution) have been considered to compare algorithms and evaluate the performance of alternatives to reach the ideal solution. Moreover, the attributes analysis such as Rough Set method has been used in analysis of vague description of decisions.

1.1 Rainwater Harvesting (RWH) Systems

The combined effect of global urbanization, climate change and water scarcity, requires a transition towards a sustainable, smart and resilient urban water management. In this regard, nowadays the sustainability concept is a basilar element for scientific, technical and socio-economic discussion. Therefore, the implementation of decentralized stormwater controls systems, as LID (Low Impact Development) systems, represents a promising strategy to achieve several benefits at multiple scales [1, 2].

Among these techniques, Rainwater Harvesting (RWH), considered an ancient practice used all over the world to meet the water demand, is now supported by many countries as a suitable solution to limit potable water demand, reduce frequency, peaks and volumes of stormwater runoff at the source, and participate in the restoration of natural hydrological cycle [3–6].

The principal component of a conventional RWH system is the rainwater tank which temporally stores the water from a capturing surface, normally the building roof or others impervious surfaces closely to the building. In a single-family building, above-ground tank, named "rain barrels", are generally used for irrigation and runoff control, while, in the case of multi-story building, above or below-ground concrete cisterns are implemented. In addition, a system consisting of gutters and downspouts lead the runoff from the collecting surface to the tank, while a dedicated piping network is needed for rainwater reuse. One or more pumps can be used to assure the pressure head for different usages, while other devices as first flus diverters, debris screen, and filters are generally implemented for water quality control. These information and more specific detail regarding this technique can be found in several studies [4, 7, 8].

Recent advances have showed the possibility for real-time monitoring and control of these systems in order to increase their efficiency in terms of reduction of urban flooding or combined sewer overflows [9] and optimize the rainwater reuse.

Harvested rainwater can be considered a renewable water source that is perfect for different non-potable water uses, as toilet flushing, laundry, car washing, terrace cleaning, private garden irrigation and green roof irrigation [7, 10–15].

In addition, as source control technology distributed at urban catchment scale, these systems are suitable to reduce stormwater runoff volume. In this regard, several studies have evaluated also the hydrological efficiency of RWH in terms of reduction of the runoff volume and peak discharged to the sewer system [5, 7, 11, 14, 16].

Several studies have been carried out to show the RWH efficiency for water saving and runoff mitigation, as study of Campisano and Modica [11] showed that the performance depends of site-specific factors, such as roof type and surface, precipitation regime, demand usage, tank size, number of people in the household, etc.

Based on a deeper literature review, in this paper some factors, here after called "attributes" have been selected and considered in a mathematical optimization of RWH.

2 Methodology

In the current study, the Rough Set method applied as a machine learning method to optimize rainwater-harvesting systems. The process is reviewed in details and the result is achieved with analysis of different case studies.

2.1 Rough Set Theory

The Rough Set theory is attributes analysis based on data or knowledge about a decision. The results of analysis can provide clear rules for similar decisions [17–19]. The Rough Set rules in a given approximation space apr = (U, A) can be calculated as follow:

$$\text{The lower approximations of X in A} \qquad \overline{apr}(\mathrm{A}) = \{\mathrm{x} \mid \mathrm{x} \in \mathrm{U},\ \mathrm{U/ind}\,(\mathrm{A}) \subset \mathrm{X}\} \quad (1)$$

$$\text{The upper approximations of X in A} \qquad \underline{apr}(\mathrm{A}) = \{\mathrm{x} \mid \mathrm{x} \in \mathrm{U},\ \mathrm{U/ind}\,(\mathrm{A}) \cap \mathrm{X} \neq \varphi\} \quad (2)$$

$$\mathrm{U/ind}\,(\mathrm{a}) = \{(\mathrm{xi}\,,\ \mathrm{xj}\,) \in \mathrm{U} \times \mathrm{U},\ \mathrm{f}\,(\mathrm{xi}\,, \mathrm{a}) = \mathrm{f}\,(\mathrm{xj}\,, \mathrm{a}), \forall \mathrm{a} \in \mathrm{A}\} \quad (3)$$

$$\text{Boundary is BN}\,(\mathrm{A}) = \overline{apr}(\mathrm{A}) - \underline{apr}(\mathrm{A}) \quad (4)$$

$$\text{The reduct} = \text{minimal set of attributes B} \subseteq \text{A such that } \mathrm{r_B}(\mathrm{U}) = \mathrm{r_A}(\mathrm{U}) \quad (5)$$

$$\text{The quality of approximation of U by B} \qquad r_B(\mathrm{U}) = \frac{\sum card(\underline{B}(X_i))}{card(U)} \quad (6)$$

$$\text{Decision rule is } \varphi \Rightarrow \theta \quad (7)$$

Where:

U is a set,
A is attributes of the set,
φ is the conjunction of elementary conditions,
θ is the disjunction of elementary decisions.

2.2 TOPSIS Method

TOPSIS (Technique for Order Preference by Similarity to Ideal Solution) method developed by Hwang and Yoon in 1981 is a method to solve the ranking and comparing decisions [20–22] and can be applied to wide range of multi-attribute decision making with several attributes [22–24]. The ranking in this method can be done for matrix $(n_{ij})m \times n$ according to the similarity to ideal solution as follow:

$$\text{Normalized decision matrix: } N = n_{ij} = \frac{a_{ij}}{\sqrt{\sum_{i}^{m} = 1 a_{ij}^2}}, \text{i} = 1, 2, \ldots, \text{m}, \text{j} = 1, 2, \ldots, \text{n} \quad (8)$$

$$\text{Weighted normalized decision matrix: V} = \text{N} \times \text{Wn} \times \text{n} \quad (9)$$

Determining the solutions:

$$\text{Ideal solution: } A^{+} = \left\{ \left\langle max_i \left(a_{ij} | j \in J_{-} \right) \right\rangle, \left\langle min_i \left(a_{ij} | j \in J_{+} \right) \right\rangle \right\} \quad (10)$$

$$\text{Negative-ideal solutions: } A^{-} = \left\{ \left\langle min_i \left(a_{ij} | j \in J_{-} \right) \right\rangle, \left\langle max_i \left(a_{ij} | j \in J_{+} \right) \right\rangle \right\} \quad (11)$$

$J_{+} = \{ j = q, 2, \ldots, n | j \}$ Associated with positive impact criteria
$J_{-} = \{ j = q, 2, \ldots, n | j \}$ Associated with negative impact criteria
Determining the distances from the solutions:

$$\text{Distance from ideal solution: } d_i^{+} = \sqrt{\sum_{j=1}^{n} \left(v_{ij} - v_j^{+} \right)}, \quad \text{i} = 1, 2, \ldots, \text{m} \quad (12)$$

$$\text{Distance from negative-ideal solution: } d_i^{-} = \sqrt{\sum_{j=1}^{n} \left(v_{ij} - v_j^{+} \right)}, \quad \text{i} = 1, 2, \ldots, \text{m} \quad (13)$$

Ranking in order to the highest closeness to the negative-ideal condition:

$$CL_i^{*} = \frac{d_i^{-}}{d_i^{-} + d_i^{+}}, \quad 0 \leq CL_i^{*} \leq 1 \ \& i = 1, 2, \ldots, m \quad (14)$$

2.3 Case Studies

To carry the analysis by rough set and TOPSIS a set of data is required such as case studies. The selection of the case studies has been done in a way that considers the main possible attributes/factors confronting in rainwater harvesting systems. The first and second case studies (CS1–CS2) are taken from the study carried out by Herrmann and Schimida [7] that considers the development and performance of rainwater utilization systems in Germany, and specifically in Bochum where the mean annual precipitation is 787 mm. More in detail, the data considered there for CS1, are related to a one-family house (with an effective roof area of 150 m^2, 4 persons, combined demand of 160 l/d, a storage volume of 6 m^3 and an additional retention volume of 15 m^3, with a covering efficiency of 98%). The CS2 case refers to a multi-story building (CS2) (with an effective roof area of 320 m^2, 24 persons, toilet flushing demand of 480 l/d, a storage volume of 14 m^3 and an additional retention volume of 35 m^3).

A study carried out by Domènech and Saurí [13] was considered to select the third (CS3) and the fourth (CS4) case study. Both case studies are in Sant Cugant del Vallès – Spain. More in detail, CS3 is a single-family house with a rooftop catchment area of

107 m^2, 3 residents, a toilet and laundry usage demand of 27 LCD and 16 LCD, respectively. While CS4 refers to a multi-family building with a rooftop catchment area of 625 m^2, 42 residents, a toilet and laundry usage demand of 30 LCD and 16 LCD, respectively. For CS3, we considered a model scenario in which a tank of 13 m^3 can meet 80% of the combined demand of toilet flushing and laundry; while for CS4 the model scenario is a tank of 31 m^3 covering 59.5% of the combined demand of toilet flushing and laundry.

Case studies CS5, CS6 and CS7 are considered from the study of Palla et al. [5]. These three case studies are located in Genoa (Italy) with a mean annual precipitation of 1340 mm. More in detail, CS5 is a 4-flat house with 16 inhabitants, a roof area of 420 m^2, an annual toilet flushing demand of 233.6 m^3/y and a tank capacity of 14 m^3. CS6 is a 6-flat house with 24 inhabitants, a roof area of 420 m^2, an annual toilet flushing demand of 350.4 m^3/y and a tank capacity of 21 m^3. CS7 is a condominium with 32 inhabitants, a roof area of 680 m2, an annual toilet flushing demand of 467.2 m^3/y and a tank capacity of 28 m^3. For the three case studies, the modeling results show a water saving efficiency of 0.83, 0.79 and 0.76 for CS5, CS6 and CS7, respectively.

The CS8 case study considers the values of the example of application found in Campisano and Modica [25], where a 4 people residential house with a daily toilet flushing demand of 0.168 m^3, a roof area of 186 m^2, daily precipitation of 0.0018 m and a size tank of 2.93 m^3, achieving a water saving of 67%, was considered.

The CS9 case study refers to a real case study at University of Calabria in Southern Italy [15], where a tank of 1.5 m^3 is located at the base of an university building to collect the water for an experimental full-scale green roof implementation and the water is reused to irrigate the same green roof in the dry period. Finally, three hypothetical cases, CS10, CS11 and CS12, have been considered to evaluate remain factors under different conditions. Specifically, CS10 represent the hypothetical implementation of RWH systems in the old town of Cosenza, CS11 in the old town of Matera, and CS12 in the new area of Quattromiglia, in the town of Rende, respectively.

Table 1. Case studies

Locations of case studies	Case study
Bochum – Germany [7]	CS1
Bochum – Germany [7]	CS2
Sant Cugant del Vallès – Spain [13]	CS3
Sant Cugant del Vallès – Spain [13]	CS4
Genoa – Italy [5]	CS5
Genoa – Italy [5]	CS6
Genoa – Italy [5]	CS7
Sicily – Italy [25]	CS8
University of Calabria (Rende) – Italy [15]	CS9
Old town of Cosenza – Italy	CS10
Old town of Matera – Italy	CS11
New Area of Quattromiglia (Rende) – Italy	CS12

3 Results

3.1 Application of Rough Set Theory in Optimizing Rainwater-Harvesting Systems

In real projects there is an enormous quantity of data that may be considered and this makes hard the decision making process. In Rough Set method, all data should be categorized. In this regard, the correlated RWH attributes must be determined. All the information about the case studies in form of determined attributes, classification of attributes and decision level for each of them should be provided. According to the data gathered in Table 1, the main RWH attributes have been determined and are presented in Table 2. The attributes have been classified based on 3 classes which denote the suitability conditions for decisions and are high (H), medium (M) and low (L).

Table 2. Conditional attributes for ranking decisions of selected case studies

Conditional attributes	Classification of individual situations	Decision
(a) Building type	1 - One-family building/one-office with garden	H
	2 - One-family building/one-office without garden	M
	3 - Multi-family building/multi offices with garden	
	4 - Multi-family building/multi offices without garden	L
(b) Roof type	1 - Slope roof with tiles, corrugated plastic, plastic or metal sheets	H
	2 - Flat roof covered with plastic or metal sheet	
	3 - Flat roof with concrete or asphalt slabs	
	4 - Flat roofs with gravel	M
	5 - Extensive green roof	
	6 - Intensive green roof	L
(c) Roof Size (collecting area)	1 - Big surface capture (>250)	H
	2 - Average surface capture (100–250)	M
	3 - Small surface capture (<100)	L
(d) The age of the building	1 - New building	H
	2 - Average age building	M
	3 - Old building	L
(e) Average Annual Precipitation	1 - >700 or <300	H
	2 - 300 to 700	M
(f) Number of building residents (based on demand)	1 - 1 to 4	H
	2 - 5 to 20	M
	3 - more 20	L

(*continued*)

Table 2. (*continued*)

Conditional attributes	Classification of individual situations	Decision
(g) Density of city (based on the location of the barrels)	1 - Low Density	H
	2 - Medium Density	M
	3 - High Density	L
(h) Type of urban area	1 - New urban area	H
	2 - Average age urban area	M
	3 - Old urban area	L
(i) Demand usage (m^3/y)	1 - combined usage	H
	2 - one usage (toilet flushing or garden irrigation)	M
	3 - laundry	L
	4 - terrace cleaning	
	5 - car washing	
(j) Tank size	1 - Big Tank (>20 m^3)	H
	2 - Medium Tank (6–20 m^3)	M
	3 - Low Tank (<6 m^3)	L
(k) Economic	1 - Very Economic	H
	2 - Partly Economic	M
	3 - Expensive	L

According to 11 attributes and classes, the selected case studies have been ranked from 1 to 3 and the results are presented in Table 3. For instance, in the first case study (CS1), since the conditional attribute (a) that is "Building type" is "One-family building", the highest rank, i.e. 3, has been selected. Since the table represents the correlation between the case studies and conditional attributes it is named "decision rules".

Table 3. Data Inspection for analysis of site selection decision ranking

Case study	Conditional attributes											Decision level
	a	b	c	d	e	f	g	h	i	j	k	
CS1	3	3	2	2	3	3	1	2	3	1	2	M
CS2	1	3	3	2	3	1	1	2	2	1	2	M
CS3	3	3	2	2	2	3	1	2	3	2	1	H
CS4	2	3	3	2	2	1	1	2	3	3	1	H
CS5	2	3	3	2	3	2	1	2	2	2	2	M
CS6	2	3	3	2	3	1	1	2	2	3	2	H
CS7	2	3	3	2	3	1	1	2	2	3	2	H
CS8	2	3	2	2	2	3	2	2	2	1	3	M
CS9	2	2	2	2	3	1	2	2	2	1	3	H
CS10	1	3	2	1	3	2	1	1	2	2	1	L
CS11	1	3	1	1	3	2	1	1	3	3	1	L
CS12	1	3	3	3	3	1	1	3	2	3	2	H

All the decisions and attributes have been checked to find out the existence of non-deterministic rules that means that for case studies of similar attributes decisions are different. The number of non-deterministic rules in Table 3 was zero. Therefore, the number of conditional attributes is sufficient for determining the decisions. The found reduction in the data is presented in Table 4.

Table 4. The founded reduction

Raw	Reduction	Raw	Reduction	Raw	Reduction
1	{a, b, d, j}	13:	{a, b, i, j}	25:	{a, f, j}
2	{a, c, e, j}	14:	{a, b, j, k}	26:	{d, e, g, j}
3	{b, c, e, j}	15:	{a, b, h, j}	27:	{c, f, j}
4:	{a, b, c, j}	16:	{b, c, h, j}	28:	{b, h, i, j}
5:	{b, d, e, j}	17:	{a, e, h, j}	29:	{e, g, h, j}
6:	{a, d, e, j}	18:	{b, e, h, j}	30:	{f, g, h, j}
7:	{b, c, d, j}	19:	{c, e, i, j}	31:	{b, c, i, j}
8:	{a, d, e, f	20:	{a, e, i, j}	32:	{b, d, j, k}
9:	{a, e, f, h}	21:	{d, f, g, j}	33:	{b, h, j, k}
10:	{b, d, f, j}	22:	{b, d, i, j}	34:	{e, j, k}
11:	{a, d, f, k}	23:	{c, e, g, j}	35:	{f, j, k}
12:	{a, f, h, k}	24:	{b, f, h, j}		

After deriving the reducts, the decision rules can be achieved by overlaying the determined reducts on the data. A decision table free of contradiction and determining a minimal decision algorithm can be achieved after elimination of all non-deterministic rules that was zero in this study. The contradictions have been analyzed based on the conditional attributes and the decisions in selected case studies. Moreover, if the attributes do not cause any contradiction they can be removed. In order to check the impact of an attribute on the result, the attributes can be removed one by one. For example, if the conditional attributes (a), (b), (c), and (d) be removed, the decision rules of case studies 1 and 2 might be contradictory that means the decision levels of these two case studies are subordinate to the mentioned conditional attributes. In this regard, and after elimination of all removable conditional attribute or classes, the minimal decision algorithm has been obtained and is presented in Table 5.

Table 5. Minimal decision algorithm

Rules	
Rule 1	(d = 1) => (Decision = L)
Rule 2	(b = 3) & (j = 1) => (Decision = M)
Rule 3	(a = 2) & (j = 2) => (Decision = M)
Rule 4	(f = 1) & (j = 3) => (Decision = H)
Rule 5	(b = 2) => (Decision = H)
Rule 6	(a = 3) & (e = 2) => (Decision = H)

The validation of the rules is presented in Tables 6 and 7. It must be mentioned that, since the selected case studies are only 12, the accuracy of the rules might not be high. To be able to extend the result of the method to other similar case studies in RWH systems, more field data might be required.

Table 6. Confusion matrix (sum over 10 passes)

	1	2	3	None
1	2	0	0	0
2	0	2	2	0
3	1	4	1	0

Table 7. Average accuracy [%]

	Correct	Incorrect	None
Total	40.00 ±43.59	60.00 ± 43.59	0.00 ± 0.00
1	20.00 ± 40.00	0.00 ± 0.00	0.00 ± 0.00
2	15.00 ± 32.02	15.00 ± 32.02	0.00 ± 0.00
3	5.00 ± 15.00	45.00 ± 47.17	0.00 ± 0.00

3.2 Application of TOPSIS in Ranking of Rainwater-Harvesting Systems

In this section, the TOPSIS method has been used to rank the selected case studies and the results are compared with those of a simple ranking. The results of simple ranking are presented in Tables 8 and 9 and those obtained by TOPSIS method in Tables 10, 11 and 12.

Table 8. Values of each attribute for each case study

Case study	Attributes										
	a	b	c	d	e	f	g	h	i	j	k
CS1	3	3	150	2	787	4	1	2	58.4	6	2
CS2	1	3	320	2	787	24	1	2	175.2	14	2
CS3	3	3	107	2	612	3	1	2	47.1	13	1
CS4	2	3	625	2	612	42	1	2	705.2	31	1
CS5	2	3	420	2	1086	16	1	2	233.6	14	2
CS6	2	3	420	2	1086	24	1	2	350.4	21	2
CS7	2	3	680	2	1086	32	1	2	467.2	28	2
CS8	2	3	186	2	657	4	2	2	61.3	2.93	3

Table 9. Simple ranking of the factors for each case study

Case study	Rank of attributes											Sum of ranking	Final rank
	a	b	c	d	e	f	g	h	i	j	k		
CS1	1	1	6	1	2	2	4	1	7	6	2	33	6
CS2	3	1	4	1	2	4	4	1	5	4	2	23	4
CS3	1	1	7	1	4	1	1	1	8	5	3	24	5
CS4	2	1	2	1	4	6	1	1	1	1	3	18	2
CS5	2	1	3	1	1	3	3	1	4	4	2	19	3
CS6	2	1	3	1	1	4	3	1	3	3	2	18	2
CS7	2	1	1	1	1	5	3	1	2	2	2	17	1
CS8	2	1	5	1	3	2	2	1	6	7	1	23	4

Table 10. TOPSIS matrix without scale (Normalized)

Case study	Attributes										
	a	b	c	d	e	f	g	h	i	j	k
CS1	0.48	0.35	0.13	0.35	0.32	0.11	0.46	0.35	0.06	0.11	0.36
CS2	0.16	0.35	0.27	0.35	0.32	0.26	0.46	0.35	0.18	0.26	0.36
CS3	0.48	0.35	0.09	0.35	0.25	0.25	0.03	0.35	0.05	0.25	0.18
CS4	0.32	0.35	0.53	0.35	0.25	0.59	0.03	0.35	0.73	0.59	0.18
CS5	0.32	0.35	0.36	0.35	0.44	0.26	0.44	0.35	0.24	0.26	0.36
CS6	0.32	0.35	0.36	0.35	0.44	0.40	0.44	0.35	0.36	0.40	0.36
CS7	0.32	0.35	0.58	0.35	0.44	0.53	0.44	0.35	0.48	0.53	0.36
CS8	0.32	0.35	0.16	0.35	0.27	0.06	0.04	0.35	0.06	0.06	0.54

Table 11. TOPSIS matrix without scale and equal weighted

Case study	Attributes										
	a	b	c	d	e	f	g	h	i	j	k
CS1	0.044	0.032	0.012	0.032	0.029	0.010	0.041	0.032	0.005	0.010	0.033
CS2	0.015	0.032	0.025	0.032	0.029	0.024	0.041	0.032	0.016	0.024	0.033
CS3	0.044	0.032	0.008	0.032	0.023	0.022	0.003	0.032	0.004	0.022	0.016
CS4	0.029	0.032	0.048	0.032	0.023	0.053	0.003	0.032	0.066	0.053	0.016
CS5	0.029	0.032	0.033	0.032	0.040	0.024	0.040	0.032	0.022	0.024	0.033
CS6	0.029	0.032	0.033	0.032	0.040	0.036	0.040	0.032	0.033	0.036	0.033
CS7	0.029	0.032	0.053	0.032	0.040	0.048	0.040	0.032	0.044	0.048	0.033
CS8	0.029	0.032	0.014	0.032	0.024	0.005	0.003	0.032	0.006	0.005	0.049
V+	**0.044**	**0.032**	**0.053**	**0.032**	**0.040**	**0.053**	**0.003**	**0.032**	**0.066**	**0.053**	**0.049**
V−	**0.015**	**0.032**	**0.008**	**0.032**	**0.023**	**0.005**	**0.041**	**0.032**	**0.004**	**0.005**	**0.016**

Table 12. Ranking in TOPSIS based on higher CL and comparison with simple ranking

Case study	d+	d−	CL	Rank in TOPSIS	Simple rank method	Decision level
CS4	0.040	0.109	0.731	1	2	H
CS7	0.049	0.090	0.645	2	1	H
CS6	0.063	0.064	0.504	**3**	**3**	**H**
CS5	0.077	0.049	0.389	**4**	**4**	**M**
CS3	0.095	0.054	0.363	5	7	H
CS8	0.101	0.053	0.342	**6**	**6**	**M**
CS2	0.088	0.038	0.302	7	5	M
CS1	0.105	0.035	0.250	**8**	**8**	**M**

Despite the fact that in some case studies the difference in ranking methods are minor since in TOPSIS all correlated attributes and the differences among the values are taken into consideration the results could be more accurate.

4 Conclusions

There are many benefits in Rainwater harvesting (RWH) systems mainly water saving for non-potable water uses and surface runoff mitigation. Moreover, the collected rainwater can be re-used for several purposes including green roofs and garden, flushing toilets, etc. Our analysis showed that, in previous studies, some important factors in the analysis and the feasibility of the RWH systems have been neglected and the optimization of RWH systems mostly is limited to optimize the size of the tankers according to hydrological and hydraulic analysis and in some cases, this is combined with an economic analysis. In this paper, multi-objective optimization approaches have been considered for comparing algorithms and evaluating the performance of alternatives to identify the ideal solution. For this, a limited set of data extracted from several case studies has been used. The selection of the case studies has been made considering the main possible attributes/factors confronting in rainwater harvesting systems. The results show that the Rough Set method is a suitable way for analysis of RWH systems and the outcomes can be useful in decision making by decreasing the uncertainties, reducing the cost, and increasing the efficiency. According to the results, TOPSIS ranking method showed good agreement with the decision levels in the case studies. This may be due to the consideration of all correlated attributes and of the differences between the values of this ranking method. In conclusion, the numerical optimization of RWH systems may improve previous studies in the field. Moreover, the Rough Set and TOPSIS methods could be applied as a useful approach in rainwater harvesting systems investigations and provide an additional tool to identify the optimal system and the best site.

Acknowledgements. The study was co-funded by the "Innovative Building Envelope through Smart Technology (I-Best)" Project funded by the Italian National Operational Program "Enterprise and Competitiveness" 2014–2020 ERDF – I AXIS "Innovation" - Action 1.1.3 – "Support for the economic enhancement of innovation through experimentation and the adoption of innovative solutions in processes, products and organizational formulas, as well as through the financing of the industrialization of research results".

References

1. Palermo, S.A., Zischg, J., Sitzenfrei, R., Rauch, W., Piro, P.: Parameter sensitivity of a microscale hydrodynamic model. In: Mannina, G. (ed.) UDM 2018. GET, pp. 982–987. Springer, Cham (2019). https://doi.org/10.1007/978-3-319-99867-1_169
2. Maiolo, M., Pantusa, D.: Sustainable water management index, SWaM_Index. Cogent Eng. **6**(1), 1603817 (2019). https://doi.org/10.1080/23311916.2019.1603817
3. Christian Amos, C., Rahman, A., Mwangi Gathenya, J.: Economic analysis and feasibility of rainwater harvesting systems in urban and peri-urban environments: a review of the global situation with a special focus on Australia and Kenya. Water **8**(4), 149 (2016). https://doi.org/10.3390/w8040149
4. Campisano, A., et al.: Urban rainwater harvesting systems: research, implementation and future perspectives. Water Res. **115**, 195–209 (2017). https://doi.org/10.1016/j.watres.2017.02.056
5. Palla, A., Gnecco, I., La Barbera, P.: The impact of domestic rainwater harvesting systems in storm water runoff mitigation at the urban block scale. J. Environ. Manag. **191**, 297–305 (2017). https://doi.org/10.1016/j.jenvman.2017.01.025
6. Petrucci, G., Deroubaix, J.F., De Gouvello, B., Deutsch, J.C., Bompard, P., Tassin, B.: Rainwater harvesting to control stormwater runoff in suburban areas. An experimental case-study. Urban Water J. **9**(1), 45–55 (2012). https://doi.org/10.1080/1573062X.2011.633610
7. Herrmann, T., Schmida, U.: Rainwater utilisation in Germany: efficiency, dimensioning, hydraulic and environmental aspects. Urban Water **1**(4), 307–316 (2000). https://doi.org/10.1016/S1462-0758(00)00024-8
8. GhaffarianHoseini, A., Tookey, J., GhaffarianHoseini, A., Yusoff, S.M., Hassan, N.B.: State of the art of rainwater harvesting systems towards promoting green built environments: a review. Desalin. Water Treat. **57**(1), 95–104 (2016). https://doi.org/10.1080/19443994.2015.1021097
9. Oberascher, M., Zischg, J., Palermo, S.A., Kinzel, C., Rauch, W., Sitzenfrei, R.: Smart rain barrels: advanced LID management through measurement and control. In: Mannina, G. (ed.) UDM 2018. GET, pp. 777–782. Springer, Cham (2019). https://doi.org/10.1007/978-3-319-99867-1_134
10. Li, Z., Boyle, F., Reynolds, A.: Rainwater harvesting and greywater treatment systems for domestic application in Ireland. Desalination **260**(1–3), 1–8 (2010). https://doi.org/10.1016/j.desal.2010.05.035
11. Campisano, A., Modica, C.: Rainwater harvesting as source control option to reduce roof runoff peaks to downstream drainage systems. J. Hydroinform. **18**(1), 23–32 (2016). https://doi.org/10.2166/hydro.2015.133
12. Jones, M.P., Hunt, W.F.: Performance of rainwater harvesting systems in the southeastern United States. Resour. Conserv. Recycl. **54**(10), 623–629 (2010). https://doi.org/10.1016/j.resconrec.2009.11.002
13. Domènech, L., Saurí, D.: A comparative appraisal of the use of rainwater harvesting in single and multi-family buildings of the Metropolitan Area of Barcelona (Spain): social experience, drinking water savings and economic costs. J. Clean. Prod. **19**(6–7), 598–608 (2011). https://doi.org/10.1016/j.jclepro.2010.11.010
14. Cipolla, S.S., Altobelli, M., Maglionico, M.: Decentralized water management: rainwater harvesting, greywater reuse and green roofs within the GST4Water project. In: Multidisciplinary Digital Publishing Institute Proceedings, vol. 2, no. 11, p. 673 (2018). https://doi.org/10.3390/proceedings2110673

15. Piro, P., Turco, M., Palermo, S.A., Principato, F., Brunetti, G.: A comprehensive approach to stormwater management problems in the next generation drainage networks. In: Cicirelli, F., Guerrieri, A., Mastroianni, C., Spezzano, G., Vinci, A. (eds.) The Internet of Things for Smart Urban Ecosystems. IT, pp. 275–304. Springer, Cham (2019). https://doi.org/10.1007/978-3-319-96550-5_12
16. Becciu, G., Raimondi, A., Dresti, C.: Semi-probabilistic design of rainwater tanks: a case study in Northern Italy. Urban Water J. **15**(3), 192–199 (2018). https://doi.org/10.1080/1573062X.2016.1148177
17. Pawlak, Z.: Rough set theory and its applications to data analysis. Cybern. Syst. **29**(7), 661–688 (1998). https://doi.org/10.1080/019697298125470
18. Arabani, M., Sasanian, S., Farmand, Y., Pirouz, M.: Rough-set theory in solving road pavement management problems (Case Study: Ahwaz-Shush Highway). Comput. Res. Prog. Appl. Sci. Eng. (CRPASE) **3**(2), 62–70 (2017)
19. Arabani, M., Pirouz, M., Pirouz, B.: Optimization of geotechnical studies using basic set theory. In: 1st Conference of Civil and Development, Zibakenar, Iran (2012)
20. Hwang, C.L., Yoon, K.P.: Multiple Attributes Decision-Making Methods and Applications. Springer, Berlin (1981). https://doi.org/10.1007/978-3-642-48318-9
21. Balioti, V., Tzimopoulos, C., Evangelides, C.: Multi-criteria decision making using TOPSIS method under fuzzy environment. Appl. Spillway Sel. Proc. **2**, 637 (2018). https://doi.org/10.3390/proceedings2110637
22. Krohling, R.A., Pacheco, A.G.: A-TOPSIS an approach based on TOPSIS for ranking evolutionary algorithms. Procedia Comput. Sci. **55**, 308–317 (2015). https://doi.org/10.1016/j.procs.2015.07.054
23. Haghshenas, S.S., Neshaei, M.A.L., Pourkazem, P., Haghshenas, S.S.: The risk assessment of dam construction projects using fuzzy TOPSIS (case study: Alavian Earth Dam). Civil Eng. J. **2**(4), 158–167 (2016). https://doi.org/10.28991/cej-2016-00000022
24. Haghshenas, S.S., Mikaeil, R., Haghshenas, S.S., Naghadehi, M.Z., Moghadam, P.S.: Fuzzy and classical MCDM techniques to rank the slope stabilization methods in a rock-fill reservoir dam. Civil Eng. J. **3**(6), 382–394 (2017). https://doi.org/10.28991/cej-2017-00000099
25. Campisano, A., Modica, C.: Optimal sizing of storage tanks for domestic rainwater harvesting in Sicily. Resour. Conserv. Recycl. **63**, 9–16 (2012). https://doi.org/10.1016/j.resconrec.2012.03.007

Paper IX

New Mathematical Optimization Approaches for LID Systems

Pirouz, B., **Palermo, S. A.,** Turco, M., & Piro, P. (2020)

Published in: Sergeyev Y., Kvasov D. (eds) Numerical Computations: Theory and Algorithms. NUMTA 2019. Lecture Notes in Computer Science, vol 11973. Springer, Cham.
https://doi.org/10.1007/978-3-030-39081-5_50

New Mathematical Optimization Approaches for LID Systems

Behrouz Pirouz[1(✉)], Stefania Anna Palermo[2], Michele Turco[3], and Patrizia Piro[2]

[1] Department of Mechanical, Energy and Management Engineering, University of Calabria, Rende, CS, Italy
behrouz.pirouz@unical.it
[2] Department of Civil Engineering, University of Calabria, Rende, CS, Italy
{stefania.palermo,patrizia.piro}@unical.it
[3] Department of Environmental and Chemical Engineering, University of Calabria, Rende, Italy
michele.turco@unical.it

Abstract. Urbanization affects ecosystem health and downstream communities by changing the natural flow regime. In this context, Low Impact Development (LID) systems are important tools in sustainable development. There are many aspects in design and operation of LID systems and the choice of the selected LID and its location in the basin can affect the results. In this regard, the Mathematical Optimization Approaches can be an ideal method to optimize LIDs use. Here we consider the application of TOPSIS (Technique for Order Preference by Similarity to Ideal Solution) and Rough Set theory (multiple attributes decision-making method). An advantage of using the Rough Set method in LID systems is that the selected decisions are explicit, and the method is not limited by restrictive assumptions. This new mathematical optimization approach for LID systems improves previous studies on this subject. Moreover, it provides an additional tool for the analysis of essential attributes to select and optimize the best LID system for a project.

Keywords: Optimization · LID · Rough Set Theory · TOPSIS method

1 Introduction

Low Impact Development (LID) systems are important tools in sustainable development. There are different types of LID practices such as green roofs, green wall, bioretention cell, permeable pavements, rainwater harvesting systems, etc. In the design and operation of LID systems, many components must be considered. When choosing and designing the best LID practices many factors can affect their efficiency in terms of flooding risk mitigation, water quality improvement, water saving, urban heat island reduction, air pollution decreasing. Previous studies are generally limited to focus the design of a type of LID based on a determined scenario and location. However, these elements are not fixed.

In this research, the application of mathematical optimization approaches by TOPSIS ranking method and attributes analysis by Rough Set in evaluation of alternative decisions is described.

Y. D. Sergeyev and D. E. Kvasov (Eds.): NUMTA 2019, LNCS 11973, pp. 583–595, 2020.
https://doi.org/10.1007/978-3-030-39081-5_50

1.1 LID Systems

In the last decades, the combined effect of urbanization and climate change produced several environmental adverse impacts as flooding risk, water and air pollution, water scarcity, and urban heat island effect [1–5].

Specifically, from a hydrologic point of view, land use changes led to significant alterations of the natural hydrological cycle with a reduction of infiltration and evapotranspiration rates, a decreasing of groundwater recharge and baseflow, and a growth of surface runoff. This phenomenon makes cities vulnerable to local flooding and combined sewer overflows (CSOs) [6, 7].

In response to these issues, a novel approach, which considers the implementation of sustainable nature-based stormwater management strategies, is necessary [8].

In this regard, several strategies, known as Low Impact Development (LID) systems [9], have gained increasing popularity. These techniques are small-scale units, which provide several benefits at multiple scales [10–13].

LID systems consist of a series of facilities - such as green roofs, green wall, rain gardens, bioretention cells, permeable pavements, infiltration trenches, rain water harvesting systems, and so on - whose purpose is to infiltrate, filter, store, evaporate, and detain runoff close to its source [14–16].

Therefore, their implementation in an urban area can create a complex system of temporal storage facilities allowing an innovative urban stormwater management approach [17].

In recent years, the implementation of these sustainable solutions has attracted widespread interest from researchers, urban planners, and city managers researchers [18] and several studies have been devoted to LID design, benefits, and simulation models of their behavior.

From these studies, as pointed out by Eckart et al. [15], it appears that: (i) the appropriate design of LID is affected by the site location (in terms of soil type/conditions, plants, rainfall regime, land use types and other meteorological and hydrological properties); (ii) the optimal selection and placement of LID is one of the most crucial factors to consider to achieve the maximum efficiency at the minimum cost.

The implementation of these systems can improve the sustainable development and mitigate several other environmental impacts in addition to urban flooding risk, such as water and air pollution, water scarcity, urban heat island effect. Therefore, a large number of factors have to be considered during the design process and for the choose of the site location.

After a deeper analysis of different studies carried out on LID solutions, several factors affecting their efficiency at multiple scale have been identified and are here considered here for optimizing their use.

2 Methodology

In this paper, we discuss the application of TOPSIS (Technique for Order Preference by Similarity to Ideal Solution) and Rough Set theory (multiple attributes decision-making method) in optimization of LIDs.

2.1 Rough Set Theory

Low Impact Development approaches are Multi-Objectives and there are many uncertainties in the selection of these objectives [19]. The Rough Set method, introduced by Pawlak [20] in 1982, can be used as an excellent mathematical tool in analysis of vague description of decisions such as quality of data, means variation or uncertainty that follows from information. The rough sets philosophy is based on assumption that, for every objects a certain information (data, knowledge) exists, that can be expressed as attributes [21].

With respect to the available data, the objects with the same description are indiscernible and a set of indiscernible objects, named elementary set, can be provided to build knowledge about a real system. Deal with quantitative or qualitative data depends on the input information and before the analysis, it is necessary to remove the irregularities. With respect to the output data, the relevance of particular attributes and their subsets to the quality of approximation can be acquired [22].

In this regard, the induction-based approach can provide clear rules for decision-makers (DMs) in the form of "if…, then…". The concept of approximation space in rough set method can be described in a given approximation space as follows:

$$\mathrm{apr} = (\mathrm{U}, \mathrm{A}) \tag{1}$$

U is a finite and non-empty set and A is set of attributes in the given space. Based on the approximation space, the lower and upper approximations of a set can be defined. Let X be a subset of U and the upper and lower approximation of X in A are:

$$\overline{apr}(\mathrm{A}) = \{\mathrm{x} | \mathrm{x} \in \mathrm{U}, \mathrm{U/ind}\,(\mathrm{A}) \subset \mathrm{X}\} \tag{2}$$

$$\underline{apr}(\mathrm{A}) = \{\mathrm{x} | \mathrm{x} \in \mathrm{U}, \mathrm{U}/\mathrm{ind}\,(\mathrm{A}) \cap \mathrm{X} \neq \varphi\} \tag{3}$$

where:

$$\mathrm{U/ind}\,(\mathrm{a}) = \{(\mathrm{xi}, \mathrm{xj}) \in \mathrm{U} \times \mathrm{U}, \mathrm{f}\,(\mathrm{xi}, \mathrm{a}) = \mathrm{f}\,(\mathrm{xj}, \mathrm{a}), \forall \mathrm{a} \in \mathrm{A}\} \tag{4}$$

Equation (2), that is the best upper approximation of X in A, means the minimum composed set in A containing X, and Eq. (3), that is the best lower approximation, means the maximum composed set in A contained in X. The graphical illustration of approximations in the rough set method is shown in Fig. 1.

The boundary represent as:

$$\mathrm{BN}\,(\mathrm{A}) = \overline{apr}(\mathrm{A}) - \underline{apr}(\mathrm{A}) \tag{5}$$

The reducts and decision rules can be defined as follows:

The reduct RED (B), is a minimal set of attributes B $\subseteq$ A such that rB (U) = rA (U). rB (U) indicates the quality of approximation of U by B.

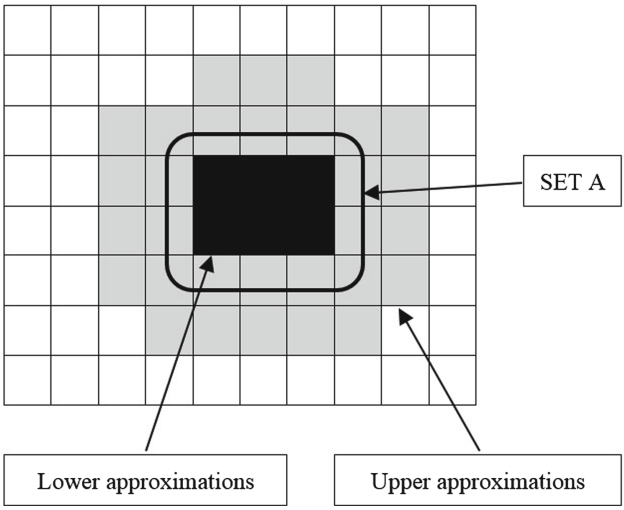

Fig. 1. Graphical illustration of the rough set approximations

The equation is:

$$r_B(\mathrm{U}) = \frac{\sum card(\underline{B}(X_i))}{card(U)} \tag{6}$$

After providing the result of reducts, the decision rules can be derived by using the overlaying of the reducts on the information systems. An expressed decision rule can be as follow:

$$\varphi \Rightarrow \theta \tag{7}$$

where:

φ is the conjunction of elementary conditions,
$\Rightarrow$ Represents indicates
θ represents the disjunction of elementary decisions.

2.2 TOPSIS Method

TOPSIS (Technique for Order Preference by Similarity to Ideal Solution) is a method developed by Hwang and Yoon in 1981 to solve the ranking and compare problems [23]. The ranking in this method is made according to the similarity to ideal solution [24, 25]. The TOPSIS method can be applied to a wide range of multi-attribute decision

making with several attributes [26–28]. The graphical illustration of the TOPSIS methodology is presented in Fig. 2.

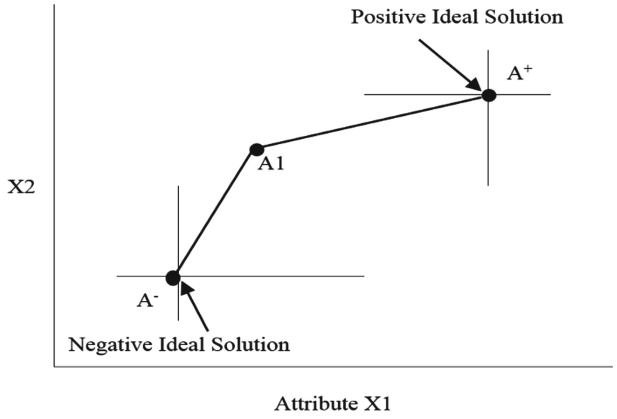

Fig. 2. Graphical illustration of the TOPSIS methodology, (A+ represent the ideal point, A− represent the negative-ideal point)

The ranking by TOPSIS is carried out through seven steps:
Step 1: Create the matrix

$$(n_{ij})m \times n \tag{8}$$

Step 2: Construct the normalized decision matrix

$$N = n_{ij} = \frac{a_{ij}}{\sqrt{\sum_i^m = 1a_{ij}^2}}, \mathrm{i} = 1, 2, \ldots, \mathrm{m} \quad \& \quad \mathrm{j} = 1, 2, \ldots, \mathrm{n} \tag{9}$$

Step 3: Construct the weighted normalized decision matrix

$$\mathrm{V} = \mathrm{N} \times \mathrm{Wn} \times \mathrm{n} \tag{10}$$

Step 4: Determine the solutions (the ideal and negative-ideal solutions)

$$\text{The ideal solution } A^+ = \left\{\left\langle max_i\left(a_{ij}|j \in J_-\right)\right\rangle, \left\langle min_i\left(a_{ij}|j \in J_+\right)\right\rangle\right\} \tag{11}$$

$$\text{The negative}-\text{ideal solutions } A^- = \left\{\left\langle min_i\left(a_{ij}|j \in J_-\right)\right\rangle, \left\langle max_i\left(a_{ij}|j \in J_+\right)\right\rangle\right\} \tag{12}$$

where,

$$J_+ = \{j = q, 2, \ldots, n|j\} \text{ Associated with positive impact criteria}$$
$$J_- = \{j = q, 2, \ldots, n|j\} \text{ Associated with negative impact criteria}$$

Step 5: Determine the distance of alternatives v_{ij} from the ideal solution and the negative-ideal solutions

$$\text{The distance from ideal solution: } d_i^+ = \sqrt{\sum_{j=1}^{n} \left(v_{ij} - v_j^+\right)}, \quad \text{i} = 1, 2, \ldots, \text{m} \tag{13}$$

$$\text{The distance from negative}-\text{ideal solution : } d_i^- = \sqrt{\sum_{j=1}^{n} \left(v_{ij} - v_j^+\right)}, \quad \text{i} = 1, 2, \ldots, \text{m} \tag{14}$$

Step 6: Calculate the closeness to the negative-ideal condition, CL^*

$$CL_i^* = \frac{d_i^-}{d_i^- + d_i^+}, \quad 0 \le CL_i^* \le 1 \ \& i = 1, 2, \ldots, m \tag{15}$$

where,

$CL_i^* = 1$ *if* The solution has the best condition and means the highest rank
$CL_i^* = 0$ *if* The solution has the worst condition and means the lowest rank

Step 7: Rank in order to the highest CL^*.

2.3 Case Studies

In order to perform the analysis of LID practices by Rough Set and TOPSIS a set of data is required. For this purpose, sites have been chosen according to different conditions and considering the main factors in the LIDs selection. The selected site along with hypothesis are presented in Table 1.

Table 1. Site selection hypothesis to rank the attributes

Site	Description
S1	An high urbanized area (78% impervious surfaces), with extremely wet condition, average age, presenting High Flooding Risk, Low Water Scarcity, High Water Pollution, Medium Heat Island Effect, High Air Pollution, supposing to replace 50% of impervious area with LID (permeable pavement and green roof); and that the inhabitants are supported to implement them, thus partially economic
S2	An urbanized area (65% of impervious surfaces), with moderately wet condition, old area, presenting High Flooding Risk, Medium Water Scarcity, High Water Pollution, High Heat Island Effect, High Air Pollution, where it is not possible to implement LID; not economic
S3	A peri-urban area (45% of impervious surfaces), with extremely dry condition, new area, presenting Low Flooding Risk, High Water Scarcity, Medium Water Pollution, Low Heat Island Effect, Medium Air Pollution, where it is possible to implement combined usage of LID (rainwater harvesting and biofiltration trench) for a percentage of 65%; high economic
S4	A peri-urban area (40% of impervious surfaces), with moderate climate condition, average age, presenting Medium Flooding Risk, Medium Water Scarcity, Low Water Pollution, Low Heat Island Effect, Medium Air Pollution, where it is possible to implement combined usage of LID (rainwater harvesting and green wall) for a percentage of 40%; partially economic
S5	A normal urban area (70% of impervious surfaces), with extremely dry climate condition, average age, presenting Low Flooding Risk, High Water Scarcity, Low Water Pollution, High Heat Island Effect, High Air Pollution, where it is possible to implement combined usage of LID (rainwater harvesting, green roof and green wall) for a percentage of 50%; partially economic
S6	A rural area (20% of impervious surface), with extremely dry climate condition, average area, presenting s Low Flooding Risk, High Water Scarcity, Low Water Pollution, Low Heat Island Effect, Low Air Pollution, where it would be better to implement rainwater harvesting for a percentage of 70%; partially economic

As it can be recognized, in Table 1. The main factors considered to define the case studies include climate condition, urbanization level, age of site, flood risk, water scarcity, water and air pollution, Heat Island Effect, LID implementation percentage and economical condition.

3 Results

3.1 Application of Rough Set Theory in Optimizing LIDs

In Rough Set method, at the first stage all factors must be categorized in form of attributes that are classified. This, and the decision level for each of them, can be done according to previous standards, papers or experts. We identified 12 conditional decision attributes for LIDs that are presented in Tables 2 and 3.

Table 2. Conditional decision attributes in selected sites, part 1

Conditional attributes	Classification	Decision
(a) Type of area	1- Urban	H
	2- Peri-urban	M
	3- Rural	L
(b) Climate condition based on precipitation	1- Extremely wet or extremely dry	H
	2- Moderately wet or moderately dry	M
(c) Age of area	1- New area	H
	2- Average age area	M
	3- Old area	L
(d) Impervious surfaces of the selected area	1- >75% of area	H
	2- 50%–75% of area	M
	3- 25%–50% of area	L
	4- <25% of area	N
(e) Flooding risk	1- High risk	H
	2- Medium risk	M
	3- Low risk	L
(f) Water scarcity	1- High water scarcity	H
	2- Medium water scarcity	M
	3- Low water scarcity	L
(g) Water pollution	1- High water pollution	H
	2- Medium water pollution	M
	3- Low water pollution	L

Table 3. Conditional decision attributes in selected sites, part 2

Conditional attributes	Classification	Decision
(h) Urban heat island effect	1- High heat island effect	H
	2- Medium heat island effect	M
	3- Low heat island effect	L
(i) Air pollution	1- High air pollution	H
	2- Medium air pollution	M
	3- Low air pollution	L
(j) LID percentage implementation	1- >60% of area	H
	2- 30%–60% of area	M
	3- <30% of area	L
(k) LID usage	1- Combined implementation (more than 1 LID)	H
	2- Only one type implementation	M
	3- No implementation	N
(l) Economic	1- Economic	H
	2- Partially economic	M
	3- Not economic	L

As it is clear from Tables 2 and 3 the conditional attributes have been categorized in at most four classes with high (H), medium (M), low (L) and no (N) suitability conditions for decisions. As next step, the selected sites presented in Table 1 have been ranked according to the attributes of Tables 2 and 3. The result is presented in Table 4. In Table 4 the ranks are based on the conditional attribute in the site and for ranks from 0 to 4. For example, in site 1 (S1), the conditional attribute (a) that is "Type of Area" is "Urban", and therefore the highest rank (3) has been selected.

Table 4. Ranking of decisions attributes in selected sites

Sites	Conditional attributes												Decision levels
	a	b	c	d	e	f	g	h	i	j	k	l	
S1	3	3	2	3	3	1	3	2	3	2	3	2	H
S2	3	2	1	2	3	2	3	3	3	1	0	1	L
S3	2	3	3	1	1	3	2	1	2	3	3	3	H
S4	2	2	2	1	2	2	1	1	2	2	3	2	M
S5	3	3	2	2	1	3	1	3	3	2	3	2	H
S6	1	3	2	0	1	3	1	1	1	3	2	2	M

3.2 Determining Minimal Decision Algorithm

The finding of a minimal decision algorithm can be achieved by analysis of decision rules in all sites and finding non-deterministic rules or sites, thus assigning different decision levels for different sites under the same class for every conditional attribute. In this regard, at the next stage, the contradiction between data can be checked according to the conditional attributes ranks and the correlated decisions and some of the attributes can be removed if this does not cause any contradiction. For this purpose, the conditional attribute can be eliminated one by one to check the role of that attribute in the result. For instance, if the conditional attributes (a), (b), and (c) were removed, the decision rules of sites S1 and S2 might be contradictory to each other, which means that the decision levels of these two sites are subordinate to one of the conditional attributes. Finally, and after checking all of the combinations, the minimal decision algorithm can be extracted that will be the main rules for each level of decisions. The determined rules according to the attributes data of Table 4 and the six case studies of Table 1 are as follows:

$$\text{Rule 1}: (c = 1) \Rightarrow (D = L)$$
$$\text{Rule 2}: (g = 1) \,\&\, (h = 1) \Rightarrow (D = M)$$
$$\text{Rule 3}: (b = 3) \,\&\, (k = 3) \Rightarrow (D = H)$$

Thus, by the determined rules it is possible to make a decision with minimum attributes. However, these rules have been generated by the decision on the selected case studies. Therefore, by increasing the number of the case studies, the accuracy of

the rules will increase and after checking the validation and accuracy of the rules, it will be possible to extend the rules for other sites.

3.3 Application of TOPSIS in Selection of LID Practices

In this section, the application of TOPSIS method in ranking the selected sites for LIDs is presented. To provide the final ranking, the data of Tables 2 and 3 that are the decision attributes for the selected sites have been used. The result of the process as explained in the methodology section are presented in Tables 5, 6 and 7.

Table 5. Attributes matrix without scale

Case study	Attributes											
	a	b	c	d	e	f	g	h	i	j	k	l
S1	0.50	0.45	0.39	0.69	0.60	0.17	0.60	0.40	0.50	0.36	0.47	0.54
S2	0.50	0.30	0.20	0.46	0.60	0.33	0.60	0.60	0.50	0.18	0.00	0.18
S3	0.33	0.45	0.59	0.23	0.20	0.50	0.40	0.20	0.33	0.54	0.47	0.54
S4	0.33	0.30	0.39	0.23	0.40	0.33	0.20	0.20	0.33	0.36	0.47	0.36
S5	0.50	0.45	0.39	0.46	0.20	0.50	0.20	0.60	0.50	0.36	0.47	0.36
S6	0.17	0.45	0.39	0.00	0.20	0.50	0.20	0.20	0.17	0.54	0.32	0.36

Table 6. Attributes matrix without scale and with equal weight

Case study	Attributes											
	a	b	c	d	e	f	g	h	i	j	k	l
S1	0.04	0.04	0.03	0.06	0.05	0.01	0.05	0.03	0.04	0.03	0.04	0.04
S2	0.04	0.03	0.02	0.04	0.05	0.03	0.05	0.05	0.04	0.01	0.00	0.01
S3	0.03	0.04	0.05	0.02	0.02	0.04	0.03	0.02	0.03	0.04	0.04	0.04
S4	0.03	0.03	0.03	0.02	0.03	0.03	0.02	0.02	0.03	0.03	0.04	0.03
S5	0.04	0.04	0.03	0.04	0.02	0.04	0.02	0.05	0.04	0.03	0.04	0.03
S6	0.01	0.04	0.03	0.00	0.02	0.04	0.02	0.02	0.01	0.04	0.03	0.03

Table 7. Final ranking in based on higher CL and comparison with initial decision level

Case study	d+	d−	CL	Rank by TOPSIS	The initial decision level
S1	0.039	0.102	0.722	1	H
S5	0.057	0.086	0.598	2	M
S3	0.066	0.080	0.548	3	H
S2	0.072	0.081	0.530	4	H
S4	0.074	0.059	0.446	5	L
S6	0.094	0.055	0.369	6	M

The results of ranking by TOPSIS in Table 7 and the comparisons with the initial decision levels represent that in some sites the results are the same such as S1, S3, S2 and S4. However, the decision levels in S6 was M but it is at the end of TOPSIs ranking. This might be based on the consideration of all correlated factors at the same time and more exact.

4 Conclusions

The analysis showed that in design and operation of the LID systems, many components can be considered and that in choosing the best LID practices and implementation percentage many factors can affect the results. In previous studies, generally, the attentions was limited to design a type of LID based on determined scenarios and for a selected site that both are not fixed elements and might need to be optimized.

The results of this application of mathematical optimization approaches by TOPSIS ranking method and attributes analysis by Rough Set in evaluation of alternative decisions confirm the advantage of using these methods. The rules provided by Rough Set method can improve the designing decisions. The generated decisions are explicit, and the results are not limited to restrictive assumptions. With consideration of more case studies, more stringent decision rules can be achieved. Moreover, the final ranks of TOPSIS shows the advantages in compared with simple ranking method.

In conclusion, the new presented mathematical optimization approaches can improve the previous studies about LIDs. They provide an additional tool for engineers in analysis of essential attributes to select and optimize the best LID system for a project and accordingly define the scenarios and hydrologic or hydraulic modeling. This means that the presented methods would provide a baseline for decision-making and would increase the efficiency of the systems and decrease the project cost by preventing uncertainties.

Acknowledgements. The study was co-funded by the Italian Operational Project (PON)—Research and Competitiveness for the convergence regions 2007/2013—I Axis "Support to structural changes" operative objective 4.1.1.1. "Scientific-technological generators of transformation processes of the productive system and creation of new sectors" Action II: "Interventions to support industrial research".

References

1. Zhang, D.L., Shou, Y.X., Dickerson, R.R.: Upstream urbanization exacerbates urban heat island effects. Geophys. Res. Lett. **36**(24), 1–5 (2009)
2. Haase, D.: Effects of urbanisation on the water balance–A long-term trajectory. Environ. Impact Assess. Rev. **29**(4), 211–219 (2009)
3. Jacob, D.J., Winner, D.A.: Effect of climate change on air quality. Atmos. Environ. **43**(1), 51–63 (2009)
4. Piro, P., et al.: Flood risk mitigation in a Mediterranean urban area: the case study of Rossano Scalo (CS – Calabria, Italy). In: Mannina, G. (ed.) UDM 2018. GET, pp. 339–343. Springer, Cham (2019). https://doi.org/10.1007/978-3-319-99867-1_57

5. Miller, J.D., Hutchins, M.: The impacts of urbanisation and climate change on urban flooding and urban water quality: a review of the evidence concerning the United Kingdom. J. Hydrol.: Reg. Stud. **12**, 345–362 (2017)
6. Piro, P., Turco, M., Palermo, S.A., Principato, F., Brunetti, G.: A comprehensive approach to stormwater management problems in the next generation drainage networks. In: Cicirelli, F., Guerrieri, A., Mastroianni, C., Spezzano, G., Vinci, A. (eds.) The Internet of Things for Smart Urban Ecosystems. IT, pp. 275–304. Springer, Cham (2019). https://doi.org/10.1007/978-3-319-96550-5_12
7. Raimondi, A., Becciu, G.: On pre-filling probability of flood control detention facilities. Urban Water J. **12**, 344–351 (2015)
8. Zischg, J., Rogers, B., Gunn, A., Rauch, W., Sitzenfrei, R.: Future trajectories of urban drainage systems: a simple exploratory modeling approach for assessing socio-technical transitions. Sci. Total Environ. **651**, 1709–1719 (2019)
9. Fletcher, T.D., et al.: SUDS, LID, BMPs, WSUD and more–The evolution and application of terminology surrounding urban drainage. Urban Water J. **12**(7), 525–542 (2015)
10. Razzaghmanesh, M., Beecham, S., Salemi, T.: The role of green roofs in mitigating Urban Heat Island effects in the metropolitan area of Adelaide, South Australia. Urban For. Urban Green. **15**, 89–102 (2016)
11. Maiolo, M., Carini, M., Capano, G., Piro, P.: Synthetic sustainability index (SSI) based on life cycle assessment approach of low impact development in the Mediterranean area. Cogent Eng. **4**(1), 1410272 (2017)
12. Zahmatkesh, Z., Burian, S.J., Karamouz, M., Tavakol-Davani, H., Goharian, E.: Low-impact development practices to mitigate climate change effects on urban stormwater runoff: case study of New York City. J. Irrig. Drain. Eng. **141**(1), 04014043 (2014)
13. Jia, H., Yao, H., Shaw, L.Y.: Advances in LID BMPs research and practice for urban runoff control in China. Front. Environ. Sci. Eng. **7**(5), 709–720 (2013)
14. Piro, P., Carbone, M., Morimanno, F., Palermo, S.A.: Simple flowmeter device for LID systems: from laboratory procedure to full-scale implementation. Flow Meas. Instrum. **65**, 240–249 (2019)
15. Turco, M., Brunetti, G., Carbone, M., Piro, P.: Modelling the hydraulic behaviour of permeable pavements through a reservoir element model. In: International Multidisciplinary Scientific Geo Conference: SGEM: Surveying Geology & mining Ecology Management, vol. 18, pp. 507–514 (2018)
16. Eckart, K., McPhee, Z., Bolisetti, T.: Performance and implementation of low impact development–a review. Sci. Total Environ. **607**, 413–432 (2017)
17. Palermo, S.A., Zischg, J., Sitzenfrei, R., Rauch, W., Piro, P.: Parameter sensitivity of a microscale hydrodynamic model. In: Mannina, G. (ed.) UDM 2018. GET, pp. 982–987. Springer, Cham (2019). https://doi.org/10.1007/978-3-319-99867-1_169
18. Jia, H., et al.: Field monitoring of a LID-BMP treatment train system in China. Environ. Monit. Assess. **187**(6), 373 (2015)
19. Zhang, G., Hamlett, J.M., Reed, P., Tang, Y.: Multi-objective optimization of low impact development designs in an urbanizing watershed. Open J. Optim. **2**, 95–108 (2013)
20. Pawlak, Z.: Rough set theory and its applications. J. Telecommun. Inf. Technol. **3**, 7–10 (2002)
21. Arabani, M., Sasanian, S., Farmand, Y., Pirouz, M.: Rough-set theory in solving road pavement management problems (case study: Ahwaz-Shush Highway). Comput. Res. Prog. Appl. Sci. Eng. (CRPASE) **3**(2), 62–70 (2017)
22. Arabani, M., Pirouz, M., Pirouz, B.: Geotechnical investigation optimization using rough set theory. In: 9th International Congress on Civil Engineering (9ICCE), Isfahan, Iran (2012)

23. Hwang, C.L., Yoon, K.P.: Multiple Attributes Decision-Making Methods and Applications. Springer, Berlin (1981). https://doi.org/10.1007/978-3-642-48318-9
24. Haghshenas, S.S., Neshaei, M.A.L., Pourkazem, P., Haghshenas, S.S.: The risk assessment of dam construction projects using fuzzy TOPSIS (case study: Alavian Earth Dam). Civ. Eng. J. **2**(4), 158–167 (2016)
25. Balioti, V., Tzimopoulos, C., Evangelides, C.: Multi-criteria decision making using TOPSIS method under fuzzy environment, application in spillway selection. In: Multidisciplinary Digital Publishing Institute Proceedings, vol. 2, p. 637 (2018)
26. İç, Y.T.: A TOPSIS based design of experiment approach to assess company ranking. Appl. Math. Comput. **227**, 630–647 (2014)
27. Krohling, R.A., Pacheco, A.G.: A-TOPSIS an approach based on TOPSIS for ranking evolutionary algorithms. Procedia Comput. Sci. **55**, 308–317 (2015)
28. Haghshenas, S.S., Mikaeil, R., Haghshenas, S.S., Naghadehi, M.Z., Moghadam, P.S.: Fuzzy and classical MCDM techniques to rank the slope stabilization methods in a rock-fill reservoir dam. Civ. Eng. J. **3**(6), 382–394 (2017)